EXPERIMENTAL STUDY ON EFFECTS OF GEOGRID REINFORCED ZONE ON SEISMIC PERFORMANCE OF LOW-TO-MEDIUM RISE BUILDINGS

by

Okan Küçükakyüz

B.S., Civil Engineering, Yıldız Technical University, 2013

Submitted to the Kandilli Observatory and Earthquake Research Institute
in partial fulfillment of the requirements for the degree of
Master of Science

Graduate Program in Earthquake Engineering

Boğaziçi University

2020

EXPERIMENTAL STUDY ON EFFECTS OF GEOGRID REINFORCED ZONE ON SEISMIC PERFORMANCE OF LOW-TO-MEDIUM RISE BUILDINGS

APPROVED BY:

……

……

……

DATE OF APPROVAL: 05.11.2020

ACKNOWLEDGEMENTS

I would like to express my deepest gratitude and kind regards to my supervisor Prof. Dr. Ayşe Edinçliler for her invaluable contributions and support. Along with putting effort to our studies and expanding our vision for our work; she also set an example for what it means to be a good academician and a teacher.

I would like to thank my committee members Prof. Dr. Ali Pınar and Prof. Dr. Ayfer Erken for their valuable contributions.

I would like to express my gratitude to Prof. Dr. Bilge Doran, for his significant contributions to me through my undergraduate education by means of personal values and sincere guidance. He has always been supportive and positive to his students.

I also present thanks to my dear brother Ozan Küçükakyüz and sister Mehtap Küçükakyüz for their priceless presence and consistent support.

I would like to thank beloved Yaren Türkkan for her invaluable support and presence throughout the difficult times with her love and encouragement all along the journey.

I thank my dear friends Mahir Çetin and Uçkan Mertcan Arslan for their invaluable contributions and helpful attitude.

I also would like to thank my parents for their support and patience, throughout my education.

ABSTRACT

EXPERIMENTAL STUDY ON EFFECTS OF GEOGRID REINFORCED ZONE ON SEISMIC PERFORMANCE OF LOW-TO-MEDIUM RISE BUILDINGS

This study aims to investigate the effectiveness and reliability of geogrids as a soil reinforcing system. In order to prevent or minimize the earthquake impact on structures, this study focuses on reducing the effect of earthquake loads by creating the geogrid reinforced zones. This system is composed of various layers of geogrid configurations to be able to create a reinforced geogrid foundation under the structure. To present reliable results through observing the soil-structure interaction and structural behaviour and digital comparisons via data outputs; an experimental setup was established. With this purpose in mind, the seismic behavior of the two 1:10 scaled structure models without and with the different geogrid reinforcement configurations under different earthquake conditions were studied. A series of shaking table tests were performed to evaluate the seismic response of the building models depending on the selected performance criteria. The effects of geogrid reinforced zone which is dependent on the number of geogrid layers on the seismic behaviour of the low-rise and medium rise buildings were discussed with comparing test results of the unreinforced and reinforced cases. Comparison results of the tests revealed that the inclusion of the geogrid reinforcement to the sand can reduce earthquake impacts by decreasing the transmitted seismic energy from soil to structure via the interlocking mechanism between geogrid layers and soil. Significant improvements in reducing forces of strong ground motions are able to make geogrid reinforced soil systems an option to improve seismic performance of the structures.

ÖZET

GEOGRİD İLE GÜÇLENDİRİLMİŞ BÖLGENİN AZ VE ORTA KATLI BİNALARIN SİSMİK PERFORMANSI ÜZERİNE ETKİLERİNİN DENEYSEL OLARAK İNCELENMESİ

Bu çalışmada, geogridlerin zemin güçlendirme sistemi olarak etkinliğinin ve güvenilirliğinin incelemesi amaçlanmaktadır. Depremin yapılar üzerindeki etkisini önlemek veya en aza indirmek için, geogrid donatı bölgeleri oluşturularak deprem yüklerinin etkisinin azaltılmasına odaklanılmıştır. Bu sistem, yapının altında güçlendirilmiş geogrid temel oluşturabilmek için çeşitli geogrid konfigürasyon katmanlarından oluşur. Veri çıktıları üzerinden zemin-yapı etkileşimini ve yapısal davranışı ve dijital karşılaştırmaları gözlemleyerek güvenilir sonuçlar sunabilmek adına, laboratuvar düzeneği oluşturulmuştur. Bu amaçla, farklı geogrid donatı konfigürasyonları olan ve olmayan 1:10 ölçekli iki yapı modelinin farklı deprem koşullarında sismik davranışı incelenmiştir. Seçilen performans kriterlerine bağlı olarak bina modellerinin sismik tepkisini değerlendirmek için bir dizi sarsma masası testi yapılmıştır. Geogrid katman sayısına bağlı olarak geogrid donatı bölgesinin alçak ve orta katlı binaların sismik davranışına etkileri, donatılmış ve donatılmamış durumların test sonuçları karşılaştırılarak tartışılmıştır. Testlerin karşılaştırma sonuçları, zemine geogrid donatı ilave edilmesinin, geogrid tabakaları ile zemin arasındaki kenetlenme mekanizması aracılığıyla zeminden yapıya iletilen sismik enerjiyi sönümleyerek deprem etkilerini azaltabileceğini ortaya koymuştur. Kuvvetli yer hareketlerinin etkisinin azaltılması ile elde edilen önemli iyileştirmeler, geogrid takviyeli zemin sistemlerini yapıların sismik performansını iyileştirmek için önemli bir seçenek haline getirebilir.

TABLE OF CONTENTS

LIST OF FIGURES

LIST OF TABLES

LIST OF SYMBOLS AND ABBREVIATIONS

a'	Acceleration of the soil without container effect
A	Accelerometer
b	Width of geogrid layers
B	Width and depth of square shaped foundation
BCR	Bearing Capacity Ratio
d	Depth of reinforcement below the bottom of foundation
ESB	Equivalent shear beam
g	Gravitational acceleration
h	Vertical spacing between consecutive geogrid layers
Hz	Hertz
F_d	Dynamic force
N	Number of geogrid layers
ODS	Optical Distance Sensors
PGA	Peak Ground Acceleration
PGV	Peak Ground Velocity
PGD	Peak Ground Displacement
RMS	Root mean square
q	Load per unit area
q_{ult}	Ultimate bearing load capacity per unit area
u	Top layer depth of geogrid

1. INTRODUCTION

1.1. General

Methods of building structures have been developed more than ever before by the help of advancing engineering capabilities and building technologies. In addition to this, it is much safer, faster and reliable to conduct different engineering analysis, as well as building constructions and improved material qualities. Even so, various solutions for structural safety problems which are caused by phenomena like earthquake, fire, tsunami etc. hazards are required. Even with multiple solutions and precautions, destructive effects of significant earthquakes such as Haiti (2010), Japan (2011), Nepal (2015), Turkey (2020) could not be prevented. In Chang et al. (2002) study, it is expressed the seismic resistance capacity can be improved by adding shear wall braced frames or moment resistant frames, however, this solution may cause higher story accelerations for stiff buildings or, large inter-story drift ratios for flexible buildings. Since the inter-story drift ratios and structural performance criteria are strictly defined in many earthquake codes as well as in Turkish Building Seismic Code (2019), an answer to these eccentric demands, should not only include the structure itself, but also other non-structural parameters of construction site and geological characteristics. Additionally, some vital buildings as fire stations, hospitals and communication station which may contain sensitive instruments that have crucial importance after an earthquake, may include additional non-structural precautions.

Concept of reducing strong ground motion impact covers a wide range of applications. For instance, seismic isolation aims to decrease horizontal loads transferred to building, via improving the damping ratio or changing the natural period of the structure. Conventional seismic isolation includes different systems, laminated bearing, lead-rubber bearing and friction pendulum elements. Although the multiple options on this method have, it is generally expensive depending on experience levels at design and implementation, and requires specialization to implement these solutions, especially in developing countries.

Alternative ways were offered in many studies to provide low-cost applications to improve earthquake performance of the structural elements by using geogrid materials, by Omar et al. (1993), Yetimoglu et al. (1994), Alawaji (2001), Patra et al. (2005), Edincliler et al. (2017). Different geometrical configurations of geosynthetics were researched in similar studies. Barely, these studies are generally conducted via numerical analysis or stick dependent on analyzing specific structural elements, such as foundations.

The content of this study includes the experimental study and evaluation of low-cost geogrid reinforced zone on seismic performance of low-to-medium rise buildings under different earthquake motions. Related studies of such systems were conducted as geogrid-reinforced sand as Laman & Yildiz (2003) and Edincliler et al. (2019).

In this context, experimental studies contain the performance tests of the laminar box and the seismic performance tests of the two 1:10 scaled building models as 3-story and 5-story buildings with and without the geogrid reinforcement by performing a series of the shaking table tests. Different geogrid reinforced zones were created to determine the effects of the geogrid reinforcement under destructive earthquake motions. Eight different scenarios of geogrid configuration were investigated to define seismic performance of the test setups. In addition to this, eight performance criteria were determined, and a parametric study was conducted to compare the results of all cases. Thus, it is aimed to experimentally develop a display for the level of interlocking effect between soil and geogrid, as well as earthquake performance of the geogrid reinforced zones in terms of mentioned performance criteria.

1.2. Problem Statement

Many numerical and some experimental researches were done for examining of seismic performance of geogrid materials. Since material and geometry of the geogrid element is quite changeable and has an impact on the behaviour of the soil, therefore the structure; it is still relatively difficult to decide the characteristics of the setup within such a combination pool. Additionally, the previous studies lack of adequate data on behalf of providing the soil-structure interaction, as well as providing experimental check of numerical researches. This study also aims to observe both superstructure and geogrid

reinforced soil at the same time. Thus, identifying the systems of laminar box, soil type, model structures and geogrid zone characteristics will improve the understanding and application of similar techniques. Actualizing the image of an environment when a strong ground motion occurs will help to provide a realistic experiment to verify effectiveness of such systems.

1.3. Objective of the Thesis

The main purpose of this study is to determine the influence of geogrid reinforced zones on the seismic behaviour of low-rise and mid-rise structures under strong ground motions via shake table tests. This study is the first experimental study in the literature in which the effects of geogrid reinforced zone on the reinforced soil and superstructure model are investigated together. Mentioned researches lacked such a characteristic and stayed on numerical basis, or either took only specific structural elements into account. In this case, considering the geogrid reinforced area, it is possible to observe both the seismic behavior of the foundation and the soil-structure interaction.

This thesis consists of checking the outputs of the previous static experiments and determining the contributions of geogrid reinforcement, therefore their performances under strong ground motions. By using the experiences from the previous numerical and experimental studies, a new test setup for the shaking table experiments was designed and modeled to validate the effects of the inclusion of the geogrid reinforcement by observing both soil and structural behaviour under the scaled real earthquake records. It is aimed to evaluate the effects of the depth of the geogrid reinforced zone on the seismic performance of the low-to-medium rise buildings.

2. LITERATURE REVIEW

2.1. Geogrid Material

A Geogrid is defined as; “a geosynthetic material consisting of connected parallel sets of tensile ribs with apertures of sufficient size to allow strike-through of surrounding soil, stone or other geotechnical material". Geogrids are commercially available materials, primarily in three main categories as displayed in Figure 2.1 (Koerner, 2005):

- Unitized polyolefin geogrids
- Coated yarn geogrids,
- Polyester rod (or strap) geogrids.

Since the one of the primary functions of the geogrids is reinforcement, type of reinforcement applications also varies to a very large range. In those applications where the direction of the major stresses are known, as walls and slopes, unidirectional, or uniaxial, geogrids are used. In those where the applied stresses come from random directions, as in pavements and foundations, bidirectional, or biaxial, geogrids are used. In addition, geogrids have been used as an improvement method for increasing bearing capacity of poor foundation soils in different ways; as a continuous layer, as multiple closely spaced continuous layers with granular soil between layers and as mattresses consisting of three-dimensional inter-connected cells. It is also mentioned to be used to stabilize and reinforce multiple application areas; such as paved roads, pavements, unpaved roads, embankments and slopes, reinforced walls, foundation and basal reinforcement, veneer cover soils (Koerner, 2005).

Furthermore, Koerner (2005) highlighted some of the useful aspects of geogrid reinforcement for foundation soil stability as;

- Global slope stability,
- Bearing capacity,
- Lateral extrusion (or squeeze-out).

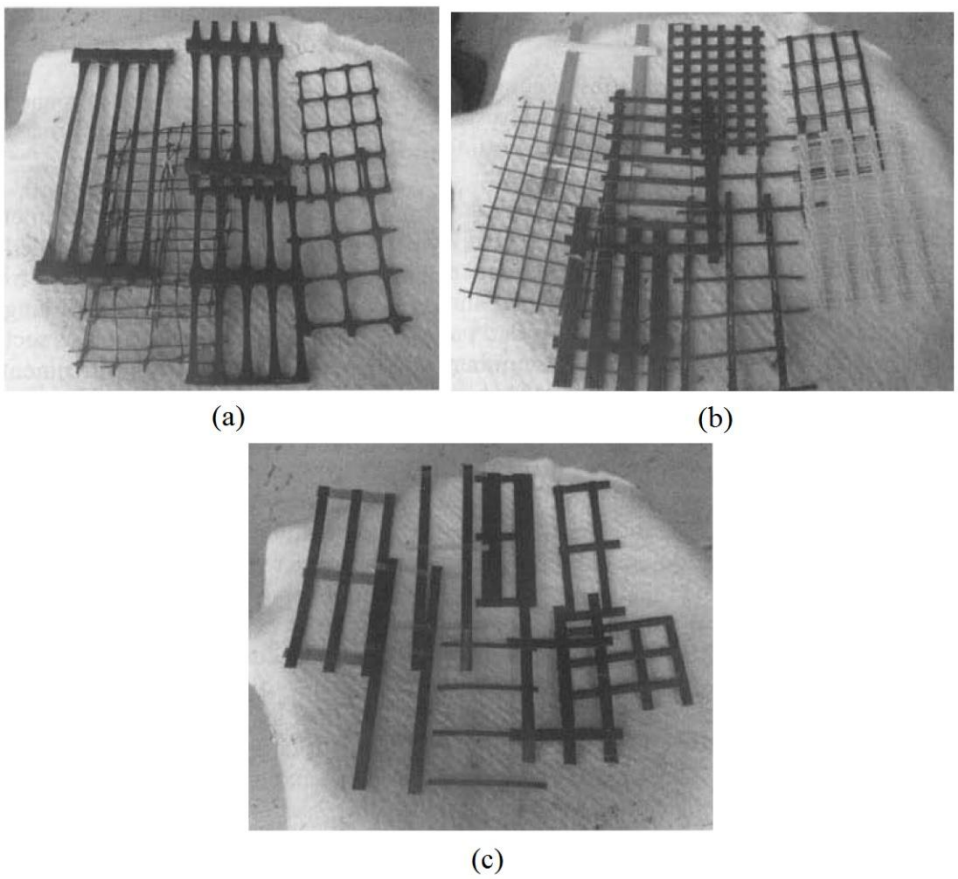

Figure 2.1. Some types of geogrids: (a) Unitized polyolefin geogrids, (b)Coated yarn geogrids, (c) Polymer rod (or strap) geogrids (Koerner, 2005).

Geogrids are nearly always serving the primary function of reinforcement, making their physical properties important; such as type of structure, rib dimensions, junction type, aperture size and thickness. Density and out-of-plane bending stiffness and in-plane torsional stiffness parameters are other substantial parameters. Mechanical properties of geogrids can be summarized as; single rib and junction (node) strength, wide-width tensile strength, shear strength, anchorage strength from wall connections and anchorage strength from soil pullout (Koerner, 2005). Since the utilization of geogrids are case specific, many forms of geogrids are still in development.

2.2. Geogrid Reinforcement

As mentioned in Section 2.1, the primary function of geogrid materials is reinforcement. This genuine characteristic transform geogrid material into a subject of multiple researches in the literature to explore the beneficial ways of geogrid usage.

Since the geogrid materials are completely produced and preferred depending on their purpose of use, there are huge numbers of geogrid utilizations in the field, in truly particular ways. Thereby, there are various studies accounting geogrid materials as their subject, mainly depending on their physical, chemical or practical characteristics. In addition, these studies also diverge depending on the experiments are numerical or experimental. Although there are hybrid studies that extent both experimental and numerical test setups, most commonly they differentiate based on that parameter, because of the reason that experimental and numerical outputs of the same conditions are generally have a degree of contrast with each other. Since the scope of this study extent an experimental study, numerical studies are going to be reviewed in the following sections.

2.2.1. Experimental Studies on Geogrid Reinforcement

Guido et al. (1986), introduced various configurations for geogrid reinforcement systems and completed a comparing study in between geotextiles and geogrids, during the period of geogrids were becoming a useful member to be utilized in many fields of construction site. The study on bearing capacity of geogrid and geotextile reinforced slabs were a set of experimental laboratory model tests. According to the analysis results, the bearing capacity of an unreinforced earth slab is able to increase essentially with the integration of either type of reinforcement.

Study genuinely notes that; to properly use geotextiles as reinforcement, friction forces must be developed between soil layers and reinforcement itself to prevent sliding; although for geogrids, it is the interlocking mechanism of the soil through the apertures of the grid that generates an efficient anchoring effect. Therefore, it is proposed to determine failure mechanisms of geotextiles by fixed shear box tests and geogrids by pull-out tests.

Primarily, the type of the reinforcement is generally site specific and depends on the purpose, however, for the same case, the grids displayed greater performance on behalf of bearing capacity ratio, as in Figure 2.2 and Figure 2.3.

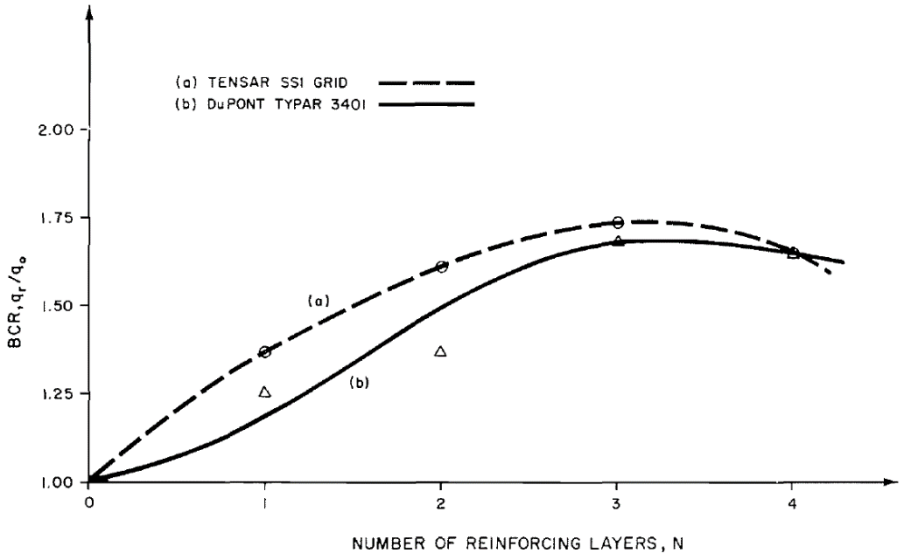

Figure 2.2. Bearing Capacity Ratio (BCR) variation with number of reinforcing layers (Guido *et al.*, 1986).

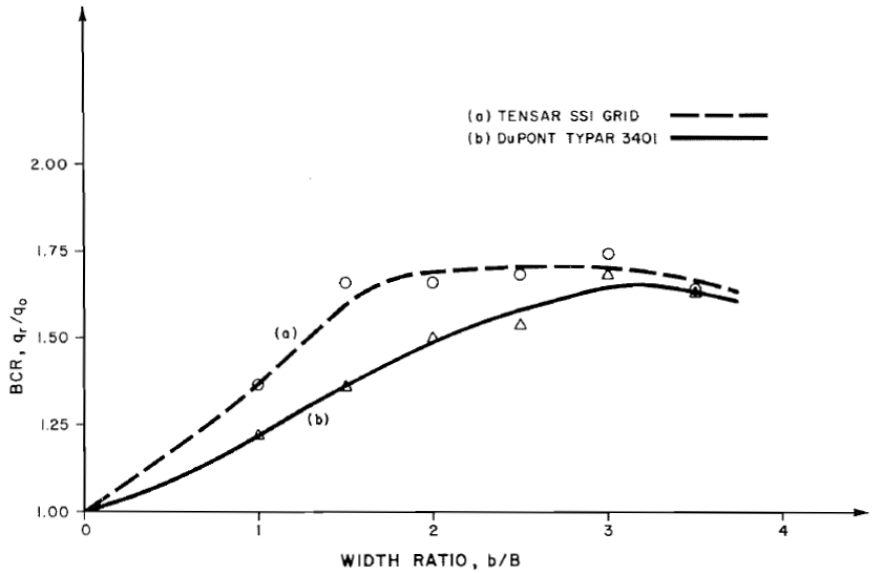

Figure 2.3. Bearing Capacity Ratio (BCR) variation with width ratio (Guido *et al.*, 1986).

Since geogrids are a specific element as a reinforcement material as noted in Section 2.1, while geotextiles have other multi-functional usage areas (i.e. separation, drainage, filtration). Geogrids are mentioned as a superior form of reinforcement owing to the interlocking of the soil surface with the grid membrane, compared to geotextiles.

Omar *et al.* (1993), addressed various studies of soil reinforcement, including geogrid soil reinforcements on bearing capacity of shallow foundations and conducted a similar study about ultimate bearing capacity of shallow foundations on sand reinforced with geogrid. Former laboratory model studies were all conducted with geosynthetic reinforcement with square foundations, however, their experimental model tests were carried out with also strip foundations supported by geogrid reinforced layers of sand. Example sketch of test setup is displayed in Figure 2.4.

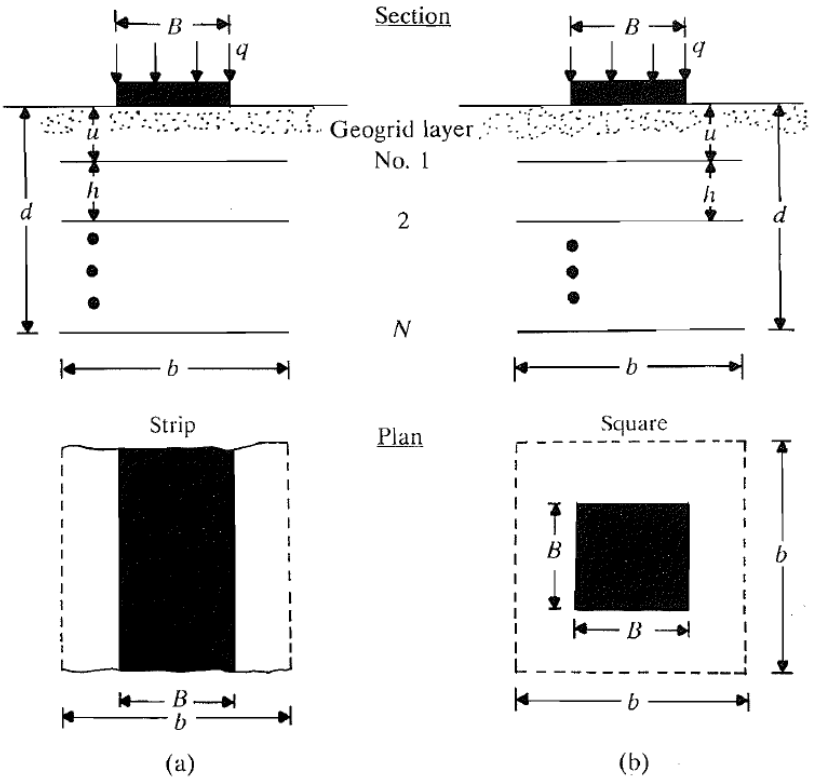

Figure 2.4. Square and strip foundations supported by sand reinforced with layers of geogrid, q, load per unit area (Omar *et al.*, 1993).

Two test series were conducted as reinforced and unreinforced cases and also variable number of geogrid layers are taken into account. It was displayed that, for a given foundation, the applied load (q) capacity increased with number of geogrid layers (N), along with an increase of the settlement at ultimate load, as in Figure 2.5. Thereby, the study displayed basic information on geogrid soil reinforcement geometry, including depth and width parameters for different foundation types.

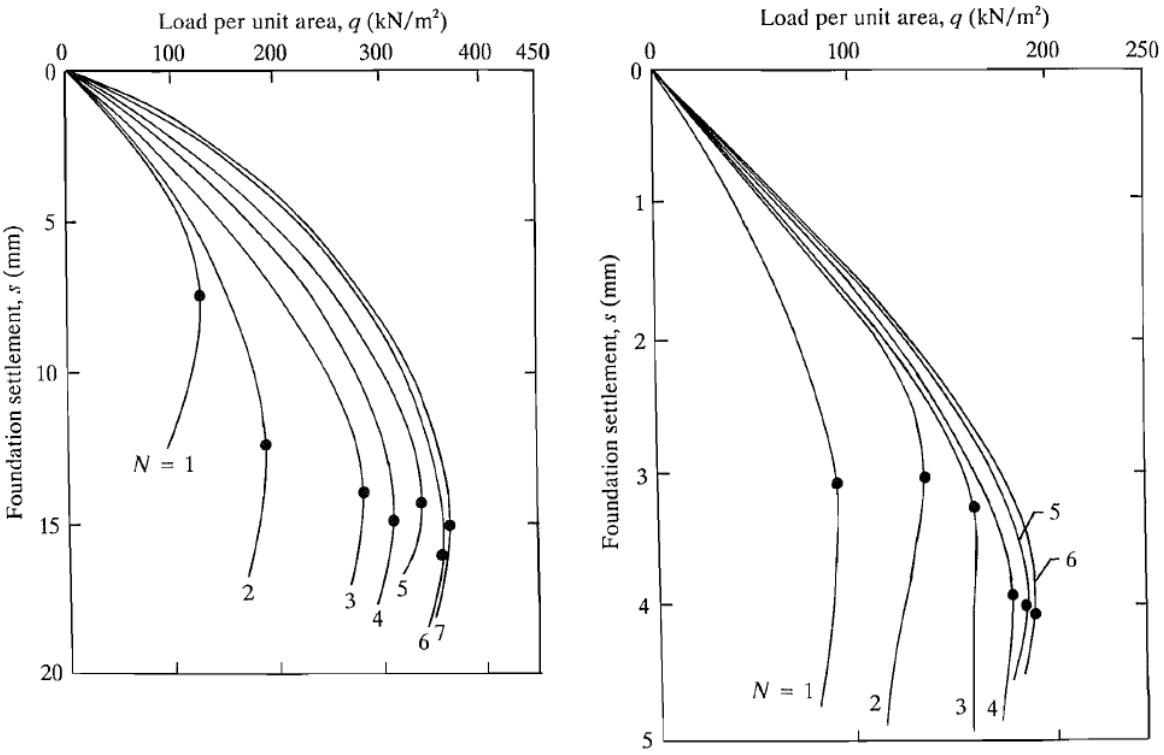

Figure 2.5. Applied load per unit area vs. settlement for strip foundations (left) and square foundations (right) (Omar *et al.*, 1993).

Additionally, following conclusions are drawn from the experimental tests conducted to investigate the study on bearing capacity on sand with geogrid reinforcement (Omar *et al.*, 1993):

- On the purpose of reaching maximum bearing capacity, effective depth shall be approximately $2B$ for strip foundations and $1{,}4B$ for square foundations (B: width of the foundation, Figure 2.4),
- For utilization of maximum bearing capacity, width of reinforcement layers shall be approximately $8B$ for strip foundations and $4{,}5B$ for square foundations,

- To utilize the first layer of geogrid properly, maximum depth of the first geogrid reinforcement layer shall be less than B.

Yetimoglu *et al.* (1994), conducted a hybrid study on bearing capacity of rectangular footings on geogrid reinforced sand. The study investigated the effects of depth to the first layer of reinforcement, vertical spacing of reinforcement layers, number of reinforcement layers, size of reinforcement sheet and stiffness of reinforcement on bearing capacity. Again, as in the previous studies, static vertical loads were applied. As the experimental study, they operated an analytical study by the finite element method and compared output data. Their test setup can be seen in Figure 2.6.

While measuring the ultimate bearing capacity, the study took into account the settlements which keep increasing without further increase in loads and abrupt changes in the load-settlement relationships. To compare applied load-foundation settlement behaviour of both unreinforced and reinforced sands, bearing capacity ratios (BCR) were treated, as defined in Binquet and Lee in 1975.

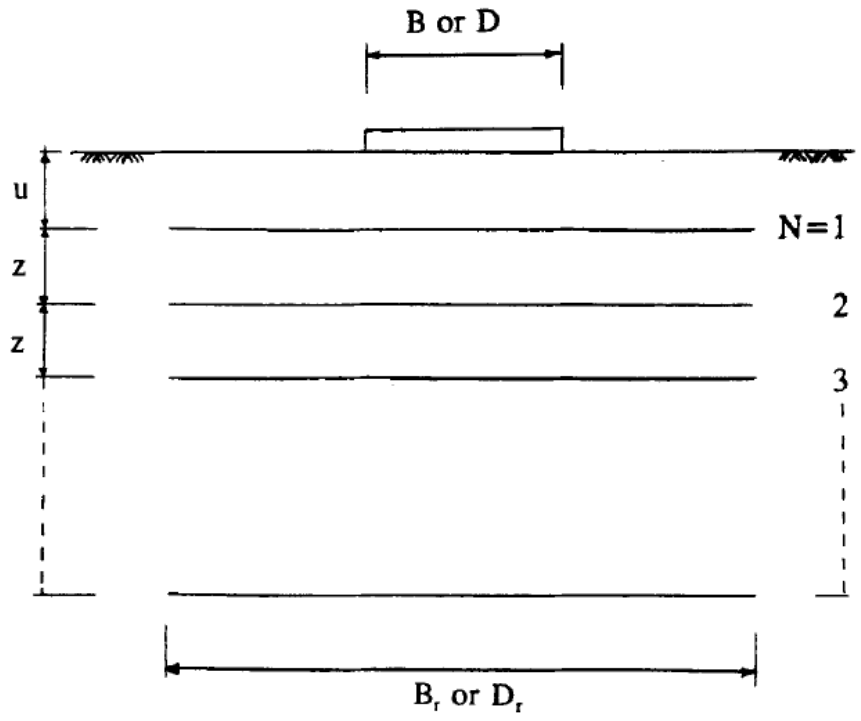

Figure 2.6. Geometric Parameters of Reinforced Foundation (Yetimoglu *et al.*, 1994).

As shown in Table 2.1, BCR of some significant cases were detected in a range of ~0 to ~3.9 for the experimental comparison results. In contrast, experimental test and numerical analysis results displayed incompatibility with each other for many of the test groups. For all investigated parameters (depth to the first layer of reinforcement, vertical spacing of reinforcement layers, number of reinforcement layers, size of reinforcement sheet and stiffness of reinforcement on bearing capacity), the results were different in various ranges. Briefly, only two examples are displayed (Figure 2.7 and Figure 2.8).

Table 2.1. Summary of test results for test groups of reinforced and unreinforced sand (Yetimoglu *et al.*, 1994).

	Group 1 $u/B = 0.30$ $z/B = 0.30$ $B_r/B = 4.5$			Group 2 $u/B = 0.45$ $z/B = 0.30$ $B_r/B = 4.5$			Group 3 $u/B = 0.30$ $z/B = 0.30$ $B_r/B = 6.0$		
N (1)	s/B^a (percent) (2)	q_{ult} (kPa) (3)	BCR^b (4)	s/B^a (percent) (5)	q_{ult} (kPa) (6)	BCR^b (7)	s/B^a (percent) (8)	q_{ult} (kPa) (9)	BCR^b (10)
0	2.7	316	-	2.7	316	-	2.7	316	-
1	3.4	586	1.85	3.1	558	1.77	3.8	579	1.83
2	4.8	790	2.50	3.1	718	2.27	3.4	795	2.52
3	4.8	1002	3.17	3.0	768	2.43	4.9	1081	3.42
4	3.9	1147	3.63	2.8	766	2.42	4.4	1225	3.88

^{a}Ratio of the settlement at failure to the width of footing.
^{b}Ratio of the ultimate bearing capacity of reinforced sand to the ultimate bearing capacity of unreinforced sand.

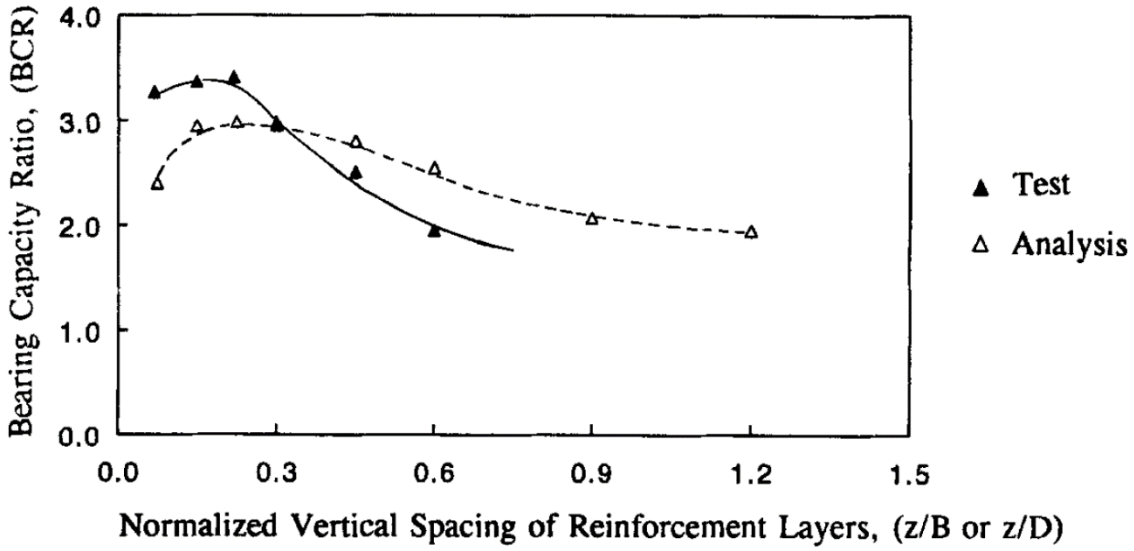

Figure 2.7. Typical variation of BCR with Vertical Spacing of Reinforcement Layers (Yetimoglu *et al.*, 1994).

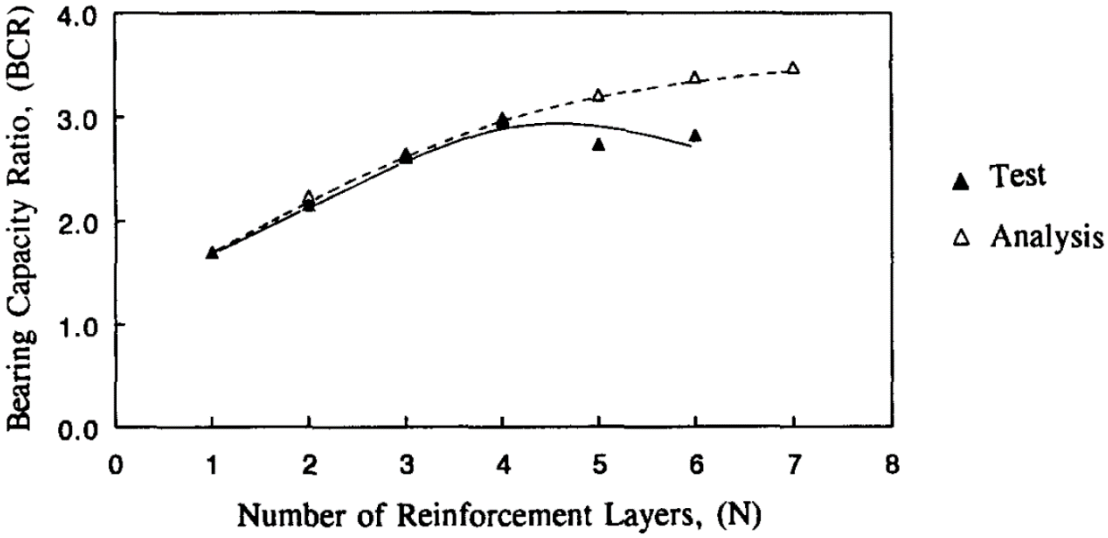

Figure 2.8. Typical variation of BCR with Number of Reinforcement Layers (Yetimoglu *et al.*, 1994).

Overall, study verified that, both from the test setup and finite-element analyses, bearing capacity of rectangular footings could be increased significantly by incorporating geogrid elements at different depths in the foundation soil. Model tests clearly indicated that the failure point at the settlement may not be affected substantially by the geogrid reinforcement, nonetheless; reinforcement configuration, vertical spacing of reinforcement

layers, size of reinforcement sheet and specifically number of reinforcement layers are able to have an apparent effect on the bearing capacity of foundation.

For the single layer reinforced cases, it is noted that there is an optimum embedment depth for the first reinforcement layer, where the bearing capacity is at its highest value. Experimental tests pointed out, that optimum depth is near $0.3B$. This value also verifies the findings of the study of Omar *et al.* (1993).

Alawaji (2001) was studied on the topic of settlement and bearing capacity of geogrid reinforced sand over collapsible soil material. The possible improvement fields of geogrid reinforced sands were researched over collapsible soil. The purpose was to control wetting induced collapse settlement. Model tests were applied within the study by using a circular shell element of 100 mm diameter with a case specific geogrid material (Figure 2.9).

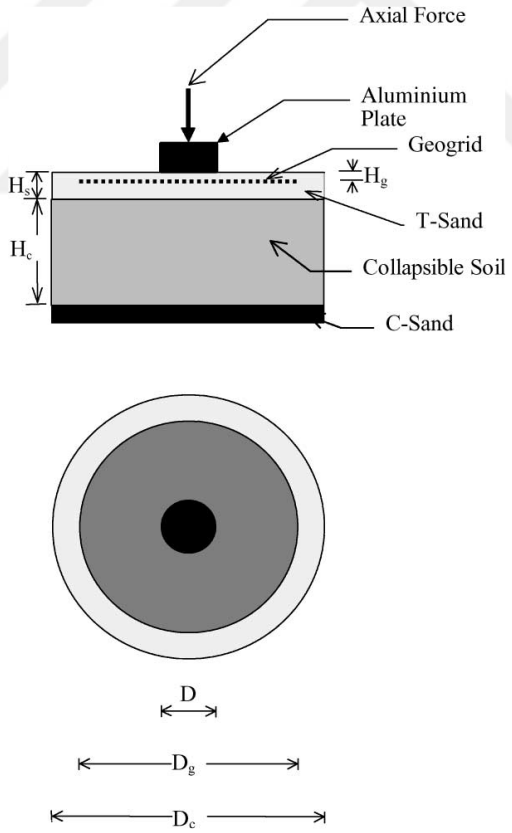

Figure 2.9. Model Plate supported by geogrid reinforced sand over collapsible soil (Alawaji, 2001).

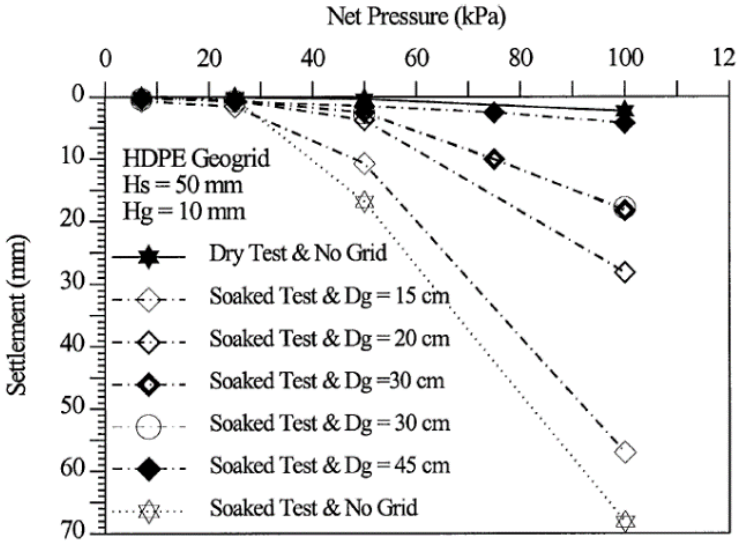

Figure 2.10. Pressure settlement curves for geogrid-reinforced sand over collapsible soils (Alawaji, 2001).

Variables of the study were width and depth of the geogrid layers during the tests to determine reinforcement effects on the deformation modulus, collapse settlement and bearing capacity ratios. Since wetting-induced collapse settlement is defined as a leading parameter to a low bearing capacity in arid and semi-arid regions in previous studies; geogrid reinforcement was used as a remarkable way of improvement practice in terms of such performance upgrades.

Outputs of the study mentioned that the impact of the geogrid reinforced sand system was improved with higher geogrid width and smaller geogrid depth (Figure 2.10). Depending on these parameters, the study introduced an economic form of sand-geogrid system.

Outcomes are mainly outlined in the analysis of the load settlement response of the reinforced and unreinforced sand as follows (Alawaji, 2001):

- Integration of the geogrid into the system, improves the load-carrying capacity and decreases wetting-induced collapse settlement,
- Geogrid reinforced sand over normal sand, depth of the sand below base level can be decreased,

- Effectiveness of geogrid layer improves with the decreased depth of geogrid layer,
- Wetting induced collapse settlement was considerably decreased below the circular loaded area, as a result of capping effects of geogrid reinforced sand.
- Geogrid reinforcement increases elastic modulus of the sand layer,
- Recommended width of the geogrid shall be greater or equal to 4 times of the diameter of the loaded area.
- Real practical conditions (like non-uniform wetting or various boundary conditions) may cause different full-scale performance experiences.

Wang *et al.* (2015), investigated retaining walls with geogrid reinforcement and saturated backfill sand, checked seismic response; by using an experimental test setup with laminar shear container mounted on shaking table.

Tests were conducted in a large scaled laminar shear container (Figure 2.11) and included both rigid retaining walls with geogrid reinforcement and soil retaining walls without reinforcement. A seismic dilatometer was used to measure wave velocities of the test models and seismic response of the models were examined. Additional parameters were also used to define seismic performance of these two models (i.e. strains of geogrids, lateral displacements of walls, wall accelerations after seismic impact, seismic induced settlements of backfill sand at surface levels, and pore water pressure differences of the backfill sand). As in many studies, scale factors were also used in this particular study. Laser displacement sensors were installed during the experiment to measure the variation of displacements (Figure 2.12).

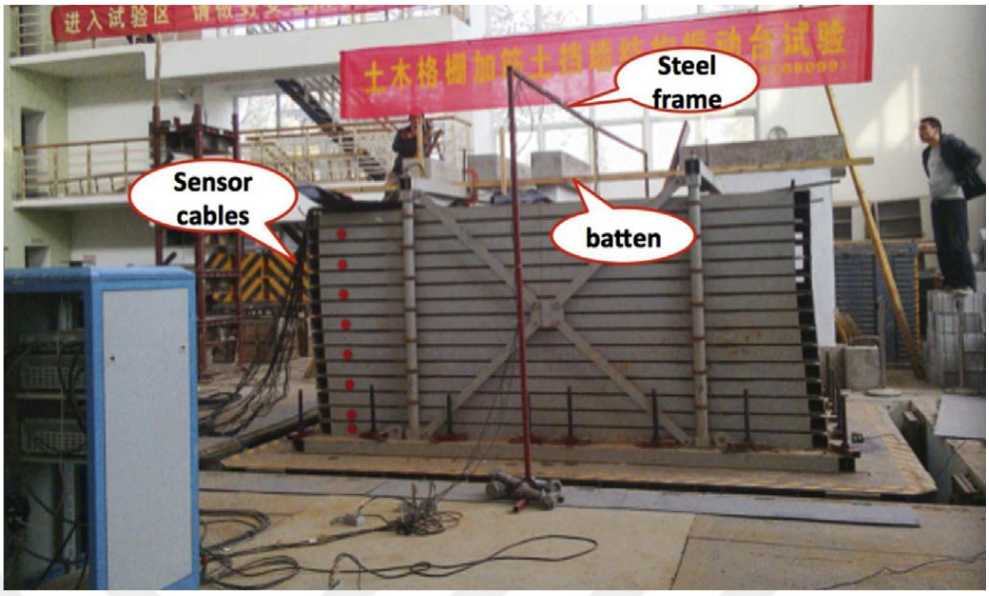

Figure 2.11. Laminar shear container mounted on shaking table (Wang *et al.*, 2015).

Considering the results of the experimental models; although the geogrid reinforcement affected to improve seismic behavior and seismic resistance deformation abilities for the reinforced case, it is found that long-time high acceleration values of the far field had larger effects on the seismic response, than those in the near field. Additionally, in the reinforced case, while improving the seismic stability of the wall, geogrid layers in the middle levels had greater influence than layers at the lower and higher levels.

Figure 2.12. Installation of laser displacement meters (Wang *et al.*, 2015).

In Figure 2.13, time histories of the lateral displacements are displayed for different ground motions. Unreinforced wall (URW) and reinforced wall (RW) cases are plotted under the strong ground motions, where SF-2 (Shifang earthquake in China, 2008, scaled PGA: 0.3g), TA-1(Taft earthquake in USA, middle-far-field seismic wave, scaled PGA: 0.3g) and SP-2(Songpan earthquake in China, 2008, scaled PGA: 0.3g). For the same seismic intensity, it can be seen that lateral displacements generated by SP and TA motions are larger than the SF ground motion. The study explained this by the specifications of the input seismic motions and noted that seismic responses were stronger for the far field and mid-far field cases. Therefore; it is displayed that for the same earthquake records, lateral displacement responses for the reinforced case are weaker than the unreinforced case. Thus, the presence of the geogrid reinforcement layers practically improved the lateral displacement performance caused by seismic movements and demonstrated a lateral deformation resistance capability.

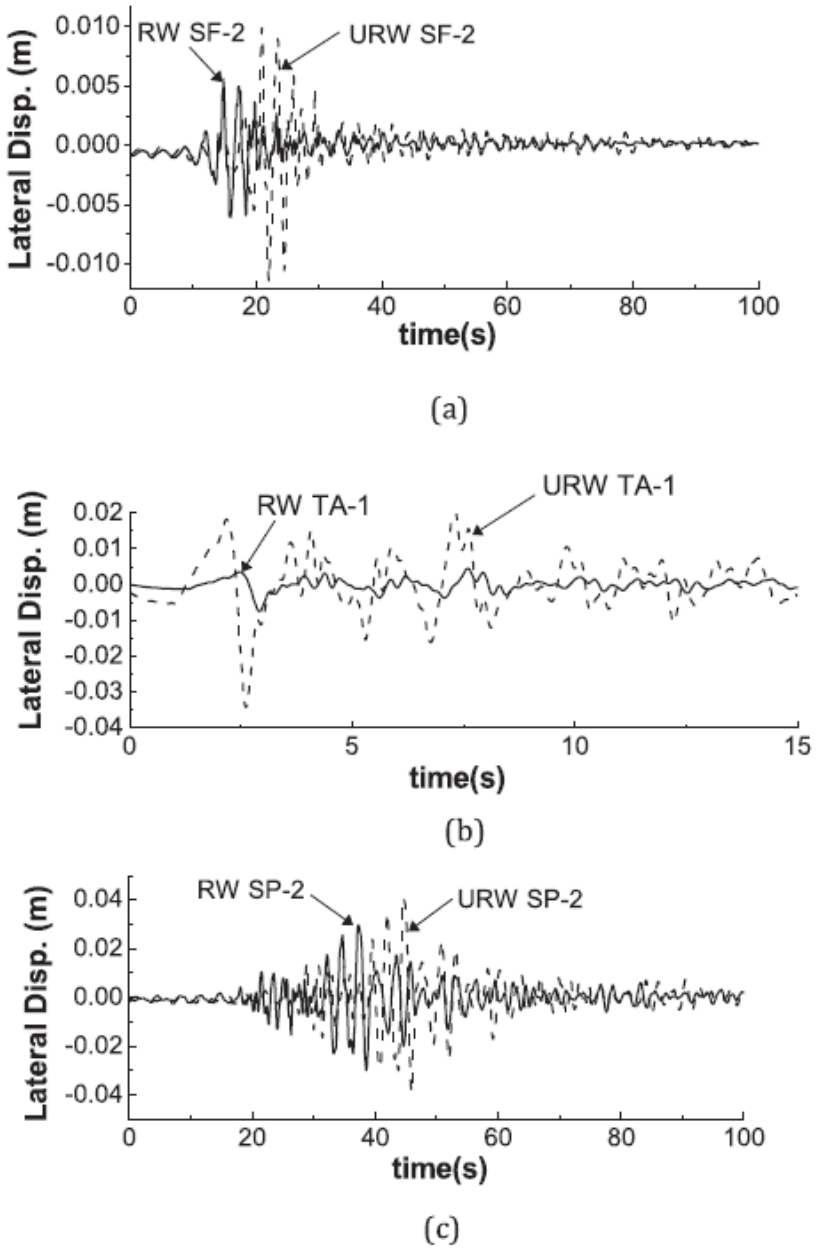

Figure 2.13. Time histories of lateral displacements of the two model wall tops: (a) SF-2, (b)TA-1, (c) SP-2 (Wang *et al.*, 2015).

From the results of large-scale shaking table tests on the seismic response of the geogrid reinforced rigid retaining walls, the following results are summarized (Wang *et al.*, 2015);

- Spectrum peak values of the Fourier spectra were adjusted backwards, while Fourier spectra of the walls presented similar symmetrical distribution, before tests. In all

earthquake cases, acceleration and spectrum responses of geogrid reinforced walls were less than unreinforced walls.

- Middle-layer geogrids had the largest strains among other geogrid layers and had the greatest effect while providing seismic stability to reinforced wall (Figure 2.14)

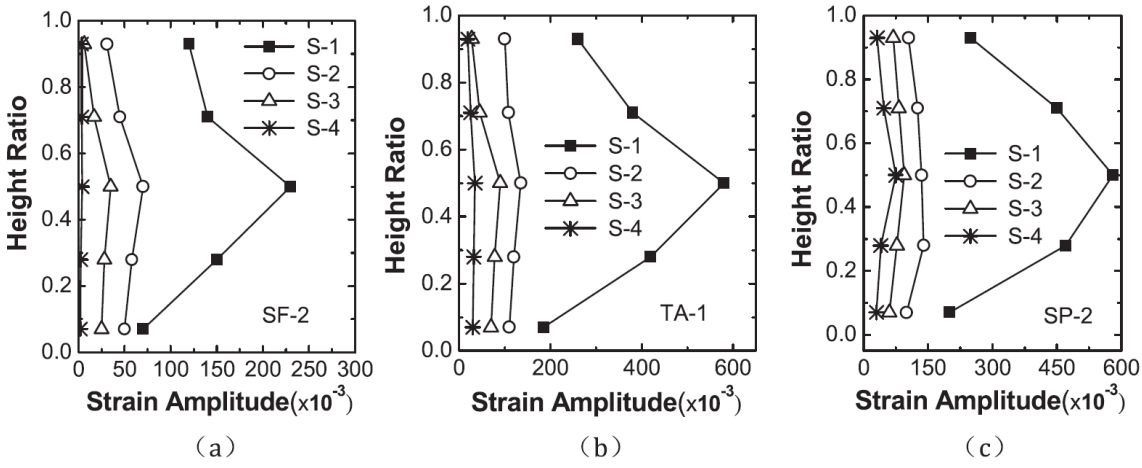

Figure 2.14. Strain amplitude distributions of geogrid layers along wall heights: (a) SF-2, (b) TA-1, (c) SP-2 (Wang *et al.*, 2015).

- Geogrid reinforcement layers effectively decreased seismic deformations in the reinforced wall and provided a resistance in terms of lateral deformation capability in all cases. Therefore, geogrid reinforced wall models were performing better than unreinforced wall models in terms of lateral displacements.
- Specific seismic response parameters within this study verified the effect of additional seismic resistance ability provided by the geogrid reinforcement.
- Settlements of the backfill surface level are directly dependent on the presence of the reinforcement in the soil material. Surface settlement of the reinforced cases were much smaller than unreinforced cases. Thus, the reinforcements provided settlement resistance ability for seismic conditions.

2.2.2. Numerical Studies on Geogrid Reinforced Foundations

In the literature, test models of geogrid reinforcement under static loads and the effects of the parameters on bearing capacity or settlement were studied. Nevertheless, various application fields of geogrid reinforcement require extensive researches under

dynamic loads, such as the cases in railway roads or super structure cases. However, conducting the large scaled experimental model test is not possible for most of the cases. Thereby, few of the mentioned scenarios are researched with the help of computer aided numerical models.

Yildiz *et al.* (2006) studied on numerical analysis of circular foundations supported by geogrid reinforced sand. As the first experimental researches, the study was conducted in terms of bearing capacity parameter. Study concluded that the reinforced soil material improved the bearing capacity ratio and various parameters for the geogrid configuration was introduced in terms of improving bearing capacity.

Alamshahi and Hataf (2009) studied on bearing capacity of strip footings on sand slopes reinforced with geogrid and grid-anchor materials. Again, various geometric parameters and configuration variations for geogrids were introduced to improve ultimate bearing capacity and settlement characteristics of such footings.

Edincliler *et al.* (2017) conducted a parametric study on the seismic performance of low and mid-rise buildings on geogrid reinforced sand by numerical models. A comparative set of numerical studies were performed on low-rise and mid-rise models, under different ground motions and structural performances were evaluated. Foundation soil was reinforced with 12 geogrid layers by using finite element modelling software. Total displacements, transmitted accelerations, earthquake induced axial and shear forces and bending moment parameters were researched under different earthquake scenarios, for each model. Study showed that utilization of geogrid layers in soil reinforcement may provide additional stability for the foundation soil. Although the results were showing dissimilarities on behalf of structure height, the common behaviors of structural responses displayed that the reinforced cases reduced strong ground motion effects for the mentioned parameters.

In addition, the study particularly concludes that in comparison of the output data in terms of height of the structures, soil-geogrid reinforcement is noted as more effective for the low-rise structures, since the acquired earthquake response reduction ratios are comparatively higher for the low-rise model.

Edincliler and Toksoy (2019), conducted a numerical study on the effects of geogrid reinforcements on behalf of mitigating earthquake risks of medium-rise buildings under different strong ground motions. Study notes that soils with a low bearing capacity may have the undesired consequences such as excessive settlement, structural damage, deterioration in durability or performance level. Therefore, the comparative results were obtained via numerical simulations of medium rise buildings on unreinforced and reinforced sand material, to be able to generate a comparison. Basically, effects of various strong ground motion features and length of geogrid reinforcement material parameters are researched and introduced. A mid-rise (5-story) building was modelled and foundation was reinforced with 4 layers of geogrid material. In this extent, Kocaeli earthquake (1999, Yarimca Station, Mw: 7.6, PGA of 0.32g) and Gokceada earthquake (2014, Meteoroloji Station, Mw: 6.5, PGA of 0.18g) motions were chosen as dynamic excitations.

Comparing the dynamic responses upon the performance in terms of total displacement and transmitted acceleration parameters, unreinforced and reinforced models showed a significant difference through the applied reinforcement material.

Numerical analysis showed that the geogrid-reinforced sand foundations displayed a superior performance with decreasing the total displacement values under stronger earthquakes (Kocaeli earthquake) as well as, they were superior with decreasing transferred acceleration values (energy dissipation) under weaker earthquakes (Gokceada earthquake). It is stated that the inclusion of the geogrid material as a reinforcement in the foundation soil is decreasing transmitted acceleration values, thereby, dissipating the seismic energy.

2.3. Experimental Techniques

In experimental applications of earthquake engineering, there are various techniques to define characteristics of tested materials and behavioral aspects of the system; such as soil element tests, reduced-scale model tests and full-scale field tests. In most of the cases, experimental test setups are vital to generate soil-structure interaction and to provide realistic results in both static and dynamic response behaviors.

As a geotechnical way of approach, to provide mentioned realistic behaviour, 1-g (shaking table) and N-g (geotechnical centrifuge at N times gravity of the earth) tests are two different practices. These model tests are able to display boundary effects of the models as well as failure mechanisms and analytical/experimental result verification. Additionally, physical test setups against strong ground motion cases, brings along the fundamental observation experience as well as output data, as potential failures and response behaviour (Jafarzadeh, 2004; Bhattacharya *et al.*, 2012).

Bhattacharya *et al.* (2012) defined some basic phases of designing 1-g or multi-g (centrifuge) testing environment, as follows;

- Deduction of non-dimensional parameters by understanding the governing mechanisms of the simulated behaviour, both at model and prototype scale, thereby, thinking the components of the experimental setup as a whole,
- Provide conserved and proper scaling coefficients for the prototype, to generate similar behaviour with the real model,
- Identifying these scaling coefficients in case if they are relatively satisfied, violated or require special consideration.

2.3.1. Centrifuge (N-G or Multi-G) Tests

Geotechnical centrifuge tests allow researchers to create similar stress – strain levels while testing a 1:N scaled model at N times gravity of earth, by centrifugal forces (Figure 2.15). In these tests, linear dimensions are considered by a 1/N coefficient and the stress is defined by a factor of unity. Hence, advantage of the centrifuge test setup is, it generates reproduction of the similar stress and strain level within the scope of scaled model (Bhattacharya *et al.*, 2012).

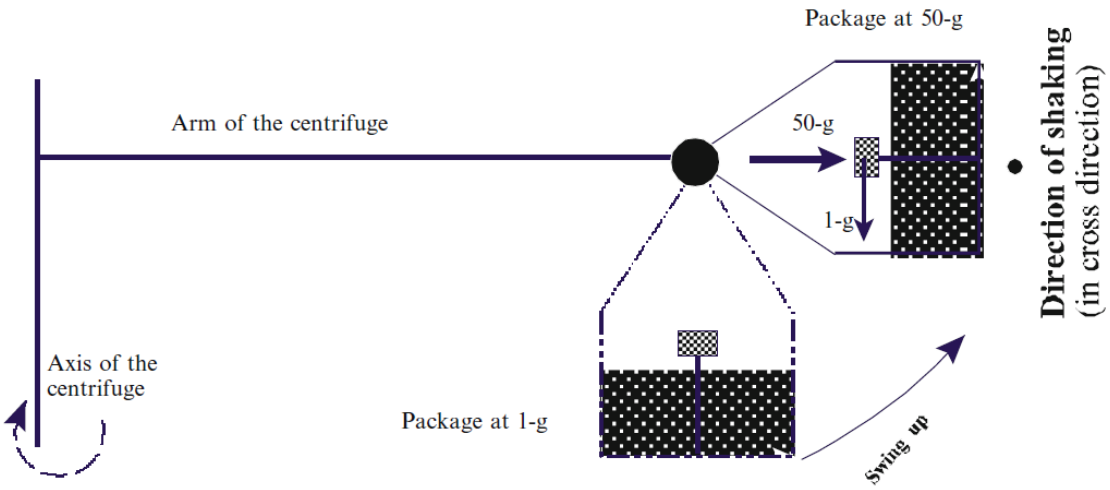

Figure 2.15. Schematic diagram showing the working principle of a geotechnical centrifuge (Bhattacharya *et al.*, 2012).

Centrifuge testing method provides output data over dynamic strong ground motion models. It is one of the very early methods of gravity testing, however, for some specific experimental conditions there are debates about the centrifugal test results in terms of creating insufficient evidences of relation between prototype data and centrifugal data, even though the cost of the creating test model is proportionally a small part of the total research cost. In advance, main problems experienced in centrifuge tests are questionable, since there are parameters that are unable to be measured because of the testing method. For similar validation reasons, large scaled model tests are needed to generate precise results (Schofield, 1981; Hushmand *et al.*, 1988; Turan *et al.*, 2009; Ecemis and Kahraman, 2012; Bhattacharya *et al.*, 2012).

2.3.2. Shaking Table (1-G Gravity) Tests

It was mentioned that model tests are a basic element to provide behavior of the prototype, among complex parameters and it is also hard to conclude with an engineering judgement on the topic. Since the aim of the model test is to simulate boundary conditions of a prototype problem in a small-scale model, model tests can be utilized to understand the response in terms of different parameters and failure points. To investigate such parameters of the structures, shaking table tests are generally used under one times gravity of earth (Figure 2.16).

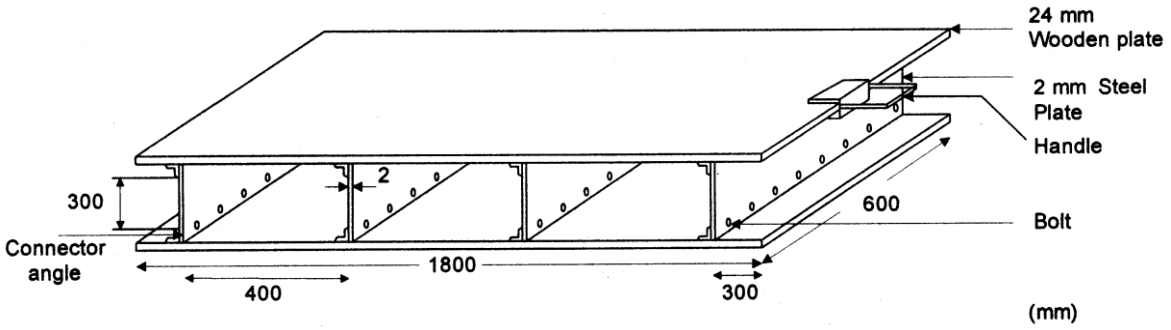

Figure 2.16. A manual shaking table scheme (Prasad *et al.*, 2004).

By the help of shaking tables, large amplitude and multi axis input motions can be analyzed and fundamental assessments can be made from the observations of experimental mechanisms of the failure point. Additionally, for precisely created test environments, parameters like post-earthquake settlements, foundation responses and liquefaction conditions are possible to obtain. Shaking table also provides the environment to compact the soil material and space for instrumentation that generally does not affect overall behavior of the setup in a large scale. Since 1-g gravitational field tests are purpose of the shake table preference, higher gravitational impact is not created in such setups. The main advantage of the shaking table is the reproduction of the strong ground motion via actuators and it is possible to create many different testing environments by various containers and instruments while measuring multiple parameters (Prasad *et al.*, 2004).

2.3.3. Soil Containers

Various types of soil containers are currently in use depending on their purpose and what advantages or disadvantages are needed to be taken by the researcher. Rigid containers, rigid containers with flexible boundaries, rigid containers with hinged end-walls, equivalent shear beam (ESB) containers, laminar containers and active boundary containers are basic types of soil containers in geotechnical earthquake experiments (Bhattacharya *et al.*, 2012). Containers will be reviewed as rigid soil containers and flexible containers, within the extent of this study.

2.3.3.1. Rigid Soil Containers. Literature contains studies with both rigid sided and flexible sided soil containers. Rigid sided containers have higher end wall shear stiffness

than the flexible sided soil containers, regarding to their structure and purpose of usage. In Table 2.2, some of the rigid sided containers are displayed from former studies. Since rigid sided containers have a higher end shear stiffness from the soil or sand at the boundaries of their walls, they may influence the soil behaviour in the container, especially at higher heights. Rigid sided soil container examples can be seen in Figure 2.17 and schematic diagram in Figure 2.18.

Table 2.2. Examples of Rigid Containers that are used for shaking table and centrifuge experiments in the literature (Bhattacharya *et al.*, 2012).

Shape	**Shaking direction**	***L* - *B* - *H* (mm)**	***L/H***	**Side - walls**	**Base & end - walls**	**Reference**
Rectangular	1 - D	597-270-150	4.0	Teflon	Rough sand paper	Adalier and Elgamal (2002)
Rectangular	1 - D	500-565-190	2.6	No-details	No-details	Whitman and Lambe (1986)
Rectangular	2 - D	712-432-440	1.6	Smooth plastic membrane	Base covered by sand-glue mixture	Ng *et al.* (2004)
Rectangular	1 - D	1,500-400-1,000	1.5	Perspex and wood plates	Terram geotextile membrane	Norton (2008)
Rectangular	1 - D	450-240-400	1.1	Perspex	PTFE (poly-tetra-fluoro-ethylene) sheets	Dash (2010)

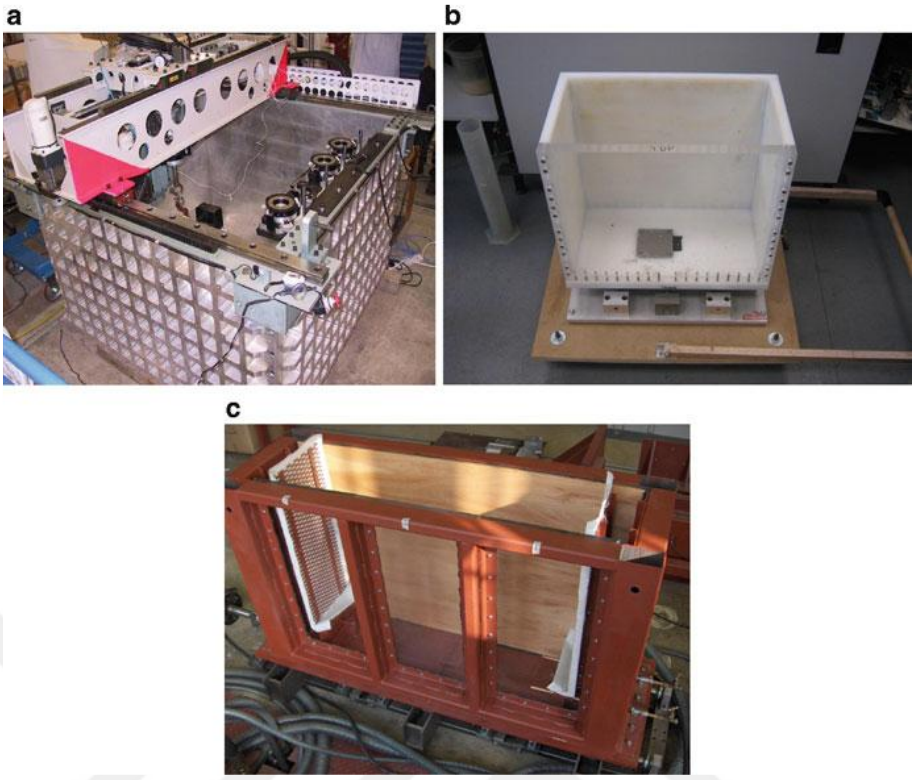

Figure 2.17. Examples of rigid container: (a) Rigid container used in centrifuge at the Hong Kong University of Science and Technology (HKUST) (Courtesy of Prof Charles W.W. Ng). (b) Rigid box used in the small shaking table at the University of Bristol. (c) Rigid box used in the shaking table at the University of Oxford (Bhattacharya *et al.*, 2012).

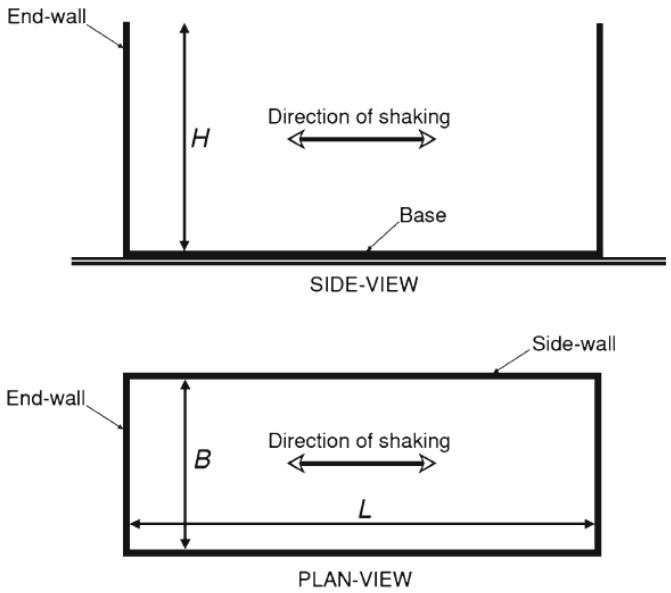

Figure 2.18. Schematic diagram of a rigid container (Bhattacharya *et al.*, 2012).

Rigid soil containers simply divide into two groups; rigid soil container with hinged end-walls and rigid soil containers with flexible boundaries.

Rigid containers with flexible boundaries, contains essential soft end-wall materials such as sponge to provide adaptive conditions within the container (Figure 2.19). As mentioned, rigid boundaries limit the reflection of waves, which is, one of the limitations of the rigid containers. Preventing such behaviour has the following advantages (Bhattacharya *et al.*, 2012);

- Partial reduction in terms of wave reflection,
- Reduction of lateral stiffness for the end wall.

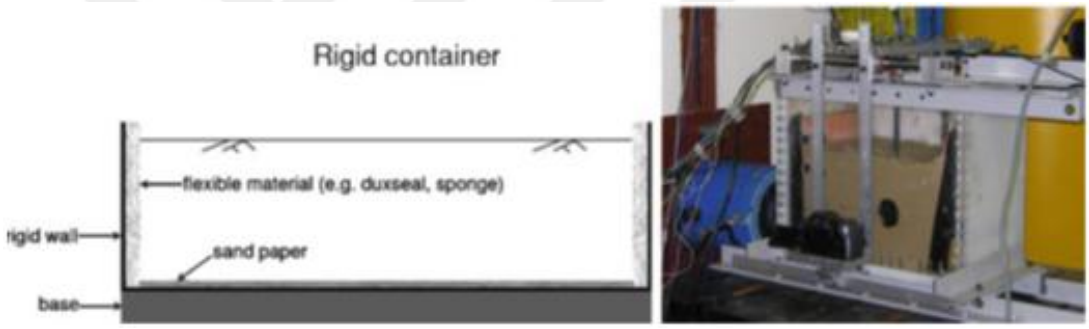

Figure 2.19. Schematic diagram (left) and rigid container with flexible boundaries in the Bristol Laboratory (right) (Bhattacharya *et al.*, 2012).

There are mainly two limitations of the rigid containers with flexible boundaries; the end-wall materials which create the actual boundary conditions by sponge or duxseal alike materials are unknown and these materials only reduce wave reflection from the artificial boundaries, thus, wave reflection from end-wall is not dissipated (Bhattacharya *et al.*, 2012). Even so, there are some examples of the rigid soil containers with flexible boundaries in the literature as displayed in Table 2.3.

Table 2.3. Some Rigid Soil Container with flexible end- in the literature reviews (Bhattacharya *et al.*, 2012).

Shape	Shaking direction	*L - B - H* (mm)	*L/H*	Side - walls	Base & end - walls	Testing	Reference
Rectangular	1 - D	4,270-910-1,220	3.5	Tempered plate-glass	Hinged to the box	Shaking table	Fishman *et al.* (1995)
Rectangular	1 - D	450-240-400	1.1	Perspex	Sponge (30 and 60 mm thick at top and bottom respectively)	Shaking table	Dash (2010)
Rectangular	1 - D	1,920-440-600	3.2	Acrylic plate	Sponge (50 mm thick)	Shaking table	Ha et al. (2011)

Rigid soil containers with hinged end-walls, contains hinges at the end-wall base to be able to create rotation, thereby reducing rigid wave reflection effects. To provide nonequivalent movement of the opposing walls, they are tied by a tie rod. Nonetheless, from the schematic demonstration in Figure 2.20, it can be seen that hinges bring some degree of flexibility to the system.

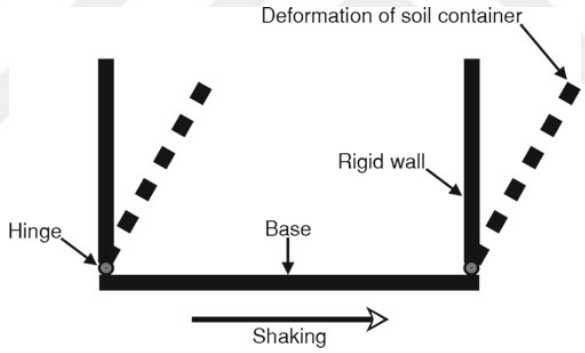

Figure 2.20. Schematic diagram of rigid container with hinged end-walls (Bhattacharya *et al.*, 2012).

2.3.3.2. Flexible Soil Containers. In real conditions, soil strata within the ground or underneath a structure is considered with infinite lateral extend while test conditions have finite boundaries. Thus, the reproduction of similar conditions for the testing environment have crucial importance. As displayed in Figure 2.21, assumption of theoretical soil deformation pattern along the soil layers, changes regarding the variation of shear modulus with depth.

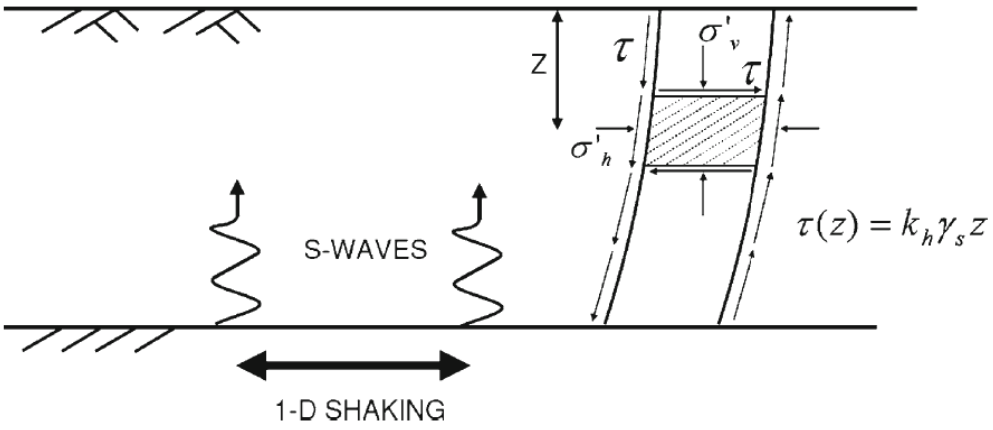

Figure 2.21. Soil layer of infinite lateral extent and finite depth subjected to a base shaking (Lombardi and Bhattacharya, 2012).

Since the displacement is constant at a particular horizontal plane and the amplitude varies with depth, the artificial soil column can be idealized as shear beam. Thus, working principle of the container is similar to "Euler-Bernoulli beam" as displayed in Figure 2.22. According to this approach, it is intended that system behaves as it has an infinite lateral extend. Thereby, soil container shall not absorb the energy generated by the strong ground motions, due to the fact that soil container has dimension restrictions, unlike real conditions. In addition, it is possible to face with inaccurate dynamic response caused by irregularities in P-wave propagation, if the boundary conditions of the container do not fulfill the mentioned behaviour (Lombardi and Bhattacharya, 2012; Bhattacharya *et al*., 2012).

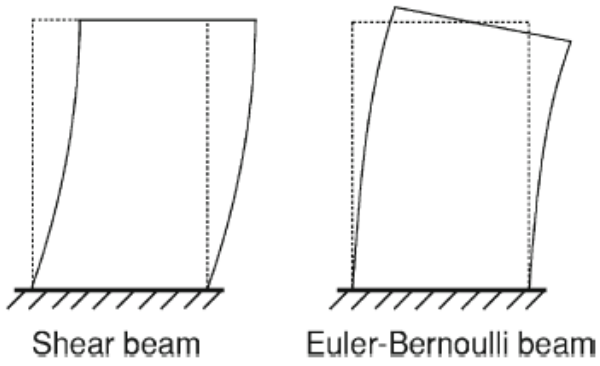

Figure 2.22. Shear beam and Euler-Bernoulli beam behaviour (Bhattacharya *et al*., 2012).

Flexible soil containers are basically divided into three groups; equivalent shear beam containers, active boundaries container and laminar boxes (flexible containers), which will be explained, respectively.

The working mechanism of the flexible sided soil containers is to divide walls into smoothly moving parts as much as possible, thereby, creating an environment for the soil to deform without the influence of exterior effects. Types of the flexible sided soil containers are generally equivalent shear beam (ESB) boxes and laminar boxes.

Since the ESB boxes composed of consecutive rubber and metal layers, their end wall stiffness is directly correlated to the rubber material used in each beam level (Figure 2.23). Example studies of ESB containers are briefly represented in Table 2.4.

According to Schofield and Zeng (1996) and Bhattacharya *et al*. (2012); the boundary conditions of an ESB container shall meet the following conditions;

- Boundary of the soil and wall-ends must have the same dynamic stiffness values to minimize energy reflection,
- Boundary of the soil and wall-ends must have the same friction to sustain complementary shear stress,
- The sidewalls should be friction free to present plane strain conditions.

Table 2.4. Examples of Equivalent Shear Beam (ESB) containers in the literature review (Bhattacharya *et al*., 2012).

Shape	Shaking direction	*L* - *B* - *H* (mm)	*L/H*	1-g/N-g	Reference
Rectangular	1 - D	2,000-750-1,750	1.1	1-g	Carvalho *et al*. (2010)
Rectangular	1 - D	1,200-550-800	1.5	1-g	Dar (1993)
Rectangular	1 - D	4,270-910-1,220	3.5	1-g	Fishman *et al.* (1995)
Rectangular	1 - D	4,800-1,000-1,200	4	1-g	Crewe *et al.* (1995)
Rectangular	1 - D	560-250-226	2.5	N-g	Zeng and Schofield (1996)
Rectangular	1 - D	800-350-600	1.3	N-g	Madabhushi *et al.* (1998)

Figure 2.23. Examples of equivalent shear beam container: ESB used in centrifuge testing, University of Cambridge – left; Shear stack used in 1-g testing, University of Bristol – right (Bhattacharya *et al.*, 2012).

As mentioned, the concept of the ESB boxes depends on the synchronization of natural frequencies of both beams and soil in each level (Sekman, 2016). The stiffness of the soil material, on the contrary, can be variable for each beam level; making practical use of ESB boxes limited and target specific (Figure 2.24).

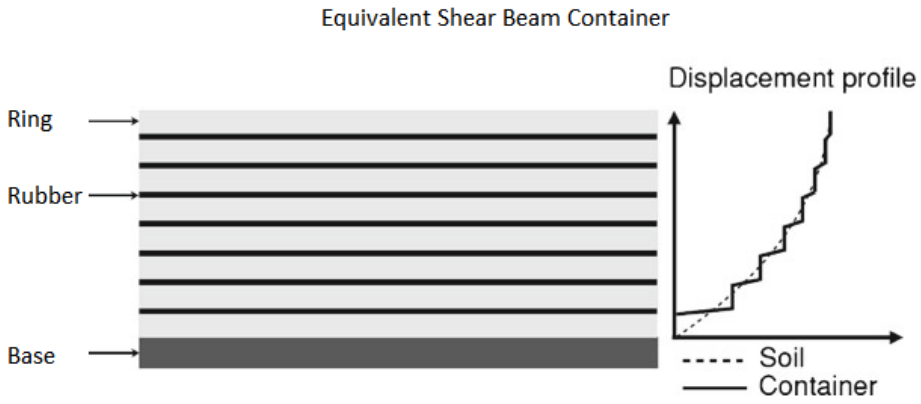

Figure 2.24. Schematic diagram showing the Equivalent Shear Beam container (Bhattacharya *et al.*, 2012).

Design principle of an active boundaries container depends on existence of external actuators, which are connected to container at each lamina level (Figure 2.25). In this point of view, they are similar to laminar boxes. In order to generate desired test model condition, different pressure levels are applied to the container via these actuators. They

are generally used in conditions, where the type of soil changes sharply during the shaking (i.e. liquefaction applications).

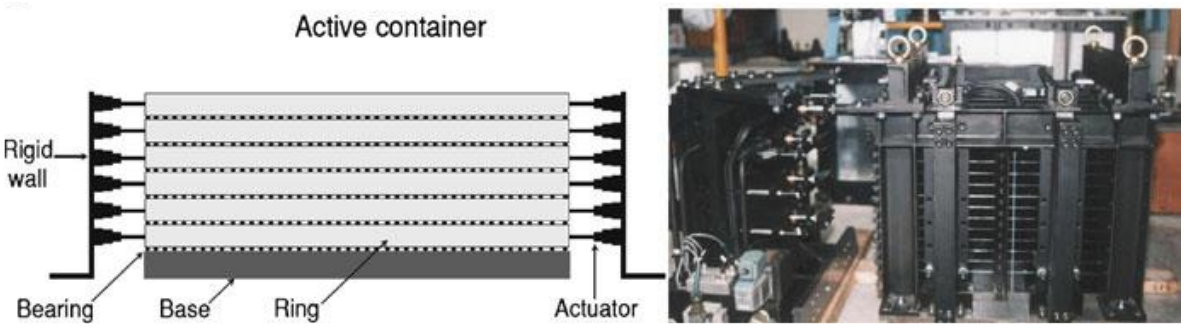

Figure 2.25. Schematic diagram of the container - left, example of active boundaries container - right (Courtesy of Professor Akihiro Takahashi), (Bhattacharya *et al.*, 2012).

To produce the mentioned behaviour in Section 2.3.3.2; a laminar box can be utilized. Laminar shear box allows each successive layer to move on top of previous one. Friction forces are minimized by roller bearings of the system. Thus, each layer can move according to soil material inside the container (Jafarzadeh, 2004; Prasad *et al.*, 2004).

The most common design of laminar boxes consists of a stack of laminates which are independently supported via bearings and steel guides, connected to external frame. The principle of the mechanism is to minimize the lateral stiffness of the container, in order to generate an environment that the soil governs in the response of the setup configuration.

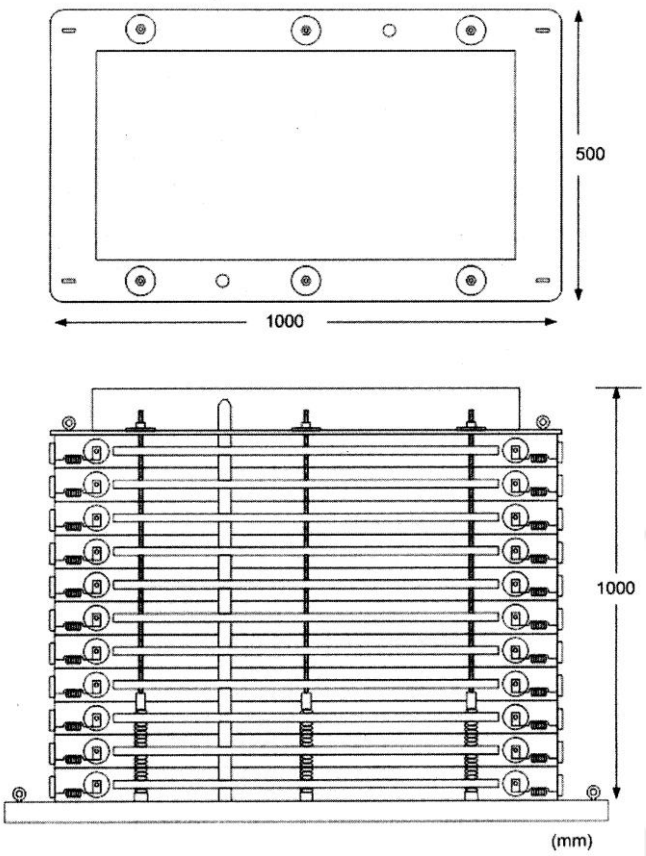

Figure 2.26. Details of a Laminar Shear Box (Prasad *et al.*, 2004).

The study of Cheung *et al.* (2013) noted that if a large-scale homogeneous soil sample is used in a laminar shear container, test provides better results in terms of representation of the effective confining stresses and boundary conditions in free field soil. Additionally, the study defines laminar soil box as "flexible soil container that can be excited using base excitations to replicate earthquake actions on the soil specimen" (Figure 2.27). The key ability in a laminar box is ability to allow constant shear deformation during presenting adequate confinement. Thus, it provides more realistic representation of the free field boundary conditions, which represented in Section 2.3.3.2.

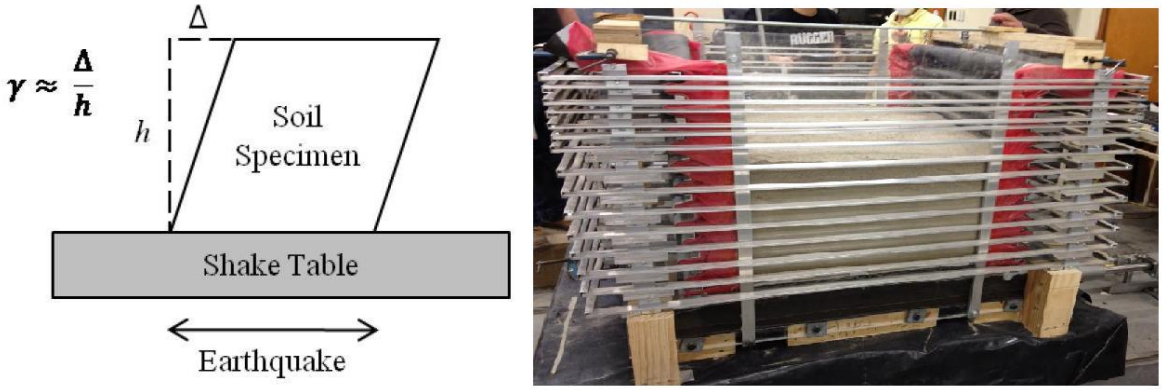

Figure 2.27. Laminar box on a shake table – right; Shear deformation of soil in a laminar box subjected to earthquake motion, where γ is the shear strain - left (Cheung *et al.*, 2013).

Table 2.5, lists different types of laminar containers presented in the previous literature reviews. Although laminar boxes can be circular, rectangular or square; common shape choice of the laminar box is rectangular. In Figure 2.28, two different types of laminar boxes can be seen (Prasad *et al.*, 2004; Bhattacharya *et al.*, 2012).

Figure 2.28. Laminar container examples: Large laminar container used in 1-g testing in Tsukuba, Japan (left); Laminar container used in centrifuge, University of Cambridge (right) (Bhattacharya *et al.*, 2012).

The main purpose in the design of the laminar container studies are summarized as follows (Cheung *et al.*, 2013);

- To create a shear box that properly grant soil the capability of shear deformation for the whole soil sample,
- To shake soil sample via a shake table and acquire the responses created by the soil at various depths,
- To set a comparison between the experimental test responses of the soil with a laminar box and equivalent numerical model responses.

Table 2.5. Examples of laminar containers in the literature (Bhattacharya *et al.*, 2012).

Shape	Shaking direction	*L - B - H* (mm)	*L/H*	1-g/N-g	Design	Reference
Rectangular	1 - D	900-350-470	1.9	1-g	Stack of laminae separated by bearing	Gibson (1997)
Rectangular	1 - D	1,000-500-1,000	1	1-g	Stack of laminae separated by bearing	Prasad *et al.* (2004)
Circular	2 - D	2,280-2,130 (D-H)	1.1	1-g	Container hanging on the top lamina supported by frame	Meymand (1998)
Rectangular	2 - D	1,888-1,888-1,520	1.2	1-g	Laminae supported by a frame and move independently	Ueng and Chen (2010)
Rectangular	1 - D	457-254-254	1.8	N-g	Stack of laminae separated by bearing	Van Laak *et al.* (1994)
Rectangular	1 - D	710-355-355	2	N-g	Stack of laminae separated by bearing	Pamuk *et al.* (2007)
12-sided polygon	2 - D	584-500 (D-H)	1.2	N-g	Stack of laminae separated by bearing	Shen *et al.* (1998)
Rectangular	1 - D	900-450-807	1.1	1-g	Laminae are supported individually by bearings and steel guide connected to an external frame	Turan *et al.* (2009)
Square	2 - D	1,000-1,000-1,000	1	1-g	Laminae are supported individually by bearings	Jafarzadeh (2004)

In the study of Chunxia *et al.* (2008), the main advantage of a laminar box described as; true propagation of response waves over the range of test conditions, while basically including the shear failure of the soil material. Some of the requirements in the study for the laminar container are described as follows;

- The self-weight of the laminar should be light as possible and size of the box is large enough to conduct large scale tests,
- Each rigid frame of the should has sufficient stiffness, thereby, distortion of frames can be ignored,
- Since unidirectional deformation is the purpose of experimental tests that extent laminar shear box, lateral deformations of the shear box should be restricted,

- The entire box should have enough durability to avoid any damage during a test,
- The friction between layers should be reduced as much as possible to generate free-field soil specimen,
- The natural frequency of laminar box should be different of the model to avoid resonance.

Based on experimental findings, comparison between model tests and numerical tests shows that the good coherence between the numerical analyses and experimental test results display the fact that the deformation of soil material in the laminar shear box resembles a shear beam behaviour (Cheung *et al.*, 2013). Thus, laminar box should meet the crucial performance criteria which are affected by (Jafarzadeh, 2004);

- Inertia effect of the lateral wall masses of the box,
- Friction effect induced by the roller bearings and layer surfaces,
- The effect of the covering membrane,
- The effect of the walls of the box, during an excitation.

Since performance criteria are vital for laminar box, maintenance is important for laminar shear boxes before establishing test setups. An example of disassembled version of a laminar box is displayed in Figure 2.29. As well as this relatively small laminer shear box when compared to this study, there are bigger shear boxes available in the literature (Figure 2.30).

Figure 2.29. View of the disassembled parts of the laminar shear box (Jafarzadeh, 2004).

Figure 2.30. A large-scaled laminar shear box, base plate, and during shaking table experiment (Thevanayagam and Ecemis, 2006).

As a result of the performed studies, friction effect was mentioned relatively negligible, because of the roller bearings between the frame layers. Also, computed resistance forces because of bearing friction and membrane effect was uniform along the container depth and negligible, compared to the shear resistance of the soil material. Thus, real soil profile simulation (as mentioned in Section 2.3.3.2) and field loading purposes within the experimental environment are possible to be reached (Prasad *et al.*, 2004; Turan *et al.*, 2008).

2.3.3.3. The laminar box used in this study. The design principle of the laminar box is to minimize lateral stiffness of the container to ensure that the soil governs the response of the soil box system. Thereby, a laminar shear box was utilized for the experiment to provide such mechanism. For the laminar box, the friction between frame layers are expected to converge approximately to zero. By doing so, the resistance between layers decreases, thus, soil can deform freely according to the natural conditions, as it has infinite lateral extend, as mentioned in Section 2.3.3.2; without artificial experimental boundary restrictions. Thus, in this experiment, a steel framed laminar box was utilized to take

advantage of minimized lateral impact (Figure 2.31). The subjected laminar soil container was designed for the former studies of Sekman (2016) and Goztepe (2016).

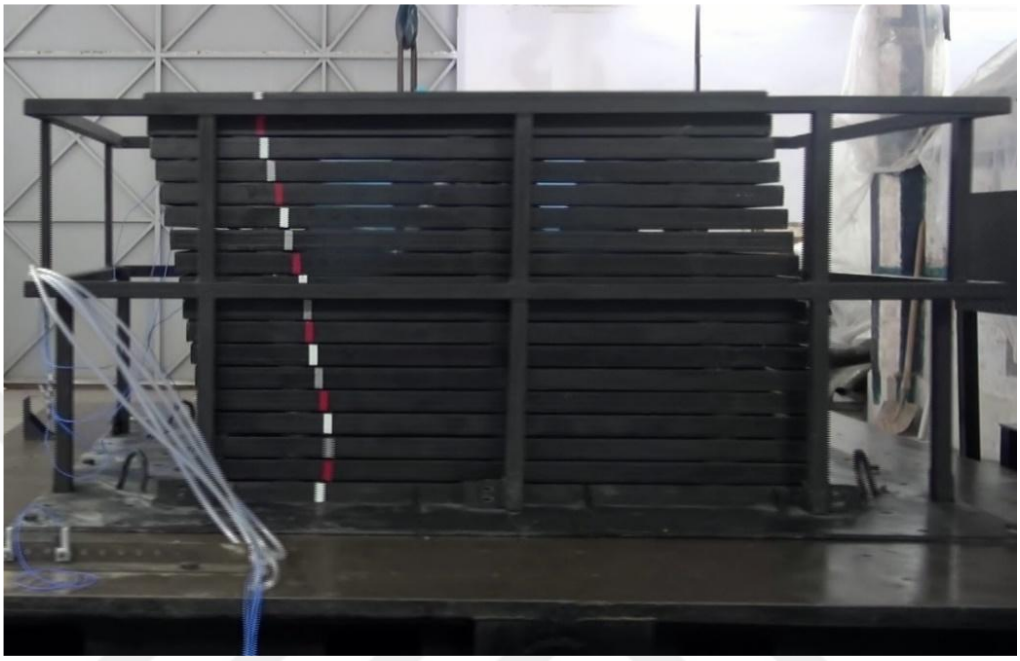

Figure 2.31. Side view of unidirectional laminar box utilized in this study (Sekman, 2016; Goztepe, 2016).

The laminar box is formed of steel frame layers, roller bearings, a steel base plate, side guides and internal membrane components. In total, there are 18 sliding layers and 324 roller bearings to provide sliding of the frame layers. Roller bearings and rubber stoppers were used to create a braking mechanism for excessive movement of the layers. Utilization of roller bearings provided reduction in friction forces between layers, by six roller bearings per laminate. Roller bearing shelters were constructed from stainless steel. Rubber strips were placed at both ends as of these shelters, as displayed in Figure 2.32 (Sekman, 2016; Goztepe, 2016).

Figure 2.32. View of roller bearing shelter with rubber strip stoppers on both side (Sekman, 2016).

Performance criteria checks recommended by Prasad *et al.* (2004); Jafarzadeh (2004) and Bhattacharya *et al.* (2012) were conducted, before the experimental tests for the studies conducted with the mentioned laminar box. These performance checks are explained in the following parts.

- Inertia Effect

Pulse absorption effect of the rubber stoppers, restricted the clashing or derailing of roller bearings, resulting further inertia effect. The first layer of laminar box was welded to steel the base plate, which is bolted to the shaking table. A membrane layer attached to the box to prevent soil leakage through layers. Also, membrane, sidewalls, roller bearings and bearing shelters were cleaned and greased to decrease any friction force (Sekman, 2016; Goztepe, 2016).

Since the inertia effect is contributed by the box mass, the measured acceleration (a) is aimed to be less than the actual acceleration to provide a superior shear beam behavior mentioned in Section 2.3.3.2, caused by the inertia effect. Considering this effect, a specific correction factor can be applied for recorded acceleration to reduce effectiveness

of this parameter. Considering m_1 and m_2 as the mass of the soil within a layer level and mass of the box layer, respectively, total dynamic force (F_d) is given as,

$$F_d = (m_1 + m_2) . a \tag{2.1}$$

Since the desired behaviour is the transferring of whole force to the soil, if the soil without container is considered,

$$F_d = m_1 . a' \tag{2.2}$$

Equating the above two equations, actual acceleration in the soil layer is given by,

$$a' = \left(\frac{m_1 + m_2}{m_1}\right) . a \tag{2.3}$$

a' = acceleration of the soil without the influence of the container
a = measured acceleration
m_1 = weight of the soil in the container
m_2 = weight of total laminates

$$a' = (1.3) . a \tag{2.4}$$

The influence coefficient was computed about 1.3 and this coefficient was normal up to 1.5 (Prasad *et al.*, 2004; Sekman, 2016; Goztepe, 2016; Calikoglu, 2017).

- Friction Effect

Static pullout tests were conducted to detect friction forces of the roller bearings to determine the force threshold for initiation of layers. Tests were conducted via load cells of 50 kg load capacity by anchoring every layer at once, gradually. Measured friction forces were the function of both the coefficient of friction between the laminates and laminate weight. Hence, the friction forces approximately increased as from top to down layers, as a result of increasing weight, as displayed in Figure 2.33.

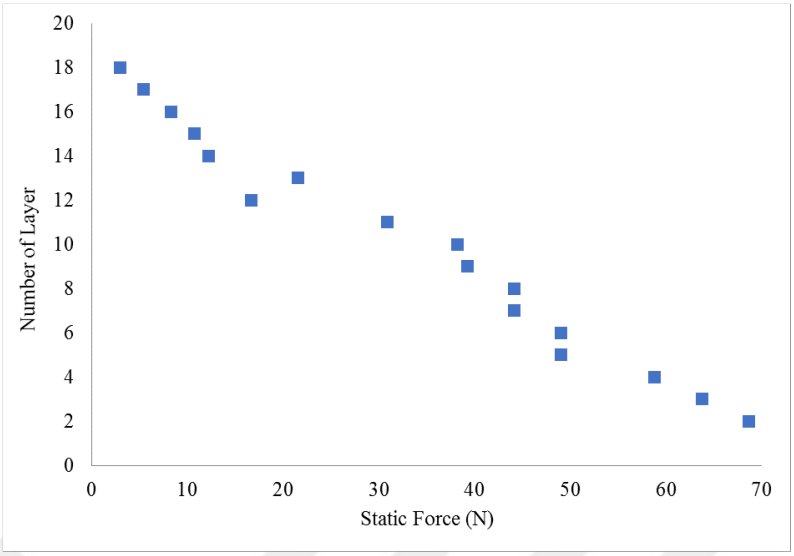

Figure 2.33. Measured friction forces from the pullout test (Sekman, 2016; Goztepe, 2016).

To cause a motion, maximum required force was measured as 69 N at the bottom layer, while average of the layer forces was 33 N. The average coefficient of friction was measured as 0.07. Resistance near the bottom was 10.5 kN while laminar box was filled with soil, approximately 0.006 of this resistance was equal to static friction. Thus, the static friction force was neglected (Sekman, 2016; Goztepe, 2016; Calikoglu, 2017).

- Membrane Effect

Rubber membrane with 1.0 mm thickness was used in the mentioned studies (Figure 2.34). Since the stiffness of the membrane was sufficiently small, in comparison with soil and stiffness of the membrane was particularly localized near the wall-ends of the laminar box than the center of the setup, effect of the membrane was negligible (Sekman, 2016; Goztepe, 2016)

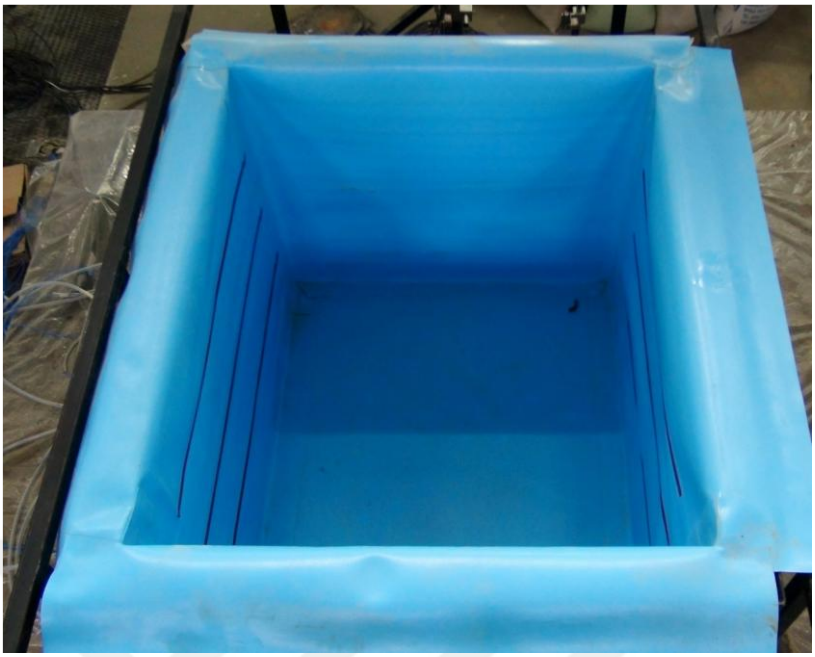

Figure 2.34. A view of thin rubber membrane located inside the laminar box (Sekman, 2016; Goztepe, 2016).

- Boundary Effect

The performance of the boundaries of laminar box was investigated through a series of shaking tests. To determine the natural behaviour of the laminar box, a group of tests were conducted without geosynthetic and soil material.

3. MATERIALS AND METHODS

In the context of this study, the efficiency and effectiveness of the geogrid reinforcement inclusions to the sand on the seismic performance of the low-to-medium rise buildings are examined. Thus, the mentioned purpose is researched through different geogrid configurations for the 1:10 scaled three story and five story models. In this regard, materials and methods section covers the information about shake table, measuring instruments, soil material properties, geogrid reinforcement material and input ground motions. The way of applications within every topic are presented in related title.

3.1. Shaking Table Facilities

This experimental research was operated in shaking table test facilities of Boğaziçi University - Kandilli Observatory and Earthquake Research Institute. Shaking table of the Institution is specified as uni-axial hydraulic shaking table which is able to generate uni-axial horizontal vibration driven by a servo-hydraulic compound. The dimensions of the table are 3 m x 3 m with a maximum 10-ton payload capacity and able to conduct 2g acceleration in horizontal direction (i.e. two times the acceleration of gravity). The shaking table can generate a stroke of +/- 12 cm (24 cm in total) which makes it suitable for seismic implementations. The actuator has a 3-stage servo-valve controlled by an analog inner-loop control system (displacement based), and a digital outer-loop control system (acceleration feedback based). It is controlled by the currently modified computer-based software system.

3.2. Measuring Instruments

±3g capacity accelerometers and ±20g capacity accelerometers were used in the experiments to measure the acceleration. Leuze ODSL 96B M/V6.XL-1200-S12 optical distance sensors (ODS) with 150 - 1200 mm measurement range and ±2% absolute measurement accuracy were utilized for measuring displacements. 27 - Channel dynamic data logger was used for data acquisition. The sample rate for cyclic sinusoidal motions

was taken as 1000 sample/sec and for earthquake motions, the sample rate was taken as 500 sample/sec.

3.3. Sand Material Properties

The soil material used in the experiments is “Silivri Sand” which is a regional soil material that can be found around Istanbul region. Sand is clean and dried in an isolated space in the laboratory. The grain-size distribution of the sand was defined corresponding to the American Standard Test Method (ASTM) of D422 as shown in Figure 3.1.

According to the Unified Soil Classification System, the sand in this experiment is categorized as poorly graded sand (SP) with the coefficient of curvature as C_u = 2.29 and the coefficient of uniformity as C_c = 1.1. The quick triaxial test conducted by Cagatay (2008) gives the internal friction angle as Φ = 41.48^o. Specific gravity of sand was obtained as G_s = 2.67 and bulk unit weight as γ_{bulk} = 16.5 kN/m^3. The maximum and minimum void ratios of the sand were obtained as in Sekman (2016); 0.73 and 0.37, respectively.

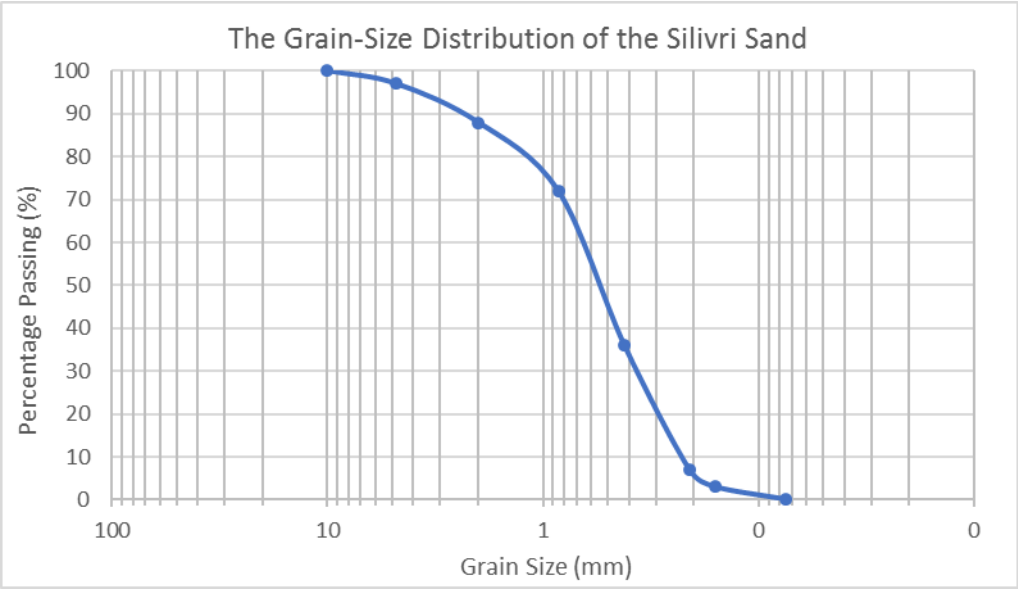

Figure 3.1. The Grain-Size Distribution of the Silivri Sand.

3.4. Input Ground Motions

Multiple earthquake motions had been selected as inputs for shake table tests. As in Sekman (2016) and Calikoglu (2017), similar strong ground motion records were chosen for this study. These are 1940 El Centro (Array #9 Station), 1995 Kobe (KJMA station), and 1999 Kocaeli (İzmit station) earthquakes. Also, Iznik station record of the 1999 Kocaeli earthquake was taken into account to examine near-fault effect. In addition, cyclic sinusoidal motions were used with different frequencies. (0.5 Hz, 1 Hz, 2 Hz, 3 Hz, 4 Hz, 5 Hz) and free vibration tests (3.93 Hz, 12.46 Hz, 18.35 Hz for 3-story model and 2.33 Hz, 8.58 Hz, 13.34 Hz, 17.52 Hz, 19.90 Hz for 5-story model). Frequencies of the cyclic sinusoidal motion were determined according to the modal frequencies obtained from free vibration tests. Motion data of selected earthquakes were obtained from the PEER Ground Motion Database (Table 3.1).

Table 3.1. Earthquake motions used in the experiments (PEER Ground Motion Database – KOERI Database).

Earthquake Event	Year	Station	Magnitude	PGA(g)	PGV(cm/sec)	PGD(cm)
Imperial Valley-02	1940	El Centro Array #9	6.95	0.32	31.74	18.01
Kobe, Japan	1995	KJMA	6.90	0.82	77.83	18.87
Kocaeli, Turkey	1999	Izmit	7.51	0.22	27.02	14.61
Kocaeli, Turkey	1999	Iznik	7.51	0.12	-	-

For the mentioned earthquake records, acceleration-time history graphs are displayed in Figure 3.2, Figure 3.3 and Figure 3.4 and Figure 3.6.

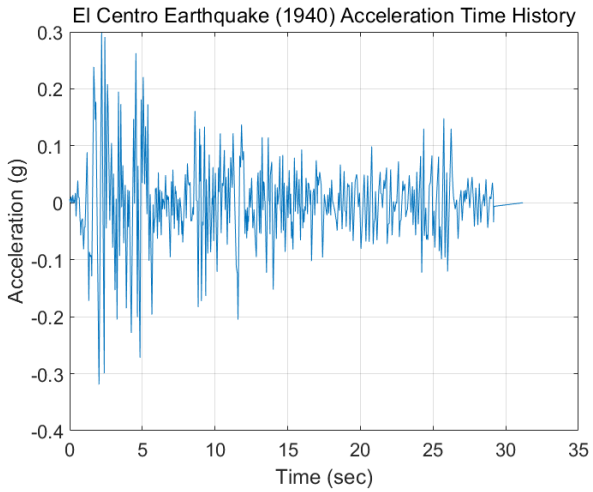

Figure 3.2. Acceleration Time History of El Centro Earthquake (1940)

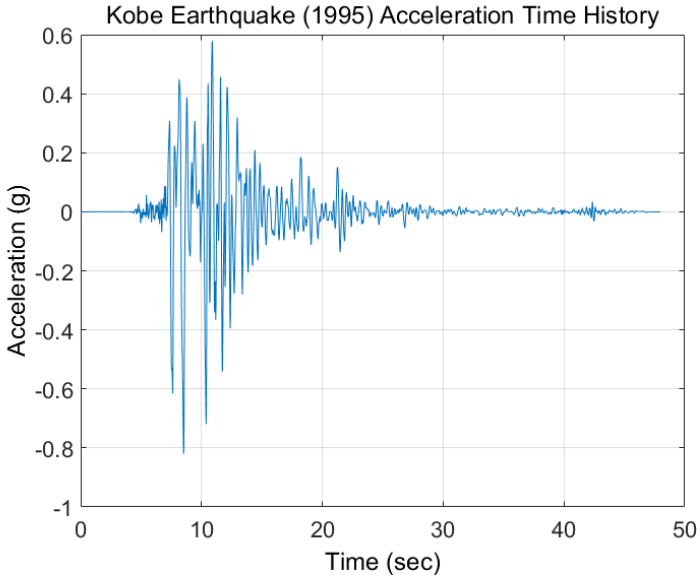

Figure 3.3. Acceleration Time History of Kobe Earthquake (1995)

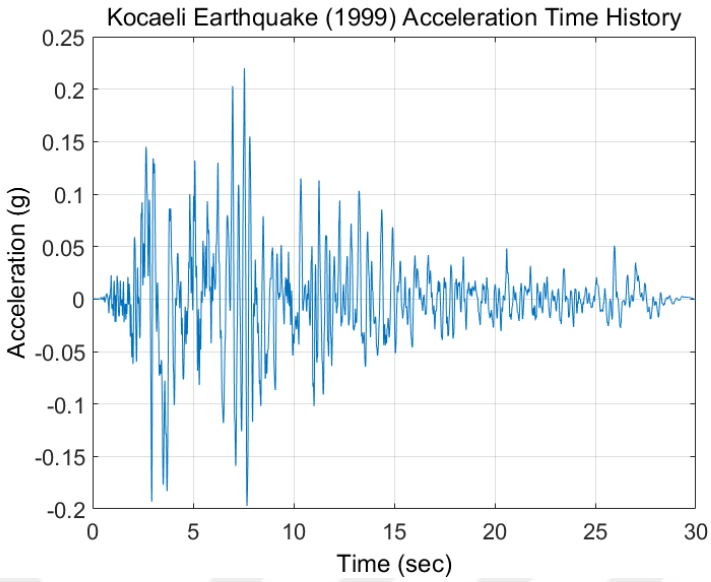

Figure 3.4. Acceleration Time History of Kocaeli Earthquake (1999)

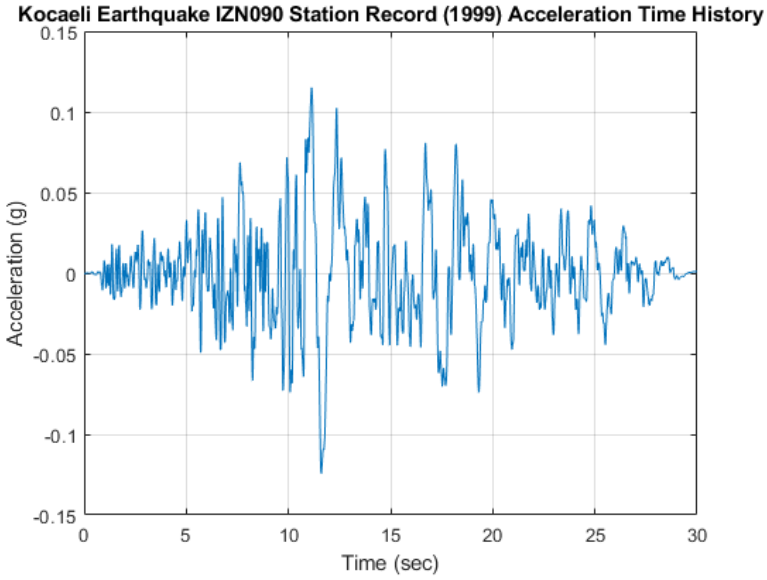

Figure 3.5. Acceleration Time History of Kocaeli Earthquake – IZN record (1999)

3.5. Experimental Setup and Preparation

The laminar box was designed and constructed according to previous studies in the literature, to be able to generate the idealized soil-box laminar interaction (Sekman, 2016; Goztepe, 2016). The dimensions of the box are; 1.3 meters length (along the shake table direction), 1.1 meters width (perpendicular to shake table direction), and 1.0 meter depth (Figure 3.6). Dimensions were decided according to maximum load capacity of the shaking table. Depending on the risk of potential torsion problems, geometry of the laminar box was preferred as a rectangular shape, instead of a square geometry (Sekman, 2016; Goztepe, 2016).

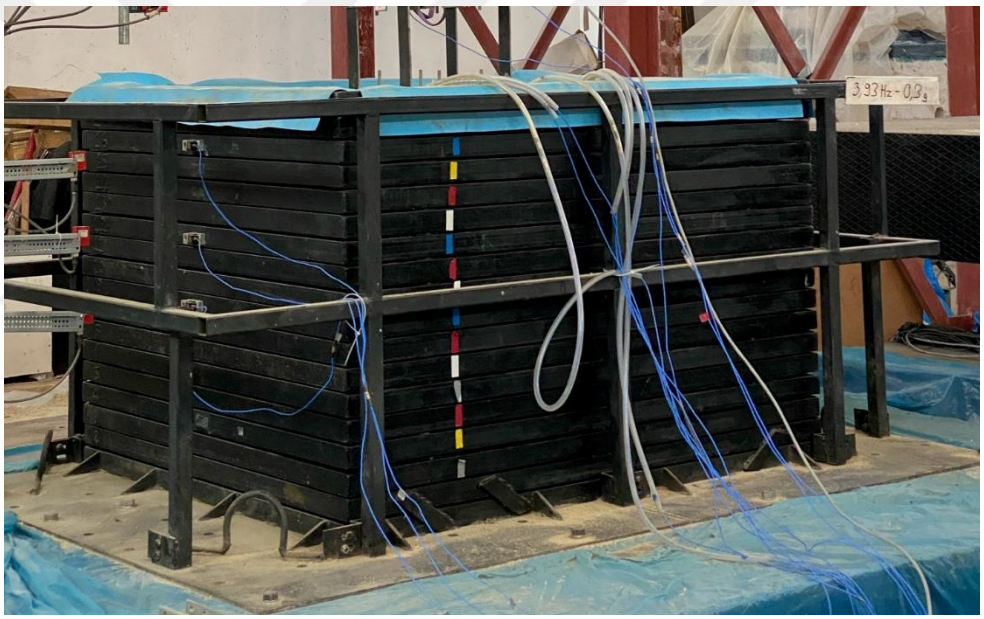

Figure 3.6. Perspective view of the Unidirectional Laminar Box used in this study.

The laminar box consists of 18 laminate plates and 324 rollers with stoppers, base plate, the protector/guide bars at each side and internal membrane component, as mentioned in detail, in Section 2.3.3.3 (Sekman, 2016).

Within the scope of this study, performance checks were repeated according to performance criteria mentioned in Section 2.3.3.3. Thus, inertia effect of the laminar box, friction effect generated through frame layers, membrane stiffness effect and boundary effect checks were repeated to validate reliability of the laminar soil container.

To control the performance of the laminar box boundaries, configuration of a setup without soil material is presented in Figure 3.7. Four accelerometers and four optical distance sensors (ODS) were placed on the front side of the laminar box. Accelerometers are signed as “A” while ODS are signed as “D” in the sketch. D19 and A1 were placed to provide data from the shaking table for checking the given input. The rest of accelerometers and displacement sensors are placed as displayed in the sketch. Cyclic sinusoidal motions of 0.5 Hz with 0.05g, 1 Hz with 0.30g, 2 Hz with 0.50g, 3 Hz with 0.60g, 4 Hz with 0.70g, and 5 Hz with 0.80g were executed to the laminar box, without soil material. The performance check results displayed that boundaries of the laminar box operated properly.

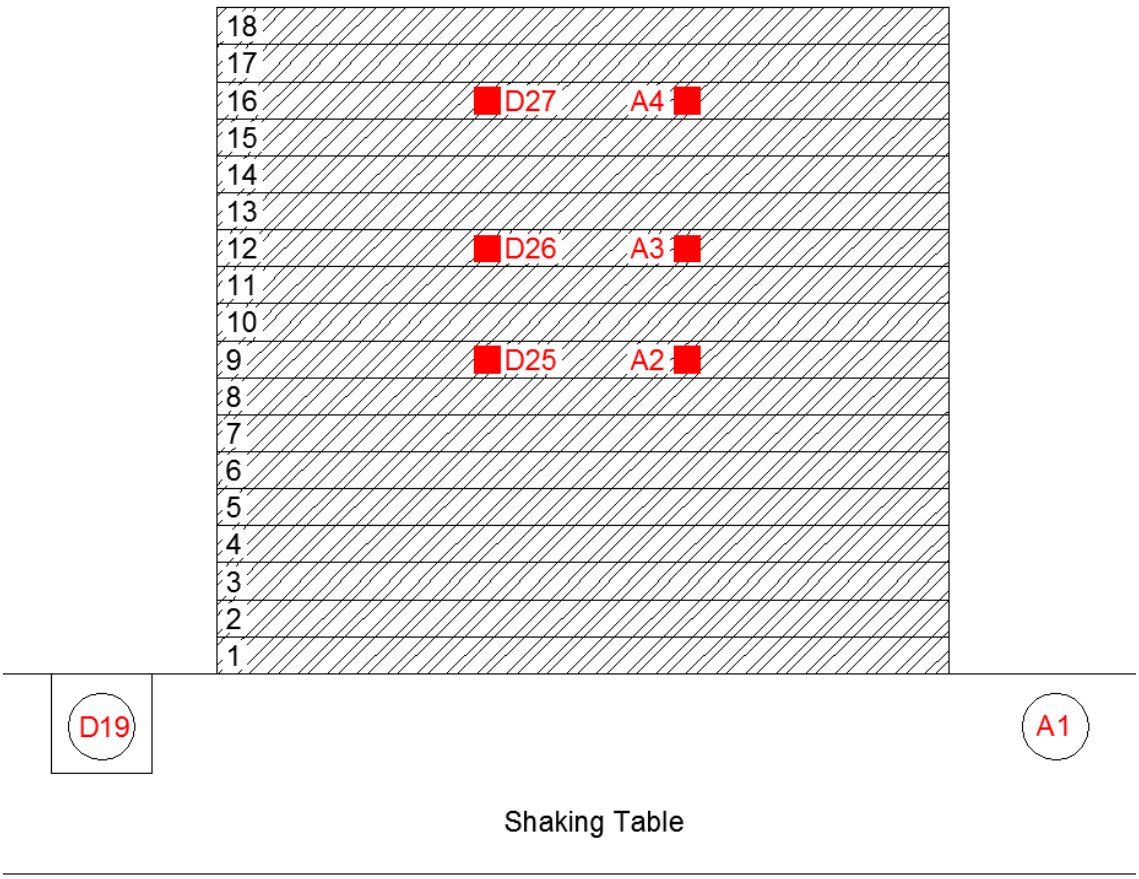

Figure 3.7. A sketch of instrumentation layout of laminar box without soil – Front view.

In Figure 3.8 (a) and Figure 3.8 (b), the measured accelerations and displacement results obtained from cyclic sinusoidal motion with 0.5 Hz are displayed. It can be seen

that both acceleration and displacement rates decreased from bottom to top, which means both effects were diminished from bottom to top, as expected.

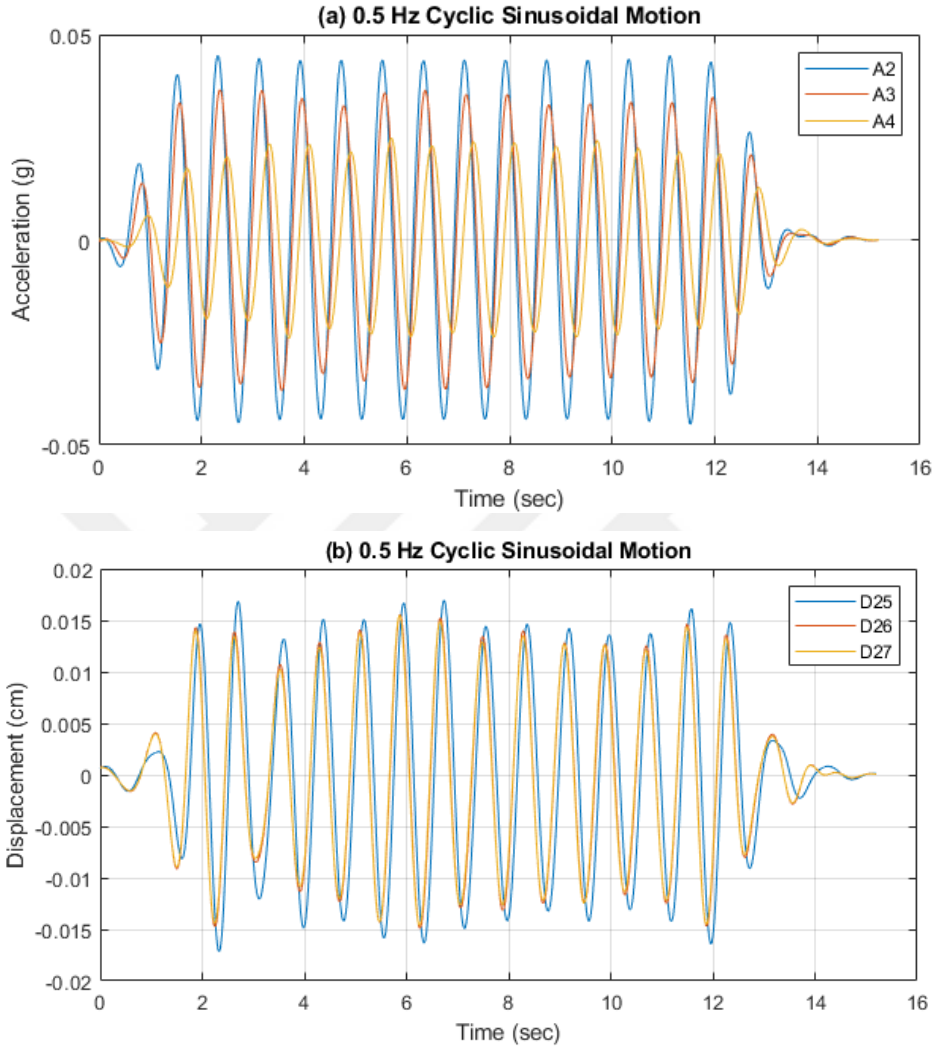

Figure 3.8. Acceleration-time history (a), displacement-time history (b) under 0.5 Hz Cyclic Sinusoidal Motion.

In the experimental setup preparations, 3 ODS (all outside the laminar box) and 11 Accelerometer (3 outside of the laminar box) as displayed in Figure 3.7. Rest of the accelerometers (A5, A6, A7, A8, A9, A10, A11, A12) are displayed in Figure 3.9 where placement and height information of accelerometers can be seen.

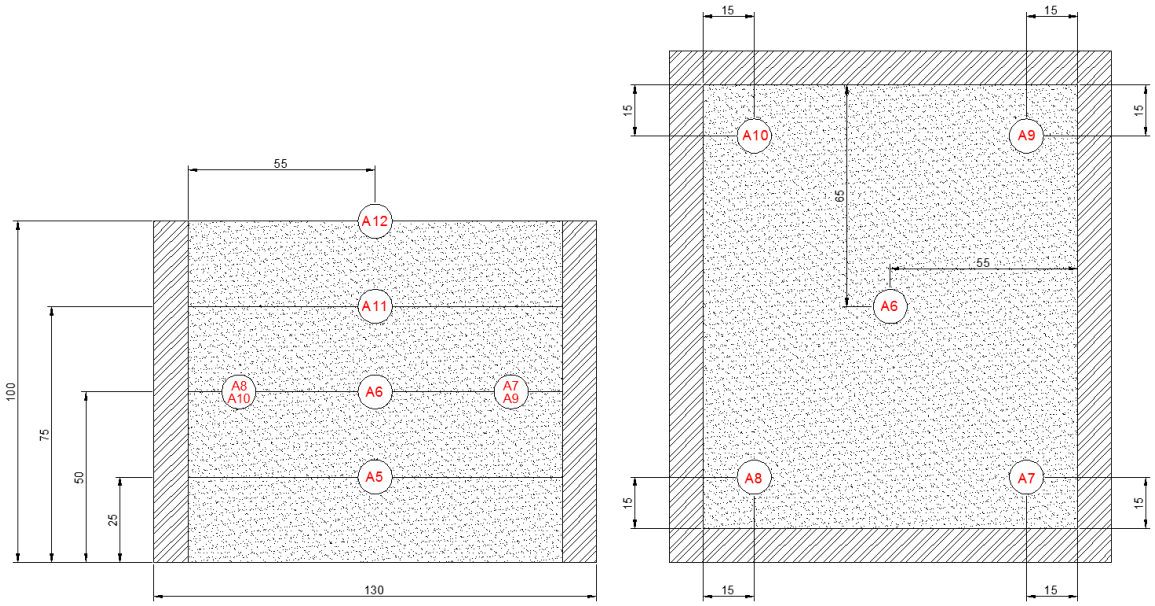

Figure 3.9. Front section view (left) and top view (right) of instrumentations in the laminar box filled with sand (Instrumentations inside the soil).

In order to evaluate the boundary effect, cyclic sinusoidal motions of 0.5 Hz (0.1g), 1 Hz (0.3g), 2Hz (0.5g), 3Hz (0.6g), 4Hz (0.7g) and 5 Hz (0.8g); Kocaeli Earthquake (1999), El Centro Earthquake (1940) and Kobe Earthquake (1995) motions were applied as a routine part of the free surface tests. Output data of the accelerometers were put in comparison to validate influence of box boundaries (Figure 3.10). The comparisons were made by the data outputs of A6, A7, A8, A9 and A10 accelerometers, based upon their same height level. As can be seen, approximately identical acceleration motions were obtained from outputs, since the mentioned horizontal levels were the same. Figure 3.10 displays the acceleration values of A6, A7, A8, A9 and A10 accelerometers for he given 0.5 Hz cyclic motion as well as, 1 Hz sinusoidal motion and Kobe earthquake (1995).

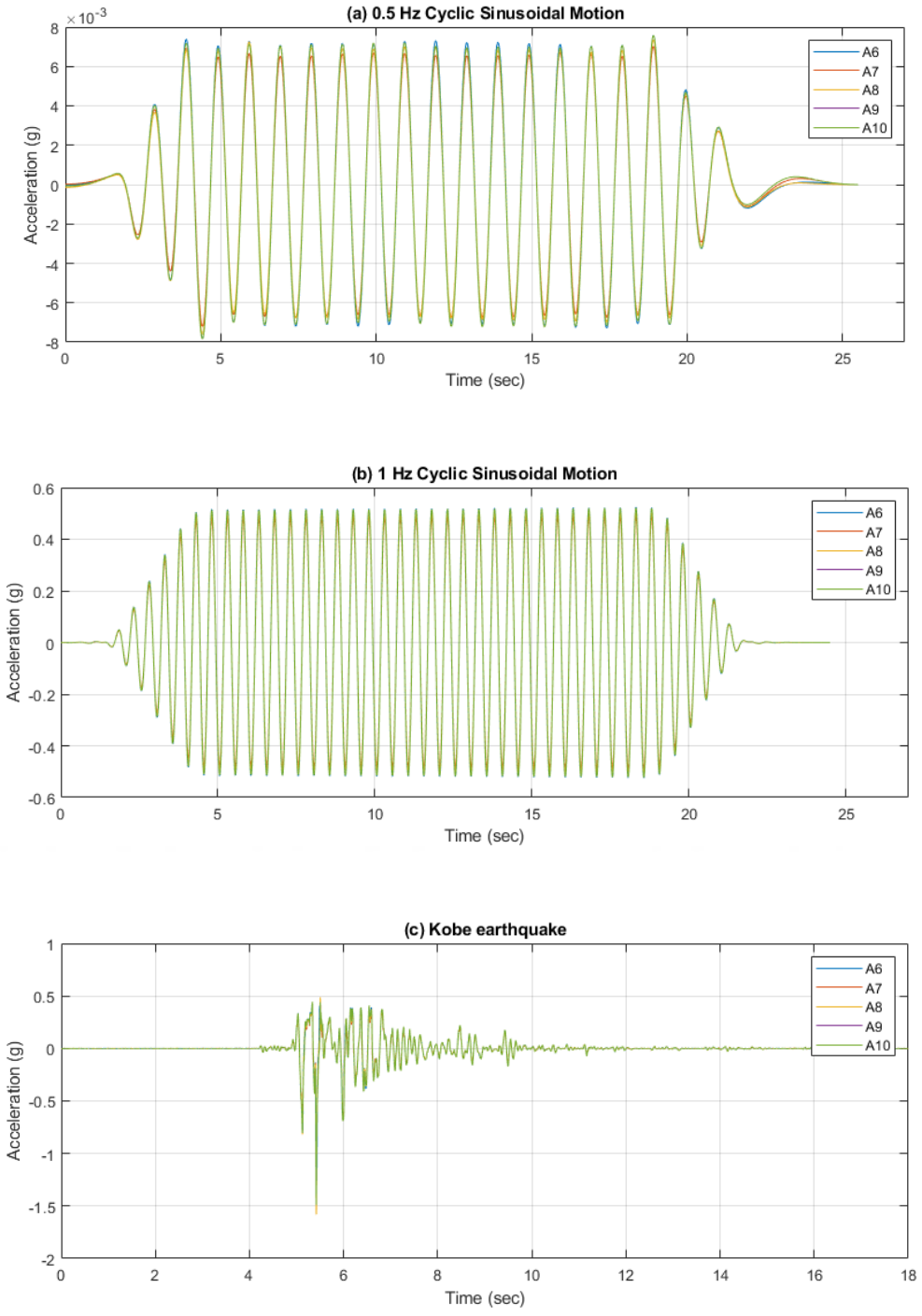

Figure 3.10. Acceleration-time history for 0.5 Hz cyclic sinusoidal motion (a), Acceleration-time history for 1 Hz cyclic sinusoidal motion (b) and Acceleration-time history for Kobe Earthquake (Laminar box is filled with sand).

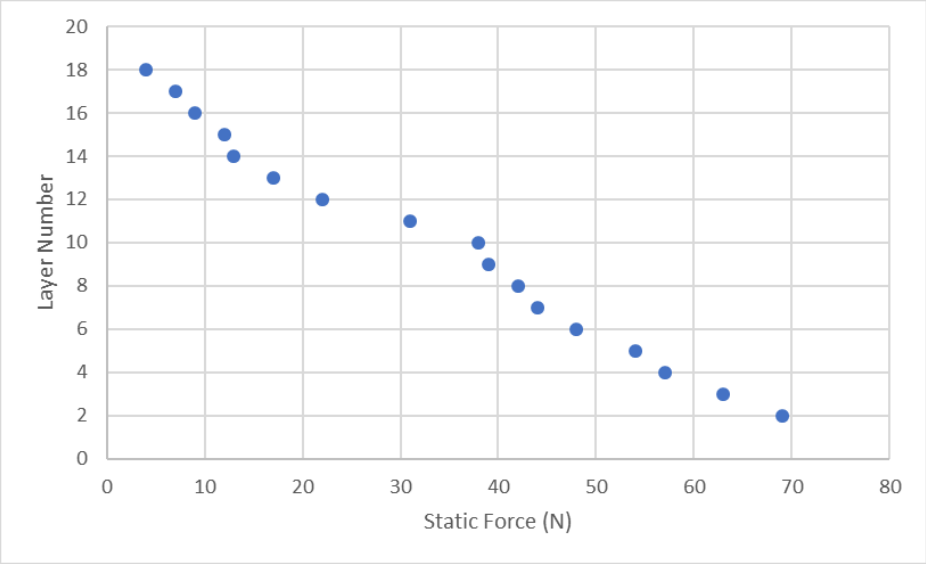

Figure 3.11. Measured friction forces of the pullout test.

Depending on the proper mechanic maintenance of the box, maximum force to start a motion was measured as 69 N at the bottom layer, and average of the layer forces was 33.47 N. Since the maximum and average forces of the laminar container are the same with previous studies of Sekman, 2016; Goztepe, 2016; Calikoglu, 2017; approximately 0.006 of this resistance was equal to static friction (Figure 3.10). Thereby, the static friction force was neglected.

3.6. Scaled Building Models

Effect of geogrid reinforced zone on the seismic performance low-to-medium rise buildings was planned to be observed. Thus, considering maximum allowable dimensions, for the building model, by the help of previous studies, 1:10 scale factor was determined and test models were selected as 3-story and 5-story buildings which are used in previous studies of Sekman (2016), Goztepe (2016) and Calikoglu (2017). Also, in literature reviews, it is seen that 1:10 factor had been commonly used due to manufacturing simplicity and reliability of calculations (Harris and Sabnis, 1999). Material characteristics were not scaled, due to unavailability of such materials during the production process of the test models. Scale factors for required parameters are described in Table 3.2. Some physical quantities, such as stress and strain; remain the same even after scaling (Harris and Sabnis, 1999; Iai, 1989).

Table 3.2. Scaling parameters of the building model (Harris and Sabnis, 1999; Iai, 1989).

Parameter	1:10 Scaled Model/Prototype	
Length	L	1/10
Time	$\sqrt{L}$	$1/\sqrt{10}$
Mass	L^2	1/100
Displacement	L	1/10
Acceleration	1	1/1
Stress	1	1/1
Strain	1	1/1
Force	L^2	1/100

Characteristics of the buildings are summarized as such: High carbon steels columns which dimensions are 26,5 cm x 5cm x 0,5 cm. They are tied with metric eight bolts to ground of the model. Weight blocks of the ground were made of St42 with a dimension of 30 cm x 30 cm x 2 cm. Four flanges were welded on every floor. Foundation was made of same St42 steel with a dimension of 35cm x 35cm x 2cm. The final height of the 5-story building was 135 cm without foundation and the final height of the 3-story building was 81 cm without foundation (Sekman, 2016; Goztepe, 2016). An example view of 3-story and 5-story building test models are presented in Figure 3.12. As displayed in the figure, instead of two identical columns, only one column was placed per edge corners, since the two columned structure was too rigid to observe the effect of geogrid reinforcement.

Figure 3.12. Building models of 1:10 Scaled 3-Story (left) and 5-Story (right) structures.

3.7. Geogrid Reinforcement Material

Since the concept of the proposed geogrid reinforcement system depends on the friction forces between soil and the reinforcement element, a geogrid element with a cellular structure was utilized for the study to provide a locking mechanism in between the soil and aperture size of the geogrid, to generate anchoring effect. Thereby, dissipating strong ground motion impact by locking mechanism via creating additional soil and geogrid layers, under the structure is vital for the concept. These layers consist of identical geogrids which have same characteristics (Table 3.3) and same geometry as displayed in Figure 3.13.

Table 3.3. Properties of geogrid material used as soil reinforcement.

Properties		**Specifications**
Name		Çevregrid UR-45
Material		Polypropylene (PP)
Area weight		390 (g/m2)
Tensile strength	Longitudinal	45 (kN/m)
	Transverse	10 (kN/m)
Breaking elongation	Longitudinal	10 (%)
	Transverse	13 (%)

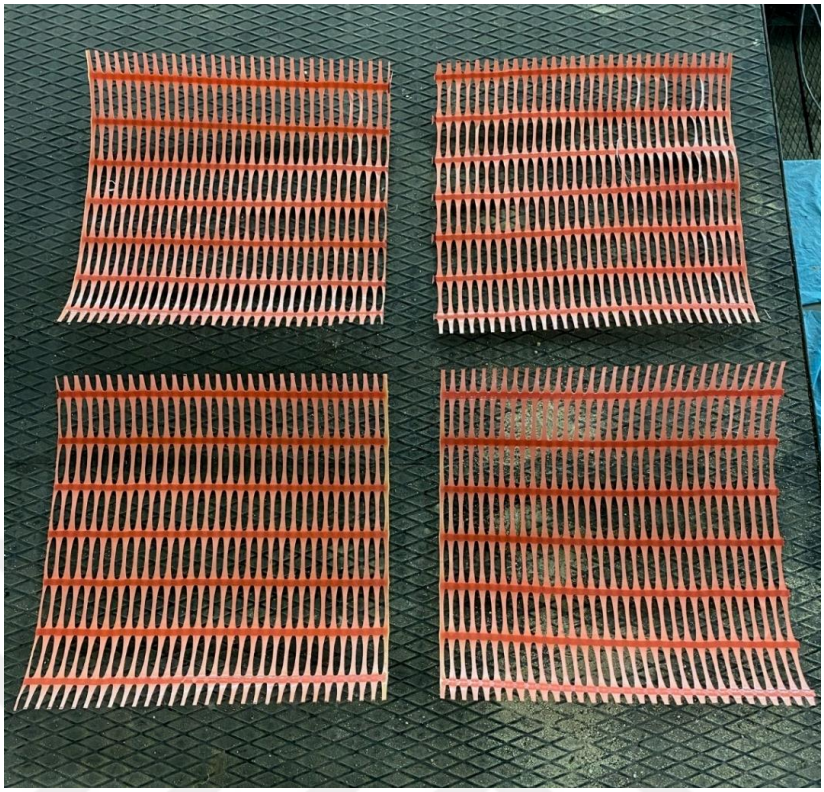

Figure 3.13. Geogrid samples which are used in the experiment.

Additionally, fundamentals of determination of appropriate geogrid materials were taken into account from the study conducted by Patra *et al.* (2005). Taking these parameters into consideration; a commercially available geogrid suitable to 1/10 scaled models was used in the studies.

3.8. Applied Ground Motions

Fundamentally, 2 types of motions were applied to test models in the experiments; which are strong ground motion records and cyclic sinusoidal motions. Free vibration tests displayed that cyclic motion frequencies are 3.93 Hz, 12.46 Hz, 18.35 Hz for 3-story model and 2.33 Hz, 8.58 Hz, 13.34 Hz, 17.52 Hz, 19.90 Hz for 5-story model buildings. In conformity with previous study of Iai (1989); duration parameter of the strong ground motions was scaled by 1:10 by multiplying duration with a scaling factor of $\sqrt{10}$. In Figure 3.14, Figure 3.15 Figure 3.16 and Figure 3.17, acceleration-time history and response spectrum figures are displayed.

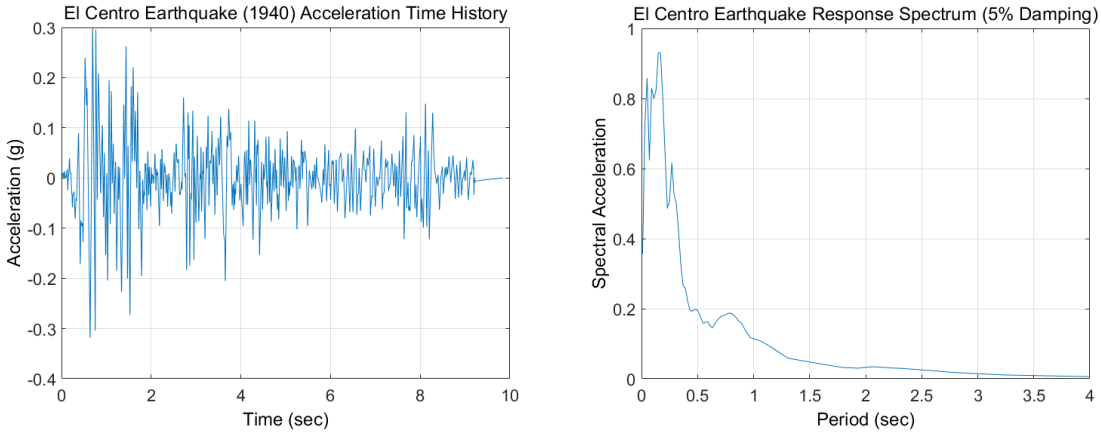

Figure 3.14. Acceleration – time history (left) and response spectrum (right) of El Centro Earthquake (1940).

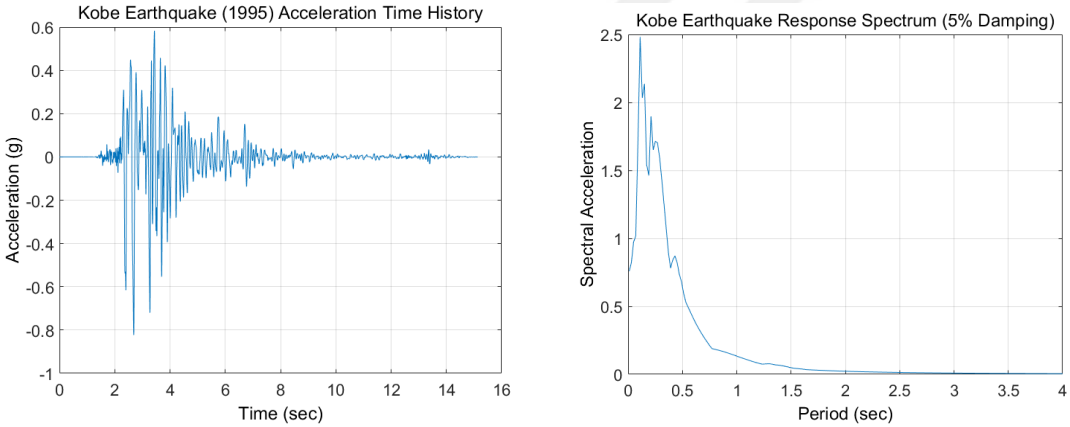

Figure 3.15. Acceleration – time history (left) and response spectrum (right) of Kobe Earthquake (1995).

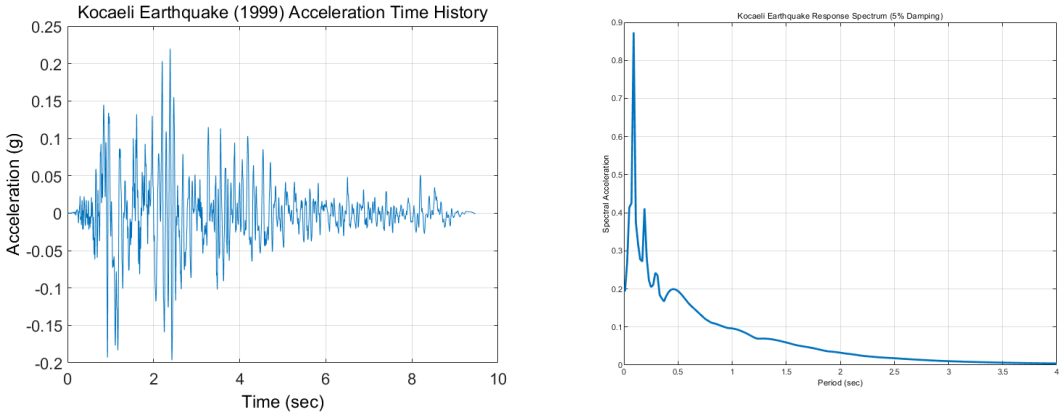

Figure 3.16. Acceleration – time history (left) and response spectrum (right) of Kocaeli Earthquake (1999).

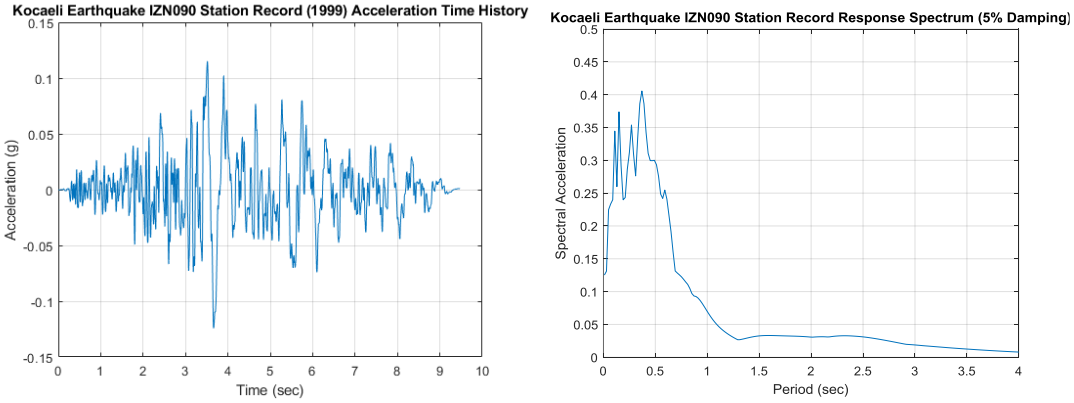

Figure 3.17. Acceleration – time history (left) and response spectrum (right) of Kocaeli Earthquake – IZN Station record (1999).

3.9. Shaking Table Experiments & Instrumentation

To be able to fill laminar shear box with soil material, approximately 2.5 tons of Silivri Sand was used by a unit weight of 16.5 kN/m^3. In Figure 3.9, nearly 0.6 tons of sand was used to reach each of the height levels. For the all height levels, compaction operation of the soil was conducted with a cylindrical rigid metal block (
Figure 3.18).

Figure 3.18. Soil Sample Preparation and Compaction.

The mentioned process was done for each level including the soil surface at the foundation level. Upon completion of the manual compaction of the soil material, compactions with shaking table were done under 9 Hz sinusoidal motion to the system for the 30 seconds (El-Emam and Bathurst, 2004). Then, soil surface was flattened to generate a uniform soil surface and elevation. Accelerometers inside the soil are displayed in Figure 3.9. Additionally, A12 accelerometer sensor was the surface accelerometer. Even more, 5 ODS were used to measure story displacements (3 for 3-story), 3 ODS were used to measure laminar box displacements at different height levels and 1 ODS was used to measure shake table displacement.

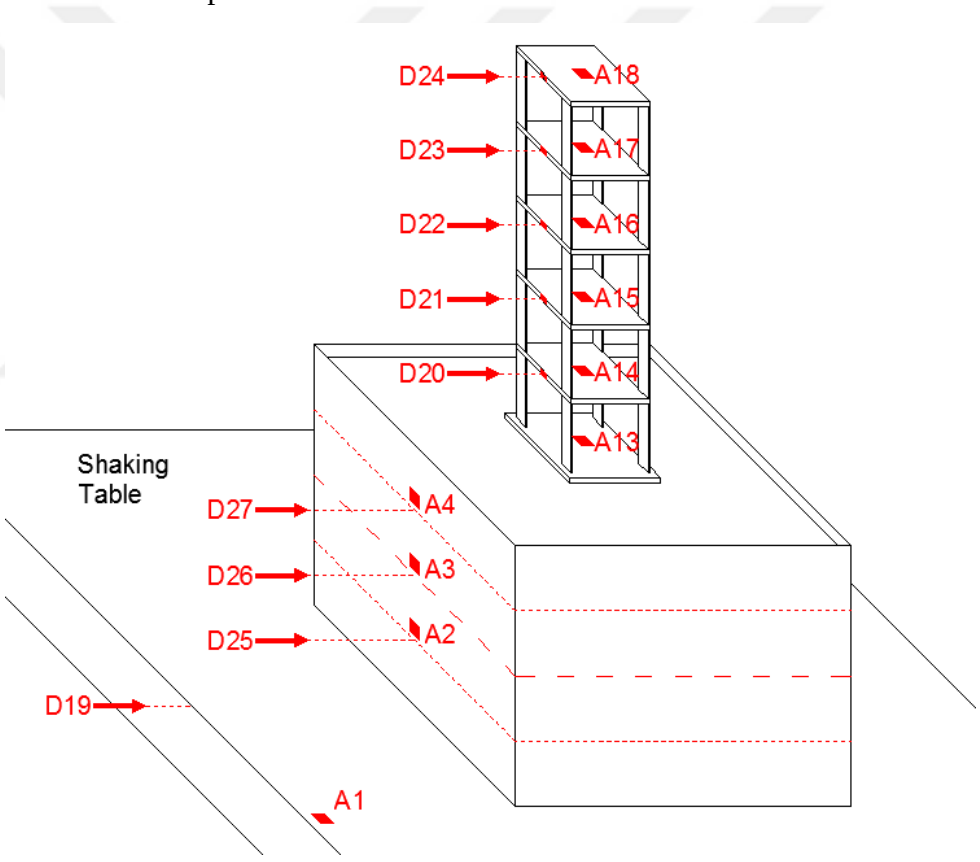

Figure 3.19. A sketch of test setup for the geogrid reinforced soil system for the 5-story model.

Also, 6 accelerometer sensors were used for structure model of 5-story model building (4 for 3-story), 3 accelerometers were used on laminar box and 1 accelerometer was used on shaking table, for the whole testing phase. A sketch of the mentioned instrumentation is displayed in Figure 3.19. For the 3-story model, D24 and D23 ODS

sensors and A17 and A18 accelerometer sensors are disabled while the rest of the setup was remaining the same. The application of the setup is displayed at Figure 3.20.

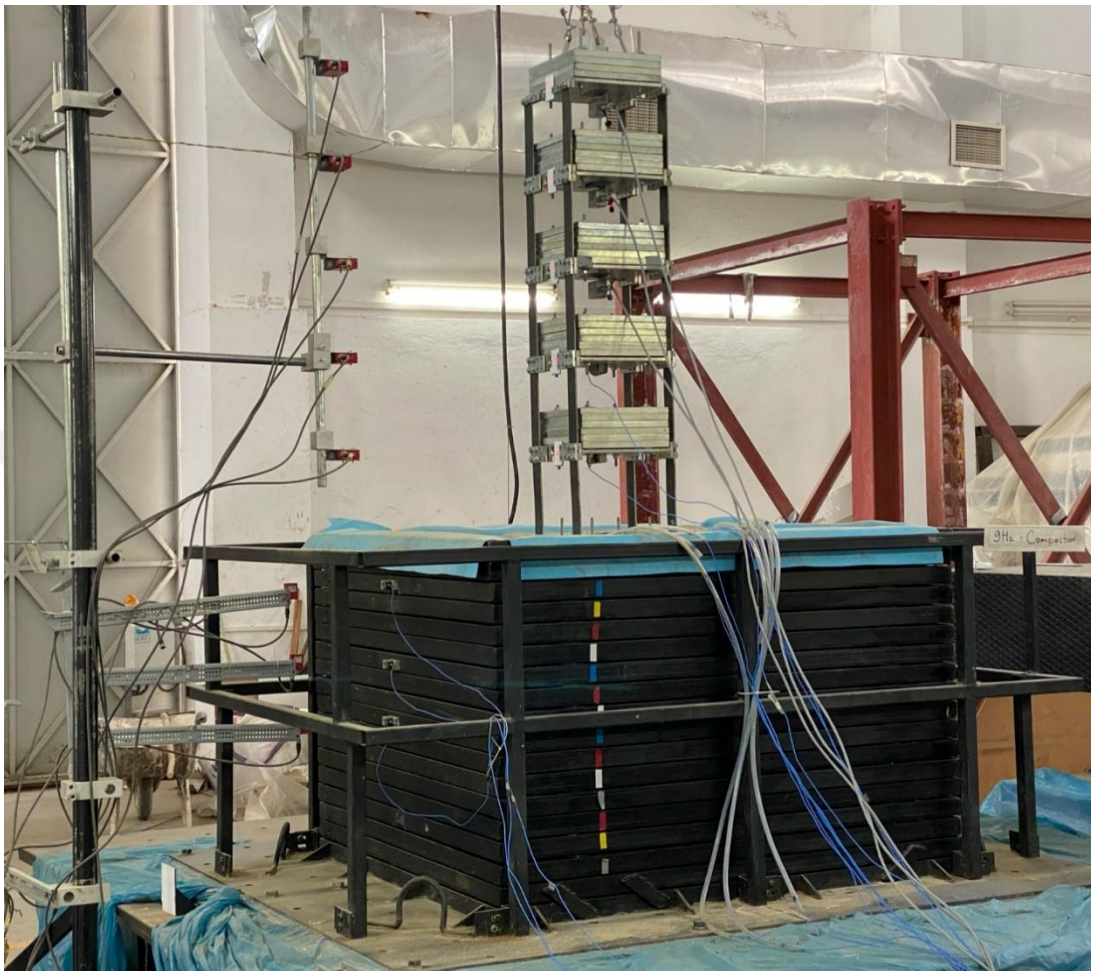

Figure 3.20. Instrumentations of the test model, laminar box and shaking table.

The parameters of the shaking table experiments include the number of geogrid layers (N number) and the number of building stories. N, the number of geogrid zone differs from 1 to 4 layers, therefore creating various reinforced soil layers. Width of the geogrids are constant at 55 cm x 55 cm, square shape. Number of building stories varies from 3 story to 5 story for the experimental setup. The effects of the reinforced zone on the seismic performance of the building models for the given parameters are researched within this study. Thereby, effect of the height of the structure is also investigated through the experiments, in terms of effectiveness of the geogrid zone. In Figure 3.21, an example of the geogrid reinforcement placement can be seen.

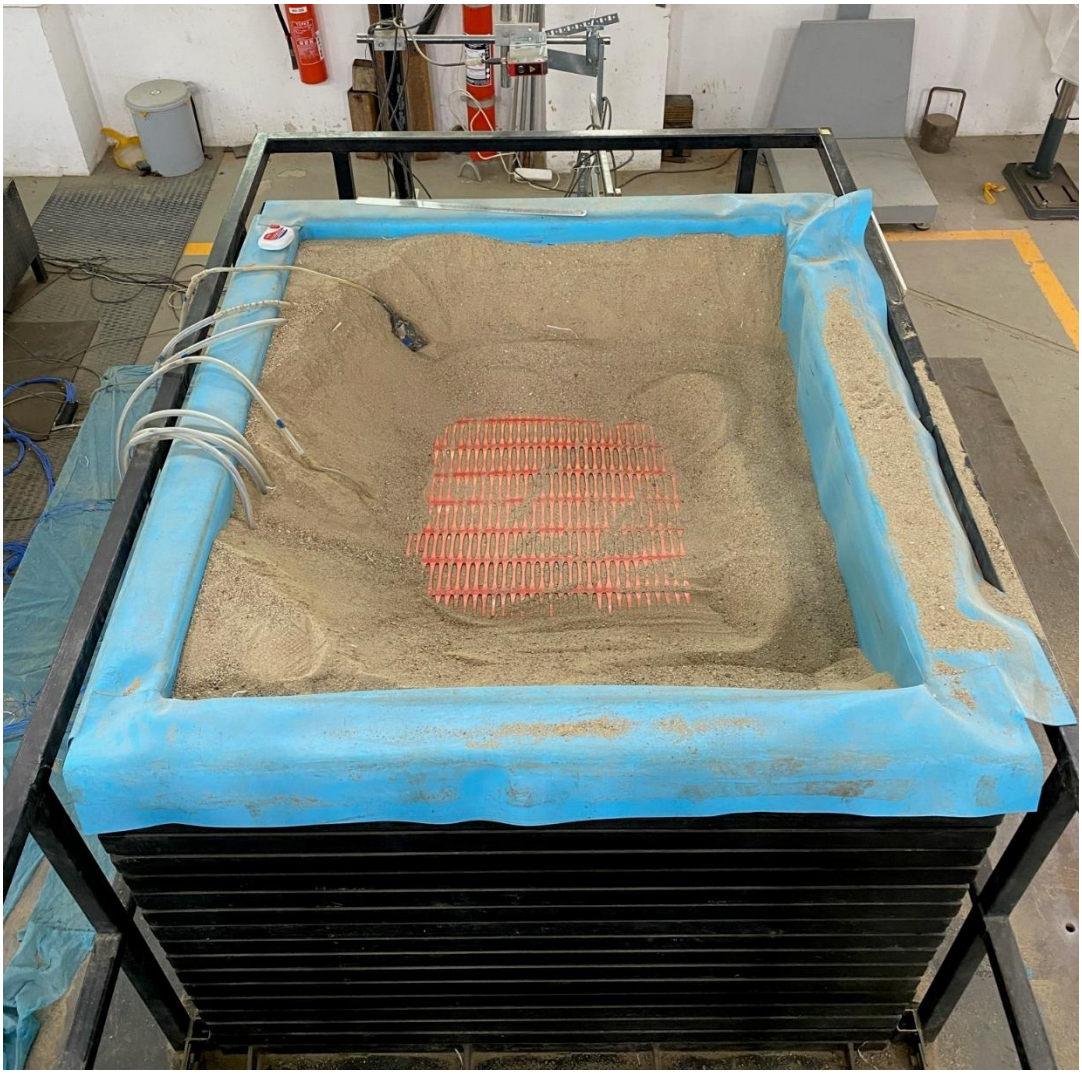

Figure 3.21. An example of the geogrid reinforcement configuration.

In the designing phase of geogrid reinforcement cases; four cases are taken into account which are applicable with the existing laminar box. In previous studies of Omar *et al.* (1993) and Yetimoglu *et al.* (1994), various references for u, N and h values are presented as;

$$d = u + (N - 1)\, h \tag{3.1}$$

Where is;

$d =$ the depth of reinforcement below the bottom of foundation

$u =$ the top layer depth of geogrid

$N =$ number of geogrid layers

$h =$ the vertical spacing between consecutive geogrid layers

Within the scope of this study, where B is the width and length parameters for a square shaped test model foundation and b is the width of the geogrid layers, following parameters are adopted for $B = 4$ (Omar *et al.*, 1993; Yetimoglu *et al.*, 1994);

$$d/B = 1.37 \quad (3.2)$$

$$u/B = 0.34 \quad (3.3)$$

$$b/B = 1.57 \quad (3.4)$$

$$h/B = 0.34 \quad (3.5)$$

Since the mentioned parameters perfectly fulfill the requirements to conduct this study, they were also chosen because of the dimensions of the soil container were also a limiting condition for the experiments. Thus, mentioned parameters are applied to test setups accordingly and geogrid reinforcement cases are generated, as represented in Figure 3.22.

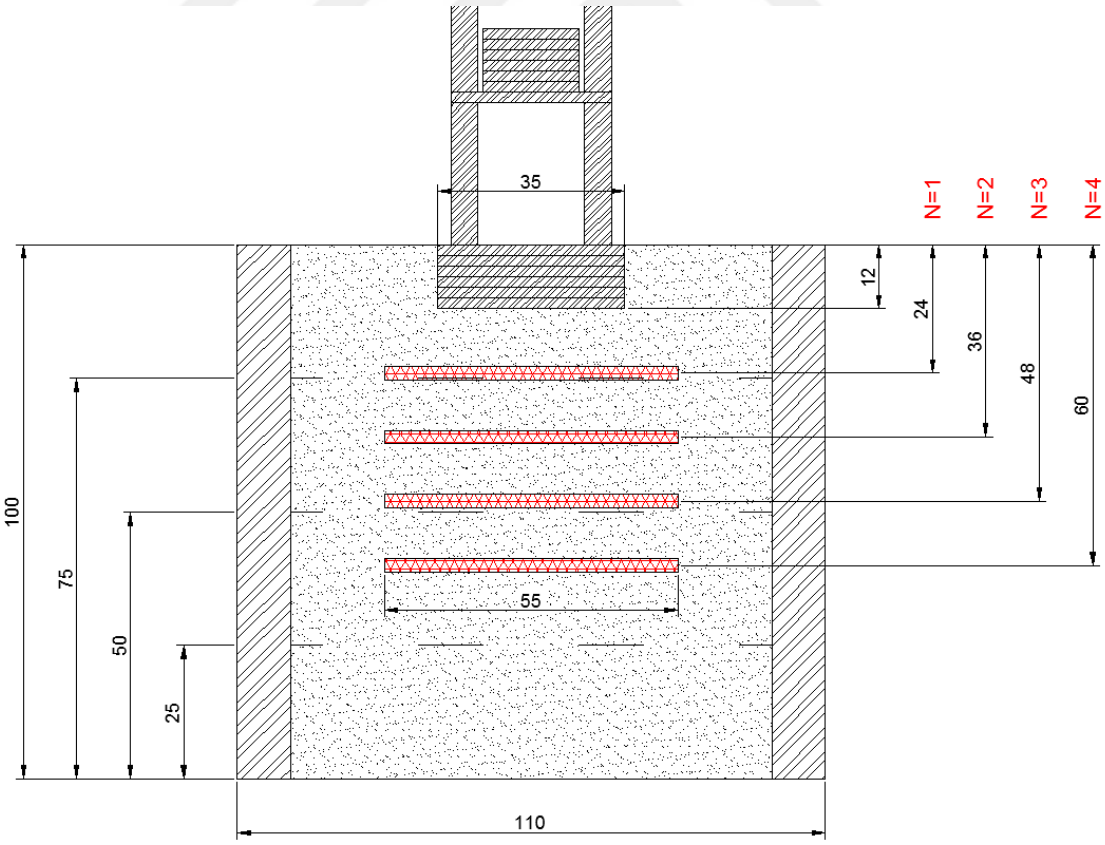

Figure 3.22. Geogrid reinforced zones for all configuration cases.

For completion of the geogrid reinforced zones, the following parameters are adopted as displayed in Table 3.4.

Table 3.4. Adopted parameters for geogrid reinforcement layers.

	$N = 1$	$N = 2$	$N = 3$	$N = 4$
d/B	0,34	0,68	1,02	1,37
u/B	0,34	0,34	0,34	0,34
b/B	1,57	1,57	1,57	1,57
h/B	0,34	0,34	0,34	0,34

After completion of the geogrid layer placement and instrumentation, free surface tests are conducted, before placing the structure models on the reinforced soil. As mentioned in Section 3.4 and 3.5, free surface tests contain 0,5 Hz (1g), 1 Hz (0,3 g), 2 Hz (0,5g), 3 Hz (0,6g), 4 Hz (0,7g), 5 Hz (0,8g) – sinusoidal – and Kocaeli (1999), El Centro (1940) and Kobe Earthquake (1995) motions. These tests were conducted for both reference (without geogrid reinforcement) setups and also, with reinforced setups. The tests also provided an additional mechanic compaction for the soil material in the laminar box and subsidence amounts of the soil were noted, and soil was added if there was an excessive soil subsidence ratio. The structure models were placed in the laminar box, after the free surface tests, in all of the cases. Then, again, the whole setup is excited with an additional 9 Hz sinusoidal motion for the 30 seconds (El-Emam and Bathurst, 2004), for an additional compaction of the soil. The resonance research of the created case setups is carried out individually for each case. Thus, along with the compaction of the soil, a stable soil-structure interaction is aimed to be generated.

An example of the experimental set-up for the 3-story model before performing an earthquake scenario can be seen in Figure 3.23.

Figure 3.23. An example of the 3-story test setup before performing an earthquake scenario.

4. EXPERIMENTAL TEST RESULTS

A series of shaking table tests conducted to evaluate effects of geogrid reinforced zones to evaluate geogrid material effect during strong ground motions, in terms of various parameters. Different reinforcement zones were created with multiple layers of geogrid. Two different 1:10 scaled 5-story and 3-story test models were utilized as a representation of medium-rise and low-rise buildings under the effect of identical strong ground motions. By 4 types of geogrid reinforced zone (N=1, N=2, N=3 and N=4) and 2 different models, 8 cases of experimental test scenarios were created, as displayed in Table 4.1. Thereby, same parameters were possible to be investigated through these cases to create comparative results. In this context, more than 300 tests were conducted and taken into account which basically contain laminar box performance tests, laminar box and soil only tests, free vibration tests, compaction tests, resonance scanning tests, and mentioned case tests.

There were also repeated tests to control accuracy of the models and setups. Among all results, one record is used for each mentioned case; although the shaking table tests were conducted for realistic PGA values of Kocaeli (0.21g), El Centro (0.35g) and Kobe (0.89g) earthquakes and with increasing/decreasing PGA values of the same motions.

Table 4.1. Experimental test setup definitions for all cases of proposed Geogrid Reinforced Zones, in the content of this study.

Case ID	Number of Story	Number of Geogrid Layers (N)	Cyclic Sinusoidal Motion	Kocaeli Eq. (1999)	El Centro Eq. (1940)	Kobe Eq. (1995)	Kocaeli Eq. - IZN (1999)
Reference -5	5	-	2.33 Hz	0.21 g 0.51 g	0.35 g 0.55 g 0.89 g	0.74 g 0.89 g	0.12 g 0.24 g
Case 1	5	1	8.58 Hz				
Case 2	5	2	13.34 Hz				
Case 3	5	3	17.52 Hz				
Case 4	5	4	19.90 Hz				
Reference -3	3	-					
Case 5	3	1	3.93 Hz				
Case 6	3	2	12.46 Hz				
Case 7	3	3	18.35 Hz				
Case 8	3	4					

As mentioned in previous studies, top floor horizontal acceleration response, foundation horizontal acceleration response and first floor story drift values of both 3 and 5-story model structures are obtained in terms of peak and root mean square (RMS) response values. These two calculation methods were compared and a reduction percentage was acquired for reinforced and unreinforced (reference) setups.

4.1. Soil Response to the Seismic Motions

To be able to understand response of the soil material under different seismic motions, mentioned strong ground motion excitations were applied to soil. Response of Silivri sand was obtained in this concept and same material was used as soil deposit of all setups. As displayed in Figure 3.9, A1 accelerometer was placed on shaking table, A5 placed in the first 25 cm-level of the soil material, close to the foundation (below all geogrid layers) and A12 accelerometer was placed near the surface of the soil, at top (free surface cases). Only soil with laminar box response is displayed in Table 4.2. The values were obtained under Kocaeli, El Centro and Kobe earthquake motions with real PGA values and cyclic sinusoidal motion with 2 Hz (0.5g) for non-structural models.

Table 4.2. Soil response to the mentioned seismic motions.

Soil Response to the Seismic Motion					
Sesimic Motions	Peak Acceleration (g)			Acceleration Difference (%)	
	A1	A5	A12	From A1 to A5	From A5 to A12
Kocaeli Earthquake	0.2144	0.2076	0.3978	-3	92
El Centro Earthquake	0.3485	0.3290	0.5813	-6	77
Kobe Earthquake	0.8812	0.8665	0.7485	-2	-14
Cyclic Sinusoidal Motion	0.4967	0.4784	0.7501	-4	57

From deeper soil to surface, acceleration values were decreased for lower level accelerometer because of the energy dissipation of seismic waves, as expected.

A different comparison was done for all N setups and unreinforced case for the non-structural case. A1 accelerometer and A12 accelerometer were compared for the same motions. Differences within the mentioned accelerometers in terms of RMS and peak acceleration response values for the accelerometers are displayed in Table 4.3 and comparison percentages were obtained for all N setups, thus, all cases.

Table 4.3. Acceleration reduction percentages from A1 to A12 depending on free surface tests of all case scenarios.

	Acceleration Reduction								
	Cases	Input Motion							
		Difference from A1 to A12 (%)							
		Kocaeli Earthquake		El Centro Earthquake		Kobe Earthquake		Cyclic Sinusoidal Motion	
		RMS	Peak	RMS	Peak	RMS	Peak	RMS	Peak
Unreinforced	A1	0.0336	0.2245	0.0442	0.3488	0.0755	0.8816	0.2423	0.4868
	A12	0.0465	0.4376	0.0587	0.5811	0.0923	0.8047	0.2252	0.7352
	Difference (%)	38.20	94.92	32.98	66.62	22.30	-8.72	-7.03	51.02
N=1	A1	0.0276	0.2141	0.0367	0.3512	0.0678	0.8768	0.2434	0.4883
	A12	0.0465	0.3405	0.0536	0.4191	0.0932	0.9371	0.3451	0.9144
	Difference (%)	68.73	59.03	46.23	19.32	37.61	6.88	41.79	87.26
N=2	A1	0.0323	0.2153	0.0401	0.3413	0.0655	0.8751	0.2292	0.5014
	A12	0.0553	0.3632	0.0594	0.4741	0.0944	0.9285	0.3229	0.9071
	Difference (%)	70.88	68.74	48.18	38.90	44.18	6.11	40.91	80.93
N=3	A1	0.0260	0.2114	0.0367	0.3470	0.0635	0.8710	0.2260	0.4682
	A12	0.0415	0.3328	0.0523	0.4557	0.0869	0.9027	0.3199	0.7891
	Difference (%)	59.26	57.37	42.36	31.33	36.78	3.63	41.57	68.56
N=4	A1	0.0254	0.2178	0.0419	0.3566	0.0714	0.8680	0.2473	0.5170
	A12	0.0383	0.3153	0.0573	0.4088	0.0944	0.9187	0.3105	0.7116
	Difference (%)	50.69	44.74	36.72	14.65	32.24	5.84	25.55	37.65

The common form among the all N cases display the A1 and A12 accelerometers are in increase since the A12 is at a higher level and A1 is on the shaking table itself. From the difference percentages, it can be seen that for Kocaeli motion, geogrid reinforcements were dissipated the acceleration responses for non-structural cases. The most energy dissipation was occurred at N=4 configuration of geogrid reinforcement, compared to unreinforced case, on behalf of peak acceleration and RMS values. N=1, N=2 and N=3 cases also diminished the seismic energy. For El Centro motion, energy dissipation was occurred for all cases, and N=4 case was the most efficient, along with N=1 case, in terms of peak acceleration responses and N=4 configuration was most effective from the point of RMS values. For Kobe motion, most effective case was N=3 configuration regarding to peak acceleration response and N=3 and N=4 configurations were performing better when compared to N=1 and N=2 in terms of RMS percentages. For the cyclic sinusoidal motion, N=4 case was the most effective configuration and N=3 was performing better even tough even though there is a slight increase in the responses in point of peak acceleration responses. N=4 case displayed better performance in terms of RMS values, even though there is an increase in the response. In general, N=4 configuration displayed the most efficient results in geogrid reinforcement for non-structural cases.

4.2. Soil Response of Vertical Accelerometers (A5-A6-A11-A12)

As the accelerometer configuration displayed in Figure 3.10, response and behaviour of the vertical acceleration-time history data of the system is examined via A5-A6-A11-A12 accelerometers, which are all in the same vertical axis within the soil deposit.

Evaluation of the vertical accelerometers are conducted through the accelerometers according to geogrid reinforced and unreinforced cases. Since there are eight cases and three main earthquakes, only the Kocaeli earthquake taken into account, in Case 4, for the sake of brevity. Results of the mentioned accelerometers are displayed in Figure 4.1, accordingly.

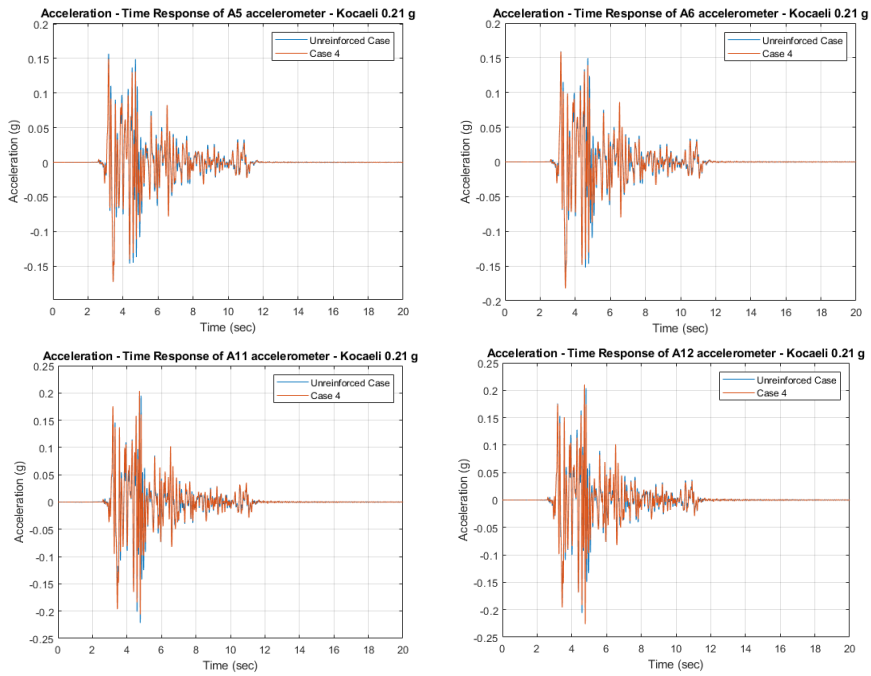

Figure 4.1. Comparison of acceleration-time histories of A5-A6-A11-A12 accelerometers, according to the Case 4 and unreinforced case under Kocaeli Earthquake.

It can be observed through the vertical accelerometers that there is nearly no difference for the A5 accelerometer for the both unreinforced and reinforced case. Since the Case 4 contains four layer of geogrid reinforcement close to the surface, A5 is the closest accelerometer to shaking table. On the other hand, the fourth layer of geogrid reinforcement stays under the A6 accelerometer and peak acceleration is reduced for this

level around 4%. In terms of A11 accelerometer, which stays above three layers of geogrid reinforcement, nearly 9% of the peak acceleration was reduced. For the A12 accelerometer, which is above all four layers of geogrid, nearly 7% of the peak acceleration was reduced, along with a clear reduction in acceleration-time history.

4.3. Unreinforced Soil with 5-Story Building

The mentioned three performance indicator parameters were evaluated for 5-story building model under Kocaeli, El Centro and Kobe earthquakes as displayed in Figure 4.2, Figure 4.3 and Figure 4.4. Maximum value of foundation acceleration response was measured as 0.35g, maximum top floor acceleration response was measured as 0.81g and maximum first floor drift was measured as 2.24cm for Kocaeli earthquake. Maximum foundation acceleration response, top floor acceleration response and first floor drift of El Centro earthquake is measured as 0.44g, 1.15g and 2.3 cm respectively. Additionally, maximum foundation acceleration response, top floor acceleration response and first floor drift of Kobe earthquake is measured as 0.81g, 1.43g and 2.28 cm respectively.

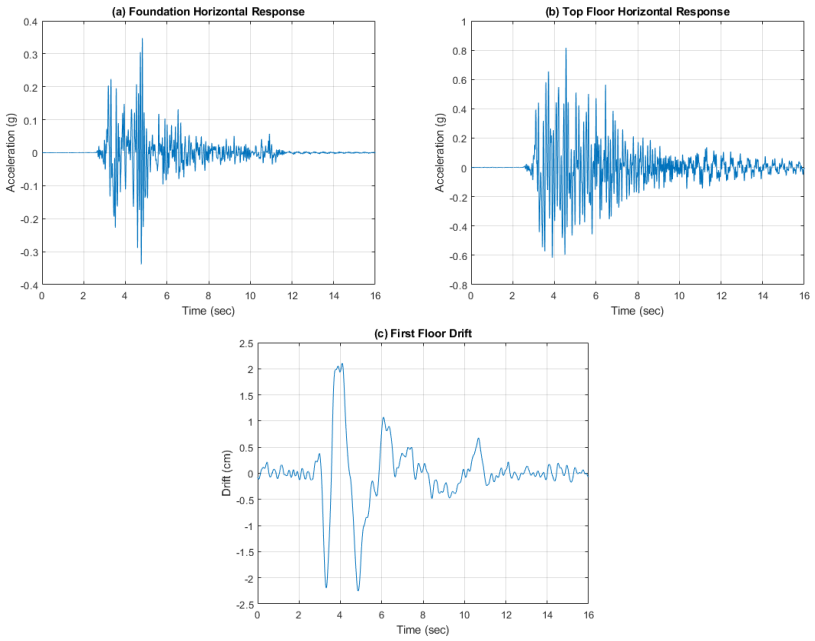

Figure 4.2. Horizontal acceleration response of foundation (a), Horizontal acceleration response of top floor (b) and First floor drift of 5-story building model under Kocaeli Earthquake.

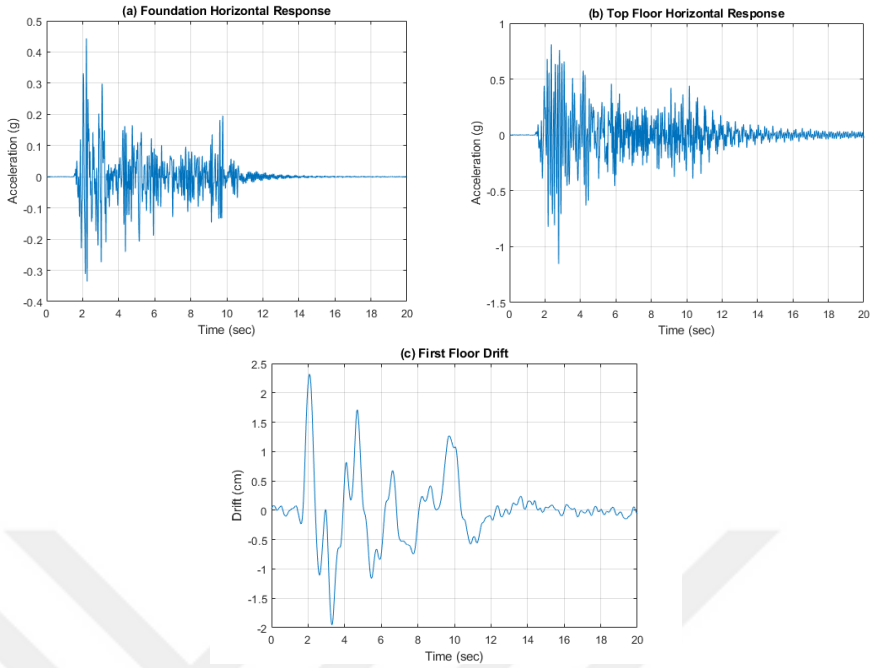

Figure 4.3. Horizontal acceleration response of foundation (a), Horizontal acceleration response of top floor (b) and First floor drift of 5-story building model under El Centro Earthquake.

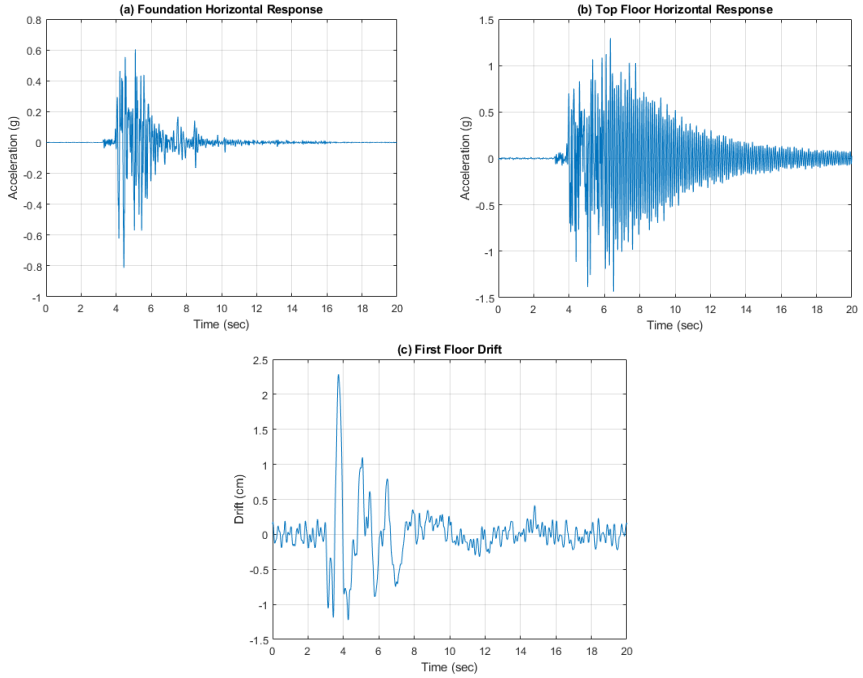

Figure 4.4. Horizontal acceleration response of foundation (a), Horizontal acceleration response of top floor (b) and First floor drift of 5-story building model under Kobe Earthquake.

4.4. Case 1 – N=1 Geogrid Reinforced 5-Story Building Model

The mentioned three performance indicator parameters were evaluated for 5-story building model under Kocaeli, Kobe and El Centro earthquakes. Applied configuration information was mentioned in Section 3.9 and configuration of geogrid reinforced zones for all configuration types was described in Figure 3.22. For this case, N=1 layer of geogrid was used for 5-story building model. Tests were conducted for all strong ground motions and sinusoidal motions. Results are demonstrated for Kocaeli, El Centro and Kobe earthquakes, respectively.

4.4.1. Seismic Response of Case 1 for Kocaeli Earthquake

Peak foundation acceleration response reduction and top floor acceleration response reduction were obtained as 11.96% and 21.77% respectively. In addition to peak values, root mean square reductions of the same acceleration responses were detected as 6.87% and -10.39% respectively, as displayed in Figure 4.5a and Figure 4.5b. A reduction of the first floor story drift was observed as 0.88% for peak value and 0.68% for RMS value, as displayed in Figure 4.5c and Figure 4.5d. All performance parameters were summarized and demonstrated in Table 4.4. Maximum reduction of arias intensity was observed at the foundation by 18.39% as in Figure 4.5e. In addition, as displayed in Figure 4.5f, base shear and base moment of the test model at the foundation level were reduced by a slight 0.48% and 0.63% respectively, in terms of peak values.

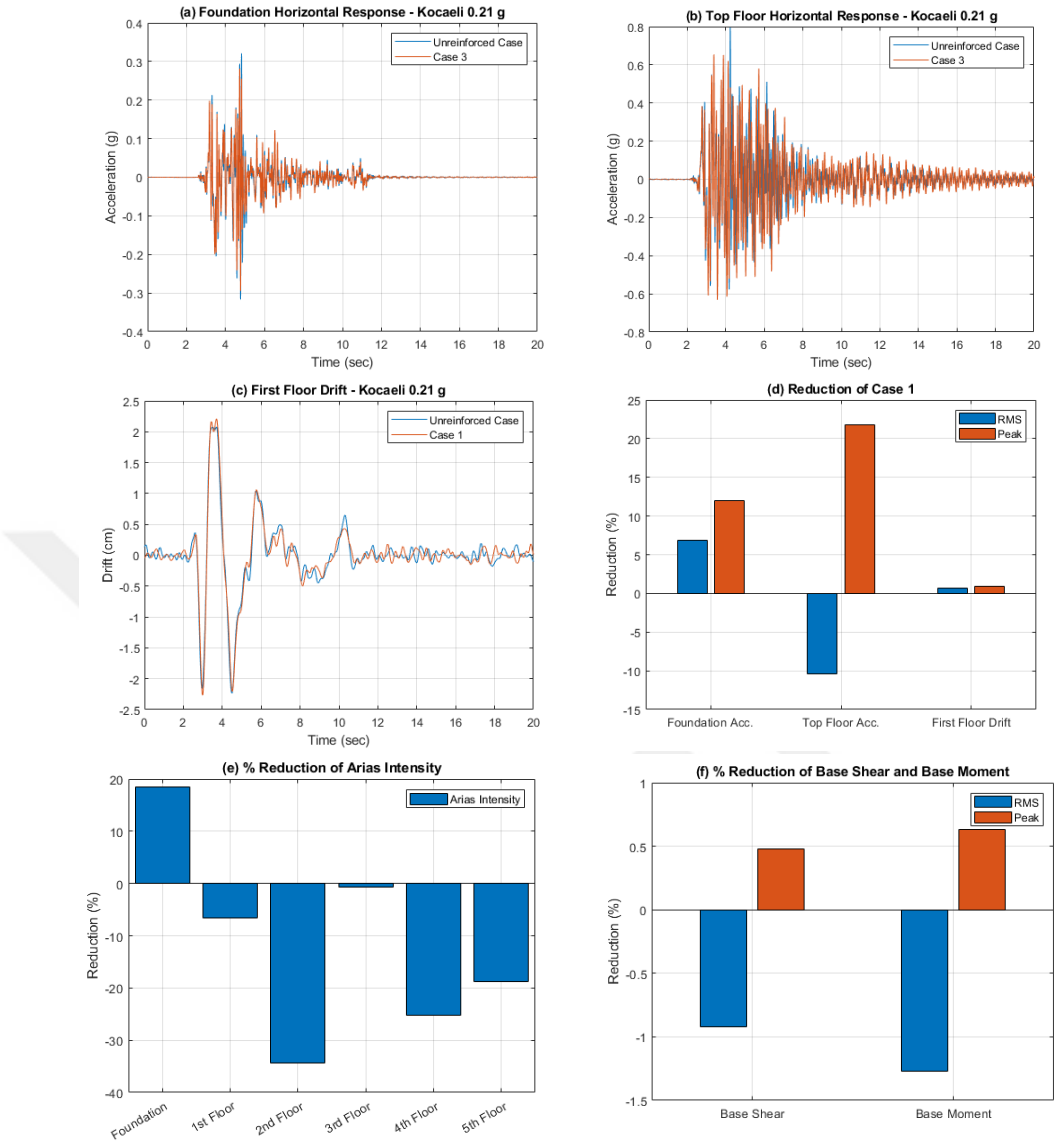

Figure 4.5. Foundation acceleration response (a), Top floor acceleration response (b), First floor acceleration response (c), (%) Reduction of Case 1 (d), (%) Reduction of arias intensity (e), (%) Reduction of base shear and base moment (f) under Kocaeli Earthquake.

Table 4.4. Horizontal acceleration, Horizontal story drift, Arias intensity, Base Shear and Base Moment reduction factors under Kocaeli Earthquake (Case 1).

Case 1 under Kocaeli (PGA=0.21g) Earthquake												
	Foundation		1st Floor		2nd Floor		3rd Floor		4th Floor		5th Floor	
	RMS	Peak	RMS	Peak	RMS	Peak	RMS	Peak	RMS	Peak	RMS	Peak
Horizontal Acceleration (g)												
Unreinforced	0.0300	0.3257	0.0758	0.5536	0.0824	0.6674	0.0663	0.5638	0.0602	0.4036	0.0959	0.8013
Case 1	0.0279	0.2868	0.0807	0.5035	0.0981	0.6444	0.0682	0.4912	0.0701	0.4909	0.1058	0.6268
Reduction (%)	6.87	11.96	-6.59	9.04	-19.05	3.45	-2.83	12.87	-16.47	-21.62	-10.39	21.77
Horizontal Story Drift (cm)												
Unreinforced	-	-	0.43	2.20	0.52	2.90	0.58	3.61	0.62	3.83	0.61	4.08
Case 1	-	-	0.43	2.18	0.52	3.01	0.58	3.44	0.62	3.88	0.62	4.03
Reduction (%)	-	-	0.68	0.88	0.71	-3.61	-0.10	4.75	-0.19	-1.35	-1.66	1.11
Arias Intensity (g-sec)												
Unreinforced	0.0047		0.0303		0.0356		0.0229		0.0191		0.0468	
Case 1	0.0039		0.0323		0.0478		0.0231		0.0240		0.0556	
Reduction (%)	18.39		-6.60		-34.33		-0.61		-25.23		-18.73	
	Base Shear (kN)				Base Moment (kN-m)							
	RMS		Peak		RMS		Peak					
Unreinforced	0.55		3.41		0.38		2.39					
Case 1	0.55		3.39		0.38		2.37					
Reduction (%)	-0.92		0.48		-1.27		0.63					

4.4.2. Seismic Response of Case 1 for El Centro Earthquake

Maximum reduction of peak acceleration response was observed in first floor by a 30.48%. Peak foundation acceleration response reduction and top floor acceleration response reduction were obtained as 5.50% and 29.47% respectively. In addition to peak values, root mean square reductions of the same acceleration responses were detected as 5.61% and 15.66% respectively, as displayed in Figure 4.6a and Figure 4.6b. A reduction of the first floor story drift was observed as 3.21% for peak value and 1.28% for RMS value, as displayed in Figure 4.6c and Figure 4.6d. All performance parameters were summarized and demonstrated in Table 4.5. Maximum reduction of arias intensity was observed at the first floor by 46.15% as in Figure 4.6e. In addition, as displayed in Figure 4.6f, base shear and base moment of the test model at the foundation level were reduced by a slight 1.05% and 1.50% respectively, in terms of peak values and 4.50% and 4.22% in terms of RMS values, respectively.

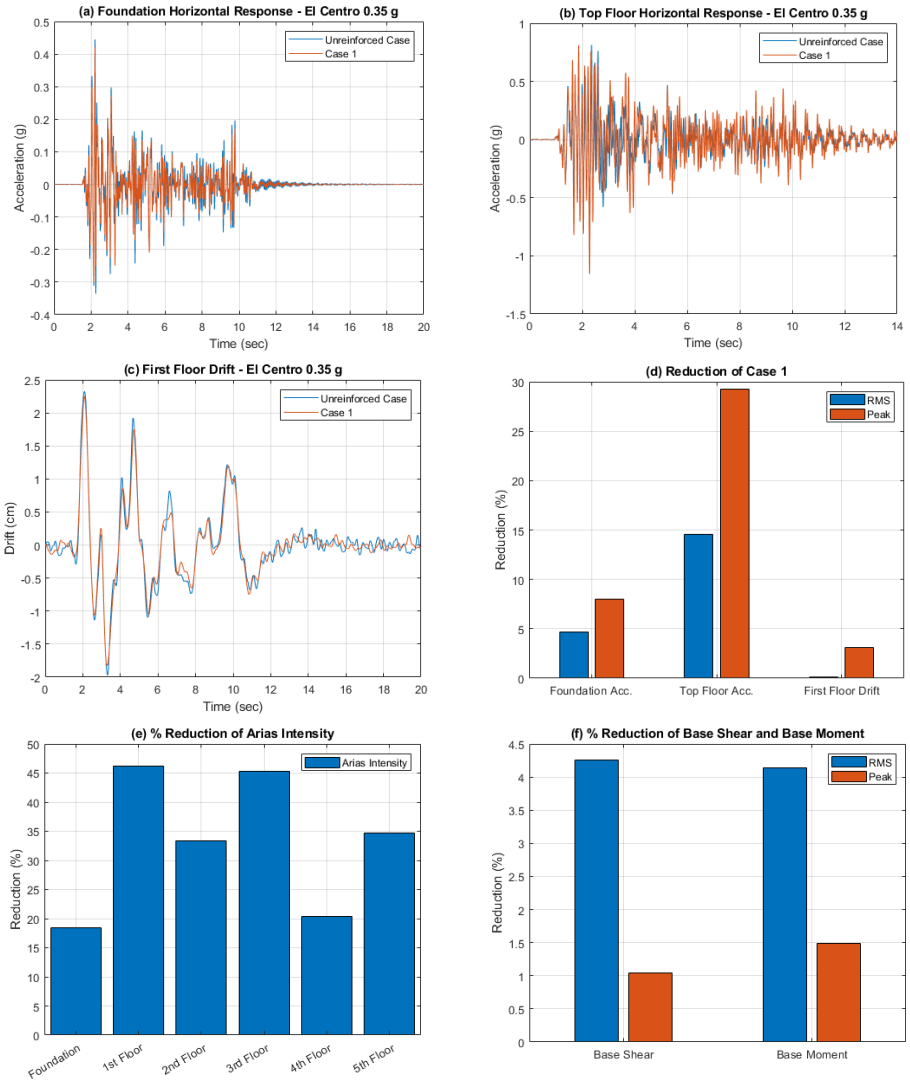

Figure 4.6. Foundation acceleration response (a), Top floor acceleration response (b), First floor acceleration response (c), (%) Reduction of Case 1 (d), (%) Reduction of arias intensity (e), (%) Reduction of base shear and base moment (f) under El Centro Earthquake.

.

Table 4.5. Horizontal acceleration, Horizontal story drift, Arias intensity, Base Shear and Base Moment reduction factors under El Centro Earthquake (Case 1).

Case 1 under El Centro (PGA=0.35g) Earthquake												
	Foundation		1st Floor		2nd Floor		3rd Floor		4th Floor		5th Floor	
	RMS	Peak	RMS	Peak	RMS	Peak	RMS	Peak	RMS	Peak	RMS	Peak
Horizontal Acceleration (g)												
Unreinforced	0.0379	0.4450	0.0927	0.8326	0.0939	0.9076	0.0793	0.5977	0.0658	0.5300	0.1122	1.1553
Case 1	0.0358	0.4205	0.0723	0.5788	0.0810	0.7044	0.0626	0.4756	0.0619	0.4389	0.0947	0.8148
Reduction (%)	5.61	5.50	22.04	30.48	13.71	22.39	20.98	20.43	5.93	17.18	15.66	29.47
Horizontal Story Drift (cm)												
Unreinforced	-	-	0.39	2.32	0.51	2.99	0.55	3.37	0.60	3.79	0.58	3.88
Case 1	-	-	0.39	2.25	0.46	3.07	0.53	3.44	0.56	3.65	0.58	3.78
Reduction (%)	-	-	1.28	3.21	8.87	-2.70	3.54	-2.01	5.95	3.81	-0.09	2.61
Arias Intensity (g-sec)												
Unreinforced	0.0097		0.0578		0.0593		0.0423		0.0291		0.0847	
Case 1	0.0077		0.0311		0.0395		0.0231		0.0232		0.0539	
Reduction (%)	20.03		46.15		33.42		45.25		20.35		36.35	
	Base Shear (kN)				Base Moment (kN-m)							
	RMS		Peak		RMS		Peak					
Unreinforced	0.52		3.62		0.36		2.50					
Case 1	0.50		3.58		0.35		2.46					
Reduction (%)	4.50		1.05		4.22		1.50					

4.4.3. Seismic Response of Case 1 for Kobe Earthquake

For the Kobe earthquake results; peak foundation acceleration response reduction and top floor acceleration response reduction were obtained as 15.16% and -3.17% respectively. In addition to peak values, root mean square reductions of the same acceleration responses were detected as 16.01% and 28.27% respectively, as displayed in Figure 4.7a and Figure 4.7b. A reduction of the first floor story drift was observed as 26.43% for peak value and 18.57% for RMS value, as displayed in Figure 4.7c and Figure 4.7d. All performance parameters were summarized and demonstrated in Table 4.6. Maximum reduction of arias intensity was observed at the first floor by 46.55% as in Figure 4.7e. In addition, as displayed in Figure 4.7f, base shear and base moment of the test model at the foundation level were reduced by 6.74% and 3.31% respectively, in terms of peak values and 16.71% and 15.69% in terms of RMS values, respectively.

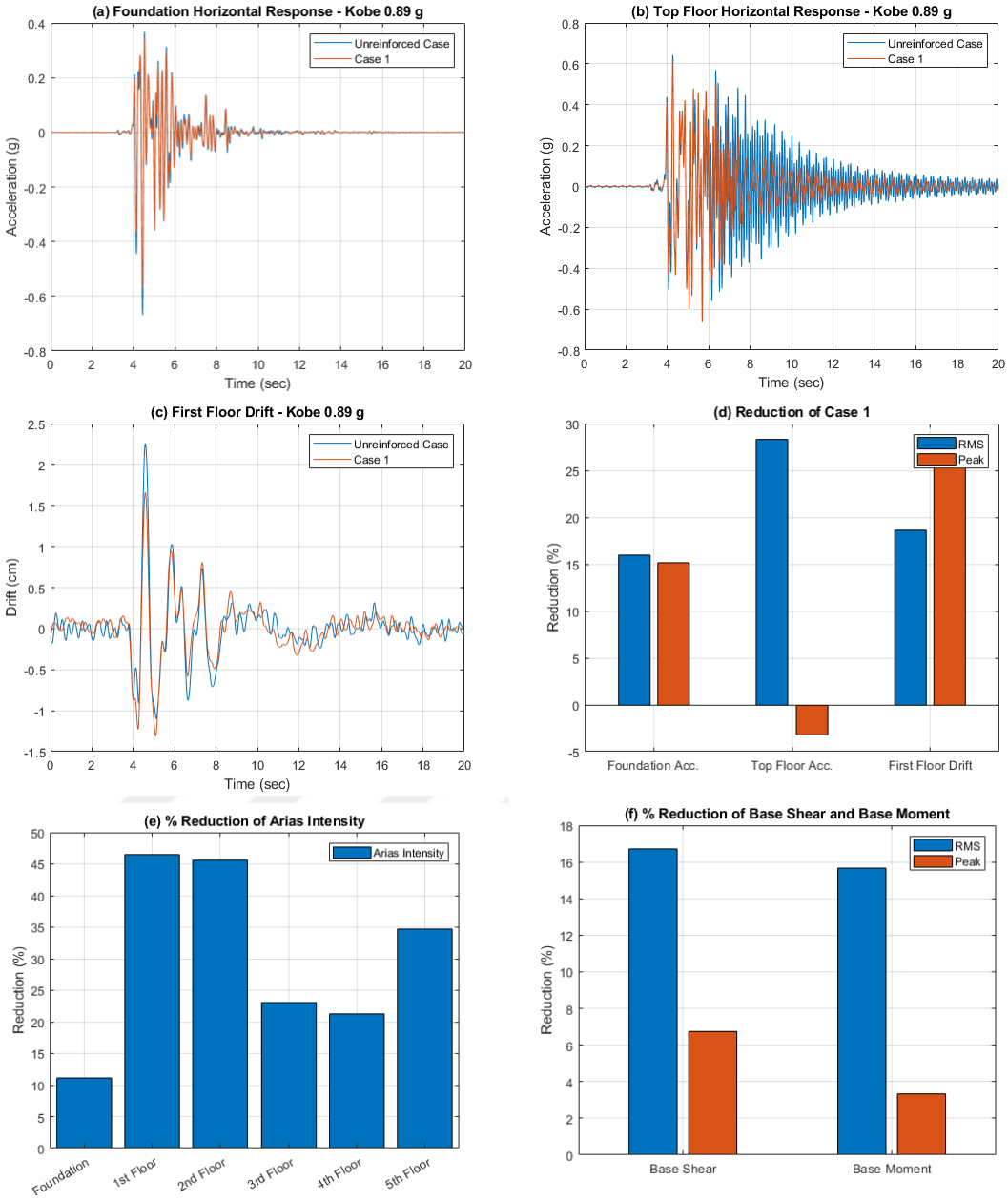

Figure 4.7. Foundation acceleration response (a), Top floor acceleration response (b), First floor acceleration response (c), (%) Reduction of Case 1 (d), (%) Reduction of arias intensity (e), (%) Reduction of base shear and base moment (f) under Kobe Earthquake.

Table 4.6. Horizontal acceleration, Horizontal story drift, Arias intensity, Base Shear and Base Moment reduction factors under Kobe Earthquake (Case 1).

Case 1 under Kobe (PGA=0.89g) Earthquake												
	Foundation		1st Floor		2nd Floor		3rd Floor		4th Floor		5th Floor	
	RMS	Peak	RMS	Peak	RMS	Peak	RMS	Peak	RMS	Peak	RMS	Peak
Horizontal Acceleration (g)												
Unreinforced	0.0508	0.6686	0.1865	1.2613	0.2041	1.1296	0.1378	1.0246	0.1192	0.8427	0.1071	0.6432
Case 1	0.0427	0.5672	0.1200	1.3895	0.1343	1.1983	0.1082	1.1252	0.0944	0.9349	0.0768	0.6636
Reduction (%)	16.01	15.16	35.63	-10.16	34.19	-6.08	21.49	-9.82	20.77	-10.95	28.27	-3.17
Horizontal Story Drift (cm)												
Unreinforced	-	-	0.28	2.26	0.55	3.08	0.59	3.83	0.67	4.52	0.68	5.17
Case 1	-	-	0.22	1.66	0.43	2.68	0.49	3.55	0.56	4.43	0.60	5.27
Reduction (%)	-	-	18.57	26.43	21.23	13.10	17.70	7.29	17.51	1.99	11.32	-1.88
Arias Intensity (g-sec)												
Unreinforced	0.0149		0.1986		0.2401		0.1095		0.0819		0.0661	
Case 1	0.0132		0.1061		0.1306		0.0843		0.0644		0.0432	
Reduction (%)	11.14		46.55		45.62		23.03		21.32		34.63	
	Base Shear (kN)						Base Moment (kN-m)					
	RMS		Peak				RMS		Peak			
Unreinforced	0.54		5.01				0.39		3.02			
Case 1	0.45		4.67				0.33		2.92			
Reduction (%)	16.71		6.74				15.69		3.31			

4.5. Case 2 – N=2 Geogrid Reinforced 5-Story Building Model

The previously evaluated performance indicator parameters were evaluated for 5-story building model under Kocaeli, Kobe and El Centro earthquakes. Applied configuration of geogrid reinforced zone was noted in Section 3.9 and geogrid reinforced zones for all configuration types was described in Figure 3.22. For this case, N=2 layer of geogrid was used for 5-story building model. Tests were conducted for all strong ground motions and sinusoidal motions. Results are demonstrated for Kocaeli, El Centro and Kobe earthquakes, respectively.

4.5.1. Seismic Response of Case 2 for Kocaeli Earthquake

For the Kocaeli earthquake results; peak foundation acceleration response reduction and top floor acceleration response reduction were obtained as 13.51% and 22.02% respectively. In addition to peak values, root mean square reductions of the same acceleration responses were detected as 17.26% and 29.28% respectively, as displayed in Figure 4.8a and Figure 4.8b. A reduction of the first floor story drift was observed as -0.50% for peak value and 21.25% for RMS value, as displayed in Figure 4.8c and Figure

4.8d. All performance parameters were summarized and demonstrated in Table 4.7. Maximum reduction of arias intensity was observed at the foundation level by 19.56% as in Figure 4.8e. In addition, as displayed in Figure 4.8f, base shear and base moment of the test model at the foundation level were reduced by -1.01% and -1.16% respectively, in terms of peak values and 6.80% and 4.51% in terms of RMS values, respectively.

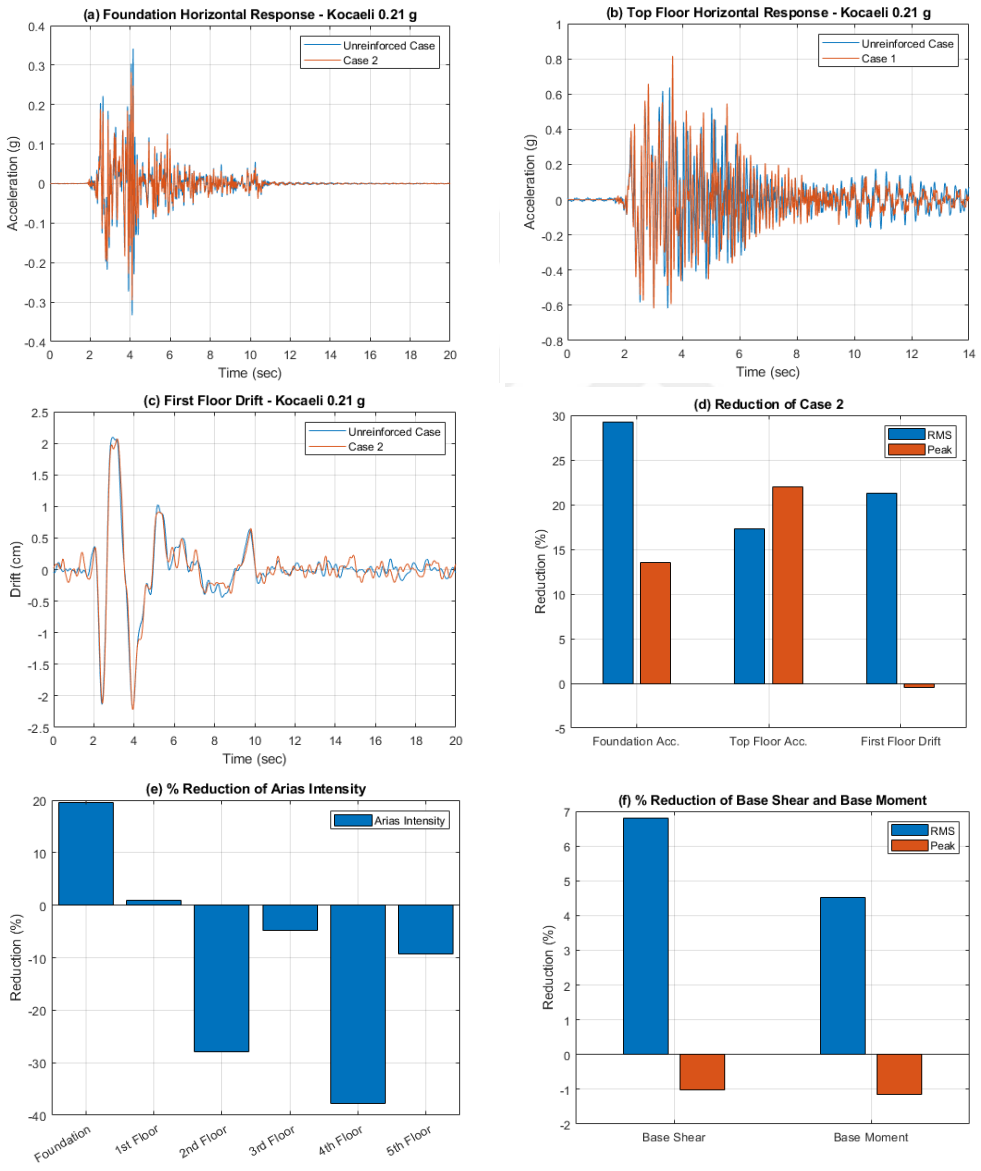

Figure 4.8. Foundation acceleration response (a), Top floor acceleration response (b), First floor acceleration response (c), (%) Reduction of Case 2 (d), (%) Reduction of arias intensity (e), (%) Reduction of base shear and base moment (f) under Kocaeli Earthquake.

Table 4.7. Horizontal acceleration, Horizontal story drift, Arias intensity, Base Shear and Base Moment reduction factors under Kocaeli Earthquake (Case 2).

Case 2 under Kocaeli (PGA=0.21g) Earthquake												
	Foundation		1st Floor		2nd Floor		3rd Floor		4th Floor		5th Floor	
	RMS	Peak	RMS	Peak	RMS	Peak	RMS	Peak	RMS	Peak	RMS	Peak
Horizontal Acceleration (g)												
Unreinforced	0.0311	0.3414	0.0773	0.5536	0.0829	0.6675	0.0666	0.5638	0.0602	0.4037	0.0967	0.8167
Case 2	0.0220	0.2953	0.0601	0.5012	0.0739	0.6428	0.0538	0.5044	0.0566	0.5207	0.0800	0.6369
Reduction (%)	29.28	13.51	22.21	9.46	10.79	3.70	19.25	10.54	5.99	-29.00	17.26	22.02
Horizontal Story Drift (cm)												
Unreinforced	-	-	0.44	2.21	0.53	2.90	0.58	3.61	0.62	3.83	0.61	4.08
Case 2	-	-	0.34	2.22	0.52	3.03	0.55	3.50	0.58	3.84	0.59	4.21
Reduction (%)	-	-	21.25	-0.50	0.85	-4.36	4.99	3.20	5.86	-0.44	4.12	-3.18
Arias Intensity (g-sec)												
Unreinforced	0.0050		0.0303		0.0356		0.0229		0.0191		0.0488	
Case 2	0.0040		0.0301		0.0455		0.0241		0.0263		0.0533	
Reduction (%)	19.56		0.85		-27.95		-4.88		-37.70		-9.24	
	Base Shear (kN)				Base Moment (kN-m)							
	RMS		Peak		RMS		Peak					
Unreinforced	0.55		3.41		0.38		2.39					
Case 2	0.51		3.44		0.36		2.41					
Reduction (%)	6.80		-1.01		4.51		-1.16					

4.5.2. Seismic Response of Case 2 for El Centro Earthquake

The maximum peak foundation acceleration response reduction and top floor acceleration response reduction were obtained as -4.74% and 19.24% respectively. In addition to peak values, root mean square reductions of the same acceleration responses were detected as 28.06% and 26.76% respectively, as displayed in Figure 4.9a and Figure 4.9b. A reduction of the first floor story drift was observed as 2.89% for peak value and 25.79% for RMS value, as displayed in Figure 4.9c and Figure 4.9d. All performance parameters were summarized and demonstrated in Table 4.8. Maximum reduction of arias intensity was observed at the first floor level by 34.66% as in Figure 4.9e. In addition, as displayed in Figure 4.9f, base shear and base moment of the test model at the foundation level were reduced by -1.62% and -2.77% respectively, in terms of peak values and 14.74% and 12.57% in terms of RMS values, respectively.

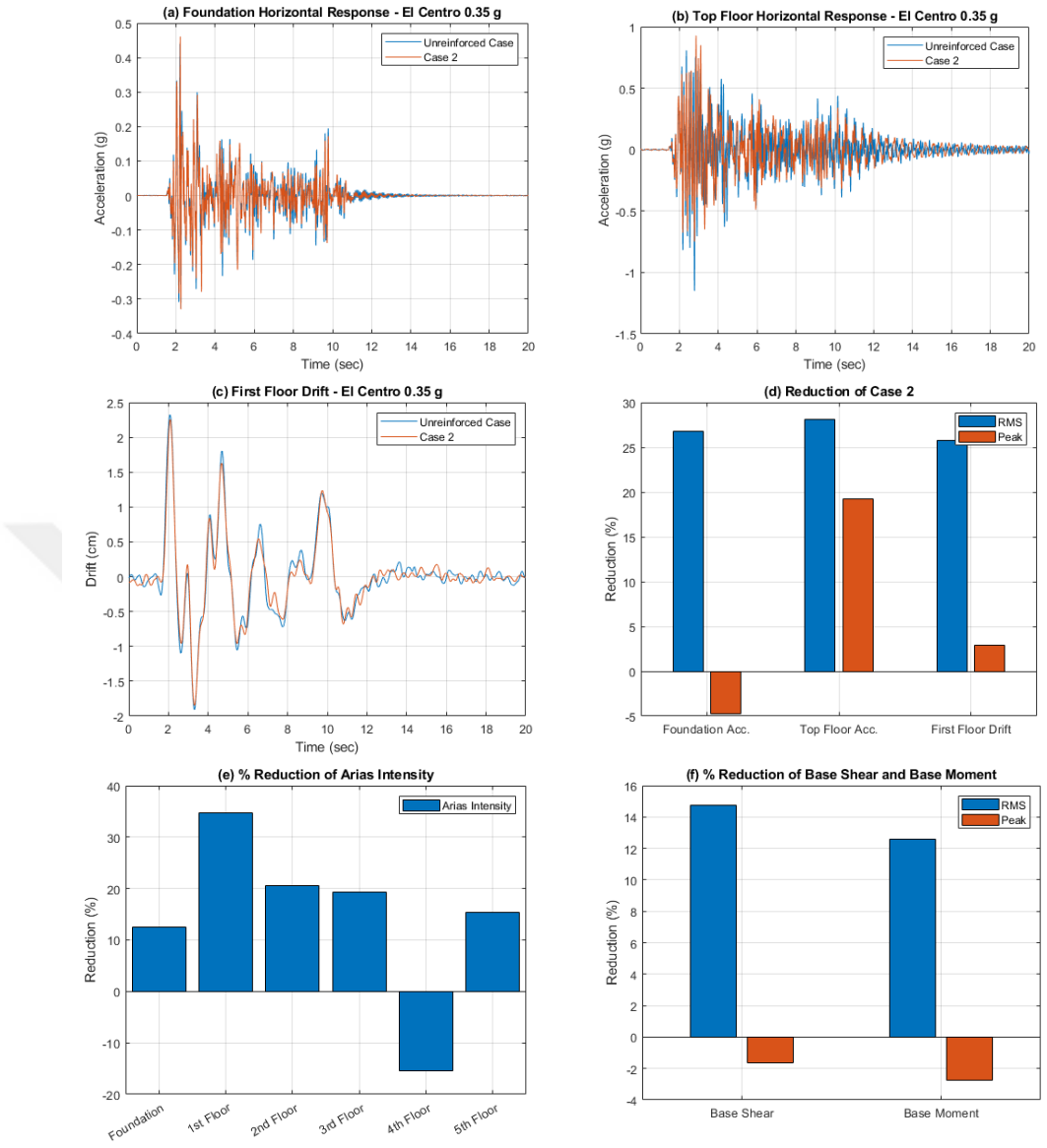

Figure 4.9. Foundation acceleration response (a), Top floor acceleration response (b), First floor acceleration response (c), (%) Reduction of Case 2 (d), (%) Reduction of arias intensity (e), (%) Reduction of base shear and base moment (f) under El Centro Earthquake.

Table 4.8. Horizontal acceleration, Horizontal story drift, Arias intensity, Base Shear and Base Moment reduction factors under El Centro Earthquake (Case 2).

Case 2 under El Centro (PGA=0.35g) Earthquake												
	Foundation		1st Floor		2nd Floor		3rd Floor		4th Floor		5th Floor	
	RMS	Peak	RMS	Peak	RMS	Peak	RMS	Peak	RMS	Peak	RMS	Peak
Horizontal Acceleration (g)												
Unreinforced	0.0377	0.4401	0.0927	0.8326	0.0939	0.9076	0.0793	0.5977	0.0658	0.5300	0.1116	1.1493
Case 2	0.0276	0.4609	0.0587	0.6232	0.0656	0.8157	0.0558	0.5380	0.0554	0.5001	0.0803	0.9281
Reduction (%)	26.76	-4.74	36.68	25.15	30.16	10.12	29.66	9.99	15.73	5.63	28.06	19.24
Horizontal Story Drift (cm)												
Unreinforced	-	-	0.39	2.32	0.51	2.99	0.55	3.37	0.60	3.79	0.58	3.88
Case 2	-	-	0.29	2.26	0.46	2.96	0.48	3.45	0.51	3.85	0.53	4.11
Reduction (%)	-	-	25.79	2.89	10.01	0.88	11.80	-2.20	14.00	-1.45	9.94	-5.90
Arias Intensity (g-sec)												
Unreinforced	0.0095		0.0578		0.0593		0.0423		0.0291		0.0838	
Case 2	0.0083		0.0378		0.0472		0.0341		0.0336		0.0709	
Reduction (%)	12.54		34.66		20.48		19.34		-15.51		15.34	
	Base Shear (kN)				Base Moment (kN-m)							
	RMS		Peak		RMS		Peak					
Unreinforced	0.52		3.62		0.36		2.50					
Case 2	0.44		3.68		0.31		2.57					
Reduction (%)	14.74		-1.62		12.57		-2.77					

4.5.3. Seismic Response of Case 2 for Kobe Earthquake

Maximum reduction in peak foundation acceleration response and top floor acceleration response were obtained as 5.51% and 10.18% respectively. In addition to peak values, root mean square reductions of the same acceleration responses were detected as 39.23% and 14.80% respectively, as displayed in Figure 4.10a and Figure 4.10b. A reduction of the first floor story drift was observed as 24.66% for peak value and 13.00% for RMS value, as displayed in Figure 4.10c and Figure 4.10d. All performance parameters were summarized and demonstrated in Table 4.9. Maximum reduction of arias intensity was observed at the second floor level by 54.45% as in Figure 4.10e. In addition, as displayed in Figure 4.10f, base shear and base moment of the test model at the foundation level were reduced by 2.97% and -1.27% respectively, in terms of peak values and -8.46% and -6.92% in terms of RMS values, respectively.

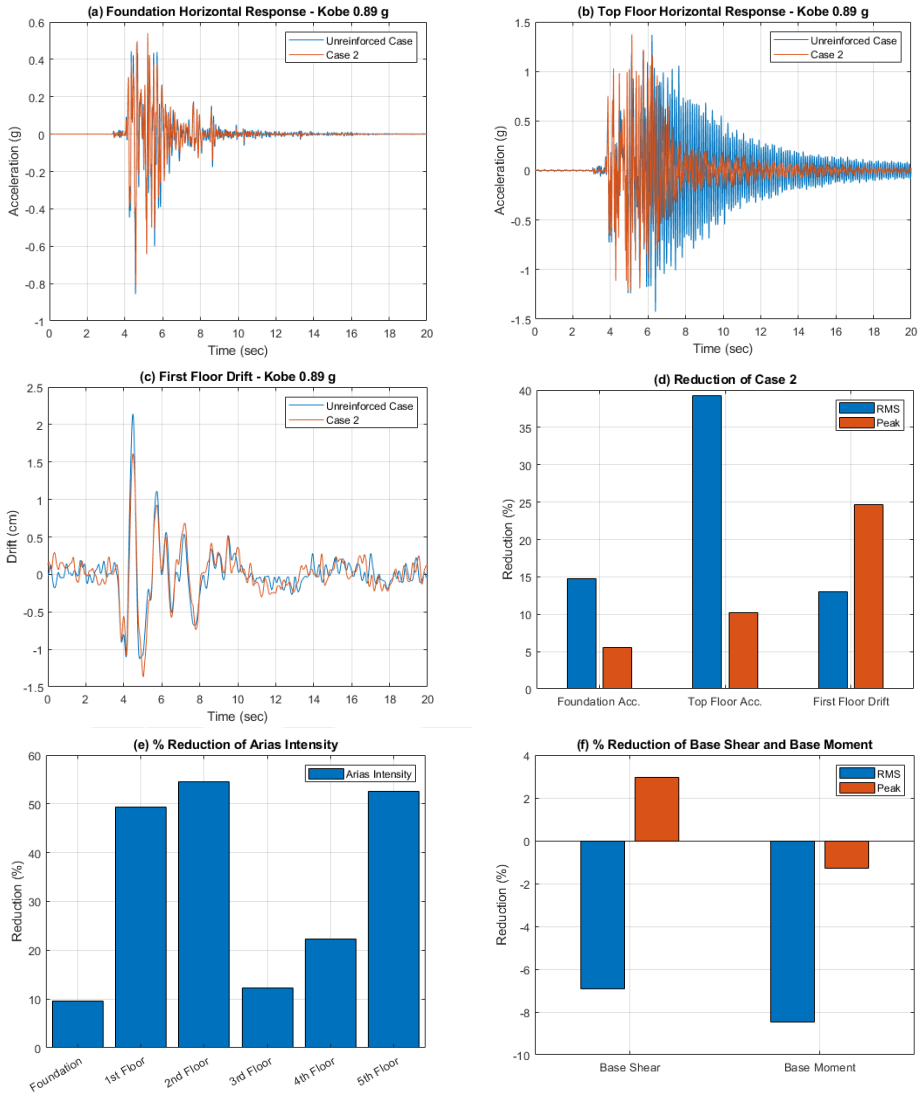

Figure 4.10. Foundation acceleration response (a), Top floor acceleration response (b), First floor acceleration response (c), (%) Reduction of Case 2 (d), (%) Reduction of arias intensity (e), (%) Reduction of base shear and base moment (f) under Kobe Earthquake.

Table 4.9. Horizontal acceleration, Horizontal story drift, Arias intensity, Base Shear and Base Moment reduction factors under Kobe Earthquake (Case 2).

Case 2 under Kobe (PGA=0.89g) Earthquake												
	Foundation		1st Floor		2nd Floor		3rd Floor		4th Floor		5th Floor	
	RMS	Peak	RMS	Peak	RMS	Peak	RMS	Peak	RMS	Peak	RMS	Peak
Horizontal Acceleration (g)												
Unreinforced	0.0617	0.8570	0.1838	1.3428	0.2074	1.2466	0.1262	1.0716	0.1169	0.8205	0.2239	1.4921
Case 2	0.0526	0.8098	0.1158	1.5007	0.1256	1.2041	0.1051	1.2079	0.0903	0.9947	0.1361	1.3403
Reduction (%)	14.80	5.51	37.04	-11.76	39.44	3.41	16.72	-12.72	22.79	-21.23	39.23	10.18
Horizontal Story Drift (cm)												
Unreinforced	-	-	0.25	2.14	0.44	3.46	0.50	4.12	0.58	4.53	0.59	5.19
Case 2	-	-	0.22	1.61	0.50	3.18	0.55	3.66	0.61	4.67	0.65	5.74
Reduction (%)	-	-	13.00	24.66	-14.08	8.09	-8.49	11.09	-4.82	-3.23	-9.21	-10.43
Arias Intensity (g-sec)												
Unreinforced	0.0259		0.2248		0.2940		0.1070		0.0890		0.3309	
Case 2	0.0235		0.1137		0.1339		0.0938		0.0691		0.1572	
Reduction (%)	9.49		49.42		54.45		12.31		22.34		52.50	
	Base Shear (kN)				Base Moment (kN-m)							
	RMS		Peak		RMS		Peak					
Unreinforced	0.46		5.17		0.34		3.09					
Case 2	0.49		5.01		0.37		3.13					
Reduction (%)	-6.92		2.97		-8.46		-1.27					

4.6. Case 3 – N=3 Geogrid Reinforced 5-Story Building Model

The previously evaluated performance indicator parameters were evaluated for 5-story building model under Kocaeli, Kobe and El Centro earthquakes. Applied configuration of geogrid reinforced zone was noted in Section 3.9 and geogrid reinforced zones for all configuration types was described in Figure 3.22. For this case, N=3 layer of geogrid was used for 5-story building model. Tests were conducted for all strong ground motions and sinusoidal motions. Results are demonstrated for Kocaeli, El Centro and Kobe earthquakes, respectively.

4.6.1. Seismic Response of Case 3 for Kocaeli Earthquake

Horizontal peak acceleration response of foundation and top floor were measured as 12.74% and 15.18% respectively. In addition to peak values, root mean square reductions of the same acceleration responses were detected as 9.50% and -3.57% respectively, as displayed in Figure 4.11a and Figure 4.11b. A reduction of the first floor story drift was observed as 6.03% for peak value and 5.83% for RMS value, as displayed in Figure 4.11c and Figure 4.11d. All performance parameters were summarized and demonstrated in

Table 4.10. Maximum reduction of arias intensity was observed at the foundation level by 16.58% as in Figure 4.11e. In addition, as displayed in Figure 4.11f, base shear and base moment of the specific case at the foundation level were reduced by -4.22% and -5.53% respectively, in terms of peak values and -3.24% and -4.62% in terms of RMS values, correspondingly.

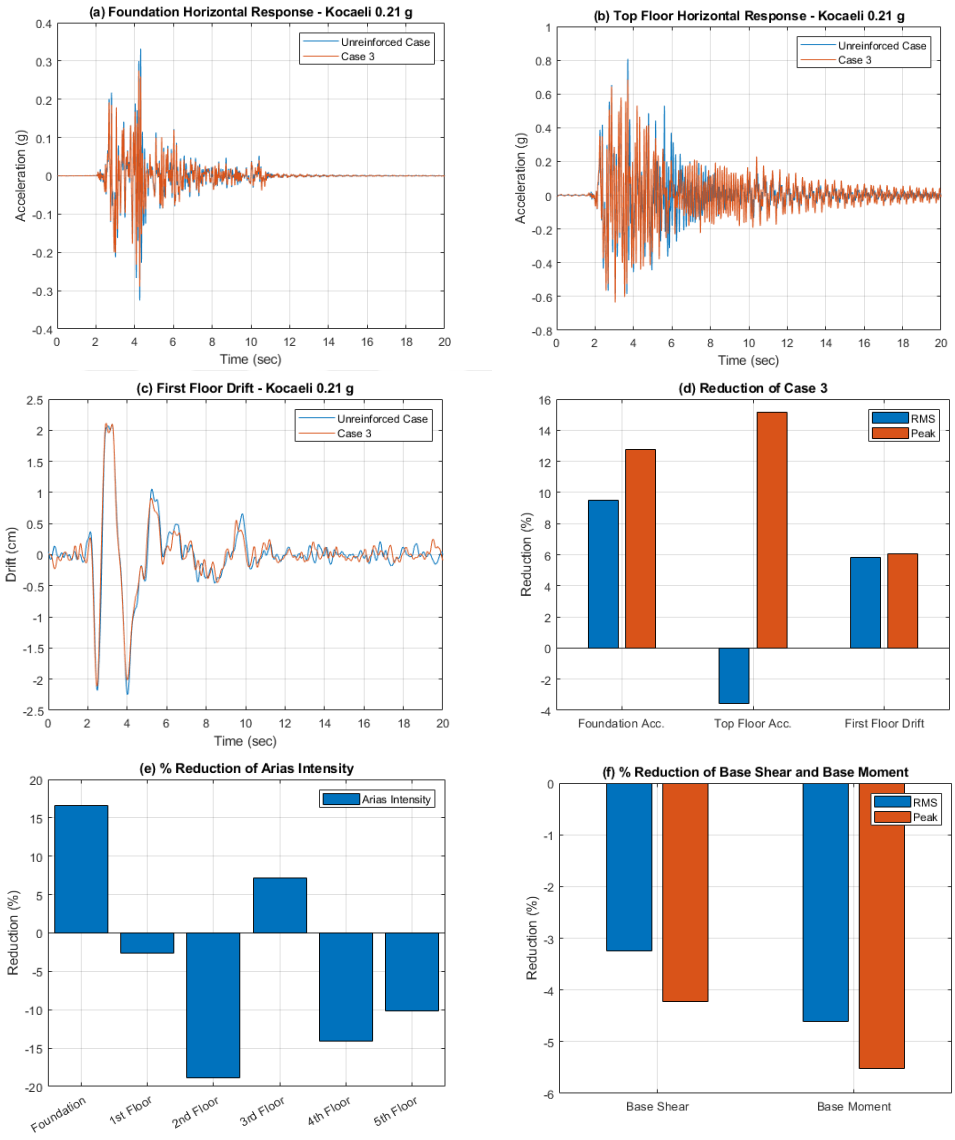

Figure 4.11. Foundation acceleration response (a), Top floor acceleration response (b), First floor acceleration response (c), (%) Reduction of Case 3 (d), (%) Reduction of arias intensity (e), (%) Reduction of base shear and base moment (f) under Kocaeli Earthquake.

Table 4.10. Horizontal acceleration, Horizontal story drift, Arias intensity, Base Shear and Base Moment reduction factors under Kocaeli Earthquake (Case 3).

Case 3 under Kocaeli (PGA=0.21g) Earthquake												
	Foundation		1st Floor		2nd Floor		3rd Floor		4th Floor		5th Floor	
	RMS	Peak	RMS	Peak	RMS	Peak	RMS	Peak	RMS	Peak	RMS	Peak
Horizontal Acceleration (g)												
Unreinforced	0.0306	0.3319	0.0762	0.5536	0.0827	0.6674	0.0674	0.5638	0.0610	0.4036	0.0962	0.8078
Case 3	0.0277	0.2896	0.0767	0.4831	0.0894	0.6519	0.0635	0.4935	0.0643	0.4392	0.0996	0.6852
Reduction (%)	9.50	12.74	-0.73	12.74	-8.20	2.33	5.78	12.47	-5.41	-8.81	-3.57	15.18
Horizontal Story Drift (cm)												
Unreinforced	-	-	0.44	2.25	0.53	2.90	0.58	3.61	0.62	3.83	0.61	4.08
Case 3	-	-	0.41	2.11	0.56	3.13	0.60	3.68	0.64	4.06	0.64	4.39
Reduction (%)	-	-	5.83	6.03	-6.37	-7.70	-3.52	-1.85	-3.67	-6.19	-4.79	-7.64
Arias Intensity (g-sec)												
Unreinforced	0.0048		0.0303		0.0356		0.0229		0.0191		0.0476	
Case 3	0.0040		0.0311		0.0423		0.0213		0.0218		0.0525	
Reduction (%)	16.58		-2.62		-18.86		7.17		-14.05		-10.13	
	Base Shear (kN)				Base Moment (kN-m)							
	RMS		Peak		RMS		Peak					
Unreinforced	0.55		3.42		0.38		2.39					
Case 3	0.57		3.56		0.39		2.52					
Reduction (%)	-3.24		-4.22		-4.62		-5.53					

4.6.2. Seismic Response of Case 3 for El Centro Earthquake

For the El Centro earthquake results; peak foundation acceleration response reduction and top floor acceleration response reduction were obtained as 8.57% and 18.33% respectively. In addition to peak values, root mean square reductions of the same acceleration responses were detected as 13.76% and 6.97% respectively, as displayed in Figure 4.12a and Figure 4.12b. A reduction of the first floor story drift was observed as 12.94% for peak value and 9.78% for RMS value, as displayed in Figure 4.12c and Figure 4.12d. All performance parameters were summarized and demonstrated in Table 4.11. Maximum reduction of arias intensity was observed at the first floor by 20.69% as in Figure 4.12e. In addition, as displayed in Figure 4.12f, base shear and base moment of the test model at the foundation level were reduced by 5.05% and 3.13% respectively, in terms of peak values and 3.75% and 2.52% in terms of RMS values, correspondingly.

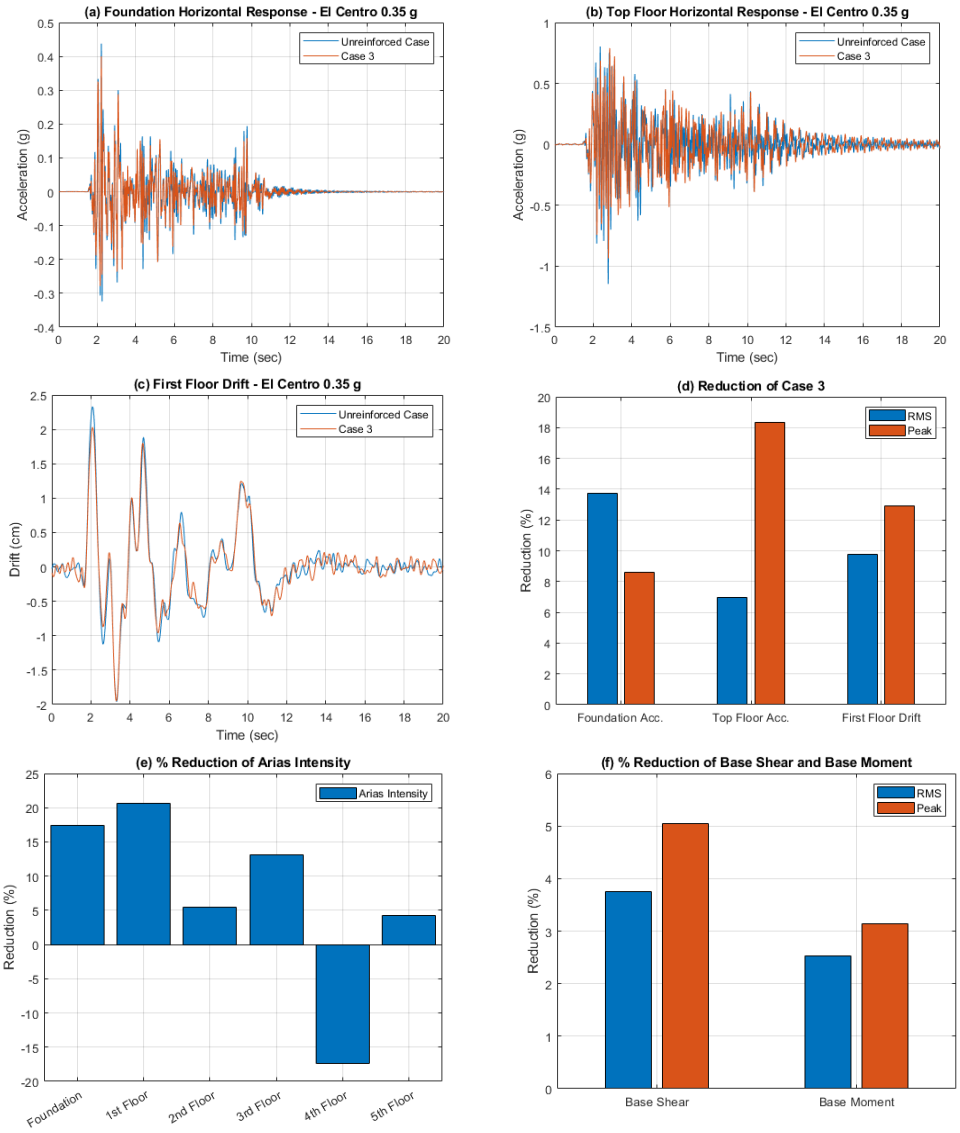

Figure 4.12. Foundation acceleration response (a), Top floor acceleration response (b), First floor acceleration response (c), (%) Reduction of Case 3 (d), (%) Reduction of arias intensity (e), (%) Reduction of base shear and base moment (f) under El Centro Earthquake.

Table 4.11. Horizontal acceleration, Horizontal story drift, Arias intensity, Base Shear and Base Moment reduction factors under El Centro Earthquake (Case 3).

Case 3 under El Centro (PGA=0.35g) Earthquake												
	Foundation		1st Floor		2nd Floor		3rd Floor		4th Floor		5th Floor	
	RMS	Peak	RMS	Peak	RMS	Peak	RMS	Peak	RMS	Peak	RMS	Peak
Horizontal Acceleration (g)												
Unreinforced	0.0375	0.4375	0.0927	0.8326	0.0939	0.9076	0.0793	0.5977	0.0658	0.5300	0.1111	1.1448
Case 3	0.0323	0.4000	0.0788	0.6890	0.0869	0.8599	0.0701	0.5342	0.0675	0.4950	0.1034	0.9349
Reduction (%)	13.76	8.57	15.03	17.25	7.45	5.25	11.53	10.62	-2.60	6.60	6.97	18.33
Horizontal Story Drift (cm)												
Unreinforced	-	-	0.39	2.33	0.51	2.99	0.55	3.37	0.60	3.79	0.58	3.88
Case 3	-	-	0.35	2.03	0.47	2.71	0.51	3.20	0.54	3.70	0.55	3.90
Reduction (%)	-	-	9.78	12.94	7.33	9.15	7.15	5.18	9.46	2.51	5.41	-0.47
Arias Intensity (g-sec)												
Unreinforced	0.0094		0.0578		0.0593		0.0423		0.0291		0.0830	
Case 3	0.0078		0.0459		0.0561		0.0367		0.0342		0.0795	
Reduction (%)	17.47		20.69		5.47		13.14		-17.38		4.22	
	Base Shear (kN)				Base Moment (kN-m)							
	RMS		Peak		RMS		Peak					
Unreinforced	0.52		3.62		0.36		2.50					
Case 3	0.50		3.44		0.35		2.42					
Reduction (%)	3.75		5.05		2.52		3.13					

4.6.3. Seismic Response of Case 3 for Kobe Earthquake

For the El Centro earthquake results; peak foundation acceleration response reduction and top floor acceleration response reduction were obtained as 5.64% and 11.46% respectively. In addition to peak values, root mean square reductions of the same acceleration responses were detected as 12.52% and 17.83% respectively, as displayed in Figure 4.13a and Figure 4.13b. A reduction of the first floor story drift was observed as 23.06% for peak value and 10.01% for RMS value, as displayed in Figure 4.13c and Figure 4.13d. All performance parameters were summarized and demonstrated in Table 4.12. Maximum reduction of arias intensity was observed at the second floor by 20.27% as in Figure 4.13e. In addition, as displayed in Figure 4.13f, base shear and base moment of the test model at the foundation level were reduced by 9.85% and 6.17% respectively, in terms of peak values and 0.48% and -0.15% in terms of RMS values, correspondingly.

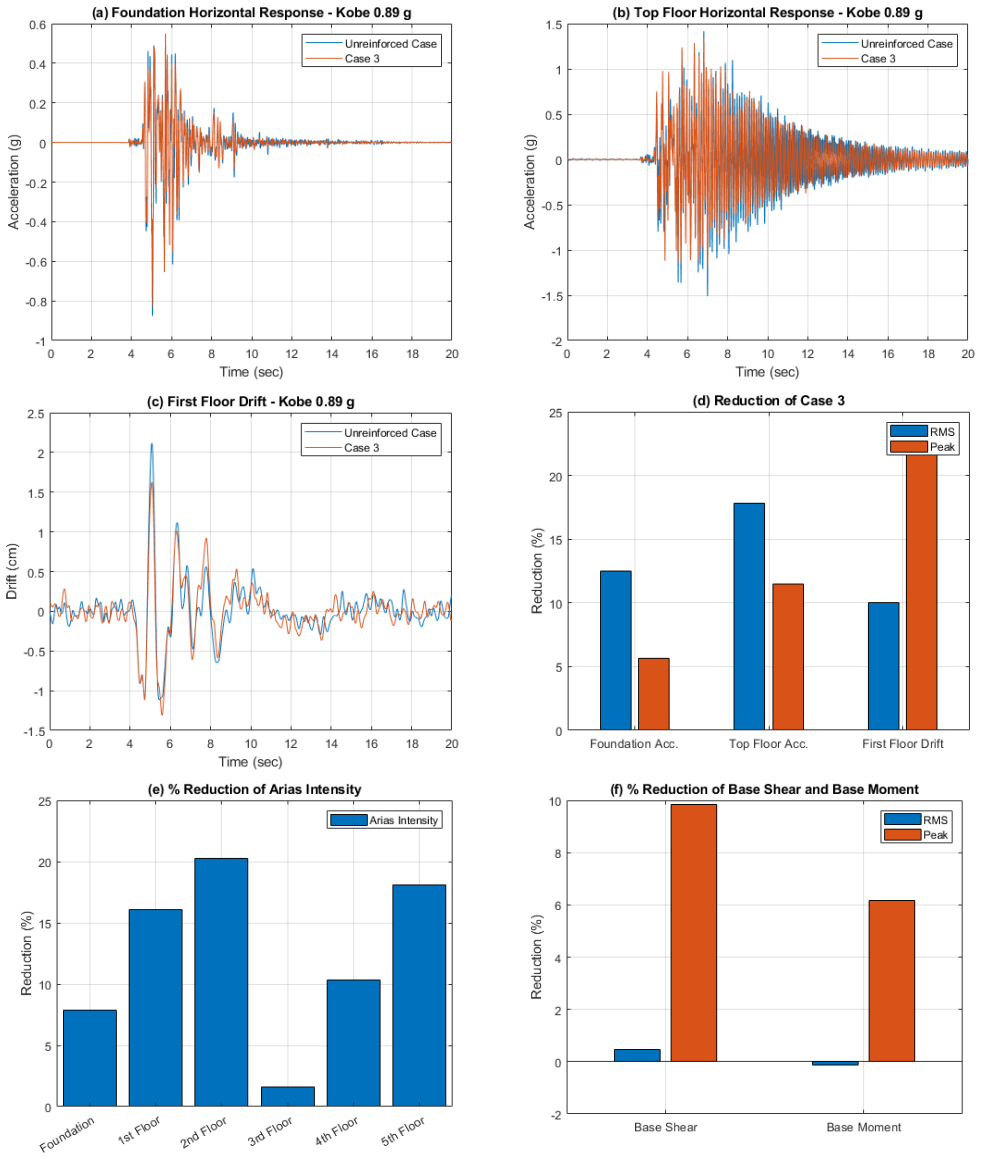

Figure 4.13. Foundation acceleration response (a), Top floor acceleration response (b), First floor acceleration response (c), (%) Reduction of Case 3 (d), (%) Reduction of arias intensity (e), (%) Reduction of base shear and base moment (f) under Kobe Earthquake.

Table 4.12. Horizontal acceleration, Horizontal story drift, Arias intensity, Base Shear and Base Moment reduction factors under Kobe Earthquake (Case 3).

Case 3 under Kobe (PGA=0.89g) Earthquake												
	Foundation		1st Floor		2nd Floor		3rd Floor		4th Floor		5th Floor	
	RMS	Peak	RMS	Peak	RMS	Peak	RMS	Peak	RMS	Peak	RMS	Peak
Horizontal Acceleration (g)												
Unreinforced	0.0618	0.8757	0.1823	1.3428	0.2066	1.2466	0.1246	1.0716	0.1140	0.8205	0.2207	1.5111
Case 3	0.0541	0.8263	0.1506	1.4025	0.1684	1.1103	0.1127	1.1908	0.0979	0.8003	0.1813	1.3379
Reduction (%)	12.52	5.64	17.42	-4.44	18.52	10.93	9.60	-11.12	14.13	2.46	17.83	11.46
Horizontal Story Drift (cm)												
Unreinforced	-	-	0.25	2.11	0.44	3.46	0.50	4.12	0.58	4.53	0.59	5.19
Case 3	-	-	0.23	1.63	0.47	2.70	0.50	3.50	0.56	4.48	0.60	5.20
Reduction (%)	-	-	10.01	23.06	-5.75	21.98	-0.21	15.11	2.75	1.09	-0.99	-0.14
Arias Intensity (g-sec)												
Unreinforced	0.0263		0.2248		0.2940		0.1070		0.0890		0.3342	
Case 3	0.0242		0.1887		0.2344		0.1053		0.0798		0.2737	
Reduction (%)	7.85		16.05		20.27		1.60		10.35		18.10	
	Base Shear (kN)						Base Moment (kN-m)					
	RMS		Peak				RMS		Peak			
Unreinforced	0.46		5.16				0.34		3.09			
Case 3	0.46		4.65				0.34		2.90			
Reduction (%)	0.48		9.85				-0.15		6.17			

4.7. Case 4 – N=4 Geogrid Reinforced 5-Story Building Model

The previously evaluated performance indicator parameters were evaluated for 5-story building model under Kocaeli, Kobe and El Centro earthquakes. Applied configuration of geogrid reinforced zone was noted in Section 3.9 and geogrid reinforced zones for all configuration types was described in Figure 3.22. For this case, N=4 layer of geogrid was used for 5-story building model. Tests were conducted for all strong ground motions and sinusoidal motions. Results are demonstrated for Kocaeli, El Centro and Kobe earthquakes, respectively.

4.7.1. Seismic Response of Case 4 for Kocaeli Earthquake

For the Kocaeli earthquake; foundation acceleration peak response reduction was measured as 16.51% and top floor acceleration peak response reduction was measured as 21.22%. Additionally, foundation and top floor root mean square acceleration response reduction was obtained as 24.57% and 13.60%, correspondingly, as displayed in Figure 4.14a and Figure 4.14b. Peak value of the first floor drift reduction was determined as 4.54% and RMS value was determined as 19.62%, as indicated in Figure 4.14c and Figure

4.14d. All performance parameters of the scenario were summarized and displayed in Table 4.13. Maximum reduction of arias intensity was observed at the foundation level by 26.83% as in Figure 4.14e. Additionally, as displayed in Figure 4.14f, base shear and base moment of the test model at the foundation level were increased by 11.31% and 10.78% respectively, in terms of peak values and there was reduction of the same parameters by 3.95% and 1.03% regarding to RMS values.

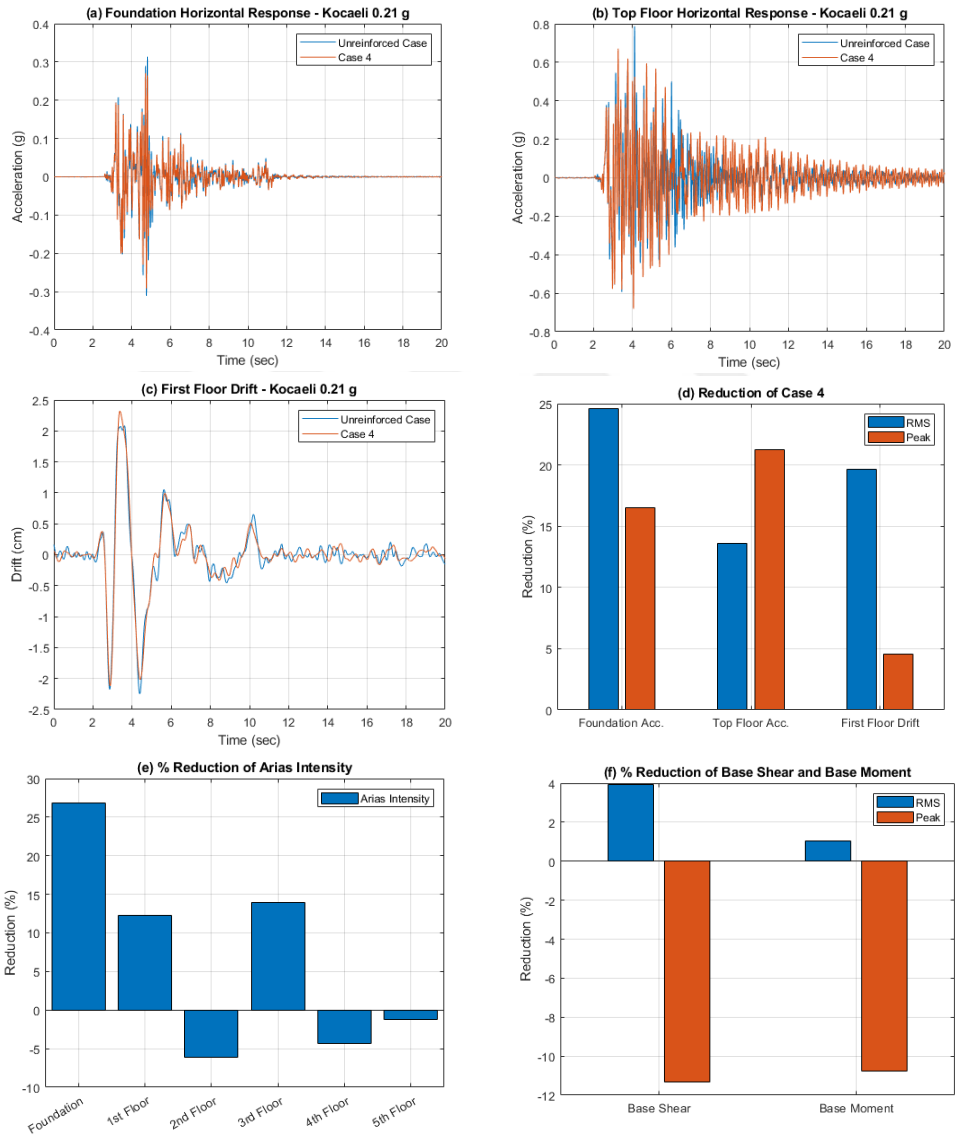

Figure 4.14. Foundation acceleration response (a), Top floor acceleration response (b), First floor acceleration response (c), (%) Reduction of Case 4 (d), (%) Reduction of arias intensity (e), (%) Reduction of base shear and base moment (f) under Kocaeli Earthquake.

Table 4.13. Horizontal acceleration, Horizontal story drift, Arias intensity, Base Shear and Base Moment reduction factors under Kocaeli Earthquake (Case 4).

Case 4 under Kocaeli (PGA=0.21g) Earthquake												
	Foundation		1st Floor		2nd Floor		3rd Floor		4th Floor		5th Floor	
	RMS	Peak	RMS	Peak	RMS	Peak	RMS	Peak	RMS	Peak	RMS	Peak
Horizontal Acceleration (g)												
Unreinforced	0.0299	0.3251	0.0758	0.5536	0.0820	0.6674	0.0661	0.5638	0.0606	0.4036	0.0960	0.8006
Case 4	0.0226	0.2714	0.0627	0.4926	0.0746	0.5755	0.0535	0.4612	0.0538	0.4022	0.0829	0.6307
Reduction (%)	24.57	16.51	17.18	11.03	9.03	13.78	18.98	18.19	11.13	0.35	13.60	21.22
Horizontal Story Drift (cm)												
Unreinforced	-	-	0.43	2.23	0.53	2.90	0.58	3.61	0.62	3.83	0.61	4.08
Case 4	-	-	0.35	2.13	0.53	3.71	0.57	4.15	0.60	4.26	0.62	4.28
Reduction (%)	-	-	19.62	4.54	-1.09	-27.85	1.46	-14.85	2.33	-11.41	-0.57	-4.96
Arias Intensity (g-sec)												
Unreinforced	0.0047		0.0303		0.0356		0.0229		0.0191		0.0468	
Case 4	0.0035		0.0266		0.0378		0.0197		0.0200		0.0474	
Reduction (%)	26.83		12.26		-6.17		13.98		-4.34		-1.26	
	Base Shear (kN)				Base Moment (kN-m)			
	RMS		Peak		RMS		Peak	
Unreinforced	0.55		3.41		0.38		2.39	
Case 4	0.53		3.80		0.37		2.64	
Reduction (%)	3.95		-11.31		1.03		-10.78	

4.7.2. Seismic Response of Case 4 for El Centro Earthquake

For the El Centro earthquake; foundation acceleration peak response reduction was measured as 11.56% and top floor acceleration peak response reduction was measured as 23.30%. Additionally, foundation and top floor root mean square acceleration response reduction was obtained as 1.17% and -0.67%, correspondingly, as displayed in Figure 4.15a and Figure 4.15b. Peak value of the first floor drift reduction was determined as 14.10% and RMS value was determined as -1.54%, as indicated in Figure 4.15c and Figure 4.15d. All performance parameters of the scenario were summarized and displayed in Table 4.14. Maximum reduction of arias intensity was observed at the first floor level by 30.70% as in Figure 4.15e. Additionally, as displayed in Figure 4.15f, base shear and base moment of the test model at the foundation level were slightly increased by 1.03% and 0.16% respectively, in terms of peak values and there was an increase of the same parameters by 0.55% and 1.00% regarding to RMS values.

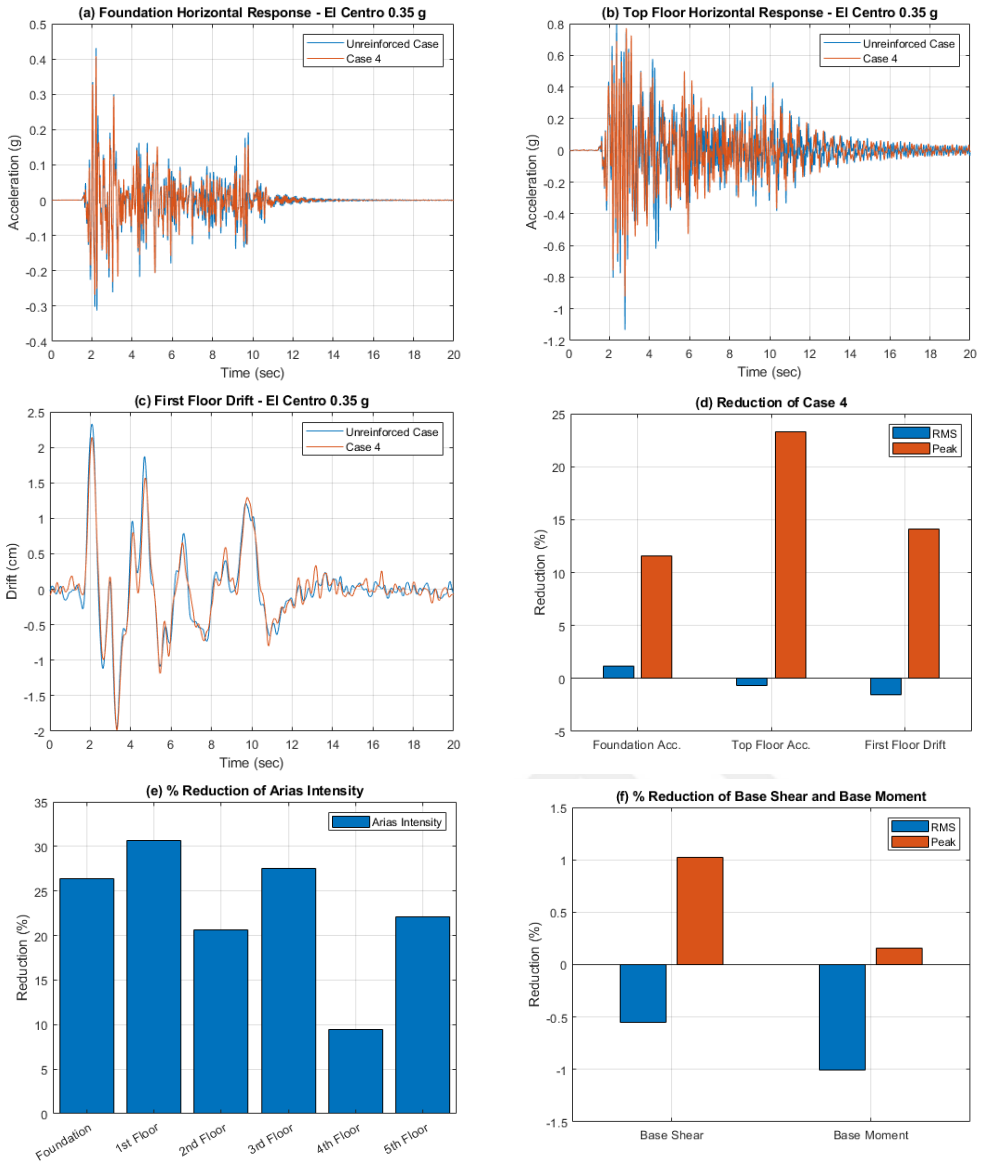

Figure 4.15. Foundation acceleration response (a), Top floor acceleration response (b), First floor acceleration response (c), (%) Reduction of Case 4 (d), (%) Reduction of arias intensity (e), (%) Reduction of base shear and base moment (f) under El Centro Earthquake.

Table 4.14. Horizontal acceleration, Horizontal story drift, Arias intensity, Base Shear and Base Moment reduction factors under El Centro Earthquake (Case 4).

Case 4 under El Centro (PGA=0.35g) Earthquake												
	Foundation		1st Floor		2nd Floor		3rd Floor		4th Floor		5th Floor	
	RMS	Peak	RMS	Peak	RMS	Peak	RMS	Peak	RMS	Peak	RMS	Peak
Horizontal Acceleration (g)												
Unreinforced	0.0373	0.4347	0.0927	0.8326	0.0939	0.9076	0.0793	0.5977	0.0658	0.5300	0.1105	1.1393
Case 4	0.0368	0.3844	0.0896	0.6565	0.0968	0.8277	0.0778	0.5235	0.0710	0.4763	0.1113	0.8738
Reduction (%)	1.17	11.56	3.36	21.15	-3.08	8.80	1.92	12.41	-7.95	10.13	-0.67	23.30
Horizontal Story Drift (cm)												
Unreinforced	-	-	0.39	2.33	0.51	2.99	0.55	3.37	0.60	3.79	0.58	3.88
Case 4	-	-	0.40	2.00	0.50	3.08	0.56	3.52	0.59	3.77	0.61	3.82
Reduction (%)	-	-	-1.54	14.10	1.18	-3.10	-1.69	-4.35	1.74	0.44	-4.15	1.62
Arias Intensity (g-sec)												
Unreinforced	0.0093		0.0578		0.0593		0.0423		0.0291		0.0822	
Case 4	0.0069		0.0401		0.0471		0.0306		0.0263		0.0640	
Reduction (%)	26.41		30.70		20.59		27.51		9.48		22.12	
	Base Shear (kN)				Base Moment (kN-m)							
	RMS		Peak		RMS		Peak					
Unreinforced	0.52		3.62		0.36		2.50					
Case 4	0.52		3.58		0.36		2.50					
Reduction (%)	-0.55		1.03		-1.00		0.16					

4.7.3. Seismic Response of Case 4 for Kobe Earthquake

For the Kobe earthquake; foundation acceleration peak response reduction was measured as 4.62% and top floor acceleration peak response reduction was measured as 14.42%. Additionally, foundation and top floor root mean square acceleration response reduction was obtained as -4.53% and 8.96%, correspondingly, as displayed in Figure 4.16a and Figure 4.16b. Peak value of the first floor drift reduction was determined as 33.41% and RMS value was determined as 2.67%, as indicated in Figure 4.16c and Figure 4.16d. All performance parameters of the scenario were summarized and displayed in Table 4.15. Maximum reduction of arias intensity was observed at the first floor level by 29.20% and fifth floor level by 29.12%, as in Figure 4.16e. Furthermore, as displayed in Figure 4.16f, base shear and base moment of the test model at the foundation level were increased by 16.60% and 14.95% respectively, in terms of peak values and there was an increase of the same parameters by 9.62% and 10.93% regarding to RMS values.

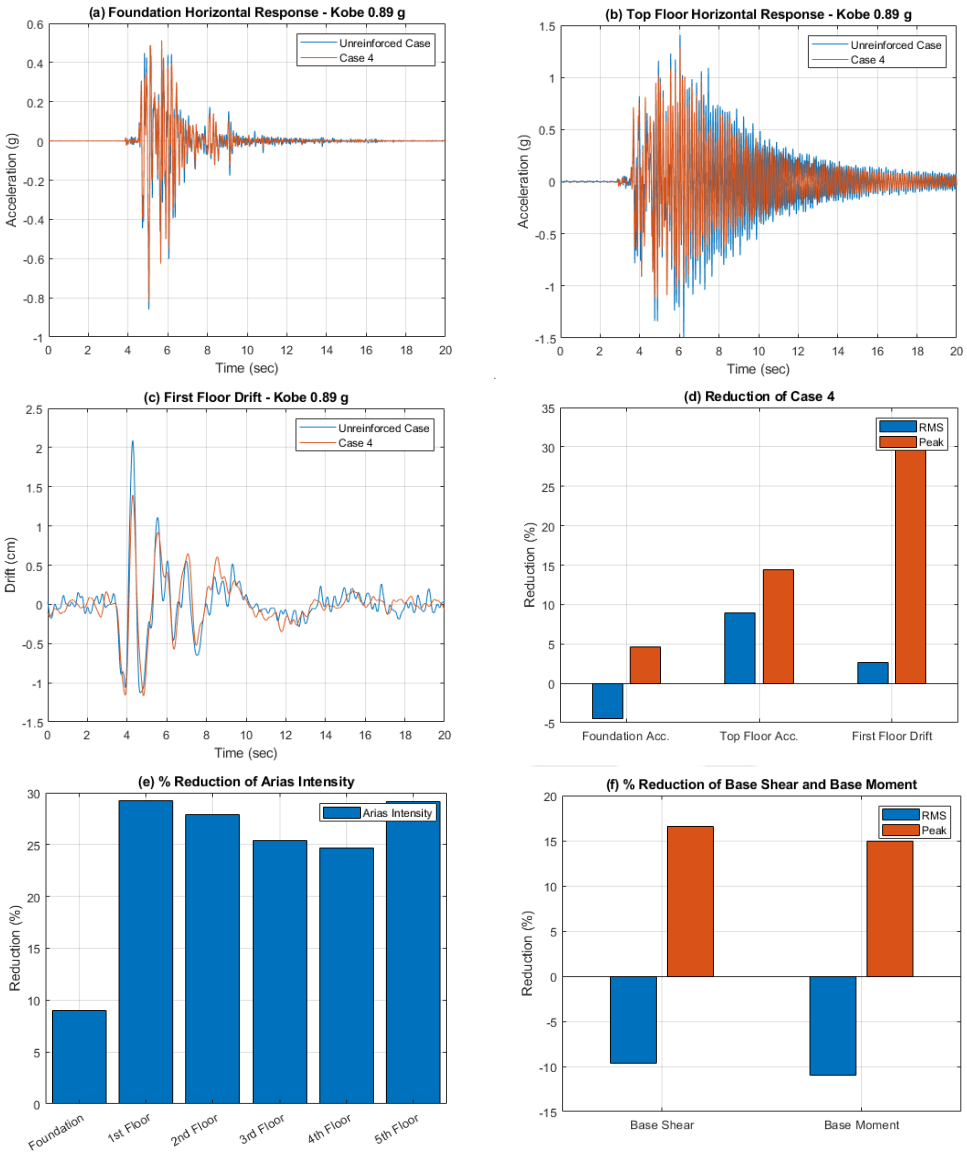

Figure 4.16. Foundation acceleration response (a), Top floor acceleration response (b), First floor acceleration response (c), (%) Reduction of Case 4 (d), (%) Reduction of arias intensity (e), (%) Reduction of base shear and base moment (f) under Kobe Earthquake.

Table 4.15. Horizontal acceleration, Horizontal story drift, Arias intensity, Base Shear and Base Moment reduction factors under Kobe Earthquake (Case 4).

Case 4 under Kobe (PGA=0.89g) Earthquake												
	Foundation		1st Floor		2nd Floor		3rd Floor		4th Floor		5th Floor	
	RMS	Peak	RMS	Peak	RMS	Peak	RMS	Peak	RMS	Peak	RMS	Peak
Horizontal Acceleration (g)												
Unreinforced	0.0614	0.8601	0.1829	1.3428	0.2066	1.2466	0.1258	1.0716	0.1149	0.8205	0.2218	1.4958
Case 4	0.0642	0.8203	0.1662	1.2399	0.1927	1.1821	0.1176	1.0611	0.1079	0.8300	0.2020	1.2800
Reduction (%)	-4.53	4.62	9.13	7.66	6.74	5.17	6.50	0.98	6.16	-1.16	8.96	14.42
Horizontal Story Drift (cm)												
Unreinforced	-	-	0.25	2.09	0.44	3.46	0.50	4.12	0.58	4.53	0.59	5.19
Case 4	-	-	0.24	1.39	0.51	2.91	0.55	3.51	0.62	3.89	0.67	4.48
Reduction (%)	-	-	2.67	33.41	-14.38	15.93	-9.37	14.80	-7.12	14.18	-12.95	13.82
Arias Intensity (g-sec)												
Unreinforced	0.0260		0.2248		0.2940		0.1070		0.0890		0.3317	
Case 4	0.0236		0.1592		0.2121		0.0798		0.0671		0.2351	
Reduction (%)	9.02		29.20		27.86		25.42		24.69		29.12	
	Base Shear (kN)				Base Moment (kN-m)							
	RMS		Peak		RMS		Peak					
Unreinforced	0.46		5.15		0.34		3.09					
Case 4	0.51		4.30		0.37		2.63					
Reduction (%)	-9.62		16.60		-10.93		14.95					

4.8. Unreinforced Soil with 3-Story Building

The mentioned three performance indicator parameters were evaluated for 3-story building model under Kocaeli, El Centro and Kobe earthquakes as displayed in Figure 4.17, Figure 4.18 and Figure 4.19. Maximum value of foundation acceleration response was measured as 0.30g, maximum top floor acceleration response was measured as 0.69g and maximum first floor drift was measured as 2.29cm for Kocaeli earthquake. Maximum foundation acceleration response, top floor acceleration response and first floor drift of El Centro earthquake is measured as 0.39g, 0.67g and 2.03 cm respectively. Additionally, maximum foundation acceleration response, top floor acceleration response and first floor drift of Kobe earthquake is measured as 0.72g, 1.20g and 2.14 cm respectively.

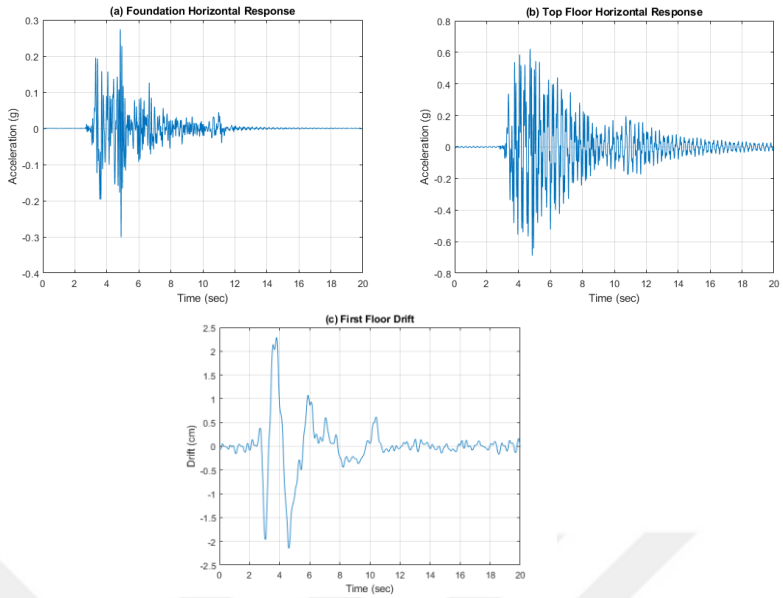

Figure 4.17. Horizontal acceleration response of foundation (a), Horizontal acceleration response of top floor (b) and First floor drift of 3-story building model under Kocaeli Earthquake.

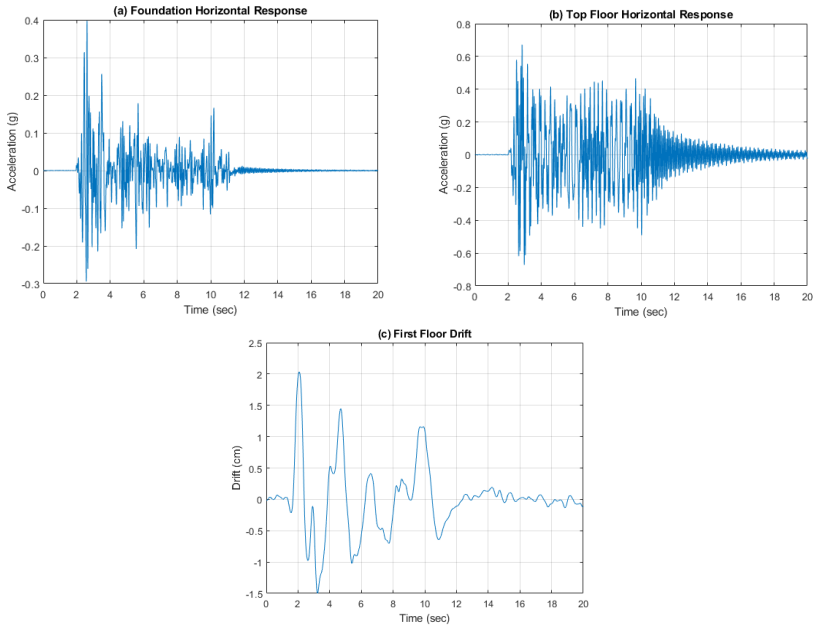

Figure 4.18. Horizontal acceleration response of foundation (a), Horizontal acceleration response of top floor (b) and First floor drift of 3-story building model under El Centro Earthquake.

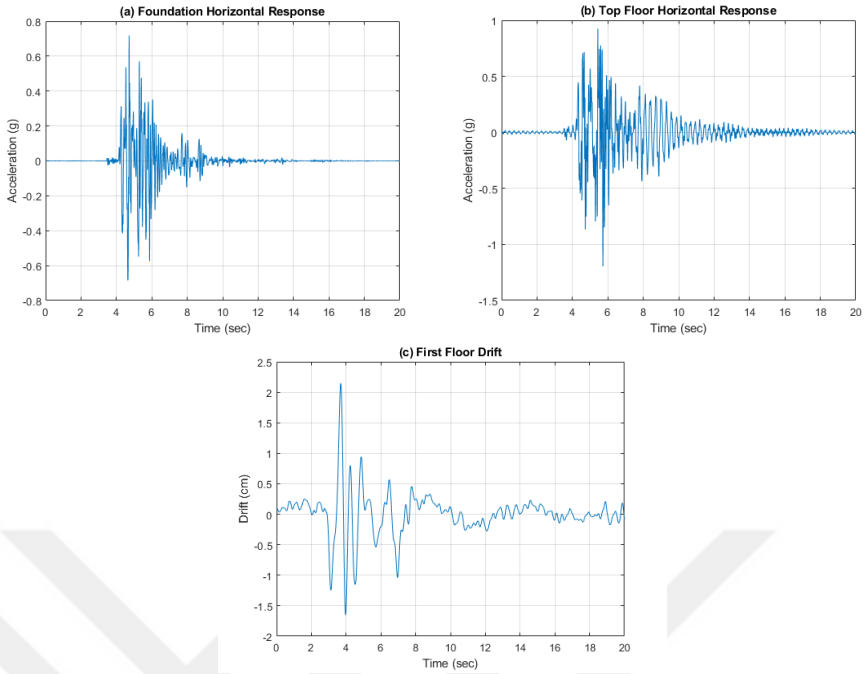

Figure 4.19. Horizontal acceleration response of foundation (a), Horizontal acceleration response of top floor (b) and First floor drift of 3-story building model under Kobe Earthquake.

4.9. Case 5 – N=1 Geogrid Reinforced 3-Story Building Model

The mentioned three performance indicator parameters were evaluated for 3-story building model under Kocaeli, Kobe and El Centro earthquakes. Applied configuration information was mentioned in Section 3.9 and configuration of geogrid reinforced zones for all configuration types was described in Figure 3.22. For this case, N=1 layer of geogrid was used for 3-story building model. Tests were conducted for all strong ground motions and sinusoidal motions. Results are demonstrated for Kocaeli, El Centro and Kobe earthquakes, respectively.

4.9.1. Seismic Response of Case 5 for Kocaeli Earthquake

Maximum foundation acceleration peak response reduction was measured as 17.66% and top floor acceleration peak response reduction was slightly increased with 5.35%. Additionally, foundation and top floor root mean square acceleration response reduction was obtained as 20.78% and 10.06%, correspondingly, as displayed in Figure 4.20a and Figure 4.20b. Peak value of the first floor drift reduction was determined as 3.00% and RMS value was determined as 12.68% reduced, as indicated in Figure 4.20c and Figure 4.20d. Maximum reduction of arias intensity was observed at the foundation level by 16.38% and fifth floor level by 11.64%, as in Figure 4.20e. Furthermore, as displayed in Figure 4.20f, base shear and base moment of the test model at the foundation level were slightly increased by 0.42% and 0.81% respectively, in terms of peak values and there was a reduction of the same parameters by 6.77% and 5.08% regarding to RMS values. All performance parameters of the case were summarized and displayed in Table 4.16.

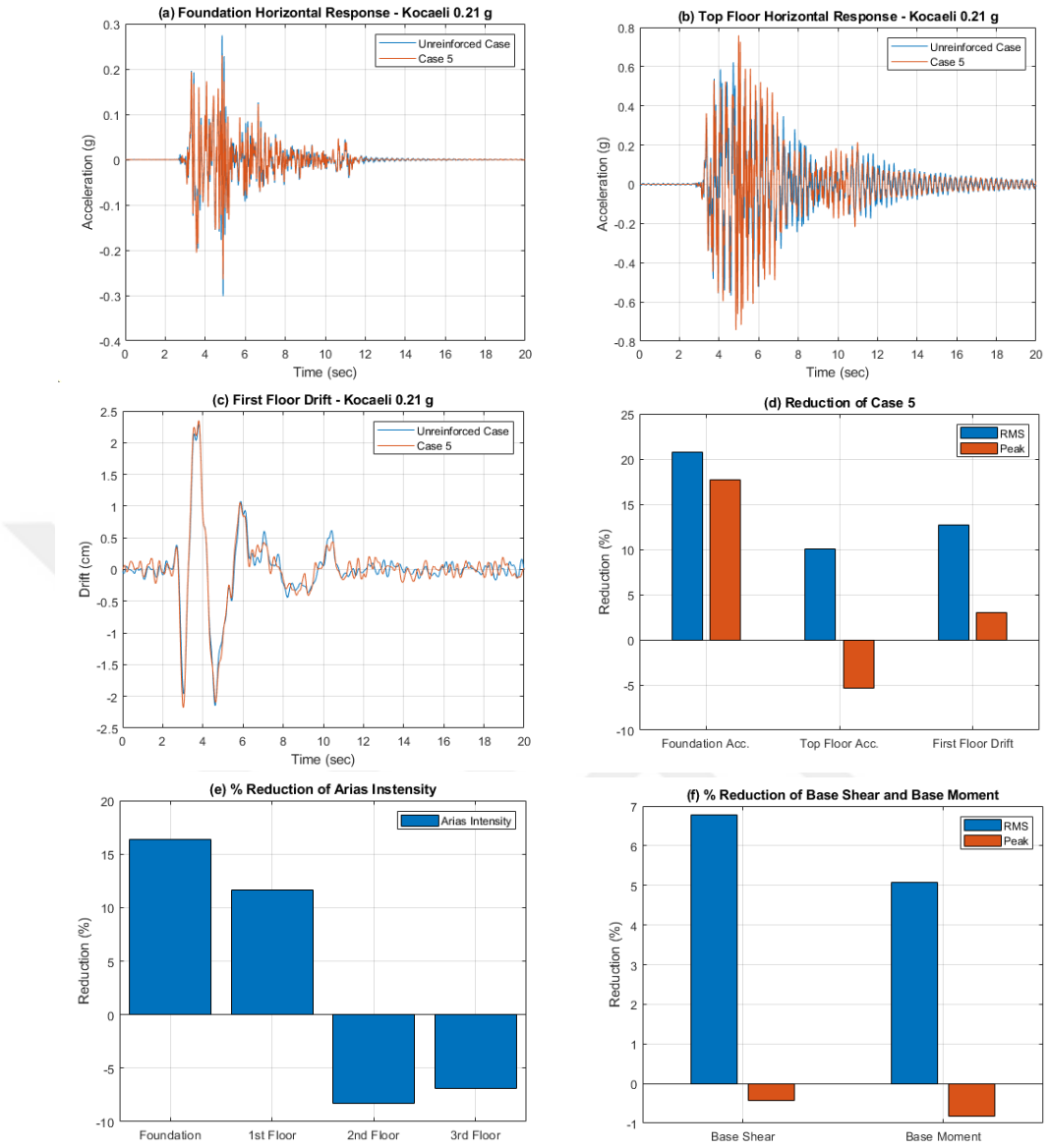

Figure 4.20. Foundation acceleration response (a), Top floor acceleration response (b), First floor acceleration response (c), (%) Reduction of Case 5 (d), (%) Reduction of arias intensity (e), (%) Reduction of base shear and base moment (f) under Kocaeli Earthquake.

Table 4.16. Horizontal acceleration, Horizontal story drift, Arias intensity, Base Shear and Base Moment reduction factors under Kocaeli Earthquake (Case 5).

Case 5 under Kocaeli (PGA=0.21g) Earthquake								
	Foundation		1st Floor		2nd Floor		3rd Floor	
	RMS	Peak	RMS	Peak	RMS	Peak	RMS	Peak
Horizontal Acceleration (g)								
Unreinforced	0.0280	0.3076	0.0864	0.7841	0.0797	0.5941	0.1047	0.6940
Case 5	0.0222	0.2533	0.0707	0.7488	0.0722	0.6605	0.0942	0.7311
Reduction (%)	20.78	17.66	18.13	4.51	9.47	-11.18	10.06	-5.35
Horizontal Story Drift (cm)								
Unreinforced	-	-	0.41	2.26	0.52	3.33	0.56	3.76
Case 5	-	-	0.36	2.19	0.51	3.42	0.53	3.77
Reduction (%)	-	-	12.68	3.00	2.52	-2.72	4.64	-0.45
Arias Intensity (g-sec)								
Unreinforced	0.0042		0.0399		0.0339		0.0585	
Case 5	0.0035		0.0352		0.0367		0.0625	
Reduction (%)	16.38		11.64		-8.27		-6.86	
	Base Shear (kN)				Base Moment (kN-m)			
	RMS		Peak		RMS		Peak	
Unreinforced	0.28		1.31		0.15		0.54	
Case 5	0.26		1.31		0.14		0.54	
Reduction (%)	6.77		-0.42		5.08		-0.81	

4.9.2. Seismic Response of Case 5 for El Centro Earthquake

Maximum foundation acceleration peak response was reduced by 23.63% and top floor acceleration peak response reduction was increased with 11.75%. Also, foundation and top floor root mean square acceleration response was both increased by a 14.19% and 21.44%, respectively, as displayed in Figure 4.21a and Figure 4.21b. Peak value of the first floor drift reduction was determined as 11.12%, in contrary, RMS value of the same parameter was increased as 19.62%, as indicated in Figure 4.21c and Figure 4.21d. Maximum reduction of arias intensity was observed at the first floor story level by 35.18% and first floor level by 15.58%, as in Figure 4.21e. Moreover, as displayed in Figure 4.21f, base shear and base moment of the test model at the foundation level were slightly reduced by a 4.28% and 2.85% respectively, in terms of peak values and there was an increase of the same parameters by 16.52% and 15.73% regarding to RMS values. All performance parameters of the case were summarized and displayed in Table 4.17, for El Centro earthquake.

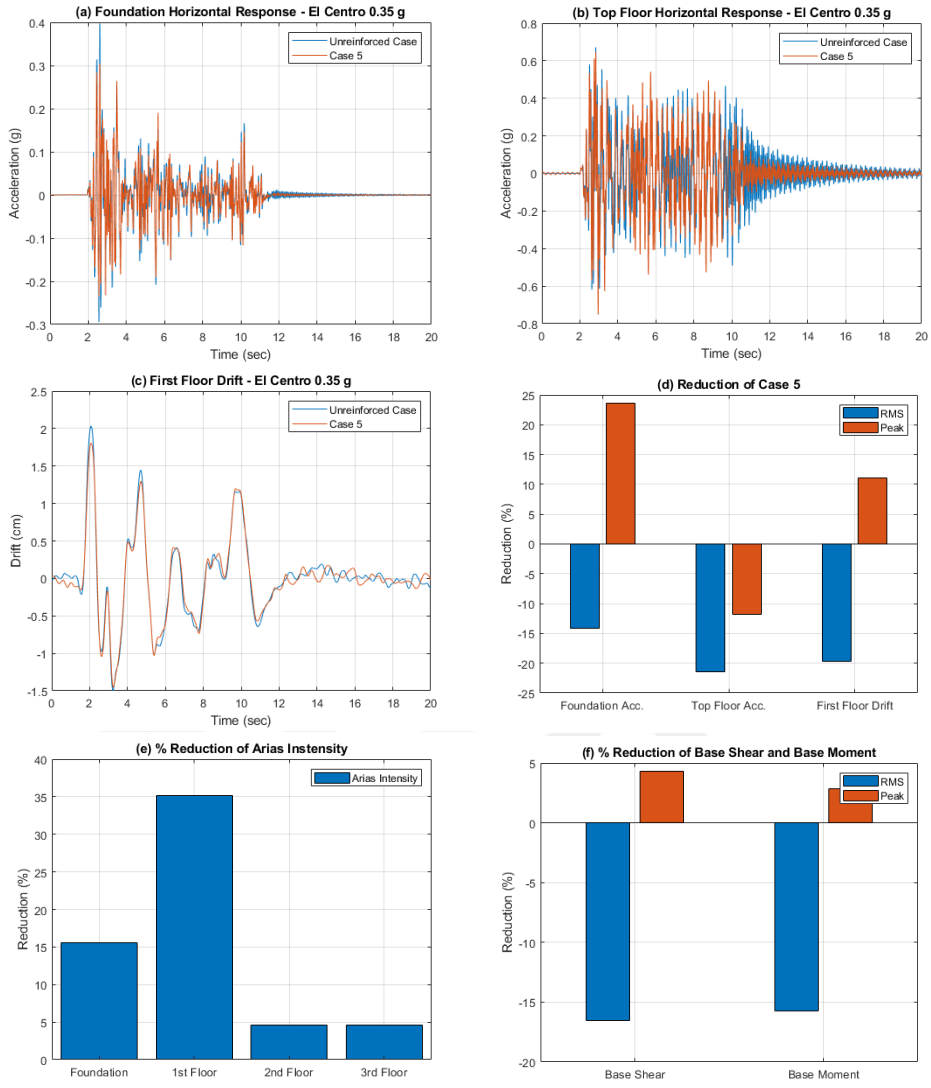

Figure 4.21. Foundation acceleration response (a), Top floor acceleration response (b), First floor acceleration response (c), (%) Reduction of Case 5 (d), (%) Reduction of arias intensity (e), (%) Reduction of base shear and base moment (f) under El Centro Earthquake.

Table 4.17. Horizontal acceleration, Horizontal story drift, Arias intensity, Base Shear and Base Moment reduction factors under El Centro Earthquake (Case 5).

Case 5 under El Centro (PGA=0.35g) Earthquake								
	Foundation		1st Floor		2nd Floor		3rd Floor	
	RMS	Peak	RMS	Peak	RMS	Peak	RMS	Peak
Horizontal Acceleration (g)								
Unreinforced	0.0328	0.3974	0.0900	0.6391	0.0743	0.5584	0.1037	0.6721
Case 5	0.0375	0.3035	0.0902	0.5738	0.0906	0.5551	0.1260	0.7511
Reduction (%)	-14.19	23.63	-0.16	10.22	-21.90	0.59	-21.44	-11.75
Horizontal Story Drift (cm)								
Unreinforced	-	-	0.36	2.03	0.46	2.73	0.50	3.07
Case 5	-	-	0.43	1.81	0.53	2.66	0.58	3.04
Reduction (%)	-	-	-19.62	11.12	-13.23	2.80	-15.82	1.06
Arias Intensity (g-sec)								
Unreinforced	0.0075		0.0562		0.0385		0.0745	
Case 5	0.0063		0.0364		0.0368		0.0711	
Reduction (%)	15.58		35.18		4.55		4.55	
	Base Shear (kN)				Base Moment (kN-m)			
	RMS		Peak		RMS		Peak	
Unreinforced	0.32		1.29		0.14		0.53	
Case 5	0.37		1.24		0.17		0.51	
Reduction (%)	-16.52		4.28		-15.73		2.85	

4.9.3. Seismic Response of Case 5 for Kobe Earthquake

There was an increase for the foundation acceleration peak response by 13.95% and top floor acceleration peak response was decreased with 8.45%. Also, foundation and top floor root mean square acceleration response was both reduced by a 15.50% and 4.96%, respectively, as displayed in Figure 4.22a and Figure 4.22b. Peak value of the first floor drift reduction was slightly increased by a 0.75%, in contrary, RMS value of the same parameter was decreased 9.37%, as indicated in Figure 4.22c and Figure 4.22d. Maximum reduction of arias intensity was observed at the first floor story level by 7.75% and there was an increase for the second floor level by 30.60%, as in Figure 4.22e. Moreover, as displayed in Figure 4.22f, base shear and base moment of the test model at the foundation level were slightly increased by 6.19% and 7.26% respectively, in terms of peak values and there was a reduction of the same parameters by 5.19% and 4.08% regarding to RMS values. All performance parameters of the case were summarized and displayed in Table 4.18, for Kobe earthquake.

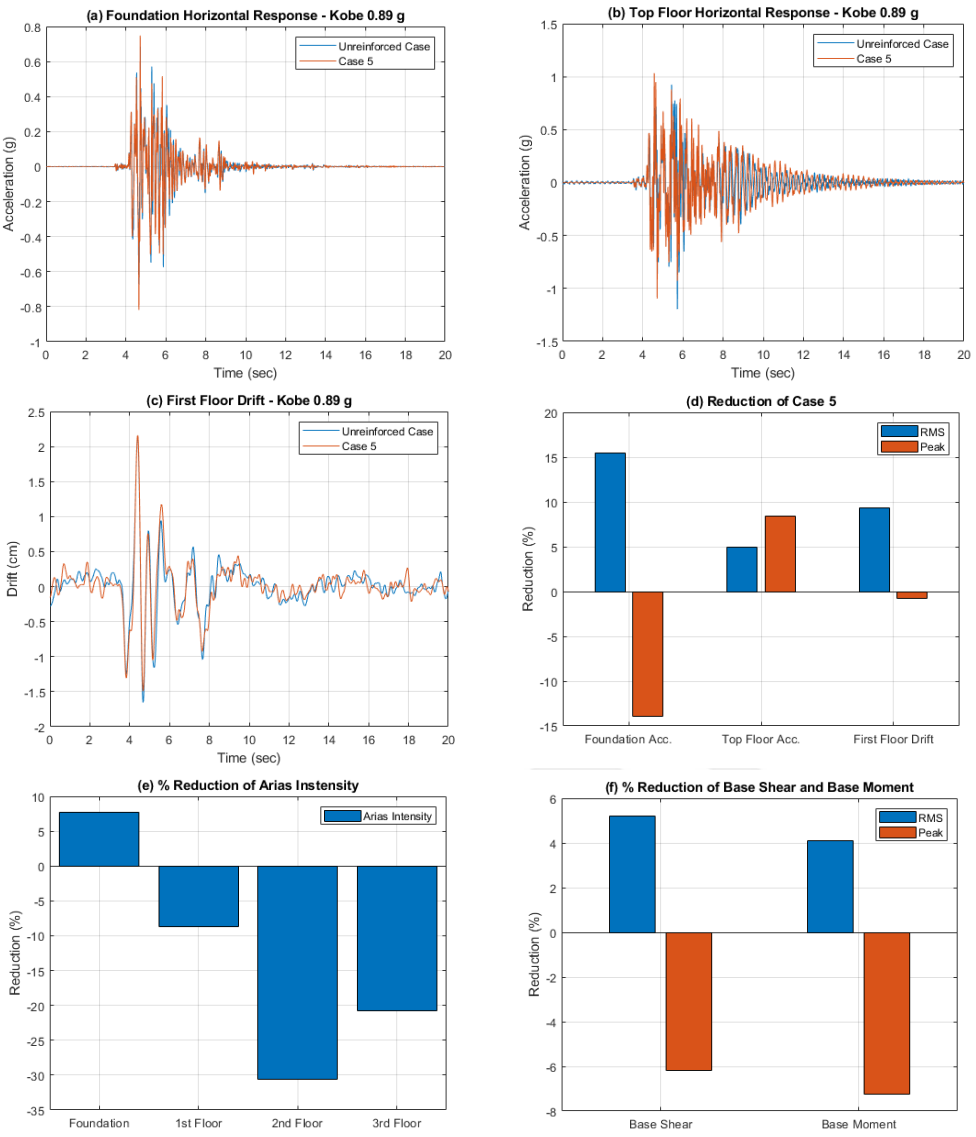

Figure 4.22. Foundation acceleration response (a), Top floor acceleration response (b), First floor acceleration response (c), (%) Reduction of Case 5 (d), (%) Reduction of arias intensity (e), (%) Reduction of base shear and base moment (f) under Kobe Earthquake.

Table 4.18. Horizontal acceleration, Horizontal story drift, Arias intensity, Base Shear and Base Moment reduction factors under Kobe Earthquake (Case 5).

Case 5 under Kobe (PGA=0.89g) Earthquake								
	Foundation		1st Floor		2nd Floor		3rd Floor	
	RMS	Peak	RMS	Peak	RMS	Peak	RMS	Peak
Horizontal Acceleration (g)								
Unreinforced	0.0705	0.7182	0.1028	1.0913	0.0933	0.7928	0.1261	1.1960
Case 5	0.0595	0.8184	0.0943	1.0445	0.0936	0.9994	0.1198	1.0950
Reduction (%)	15.50	-13.95	8.28	4.28	-0.28	-26.06	4.96	8.45
Horizontal Story Drift (cm)								
Unreinforced	-	-	0.29	2.14	0.52	3.51	0.61	4.25
Case 5	-	-	0.26	2.16	0.51	3.72	0.57	4.63
Reduction (%)	-	-	9.37	-0.75	0.77	-6.16	6.14	-8.96
Arias Intensity (g-sec)								
Unreinforced	0.0240		0.0511		0.0419		0.0743	
Case 5	0.0221		0.0555		0.0547		0.0897	
Reduction (%)	7.75		-8.68		-30.60		-20.70	
	Base Shear (kN)				Base Moment (kN-m)			
	RMS		Peak		RMS		Peak	
Unreinforced	0.37		3.41		0.15		1.25	
Case 5	0.35		3.62		0.15		1.35	
Reduction (%)	5.19		-6.19		4.08		-7.26	

4.10. Case 6 – N=2 Geogrid Reinforced 3-Story Building Model

The mentioned performance indicator parameters were evaluated for 3-story building model under Kocaeli, Kobe and El Centro earthquakes. Applied configuration information was mentioned in Section 3.9 and configuration of geogrid reinforced zones for all configuration types was described in Figure 3.22. For this case, N=2 layer of geogrid was used for 3-story building model. Tests were conducted for all strong ground motions and sinusoidal motions. Results are demonstrated for Kocaeli, El Centro and Kobe earthquakes, respectively.

4.10.1. Seismic Response of Case 6 for Kocaeli Earthquake

There was a slight increase for the foundation acceleration peak response by 2.07% and in contrary, top floor acceleration peak response was increased by a 2.00%. Also, foundation and top floor root mean square acceleration response was both reduced by a 10.54% and 12.66%, respectively, as displayed in Figure 4.23a and Figure 4.23Figure 4.22b. Peak value of the first floor drift reduction was slightly increased by a 4.88% and RMS value of the same parameter was reduced by a 8.06%, as indicated in Figure 4.23c and Figure 4.23d. Maximum reduction of arias intensity was observed at the third floor story level by 7.95% and there was an increase for the second floor level by 3.02%, as in Figure 4.23e. Moreover, as displayed in Figure 4.23f, base shear and base moment of the test model at the foundation level were increased by 11.62% and 12.51% respectively, in terms of peak values and there was a reduction of the same parameters by 7.37% and 7.58% regarding to RMS values. All performance parameters of the case were summarized and displayed in Table 4.19, for Kocaeli earthquake.

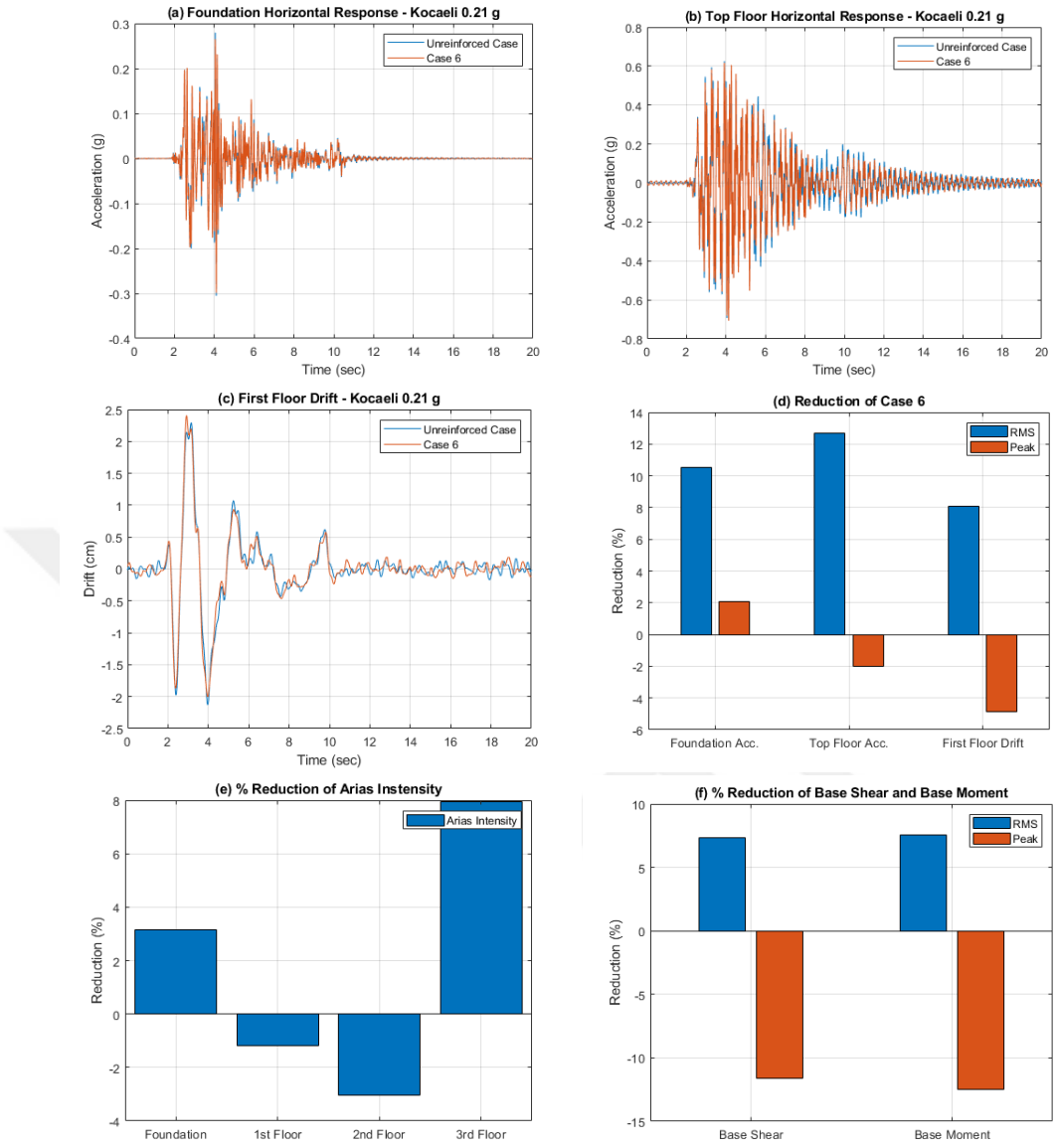

Figure 4.23. Foundation acceleration response (a), Top floor acceleration response (b), First floor acceleration response (c), (%) Reduction of Case 6 (d), (%) Reduction of arias intensity (e), (%) Reduction of base shear and base moment (f) under Kocaeli Earthquake.

Table 4.19. Horizontal acceleration, Horizontal story drift, Arias intensity, Base Shear and Base Moment reduction factors under Kocaeli Earthquake (Case 6).

Case 6 under Kocaeli (PGA=0.21g) Earthquake								
	Foundation		1st Floor		2nd Floor		3rd Floor	
	RMS	Peak	RMS	Peak	RMS	Peak	RMS	Peak
Horizontal Acceleration (g)								
Unreinforced	0.0282	0.3054	0.0879	0.7841	0.0813	0.5941	0.1059	0.6929
Case 6	0.0252	0.2991	0.0804	0.7646	0.0748	0.6585	0.0925	0.7068
Reduction (%)	10.54	2.07	8.55	2.49	8.06	-10.83	12.66	-2.00
Horizontal Story Drift (cm)								
Unreinforced	-	-	0.42	2.29	0.52	3.33	0.56	3.76
Case 6	-	-	0.38	2.41	0.48	3.85	0.51	4.22
Reduction (%)	-	-	8.06	-4.88	8.78	-15.54	8.68	-12.27
Arias Intensity (g-sec)								
Unreinforced	0.0041		0.0399		0.0339		0.0581	
Case 6	0.0040		0.0403		0.0349		0.0535	
Reduction (%)	3.15		-1.19		-3.02		7.94	
	Base Shear (kN)				Base Moment (kN-m)			
	RMS		Peak		RMS		Peak	
Unreinforced	0.28		1.31		0.15		0.54	
Case 6	0.26		1.47		0.14		0.60	
Reduction (%)	7.37		-11.62		7.58		-12.51	

4.10.2. Seismic Response of Case 6 for El Centro Earthquake

For the El Centro earthquake, foundation acceleration peak response was reduced by a 13.33% and top floor acceleration peak response was reduced by a 11.64%. Also, foundation and top floor root mean square acceleration response was both slightly increased by a 0.45% and 0.69%, respectively, as displayed in Figure 4.24a and Figure 4.24Figure 4.22b. Peak value of the first floor drift reduction was slightly increased by a 4.54% and RMS value of the same parameter was increased by a 0.97%, as indicated in Figure 4.24c and Figure 4.24d. Maximum reduction of arias intensity was observed at the foundation level by 14.48% and for the third floor level by 14.07%, as in Figure 4.24e. Moreover, as displayed in Figure 4.24f, base shear and base moment of the test model at the foundation level were slightly reduced by 2.18% and 1.35% respectively, in terms of peak values and there was a reduction of the same parameters by -0.31% and 0.07% regarding to RMS values. All performance parameters of the case were summarized and displayed in Table 4.20, for El Centro earthquake.

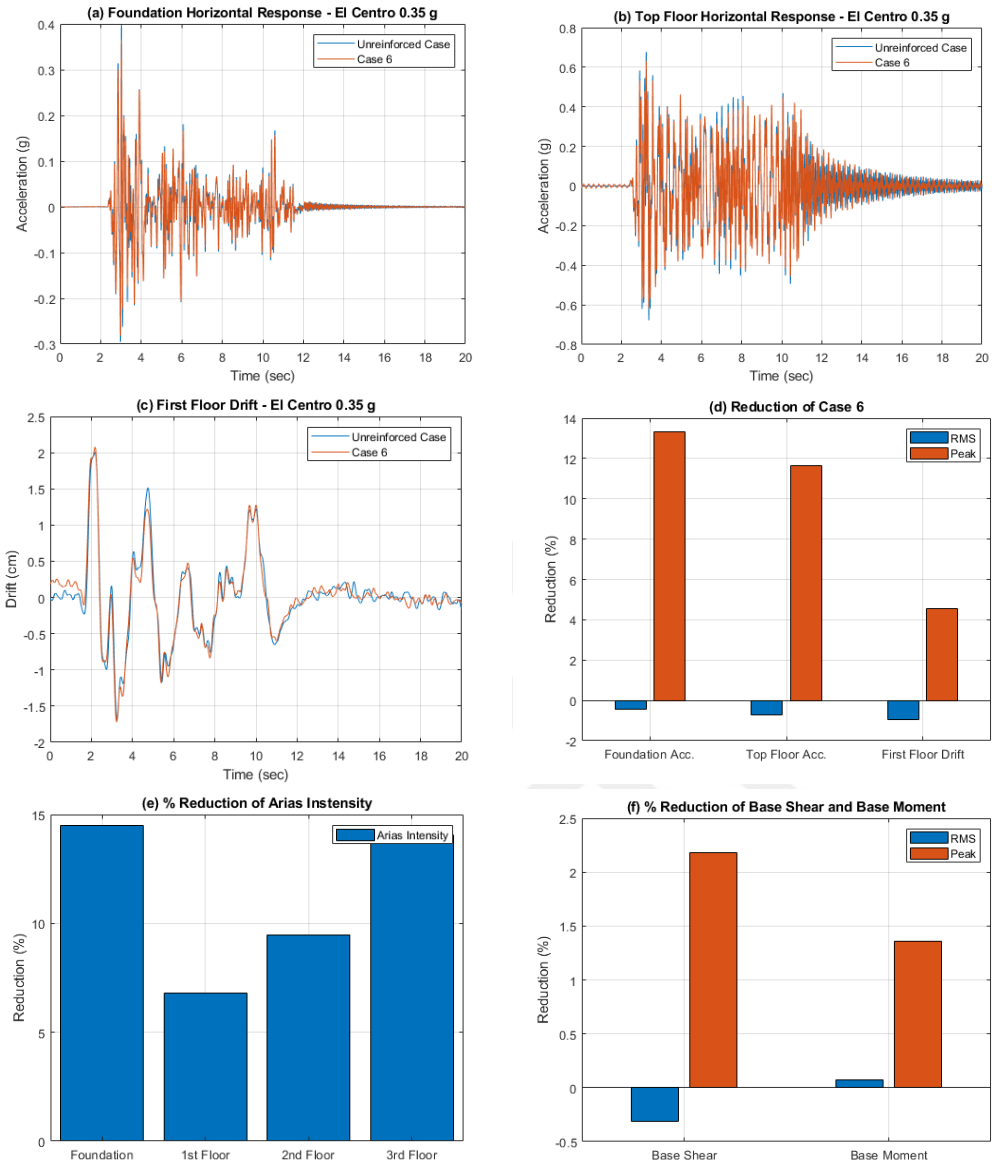

Figure 4.24. Foundation acceleration response (a), Top floor acceleration response (b), First floor acceleration response (c), (%) Reduction of Case 6 (d), (%) Reduction of arias intensity (e), (%) Reduction of base shear and base moment (f) under El Centro Earthquake.

Table 4.20. Horizontal acceleration, Horizontal story drift, Arias intensity, Base Shear and Base Moment reduction factors under El Centro Earthquake (Case 6).

Case 6 under El Centro (PGA=0.35g) Earthquake								
	Foundation		1st Floor		2nd Floor		3rd Floor	
	RMS	Peak	RMS	Peak	RMS	Peak	RMS	Peak
Horizontal Acceleration (g)								
Unreinforced	0.0322	0.3941	0.0897	0.6391	0.0742	0.5584	0.1016	0.6552
Case 6	0.0324	0.3415	0.0940	0.5652	0.0767	0.5142	0.1023	0.5790
Reduction (%)	-0.45	13.33	-4.86	11.56	-3.35	7.91	-0.69	11.64
Horizontal Story Drift (cm)								
Unreinforced	-	-	0.37	2.01	0.46	2.73	0.50	3.07
Case 6	-	-	0.37	1.92	0.45	2.63	0.50	3.09
Reduction (%)	-	-	-0.97	4.54	1.84	3.75	-0.83	-0.76
Arias Intensity (g-sec)								
Unreinforced	0.0073		0.0562		0.0385		0.0722	
Case 6	0.0062		0.0524		0.0349		0.0620	
Reduction (%)	14.48		6.82		9.49		14.07	
	Base Shear (kN)				Base Moment (kN-m)			
	RMS		Peak		RMS		Peak	
Unreinforced	0.32		1.29		0.14		0.53	
Case 6	0.32		1.26		0.14		0.52	
Reduction (%)	-0.31		2.18		0.07		1.35	

4.10.3. Seismic Response of Case 6 for Kobe Earthquake

For the Kobe earthquake, foundation acceleration peak response was reduced by a 7.76% and top floor acceleration peak response was increased by 8.65%. Also, foundation and top floor root mean square acceleration response was both slightly reduced by a 8.80% and 5.35%, respectively, as displayed in Figure 4.25a and Figure 4.25Figure 4.22b. Peak value of the first floor drift reduction was measured as 6.85% and RMS value of the same parameter was measured as 7.18%, as indicated in Figure 4.25c and Figure 4.25d. Maximum reduction of arias intensity was observed at the foundation level by 10.78% and for the third floor level by 3.93% and the percentages for first and second floor close to zero. as in Figure 4.25e. Furthermore, as displayed in Figure 4.25f, base shear and base moment of the test model at the foundation level were slightly increased by 2.65% and 4.38% respectively, in terms of peak values and there was a reduction of the same parameters by 2.24% and 1.28% in terms of RMS values. All performance parameters of the case were summarized and displayed in Table 4.21, for Kobe earthquake.

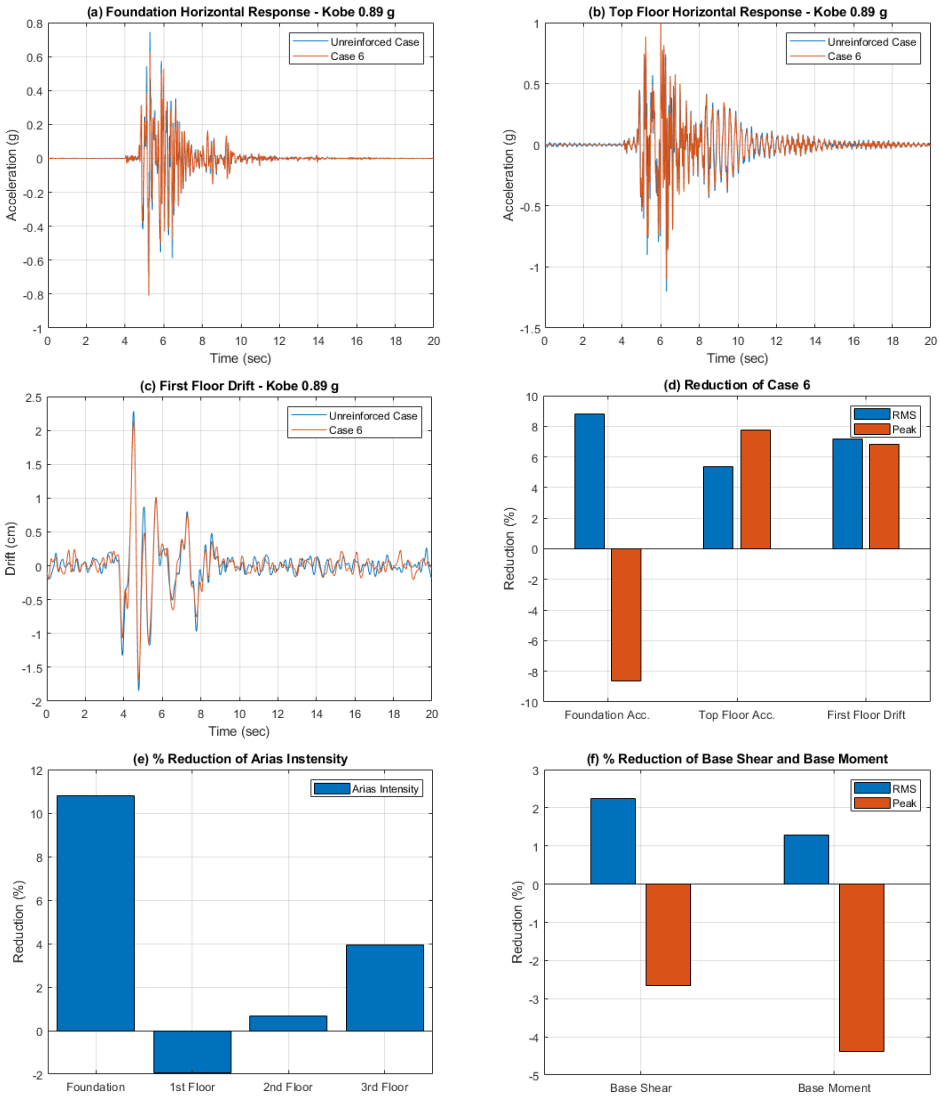

Figure 4.25. Foundation acceleration response (a), Top floor acceleration response (b), First floor acceleration response (c), (%) Reduction of Case 6 (d), (%) Reduction of arias intensity (e), (%) Reduction of base shear and base moment (f) under Kobe Earthquake.

Table 4.21. Horizontal acceleration, Horizontal story drift, Arias intensity, Base Shear and Base Moment reduction factors under Kobe Earthquake (Case 6).

Case 6 under Kobe (PGA=0.89g) Earthquake								
	Foundation		1st Floor		2nd Floor		3rd Floor	
	RMS	Peak	RMS	Peak	RMS	Peak	RMS	Peak
Horizontal Acceleration (g)								
Unreinforced	0.0700	0.7440	0.1018	1.0913	0.0924	0.7928	0.1231	1.2014
Case 6	0.0638	0.8083	0.0993	1.1766	0.0887	0.8180	0.1165	1.1081
Reduction (%)	8.80	-8.65	2.52	-7.82	3.92	-3.18	5.35	7.76
Horizontal Story Drift (cm)								
Unreinforced	-	-	0.29	2.28	0.51	3.51	0.60	4.25
Case 6	-	-	0.27	2.12	0.50	3.65	0.58	4.53
Reduction (%)	-	-	7.18	6.85	2.26	-4.09	2.57	-6.55
Arias Intensity (g-sec)								
Unreinforced	0.0241		0.0511		0.0419		0.0746	
Case 6	0.0215		0.0521		0.0416		0.0717	
Reduction (%)	10.78		-1.94		0.67		3.93	
	Base Shear (kN)				Base Moment (kN-m)			
	RMS		Peak		RMS		Peak	
Unreinforced	0.37		3.46		0.15		1.26	
Case 6	0.36		3.55		0.15		1.32	
Reduction (%)	2.24		-2.65		1.28		-4.38	

4.11. Case 7 – N=3 Geogrid Reinforced 3-Story Building Model

The mentioned performance indicator parameters were evaluated for 3-story building model under Kocaeli, Kobe and El Centro earthquakes. Applied configuration information was mentioned in Section 3.9 and configuration of geogrid reinforced zones for all configuration types was described in Figure 3.22. For this case, N=3 layer of geogrid was used for 3-story building model. Tests were conducted for all strong ground motions and sinusoidal motions. Results are demonstrated for Kocaeli, El Centro and Kobe earthquakes, respectively.

4.11.1. Seismic Response of Case 7 for Kocaeli Earthquake

Maximum increase of peak acceleration response was observed in second floor level by 8.13%. Peak foundation acceleration response reduction and top floor acceleration response reduction were obtained as 11.69% and 5.77% respectively. In addition to peak values, root mean square reductions of the same acceleration responses were detected as 5.61% and 15.66% respectively, as displayed in Figure 4.26a and Figure 4.26b. A reduction of the first floor story drift was observed as 1.22% for peak value and increased

4.50% for RMS value, regarding to unreinforced setup case, as displayed in Figure 4.26c and Figure 4.26d. All performance parameters were summarized and demonstrated in Table 4.22. Maximum reduction of arias intensity was observed at the third floor by 15.01% and at foundation level by %12.99, as in Figure 4.26e. In addition, as displayed in Figure 4.26, base shear and base moment of the test model at the foundation level were reduced slightly by 0.71% and 0.48% respectively, in terms of peak values and increased by 6.39% and 6.96% in terms of RMS values, respectively.

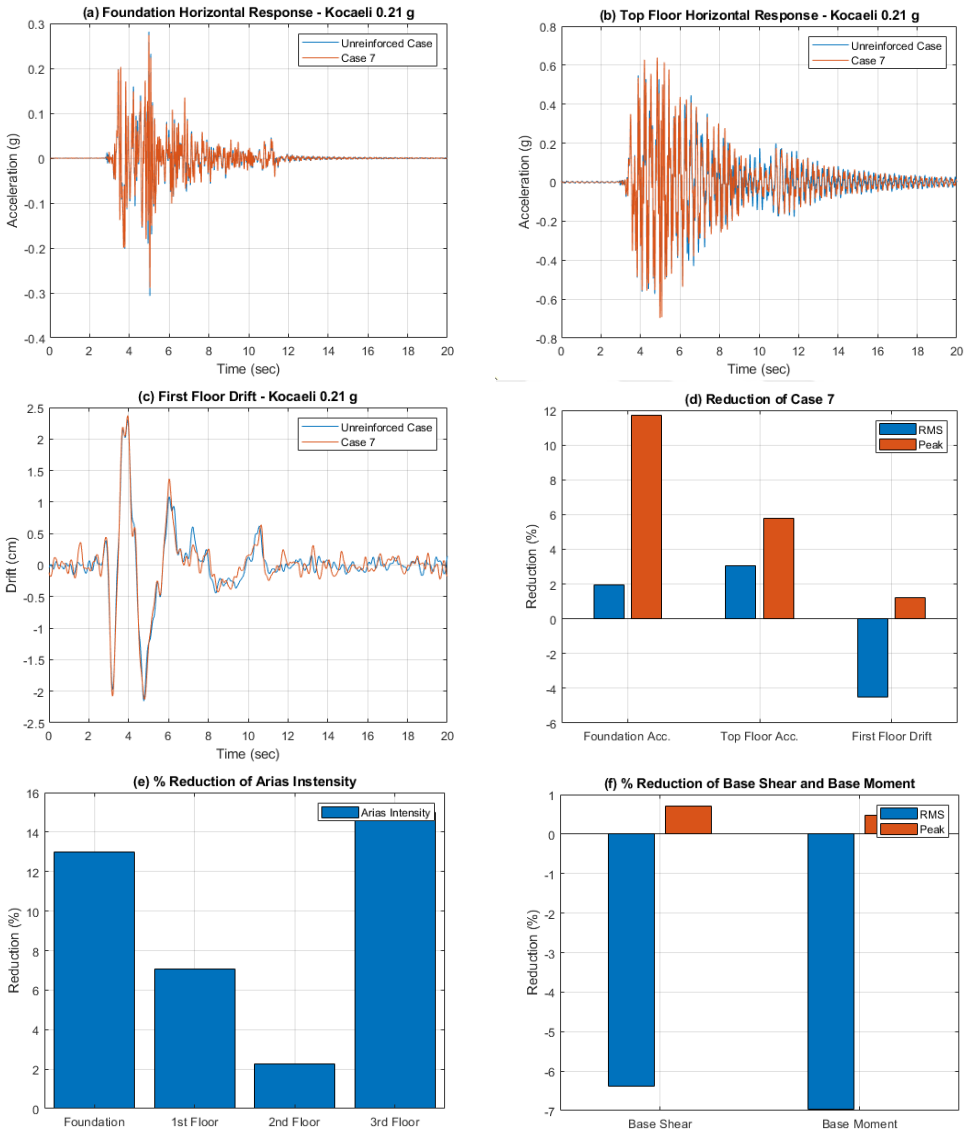

Figure 4.26. Foundation acceleration response (a), Top floor acceleration response (b), First floor acceleration response (c), (%) Reduction of Case 7 (d), (%) Reduction of arias intensity (e), (%) Reduction of base shear and base moment (f) under Kocaeli Earthquake.

Table 4.22. Horizontal acceleration, Horizontal story drift, Arias intensity, Base Shear and Base Moment reduction factors under Kocaeli Earthquake (Case 7).

Case 7 under Kocaeli (PGA=0.21g) Earthquake								
	Foundation		1st Floor		2nd Floor		3rd Floor	
	RMS	Peak	RMS	Peak	RMS	Peak	RMS	Peak
Horizontal Acceleration (g)								
Unreinforced	0.0273	0.2984	0.0862	0.7841	0.0799	0.5941	0.1032	0.6859
Case 7	0.0268	0.2635	0.0878	0.7686	0.0830	0.6424	0.1000	0.6463
Reduction (%)	1.93	11.69	-1.88	1.98	-3.95	-8.13	3.07	5.77
Horizontal Story Drift (cm)								
Unreinforced	-	-	0.41	2.29	0.52	3.33	0.56	3.76
Case 7	-	-	0.43	2.26	0.56	3.28	0.59	3.76
Reduction (%)	-	-	-4.50	1.22	-8.36	1.39	-6.77	-0.22
Arias Intensity (g-sec)								
Unreinforced	0.0040		0.0399		0.0339		0.0565	
Case 7	0.0034		0.0370		0.0331		0.0480	
Reduction (%)	12.99		7.08		2.26		15.01	
	Base Shear (kN)				Base Moment (kN-m)			
	RMS		Peak		RMS		Peak	
Unreinforced	0.28		1.31		0.15		0.54	
Case 7	0.30		1.30		0.16		0.53	
Reduction (%)	-6.39		0.71		-6.96		0.48	

4.11.2. Seismic Response of Case 7 for El Centro Earthquake

For the El Centro earthquake, maximum increase of peak acceleration response was observed in second floor level by 8.89%. Peak foundation acceleration response reduction and top floor acceleration response reduction were obtained as 29.94% and 30.30% respectively. In addition to peak values, root mean square reductions of the same acceleration responses were detected as 20.52% and 24.41% respectively, as displayed in Figure 4.27a and Figure 4.27b. An effect of increase was observed at first floor story drift as 7.45% for peak value and attenuation by 17.85% for RMS value, regarding to unreinforced setup case, as displayed in Figure 4.27c and Figure 4.27d. Maximum reduction of arias intensity was observed at the third floor by 55.59% and maximum increase in the arias intensity was at foundation level by %37.86%, as in Figure 4.27e. Additionally, as displayed in Figure 4.27f, base shear and base moment of the test model at the foundation level were reduced slightly by 3.00% and 4.10% respectively, in terms of peak values and reduced by 19.16% and 19.74% in terms of RMS values, respectively. All performance parameters were summarized and demonstrated in Table 4.23.

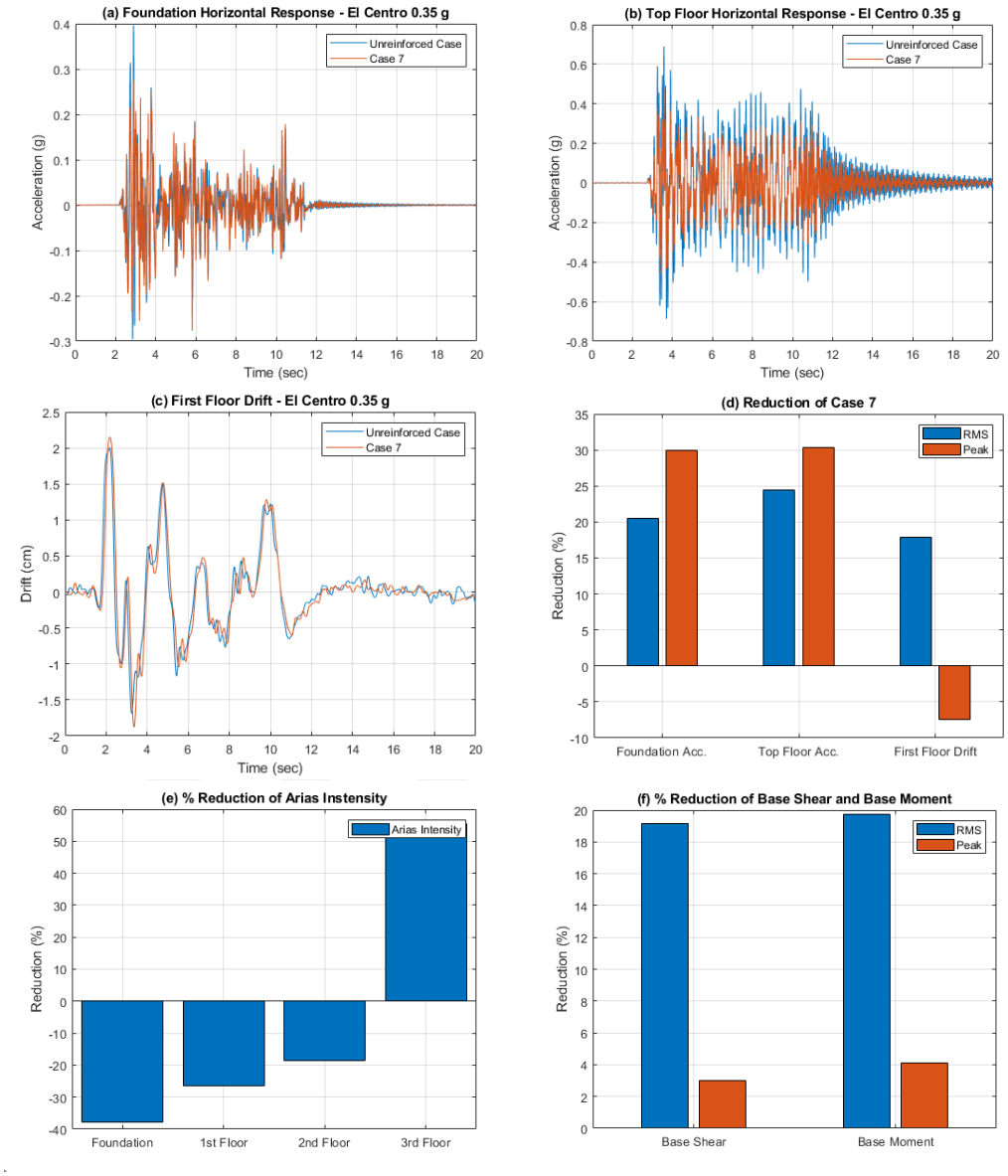

Figure 4.27. Foundation acceleration response (a), Top floor acceleration response (b), First floor acceleration response (c), (%) Reduction of Case 7 (d), (%) Reduction of arias intensity (e), (%) Reduction of base shear and base moment (f) under El Centro Earthquake.

Table 4.23. Horizontal acceleration, Horizontal story drift, Arias intensity, Base Shear and Base Moment reduction factors under El Centro Earthquake (Case 7).

Case 7 under El Centro (PGA=0.35g) Earthquake								
	Foundation		1st Floor		2nd Floor		3rd Floor	
	RMS	Peak	RMS	Peak	RMS	Peak	RMS	Peak
Horizontal Acceleration (g)								
Unreinforced	0.0332	0.3960	0.0899	0.6391	0.0744	0.5584	0.1042	0.6889
Case 7	0.0264	0.2774	0.0684	0.5138	0.0548	0.6080	0.0788	0.4801
Reduction (%)	20.52	29.94	23.96	19.61	26.31	-8.89	24.41	30.30
Horizontal Story Drift (cm)								
Unreinforced	-	-	0.37	2.00	0.46	2.73	0.50	3.07
Case 7	-	-	0.30	2.15	0.36	2.42	0.40	3.00
Reduction (%)	-	-	17.85	-7.45	21.31	11.58	19.82	2.17
Arias Intensity (g-sec)								
Unreinforced	0.0077		0.0562		0.0385		0.0765	
Case 7	0.0106		0.0711		0.0457		0.0340	
Reduction (%)	-37.86		-26.51		-18.56		55.59	
	Base Shear (kN)				Base Moment (kN-m)			
	RMS		Peak		RMS		Peak	
Unreinforced	0.32		1.29		0.14		0.53	
Case 7	0.26		1.25		0.12		0.50	
Reduction (%)	19.16		3.00		19.74		4.10	

4.11.3. Seismic Response of Case 7 for Kobe Earthquake

For the Kobe earthquake, there was an increase in peak foundation acceleration response and reduction in top floor acceleration response which were obtained as 11.23% and 6.63% respectively. There was no reduction in terms of peak values for first and second floor levels. In addition to peak values, root mean square reductions of the same acceleration responses were detected as 23.09% and 17.37% respectively, as displayed in Figure 4.28a and Figure 4.28b. An effect of increase was observed at first floor story drift as 15.45% for peak value and attenuation by 14.70% for RMS value, regarding to unreinforced setup case, as displayed in Figure 4.28c and Figure 4.28d. Maximum reduction of arias intensity was noted at the foundation floor by 10.72% and maximum increase in the arias intensity was at second floor level by 7.87%, as in Figure 4.28e. Additionally, as displayed in Figure 4.28fFigure 4.27, base shear and base moment of the test model at the foundation level were reduced by 13.36% and 13.00% respectively, in terms of peak values and reduced by 11.28% and 10.55% in terms of RMS values, respectively. All performance parameters were summarized and demonstrated in Table 4.24.

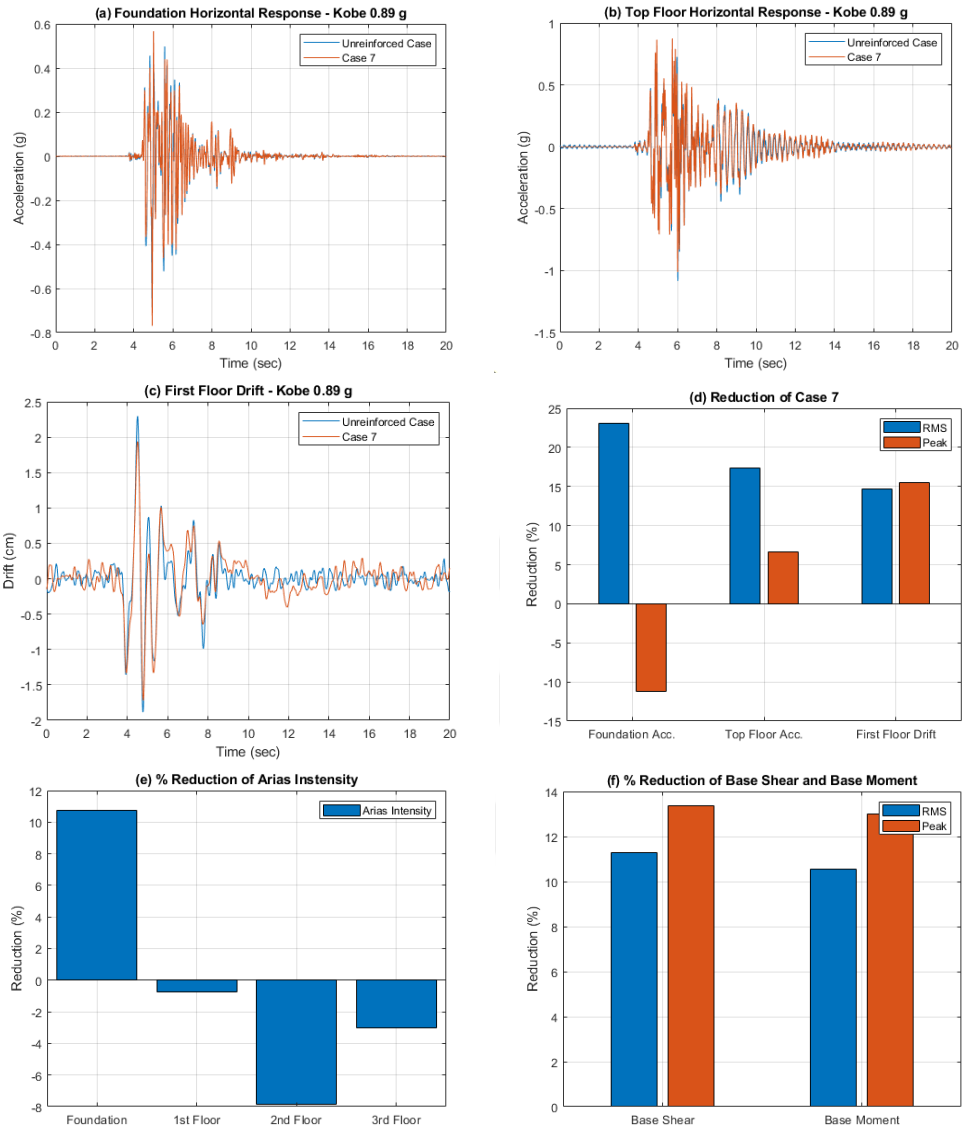

Figure 4.28. Foundation acceleration response (a), Top floor acceleration response (b), First floor acceleration response (c), (%) Reduction of Case 7 (d), (%) Reduction of arias intensity (e), (%) Reduction of base shear and base moment (f) for Kobe Earthquake.

Table 4.24. Horizontal acceleration, Horizontal story drift, Arias intensity, Base Shear and Base Moment reduction factors under Kobe Earthquake (Case 7).

Case 7 under Kobe (PGA=0.89g) Earthquake								
	Foundation		1st Floor		2nd Floor		3rd Floor	
	RMS	Peak	RMS	Peak	RMS	Peak	RMS	Peak
Horizontal Acceleration (g)								
Unreinforced	0.0678	0.6916	0.1023	1.0913	0.0928	0.7928	0.1177	1.0840
Case 7	0.0522	0.7693	0.0836	1.2121	0.0783	0.8775	0.0973	1.0121
Reduction (%)	23.09	-11.23	18.29	-11.07	15.59	-10.69	17.37	6.63
Horizontal Story Drift (cm)								
Unreinforced	-	-	0.29	2.29	0.51	3.51	0.60	4.25
Case 7	-	-	0.25	1.94	0.48	3.05	0.53	3.72
Reduction (%)	-	-	14.70	15.45	6.68	12.86	11.14	12.64
Arias Intensity (g-sec)								
Unreinforced	0.0225		0.0511		0.0419		0.0676	
Case 7	0.0200		0.0515		0.0452		0.0697	
Reduction (%)	10.72		-0.76		-7.87		-3.03	
	Base Shear (kN)				Base Moment (kN-m)			
	RMS		Peak		RMS		Peak	
Unreinforced	0.37		3.47		0.15		1.26	
Case 7	0.33		3.00		0.14		1.10	
Reduction (%)	11.28		13.36		10.55		13.00	

4.12. Case 8 – N=4 Geogrid Reinforced 3-Story Building Model

The mentioned performance indicator parameters were evaluated for 3-story building model under Kocaeli, Kobe and El Centro earthquakes. Applied configuration information was mentioned in Section 3.9 and configuration of geogrid reinforced zones for all configuration types was described in Figure 3.22. For this case, N=4 layer of geogrid was used for 3-story building model. Tests were conducted for all strong ground motions and sinusoidal motions. Results are demonstrated for Kocaeli, El Centro and Kobe earthquakes, respectively.

4.12.1. Seismic Response of Case 8 for Kocaeli Earthquake

For the Kocaeli earthquake, maximum peak acceleration response reduction was observed at first floor by a 21.55%. There was a reduction in peak foundation acceleration response and reduction in top floor acceleration response which were obtained as 2.79% and 5.67% respectively. There were also reductions in terms of peak values for first and second floor levels. In addition to peak values, root mean square effect of the same acceleration responses were identified as -1.37% and 14.42% respectively, as displayed in

Figure 4.29a and Figure 4.29b. An effect of reduction was observed at first floor story drift as 5.65% for peak value and increase was observed by 0.30% for RMS value, regarding to unreinforced setup case, as displayed in Figure 4.29c and Figure 4.29d. Maximum reduction of arias intensity was noted at the second floor by 35.49% and was at third floor level by 34.13%, as in Figure 4.29e. Furthermore, as displayed in Figure 4.29fFigure 4.27, base shear and base moment of the test model at the foundation level were reduced by 5.37% and 5.46% respectively, in terms of peak values and reduced by 0.91% and 1.75% in terms of RMS values, compared to unreinforced case. All performance parameters were summarized and demonstrated in Table 4.25.

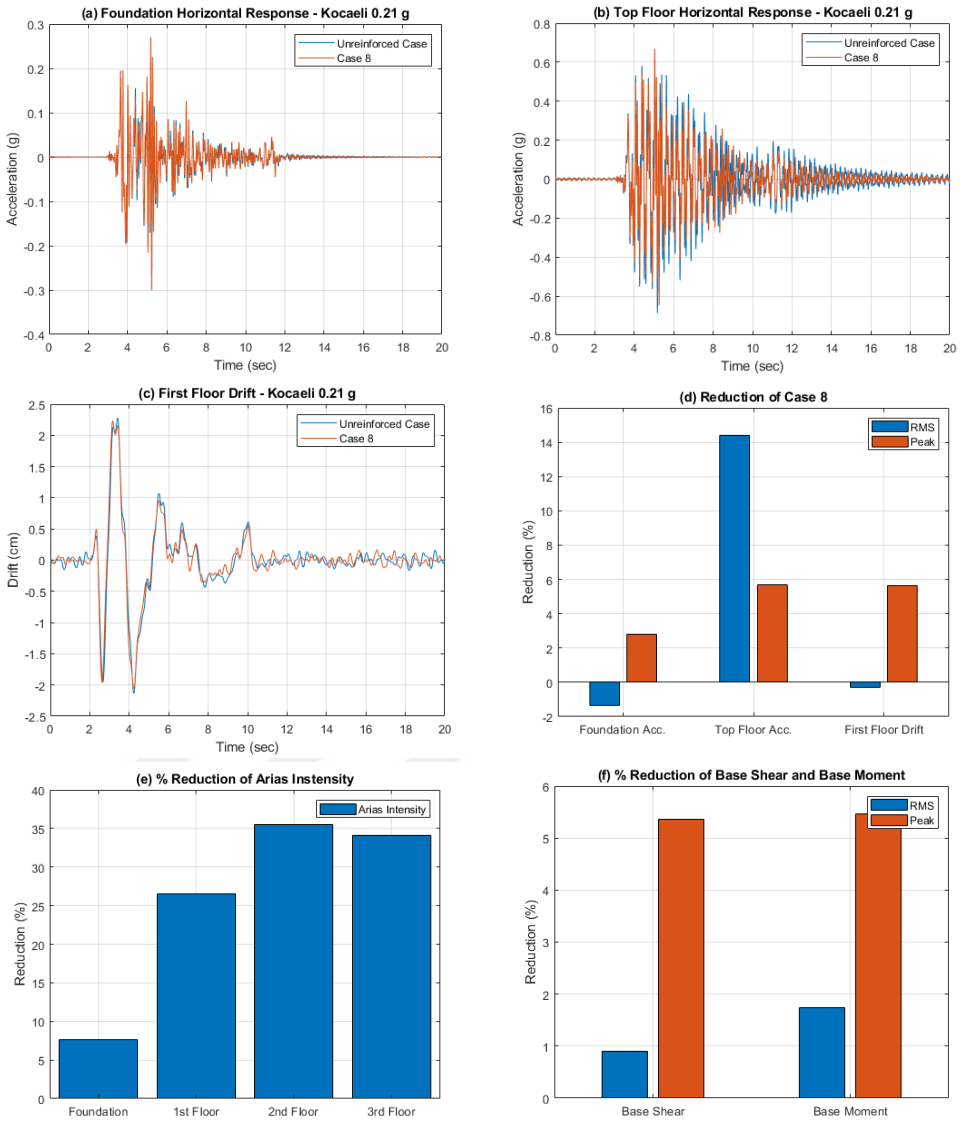

Figure 4.29. Foundation acceleration response (a), Top floor acceleration response (b), First floor acceleration response (c), (%) Reduction of Case 8 (d), (%) Reduction of arias intensity (e), (%) Reduction of base shear and base moment (f) under Kocaeli Earthquake.

Table 4.25. Horizontal acceleration, Horizontal story drift, Arias intensity, Base Shear and Base Moment reduction factors under Kocaeli Earthquake (Case 8).

Case 8 under Kocaeli (PGA=0.21g) Earthquake								
	Foundation		1st Floor		2nd Floor		3rd Floor	
	RMS	Peak	RMS	Peak	RMS	Peak	RMS	Peak
Horizontal Acceleration (g)								
Unreinforced	0.0273	0.3000	0.0862	0.7841	0.0796	0.5941	0.1033	0.6883
Case 8	0.0277	0.2916	0.0781	0.6151	0.0675	0.5654	0.0884	0.6492
Reduction (%)	-1.37	2.79	9.38	21.55	15.31	4.83	14.42	5.67
Horizontal Story Drift (cm)								
Unreinforced	-	-	0.42	2.37	0.52	3.33	0.56	3.76
Case 8	-	-	0.42	2.23	0.51	3.18	0.54	3.53
Reduction (%)	-	-	-0.30	5.65	3.53	4.41	3.51	6.04
Arias Intensity (g-sec)								
Unreinforced	0.0040		0.0399		0.0339		0.0569	
Case 8	0.0037		0.0293		0.0219		0.0375	
Reduction (%)	7.59		26.54		35.49		34.13	
	Base Shear (kN)				Base Moment (kN-m)			
	RMS		Peak		RMS		Peak	
Unreinforced	0.28		1.32		0.15		0.54	
Case 8	0.28		1.25		0.15		0.51	
Reduction (%)	0.91		5.37		1.75		5.46	

4.12.2. Seismic Response of Case 8 for El Centro Earthquake

For the El Centro earthquake, minimum peak acceleration response reduction was observed at third floor by a 1.55%. There was a reduction in peak foundation acceleration response and reduction in top floor acceleration response which were obtained as 11.26% and 9.69% respectively. There were also reductions in terms of peak values for first and second floor levels. In addition to peak values, root mean square effect of the same acceleration responses were identified as increase by 12.33% and 7.04% respectively, as displayed in Figure 4.29a and Figure 4.29b. An effect of reduction was observed at first floor story drift as 8.07% for peak value and increase was observed by 11.71% for RMS value, regarding to unreinforced setup case, as displayed in Figure 4.29c and Figure 4.29d. Maximum reduction of arias intensity was noted at the third floor by 20.62% and was at second floor level by 17.69%, as in Figure 4.29e. Furthermore, as displayed in Figure 4.29fFigure 4.27, base shear and base moment of the test model at the foundation level were reduced by 3.96% and 3.13% respectively, in terms of peak values and increased by 7.65% and 6.42% in terms of RMS values, compared to unreinforced case. All performance parameters were summarized and demonstrated in Table 4.25.

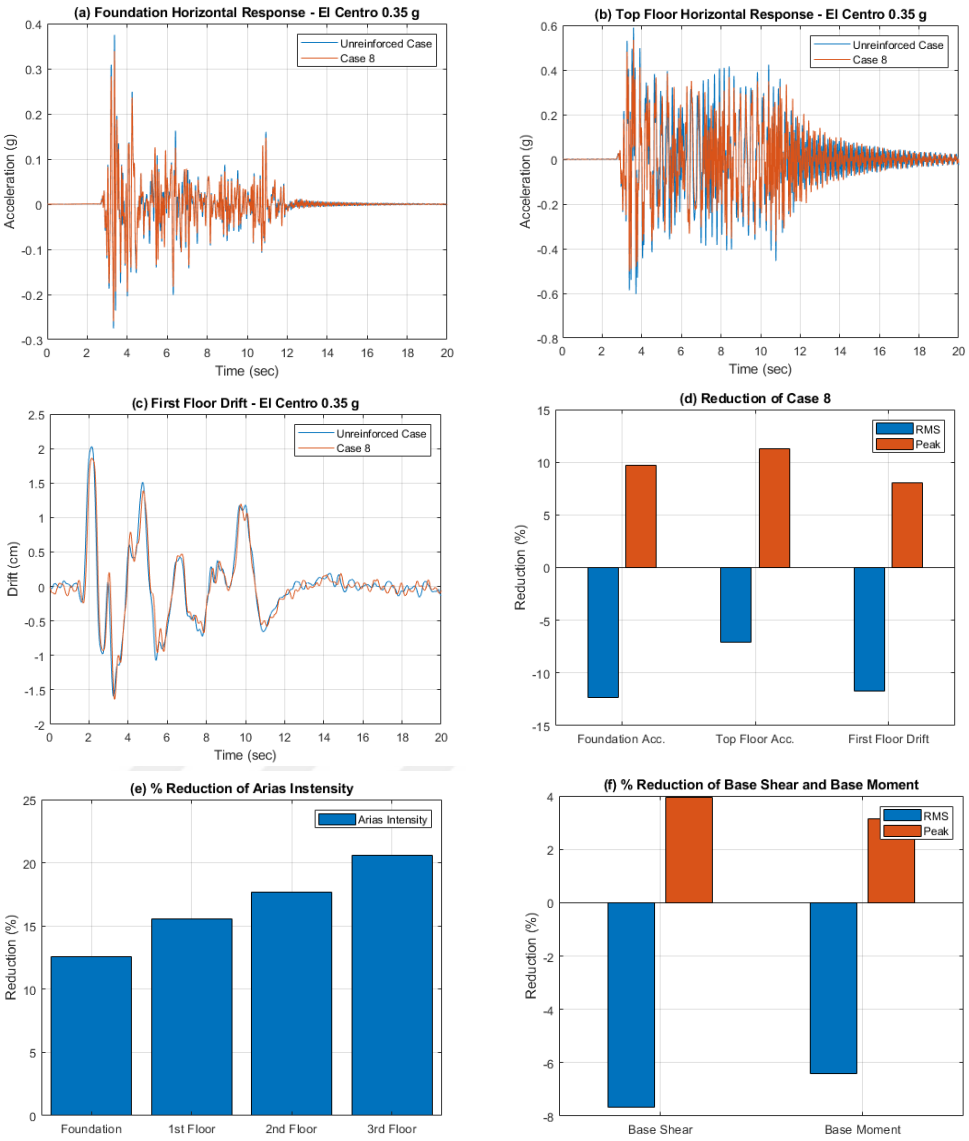

Figure 4.30. Foundation acceleration response (a), Top floor acceleration response (b), First floor acceleration response (c), (%) Reduction of Case 8 (d), (%) Reduction of arias intensity (e), (%) Reduction of base shear and base moment (f) under El Centro Earthquake.

Table 4.26. Horizontal acceleration, Horizontal story drift, Arias intensity, Base Shear and Base Moment reduction factors under El Centro Earthquake (Case 8).

Case 8 under El Centro (PGA=0.35g) Earthquake								
	Foundation		1st Floor		2nd Floor		3rd Floor	
	RMS	Peak	RMS	Peak	RMS	Peak	RMS	Peak
Horizontal Acceleration (g)								
Unreinforced	0.0308	0.3750	0.0893	0.6391	0.0739	0.5584	0.0962	0.6026
Case 8	0.0346	0.3387	0.0987	0.6017	0.0806	0.5497	0.1029	0.5347
Reduction (%)	-12.33	9.67	-10.42	5.85	-9.01	1.55	-7.04	11.26
Horizontal Story Drift (cm)								
Unreinforced	-	-	0.37	2.03	0.46	2.73	0.50	3.07
Case 8	-	-	0.41	1.86	0.48	2.65	0.53	3.00
Reduction (%)	-	-	-11.71	8.07	-3.01	2.90	-7.12	2.19
Arias Intensity (g-sec)								
Unreinforced	0.0067		0.0562		0.0385		0.0652	
Case 8	0.0059		0.0475		0.0317		0.0517	
Reduction (%)	12.59		15.53		17.69		20.62	
	Base Shear (kN)				Base Moment (kN-m)			
	RMS		Peak		RMS		Peak	
Unreinforced	0.32		1.29		0.14		0.53	
Case 8	0.34		1.24		0.15		0.51	
Reduction (%)	-7.65		3.96		-6.42		3.13	

4.12.3. Seismic Response of Case 8 for Kobe Earthquake

Comparison of Case 8 with unreinforced case displayed that, minimum peak acceleration response reduction was observed at first floor by 9.20%. There was no reduction in peak foundation acceleration response and reduction in top floor acceleration response which were obtained as 26.86% and 15.58% accordingly. In addition to peak values, root mean square effect of the same acceleration responses were identified as increase by 4.02% and 8.98% respectively, as displayed in Figure 4.31a and Figure 4.31b. An effect of reduction was observed at first floor story drift as 5.57% for peak value and reduction was observed by a slight 1.57% for RMS value, regarding to unreinforced setup case, as displayed in Figure 4.31c and Figure 4.31d. Maximum reduction of arias intensity was noted at the first floor by 16.37% and was at third floor level by 14.20%, as in Figure 4.31e. Furthermore, as displayed in Figure 4.31fFigure 4.27, base shear and base moment of the test model at the foundation level were reduced by 9.50% and 9.92% respectively, in terms of peak values and increased by 3.63% and 3.93% in terms of RMS values, compared to unreinforced case. All performance parameters were summarized and demonstrated in Table 4.27.

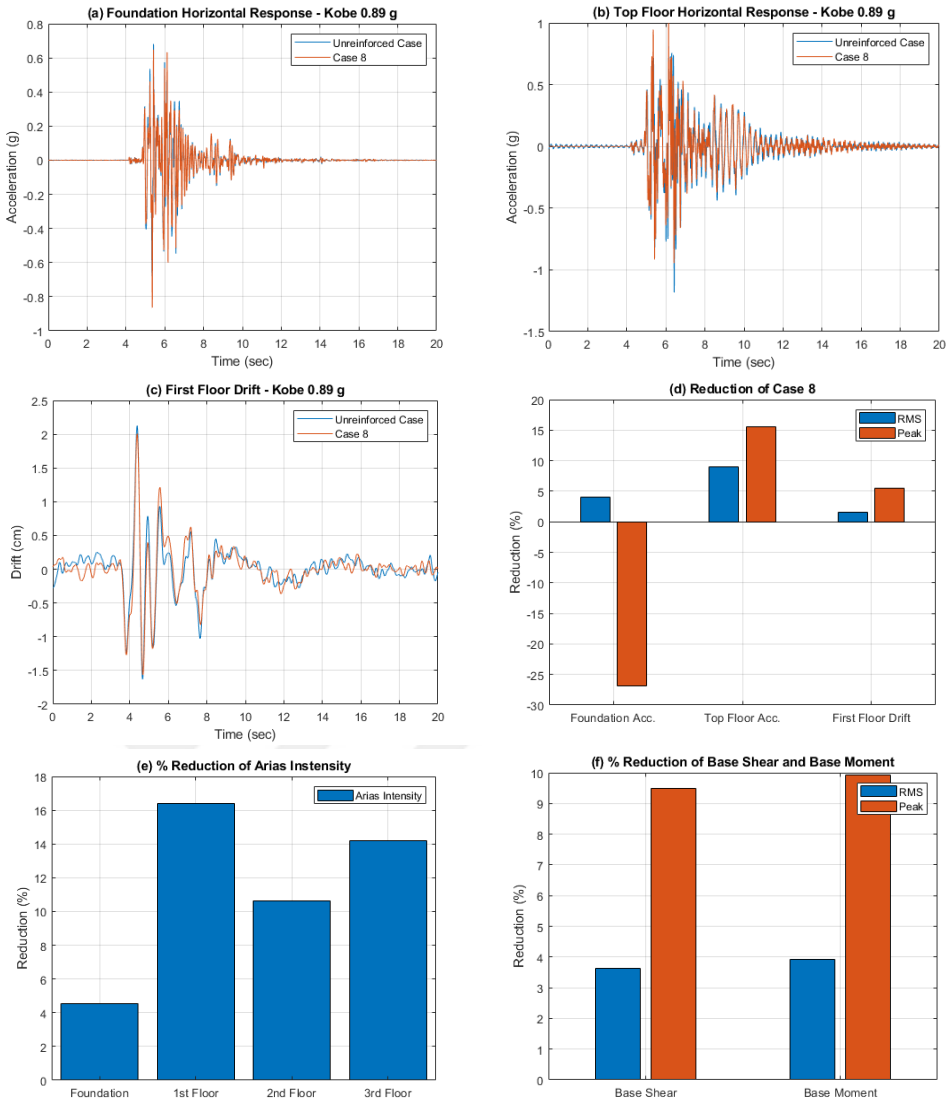

Figure 4.31. Foundation acceleration response (a), Top floor acceleration response (b), First floor acceleration response (c), (%) Reduction of Case 8 (d), (%) Reduction of arias intensity (e), (%) Reduction of base shear and base moment (f) under Kobe Earthquake.

Table 4.27. Horizontal acceleration, Horizontal story drift, Arias intensity, Base Shear and Base Moment reduction factors under Kobe Earthquake (Case 8).

Case 8 under Kobe (PGA=0.89g) Earthquake								
	Foundation		1st Floor		2nd Floor		3rd Floor	
	RMS	Peak	RMS	Peak	RMS	Peak	RMS	Peak
Horizontal Acceleration (g)								
Unreinforced	0.0691	0.6813	0.1016	1.0913	0.0922	0.7928	0.1210	1.1833
Case 8	0.0663	0.8644	0.0913	0.9909	0.0855	0.8283	0.1102	0.9989
Reduction (%)	4.02	-26.86	10.16	9.20	7.26	-4.47	8.98	15.58
Horizontal Story Drift (cm)								
Unreinforced	-	-	0.29	2.13	0.51	3.51	0.60	4.25
Case 8	-	-	0.29	2.01	0.50	3.10	0.57	3.84
Reduction (%)	-	-	1.57	5.57	3.10	11.65	4.88	9.70
Arias Intensity (g-sec)								
Unreinforced	0.0236		0.0511		0.0419		0.0725	
Case 8	0.0225		0.0427		0.0374		0.0622	
Reduction (%)	4.55		16.37		10.64		14.20	
	Base Shear (kN)				Base Moment (kN-m)			
	RMS		Peak		RMS		Peak	
Unreinforced	0.37		3.41		0.15		1.25	
Case 8	0.36		3.08		0.15		1.13	
Reduction (%)	3.63		9.50		3.93		9.92	

5. PARAMETRIC STUDY

In the context of this study, number of stories and effects of geogrid reinforced zones were evaluated in terms of performance indicator parameters for different strong ground motions. Thereby, shaking table tests were conducted and eight performance criteria of top floor acceleration reduction, foundation acceleration reduction, top floor drift reduction, first floor drift reduction, top floor arias intensity reduction, base shear reduction and base moment reduction were investigated. The efficiency of geogrid reinforced zones is checked for all eight cases and results are compared. Geogrid reinforced zone effects for different case setups are then defined and advantages and disadvantages of the systems are reviewed through each parameter characteristics.

Following parts will be expressing these reviews of experimental output, generated through motions of Kocaeli (0.21g), El Centro (0.35g) and Kobe (0.89g) earthquakes which are analyzed in Section 4. The other modified strong ground motions and cyclic sinusoidal motions which are described in Table 4.1 are also will be considered in Section 5.2. The defined Iznik station of Kocaeli earthquake record is also mentioned in the following parts to mention the near fault effect on the cases of geogrid reinforced zones.

5.1. Seismic Responses of Cases under Earthquake Motions with Real PGA Values and Specific Cyclic Sinusoidal Motion

Kocaeli, Kobe and El Centro earthquake record responses of 3-story and 5-story test models were evaluated for realistic PGA values (0.21g for Kocaeli, 0.35g for El Centro and 0.89g for Kobe) of the mentioned motions and specified cyclic sinusoidal motions (13.34 Hz – 0.4 g for 5-story and 12.46 Hz – 0.4 g for 3-story models).

In Table 5.1, outputs of Case 1, which extent 1 layer of geogrid reinforcement and 5-story test model are displayed. Case 1 presented superior results under cyclic sinusoidal motion in terms of top floor and foundation floor arias intensity reduction in addition to RMS and peak values of the first floor drift. When it comes to realistic earthquake motions, El Centro and Kocaeli earthquakes with lower PGA values displayed a better

performance in terms of top floor peak acceleration reduction, when compared with Kobe earthquake. In terms of foundation acceleration, however, Kobe earthquake with higher PGA value exhibited a better performance both for RMS and peak values. On behalf of top floor drift peak values, there were slight effects of geogrid reinforcement layer for the Case 1, since the difference for peak values are close to ±1-2%. Geogrid layer performed better for higher PGA values in terms of first floor drift and showed nearly no effect for Kocaeli earthquake and a slight additional performance for El Centro earthquake. Reinforcement setup was more efficient Kobe and El Centro earthquakes while mentioning arias intensities of both top floor and foundation floor. Additionally, Case 1 setup displayed better performance for the increasing PGA values for base shear and base moment, both for RMS and peak values, while under the Kocaeli earthquake, there was no significant difference.

Table 5.1. % Reduction of Selected performance indicator parameters for Case 1.

Case 1								
	Ground Motions							
	Kocaeli Earthquake (1999) PGA=0.21g		El Centro Earthquake (1940) PGA=0.35g		Kobe Earthquake (1995) PGA=0.89g		Cyclic Sinusoidal Motion 13.34 Hz	
Performance Indicator Parameters	Reduction (%)							
	RMS	Peak	RMS	Peak	RMS	Peak	RMS	Peak
Top Floor Acceleration	-10.39	21.77	15.66	29.47	28.27	-3.17	31.86	36.02
Foundation Acceleration	6.87	11.96	5.61	5.50	16.01	15.16	-10.70	-17.40
Top Floor Drift	-1.66	1.11	-0.09	2.61	11.32	-1.88	25.80	-15.40
First Floor Drift	0.68	0.88	1.28	3.21	18.57	26.43	43.21	31.66
Top Floor Arias Intensity	-18.73		36.35		34.63		58.45	
Foundation Arias Intensity	18.39		20.03		11.14		21.71	
Base Shear	-0.92	0.48	4.50	1.05	16.71	6.74	26.10	-9.78
Base Moment	-1.27	0.63	4.22	1.50	15.69	3.31	26.57	-12.38

For the results of Case 2, which consists of 2 layers of successive geogrid reinforcement layers and 5-story test model, output values are demonstrated in

Table 5.2. Case 2 also presented superior results under cyclic sinusoidal motion in terms of top floor and foundation floor arias intensity reduction, in addition to top floor acceleration reduction RMS and peak values. About the earthquake motions, top floor acceleration peak and RMS values for all motions are reduced under the effect of Case 2 setup. In terms of top floor acceleration peak values, reduction in earthquakes of Kocaeli and El Centro motions with the lower PGA values are higher, when compared to Kobe earthquake. Foundation acceleration peak and RMS values are both reduced under the

Kocaeli motion, and relatively small reductions were noted for Kobe earthquake, on the other hand, foundation acceleration peak value under El Centro earthquake was slightly increased. There were no reduction for top floor drift peak values for all motions and the parameter raised nearly 10% for Kobe motion and Case 2 setup was not able to significantly effect this parameter. First floor drift values displayed and increasing rate of reduction for increasing PGA values of earthquakes and 24.66% reduction was noted for Kobe earthquake. Similarly, geogrid setup of Case 2 displayed better performance for increasing PGA value of motions for top floor arias intensity and 52.50% reduction was observed under the Kobe earthquake, while the same result is negative for Kocaeli earthquake. On behalf of foundation arias intensity, Kocaeli earthquake performance was superior when compared to other earthquake motions and all there were reductions observed for all earthquake cases. In addition, Case 2 configuration displayed a slight performance improvement for base shear peak value, under Kobe earthquake and there were no behaviour update for other motions. Similar to these findings, there was no reductions noted for base moment peak values for all motions.

Table 5.2. % Reduction of Selected performance indicator parameters – Case 2.

Case 2								
	Ground Motions							
	Kocaeli Earthquake (1999) PGA=0.21g		El Centro Earthquake (1940) PGA=0.35g		Kobe Earthquake (1995) PGA=0.89g		Cyclic Sinusoidal Motion 13.34 Hz	
Performance Indicator Parameters	Reduction (%)							
	RMS	Peak	RMS	Peak	RMS	Peak	RMS	Peak
Top Floor Acceleration	17.26	22.02	28.06	19.24	39.23	10.18	51.22	35.98
Foundation Acceleration	29.28	13.51	26.76	-4.74	14.80	5.51	4.72	-17.46
Top Floor Drift	4.12	-3.18	9.94	-5.90	-9.21	-10.43	24.72	-11.38
First Floor Drift	21.25	-0.50	25.79	2.89	13.00	24.66	21.75	-5.11
Top Floor Arias Intensity	-9.24		15.34		52.50		81.13	
Foundation Arias Intensity	19.56		12.54		9.49		25.59	
Base Shear	6.80	-1.01	14.74	-1.62	-6.92	2.97	23.19	-9.80
Base Moment	4.51	-1.16	12.57	-2.77	-8.46	-1.27	24.81	-9.43

The results of Case 3, which contains 3 layers of geogrid reinforcement and 5-story test model, are displayed in Table 5.3. Similar to previously mentioned case, Case 3 presented superior results under cyclic sinusoidal motion in terms of top floor and foundation floor arias intensity reduction, as well as RMS and peak values of the first floor drift. About the earthquake motions, the most reduction was observed in El Centro earthquake for the peak top floor acceleration reduction. For the peak values of the

foundation acceleration, reduction rate was displayed a minor decrease and 12.74% reduction was noted for Kocaeli motion. In terms of top floor drift peak values, there was no reductions and instead, slight increases were noted for the parameter. Case 3 displayed a better performance on behalf of first floor drift peak value under increasing PGA values of earthquake motions, for both RMS and peak values. Thus, Case 3 configuration performed superior in Kobe earthquake in the aspect of first floor story drift and top floor arias intensity displayed a similar reaction. Foundation arias intensity gradually decreased for improving PGA values of earthquakes, therefore the specific configuration performed better under Kocaeli earthquake. In terms of base shear peak reduction as well as the base moment peak reduction, Case 3 performed better under higher PGA values and there was no reduction noted for Kocaeli motion. There were no significant improvements noted for the RMS values of both base shear and base moment parameters.

Table 5.3. % Reduction of Selected performance indicator parameters – Case 3.

Case 3								
	Ground Motions							
	Kocaeli Earthquake (1999) PGA=0.21g		El Centro Earthquake (1940) PGA=0.35g		Kobe Earthquake (1995) PGA=0.89g		Cyclic Sinusoidal Motion 13.34 Hz	
Performance Indicator Parameters	Reduction (%)							
	RMS	Peak	RMS	Peak	RMS	Peak	RMS	Peak
Top Floor Acceleration	-3.57	15.18	6.97	18.33	17.83	11.46	16.34	13.36
Foundation Acceleration	9.50	12.74	13.76	8.57	12.52	5.64	12.08	-5.06
Top Floor Drift	-4.79	-7.64	5.41	-0.47	-0.99	-0.14	20.08	-12.78
First Floor Drift	5.83	6.03	9.78	12.94	10.01	23.06	26.76	16.94
Top Floor Arias Intensity	-10.13		4.22		18.10		24.75	
Foundation Arias Intensity	16.58		17.47		7.85		36.40	
Base Shear	-3.24	-4.22	3.75	5.05	0.48	9.85	24.82	-5.81
Base Moment	-4.62	-5.53	2.52	3.13	-0.15	6.17	24.50	-7.50

The performance indicator parameters of Case 4, which consists of 4 layers of successive geogrid reinforcement and 5-story test model, are presented in Table 5.4. The configuration of Case 4 displayed superior results for top floor and foundation arias intensity under cyclic sinusoidal motion. Also, most reduction for top floor acceleration peak value was observed under the cyclic motion. Base shear and base moment peak values, on the other hand, were increased around 13-14%. For the earthquake motions, most top floor acceleration peak reduction was observed under the effect of El Centro earthquake and Kocaeli earthquake gradually, which is above 20%. Most reduction in foundation acceleration peak values was observed under Kocaeli earthquake and following

El Centro earthquake motion. These two parameters also reduced under the Kobe earthquake in a relatively small percent. Top floor peak drift value was improved under the increasing PGA value of the motions, thereby Case 4 performed better under Kobe motion, in this aspect. Similarly, first floor peak drift ratio was reduced for increasing PGA values, and additionally, there were reductions noted for all earthquake motions, as well as the RMS values, where only El Centro earthquake was an exception. Top floor arias intensity was reduced for higher PGA values and there was no reduction for the Kocaeli earthquake, however, Kobe and El Centro motion impact were reduced above the 20%. Foundation arias intensity was reduced for all motions and Case 4 performed superior under Kocaeli and El Centro earthquake, in terms of this parameter. In addition to these findings, base shear and base moment reduction peak values were greater in higher PGA values, thereby geogrid configuration performed better under Kobe earthquake. There were no reductions, but increase observed for the Kocaeli earthquake for the same parameters.

Table 5.4. % Reduction of Selected performance indicator parameters – Case 4.

Case 4								
	Ground Motions							
	Kocaeli Earthquake (1999) PGA=0.21g		El Centro Earthquake (1940) PGA=0.35g		Kobe Earthquake (1995) PGA=0.89g		Cyclic Sinusoidal Motion 13.34 Hz	
Performance Indicator Parameters	Reduction (%)							
	RMS	Peak	RMS	Peak	RMS	Peak	RMS	Peak
Top Floor Acceleration	13.60	21.22	-0.67	23.30	8.96	14.42	36.39	24.11
Foundation Acceleration	24.57	16.51	1.17	11.56	-4.53	4.62	10.77	2.28
Top Floor Drift	-0.57	-4.96	-4.15	1.62	-12.95	13.82	9.33	-13.71
First Floor Drift	19.62	4.54	-1.54	14.10	2.67	33.41	16.53	-3.30
Top Floor Arias Intensity	-1.26		22.12		29.12		53.15	
Foundation Arias Intensity	26.83		26.41		9.02		45.49	
Base Shear	3.95	-11.31	-0.55	1.03	-9.62	16.60	10.57	-13.73
Base Moment	1.03	-10.78	-1.00	0.16	-10.93	14.95	10.62	-13.90

The results of Case 5, which contains 1 layer of geogrid reinforcement and 3-story test model, are represented in Table 5.5. Similar to previously mentioned 5-story cases, Case 5 presented superior results under cyclic sinusoidal motion in terms of top floor arias intensity, however, foundation arias intensity was proportionally increased. Top floor acceleration peak and RMS values as well as first floor drift and base shear – base moment parameters were reduced most, compared to earthquake motions. When it comes to earthquake motions, there were no reductions under the effect of Kocaeli and El Centro earthquake in terms of top floor acceleration peak values. For this parameter, reduction

was observed in Kobe earthquake, as well as the RMS value. On behalf of peak value of foundation acceleration, effects under the El Centro earthquake declined the most, followed by Kocaeli earthquake. There were no reduction or significant performance improvement noted for the top floor drift peak values, similar to RMS values. Maximum first floor drift was noted under the El Centro earthquake reaction. In terms of RMS values, there were reductions for Kocaeli and Kobe motions. Thus, configuration was not providing functional performance improvements under the effect of El Centro earthquake, considering all parameters, however, peak values are smoothed for this motion. Top floor arias intensity was not reduced for the Kocaeli and Kobe earthquakes nor El Centro in a respectable amount. Base shear and moment peak values were hardly changed for Kocaeli earthquake and decreased for Kobe earthquake. Thereby, Case 5 displayed an appropriate improvement for Kocaeli motion among other strong ground motions.

Table 5.5. % Reduction of Selected performance indicator parameters – Case 5.

Case 5								
	Ground Motions							
	Kocaeli Earthquake (1999) PGA=0.21g		El Centro Earthquake (1940) PGA=0.35g		Kobe Earthquake (1995) PGA=0.89g		Cyclic Sinusoidal Motion 12.46 Hz	
Performance Indicator Parameters	Reduction (%)							
	RMS	Peak	RMS	Peak	RMS	Peak	RMS	Peak
Top Floor Acceleration	10.06	-5.35	-21.44	-11.75	4.96	8.45	57.35	56.14
Foundation Acceleration	20.78	17.66	-14.19	23.63	15.50	-13.95	-26.39	-38.10
Top Floor Drift	4.64	-0.45	-15.82	1.06	6.14	-8.96	10.17	12.18
First Floor Drift	12.68	3.00	-19.62	11.12	9.37	-0.75	54.77	35.65
Top Floor Arias Intensity	-6.86		4.55		-20.70		69.08	
Foundation Arias Intensity	16.38		15.58		7.75		-87.91	
Base Shear	6.77	-0.42	-16.52	4.28	5.19	-6.19	-8.55	10.75
Base Moment	5.08	-0.81	-15.73	2.85	4.08	-7.26	-7.83	8.95

For the results of Case 6, which consists 2 layers of successive geogrid reinforcement layers and 3-story test model, reduction values of responses are demonstrated in Table 5.6. Geogrid configuration of the case presented better performance under cyclic sinusoidal motion on behalf of first floor drift, top floor drift, base shear and base moment reduction for both RMS and peak values. About the earthquake motions, Case 6 configuration displayed better results in El Centro motion regarding to top floor acceleration and foundation acceleration peak values. RMS values for the parameters remain almost unchanged for the parameters. For the lower and higher PGAs, a proper performance advancement is not confirmed. There is no reduction detected for the top floor drift peak

ratios for all realistic earthquake motions. With reference to top floor and foundation arias intensity values, El Centro motion sample displayed better reduction results. In respect of base shear and base moment peak values, a slight improvement is noted for El Centro motion and an amplification is detected for both Kocaeli and Kobe motions. Thus, the geogrid arrangement of Case 6 set out finer performance outcomes for El Centro earthquake, when compared with other earthquake motions.

Table 5.6. % Reduction of Selected performance indicator parameters – Case 6.

Case 6								
	Ground Motions							
	Kocaeli Earthquake (1999) PGA=0.21g		El Centro Earthquake (1940) PGA=0.35g		Kobe Earthquake (1995) PGA=0.89g		Cyclic Sinusoidal Motion 12.46 Hz	
Performance Indicator Parameters	Reduction (%)							
	RMS	Peak	RMS	Peak	RMS	Peak	RMS	Peak
Top Floor Acceleration	12.66	-2.00	-0.69	11.64	5.35	7.76	19.95	5.10
Foundation Acceleration	10.54	2.07	-0.45	13.33	8.80	-8.65	9.16	-6.84
Top Floor Drift	8.68	-12.27	-0.83	-0.76	2.57	-6.55	22.90	10.13
First Floor Drift	8.06	-4.88	-0.97	4.54	7.18	6.85	26.69	12.31
Top Floor Arias Intensity	7.94		14.07		3.93		12.96	
Foundation Arias Intensity	3.15		14.48		10.78		-11.69	
Base Shear	7.37	-11.62	-0.31	2.18	2.24	-2.65	21.48	7.93
Base Moment	7.58	-12.51	0.07	1.35	1.28	-4.38	22.11	7.97

Results for Case 7, which involved 3 layers of geogrid reinforcement sheets and 3-story test model are represented in Table 5.7. Case 7 arrangement was not able to highlight a specific distinct behavioral aspect under cyclic sinusoidal motion, compared with earthquake motions. A performance improvement top floor acceleration and first floor drift peak and RMS values was confirmed. In addition, base shear and base moment peak values were reduced. In terms of earthquake motions, Case 7 configuration displayed superior reduction amount for the top floor acceleration and foundation acceleration parameters under El Centro earthquake, in comparison with Kocaeli and Kobe earthquakes. Both RMS and peak values were decreased between 20 to 30%. Top floor drift peak values decreased in correlation with the increasing PGA value of the earthquake motions. For the first floor drift, configuration displayed better reduction under the effect of Kobe motion. In terms of top floor arias intensity values, there was a slight increase for Kobe motion and huge reduction for El Centro motion, however, foundation arias intensity value for the El Centro motion was increased by a high amount. Similar to top floor drift, foundation arias intensity, base shear and base moment reduction peak values are increased according to

growing PGA values. Thereby, configuration of Case 7 with 3 geogrid layers displayed an appropriate improvement for El Centro motion among other strong ground motions, followed by the Kobe motion.

Table 5.7. % Reduction of Selected performance indicator parameters – Case 7.

Case 7								
	Ground Motions							
	Kocaeli Earthquake (1999) PGA=0.21g		El Centro Earthquake (1940) PGA=0.35g		Kobe Earthquake (1995) PGA=0.89g		Cyclic Sinusoidal Motion 12.46 Hz	
Performance Indicator Parameters	Reduction (%)							
	RMS	Peak	RMS	Peak	RMS	Peak	RMS	Peak
Top Floor Acceleration	3.07	5.77	24.41	30.30	17.37	6.63	17.96	2.39
Foundation Acceleration	1.93	11.69	20.52	29.94	23.09	-11.23	2.84	-14.25
Top Floor Drift	-6.77	-0.22	19.82	2.17	11.14	12.64	-1.75	10.67
First Floor Drift	-4.50	1.22	17.85	-7.45	14.70	15.45	17.81	9.22
Top Floor Arias Intensity	15.01		55.59		-3.03		6.34	
Foundation Arias Intensity	12.99		-37.86		10.72		-31.37	
Base Shear	-6.39	0.71	19.16	3.00	11.28	13.36	-10.62	5.49
Base Moment	-6.96	0.48	19.74	4.10	10.55	13.00	-11.64	6.17

The performance indicator parameters of Case 8, which include 4 layers of successive geogrid reinforcement and 3-story test model, are displayed in Table 5.8. The configuration of Case 8 displayed no significant reduction results for many of the performance criteria under cyclic sinusoidal motion. About the earthquake motions, the most reduction was observed in Kobe earthquake followed by El Centro earthquake for the peak top floor acceleration reduction. The reduction was increasing for the higher PGA values of motions. Foundation acceleration peak values was reduced for the earthquakes with lower PGA values and for the Kobe earthquake, there was no reduction but an increase. On behalf of top floor drift and foundation drift values, Case 8 configuration reduced peak value amplitudes under all earthquake motions. Top floor arias intensity reduction values get lower with the increasing PGA values. Foundation arias intensity was also reduced under all earthquake motions and a slight reduction factor is noted for Kobe motion. Similarly, base shear and base moment peak values were decreased under all motions and Case 8 performed better in Kobe earthquake motion, in terms of these performance indicators. Additionally, RMS factors for the same parameters were slightly reduced under Kobe motion. Consequently, for the Case 8 arrangement of geogrid layers, effects of Kobe earthquake were gradually decreased for both RMS and peak values, where only foundation acceleration peak value is an exception.

Table 5.8. % Reduction of Selected performance indicator parameters – Case 8.

Case 8								
	Ground Motions							
	Kocaeli Earthquake (1999) PGA=0.21g		El Centro Earthquake (1940) PGA=0.35g		Kobe Earthquake (1995) PGA=0.89g		Cyclic Sinusoidal Motion 12.46 Hz	
Performance Indicator Parameters	Reduction (%)							
	RMS	Peak	RMS	Peak	RMS	Peak	RMS	Peak
Top Floor Acceleration	14.42	5.67	-7.04	11.26	8.98	15.58	5.21	-0.28
Foundation Acceleration	-1.37	2.79	-12.33	9.67	4.02	-26.86	6.23	0.91
Top Floor Drift	3.51	6.04	-7.12	2.19	4.88	9.70	-7.57	8.54
First Floor Drift	-0.30	5.65	-11.71	8.07	1.57	5.57	4.15	-1.93
Top Floor Arias Intensity	34.13		20.62		14.20		2.58	
Foundation Arias Intensity	7.59		12.59		4.55		4.79	
Base Shear	0.91	5.37	-7.65	3.96	3.63	9.50	-12.82	1.34
Base Moment	1.75	5.46	-6.42	3.13	3.93	9.92	-12.18	3.02

5.2. Effects of Geogrid Reinforced Zones on Performance Parameters under Earthquake Motions with Increasing PGAs and Cyclic Sinusoidal Motions with Various Frequencies

Since the geogrid reinforced zone impact on the test setup for different cases is identified in previous chapters, the other mentioned earthquake motions which are described in Table 4.1 with various PGA values and cyclic sinusoidal motions with various frequency/PGA values are investigated in this context. The outcomes of the various tests are compared and distribution charts were generated to understand and evaluate performance range of the introduced geogrid reinforced zones, for various conditions.

Mentioned earthquake motions for this chapter will be free vibration tests; 3.93 Hz (0.3g), 12.46 Hz (0.4g), 18.35 Hz (0.5g) for 3-story model and 2.33 Hz (0.25g), 8.58 Hz (0.35g), 13.34 Hz (0.4g), 17.52 Hz (0.5g), 19.90 Hz (0.6g) for 5-story model. In terms of strong ground motions; Kocaeli earthquake with 0.21g and 0.51g, El Centro earthquake with 0.35g, 0.55g and 0.89g; Kobe earthquake with 0.74g and 0.89g; Kocaeli Iznik station record with 0.12g and 0.24g are utilized to provide distribution charts. Results and reductions are taken into account for each performance criteria individually.

5.2.1. Effects of Geogrid Reinforced Zones on Top Floor Acceleration

As demonstrated in Figure 5.1; top floor acceleration reduction parameters are presented for each motion individually. For the Kocaeli earthquake (Figure 5.1a), Case 1 test setup performed the best, which was comprised of 1 layer of geogrid with 5-story building model. For a similar 1 layer setup, Case 5 also displayed similar slope angle from a lower reduction point. Similarly, Case 8 and Case 4 displayed similar horizontal behavior, however, in a stable manner. Thus, for the improving peak ground acceleration; Case 1, 5 and followingly Case 2, displayed an increasing performance. For the El Centro earthquake (Figure 5.1b), a general behavior was exhibited by all cases, where all reductions are likely to converge to a single, lower point. Generally, cases performed better under the lower PGA values of El Centro earthquake and for higher values, the reductions were expected to shrink. In terms of Kobe earthquake (Figure 5.1c), Case 7 was functioning properly even in increasing PGA values of the motion. Cases that have similar behavior but less efficient are; Case 2, Case 3 and Case 4, which are all 5-story cases, however, Case 1 of 5-story building was less efficient among all cases. Additionally, Case 6 was in an increasing trend with the effect of increasing PGA. For the Kocaeli Iznik record (Figure 5.1d), a proper performance improvement was valid for Case 8, which was stable near the 15% reduction value and also Case 4 was progressively performing better for the increasing PGA value. The other cases displayed no significant reduction performance for the increasing PGA values, however, all were efficient to reduce the top floor acceleration to various degrees, for 0.12g. For the cyclic sinusoidal motions (Figure 5.1e); Case 1, Case 5 and Case 2 displayed the highest reductions in the middle range frequency zone and Case 1, Case 2, Case 3 and Case 4 performed better for higher frequency rates, while providing a poor performance for the smaller frequency ranges. The most reduction was noted for Case 1 under Kocaeli earthquake motion for 0.51g, which is above 30%.

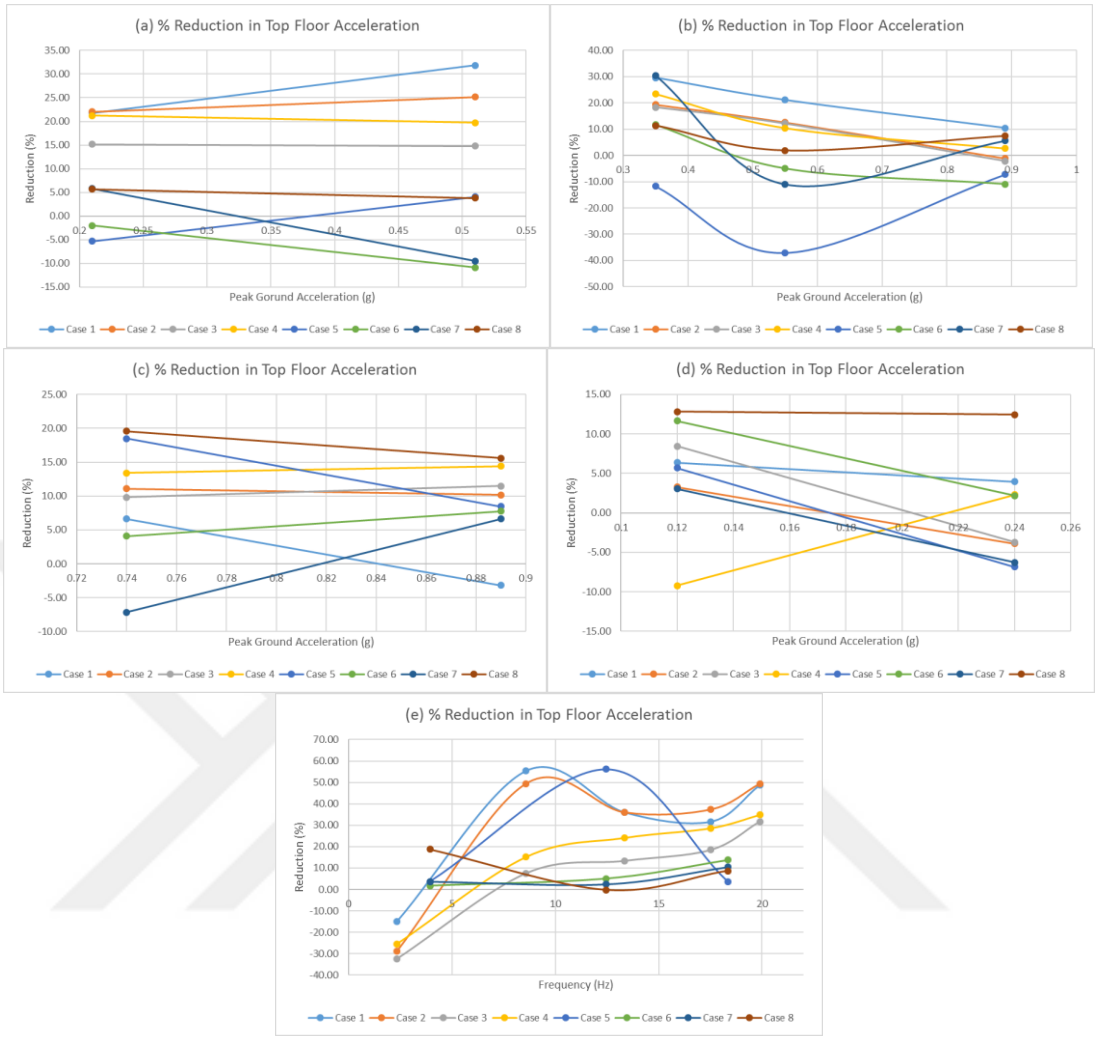

Figure 5.1. Reduction distributions of top floor acceleration for Kocaeli earthquake (a), El Centro earthquake (b), Kobe earthquake (c), Kocaeli Iznik record motion (d) and Cyclic sinusoidal motion (e) for all cases.

5.2.2. Effects of Geogrid Reinforced Zones on Foundation Acceleration

Foundation acceleration reduction distribution graphics are demonstrated in Figure 5.2 and reduction parameters are presented for each motion individually. For the Kocaeli earthquake (Figure 5.2a), Case 5 test setup performed the best, along with the Case 6 and Case 8, for the higher PGA values of the motion. Although the rest of the cases displayed a declining trend, all of the cases reduced the foundation acceleration impact above 10%, except Case 6 and Case 8, for the lower PGA values. Case 1, Case 2 and Case 3 were increasing the foundation acceleration values for the higher PGA values of the same motion. For the El Centro motion (Figure 5.2b), Case 1, Case 2, Case 3, Case 4 and Case 5

exhibited better performance for lower and higher PGA values. For the mid-range PGA value, reduction ratios were proportionally decreased and Case 1, Case 5 and Case 8 configurations displayed the effect of amplification on foundation acceleration. In the scope of Kobe earthquake (Figure 5.2c), Case 1, Case 2, Case 3 and Case 4 functioned properly and reduced the foundation acceleration in various reduction ranges. On the other hand, Case 5, Case 6, Case 7 and Case 8 increased the foundation acceleration value. Most reduction was noted by the Case 1 for the 0.89g while the least was noted by Case 7 around 0.74g. For the Iznik record of Kocaeli earthquake (Figure 5.2d), Case 6, Case 7 and Case 8 behaved in a similar way and represent the best performance at 0.12g, while the reduction effect diminished with the increasing PGA value of the record. Among the cyclic sinusoidal motions (Figure 5.2e), Case 8 functioned in a stabilized manner for increasing frequency ranges. Also, Case 1, Case 2 and Case 4 displayed positive reductions for 20 Hz frequency range. However, in overall, cyclic sinusoidal motion reductions were below 10% for all cases and there are also cases that amplifies the foundation acceleration effect. Greatest reduction in terms of foundation acceleration was identified for Case 7, under the El Centro earthquake with 0.35g, around 30%.

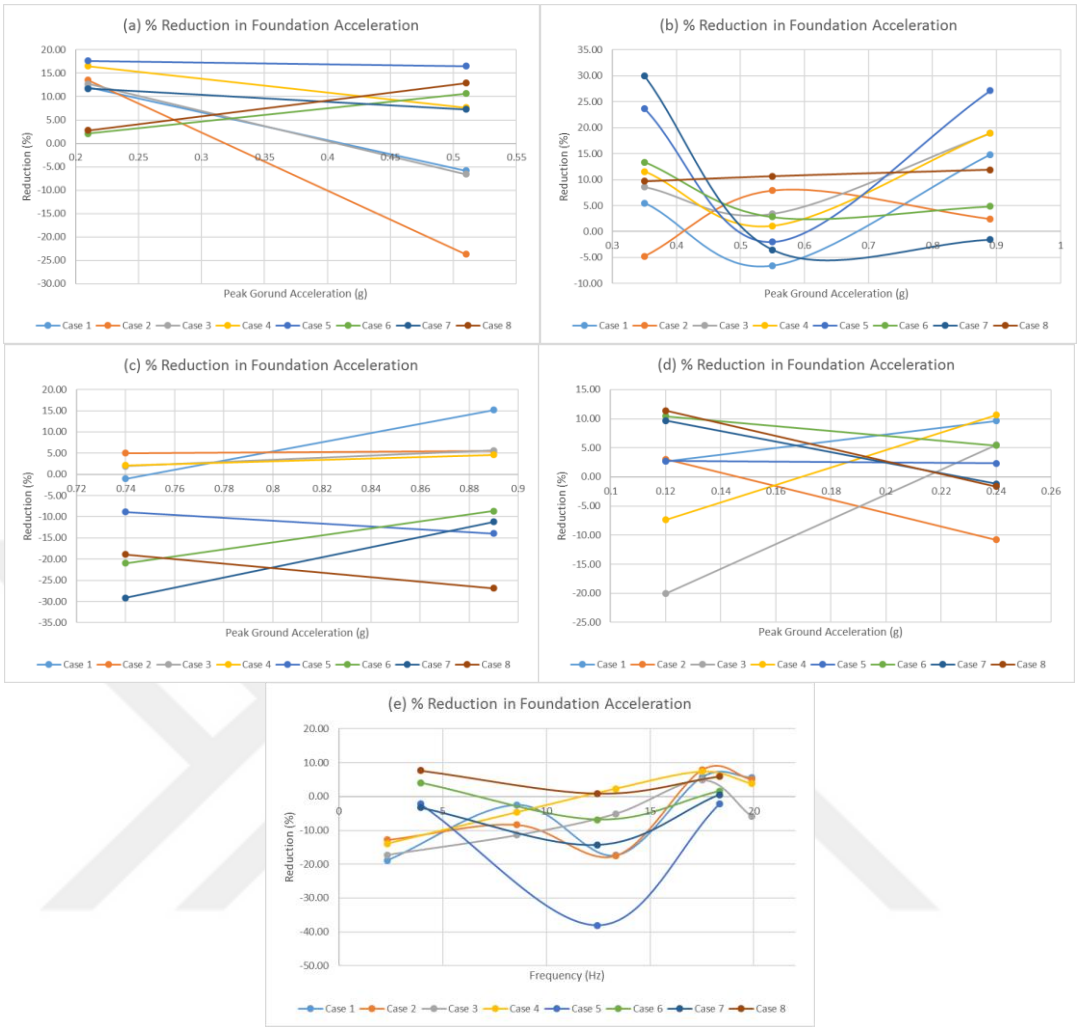

Figure 5.2. Reduction distributions of foundation acceleration for Kocaeli earthquake (a), El Centro earthquake (b), Kobe earthquake (c), Kocaeli Iznik record motion (d) and Cyclic sinusoidal motion (e) for all cases.

5.2.3. Effects of Geogrid Reinforced Zones on Top Floor Drift

Top floor drift reductions for each motion group are showed in Figure 5.3 and reduction parameters are presented. For the Kocaeli earthquake motions (Figure 5.3a), Case 1 functioned properly in all PGA values among with Case 5 and Case 7. The reduction value of Case 1 was around 20% for 0.51g, which was the highest reduction value. Case 8 was in a decreasing trend while the PGA was increasing. Among the El Centro motions (Figure 5.3b), Case 1, Case 4, Case 5 and Case 7 displayed efficient reduction values for all PGA ranges and Case 7 displayed the maximum reduction under the 0.89 PGA by 14%. For the Kobe motion (Figure 5.3c), all cases displayed similar

reduction values of their own for the increasing PGAs and outputs are generally in a steady horizontal line appearance. For the Iznik station record (Figure 5.3d), Case 6, Case 7 and Case 8 were providing better performance by displaying positive reduction values for both lower and higher PGA values of the motion. The most efficient setup appeared to be Case 8 for the 0.12g. Cyclic sinusoidal motion behavior (Figure 5.3e), varied in a large reduction range and greatest reduction was at Case 2, for 8.58 Hz, by a reduction value of 52%.

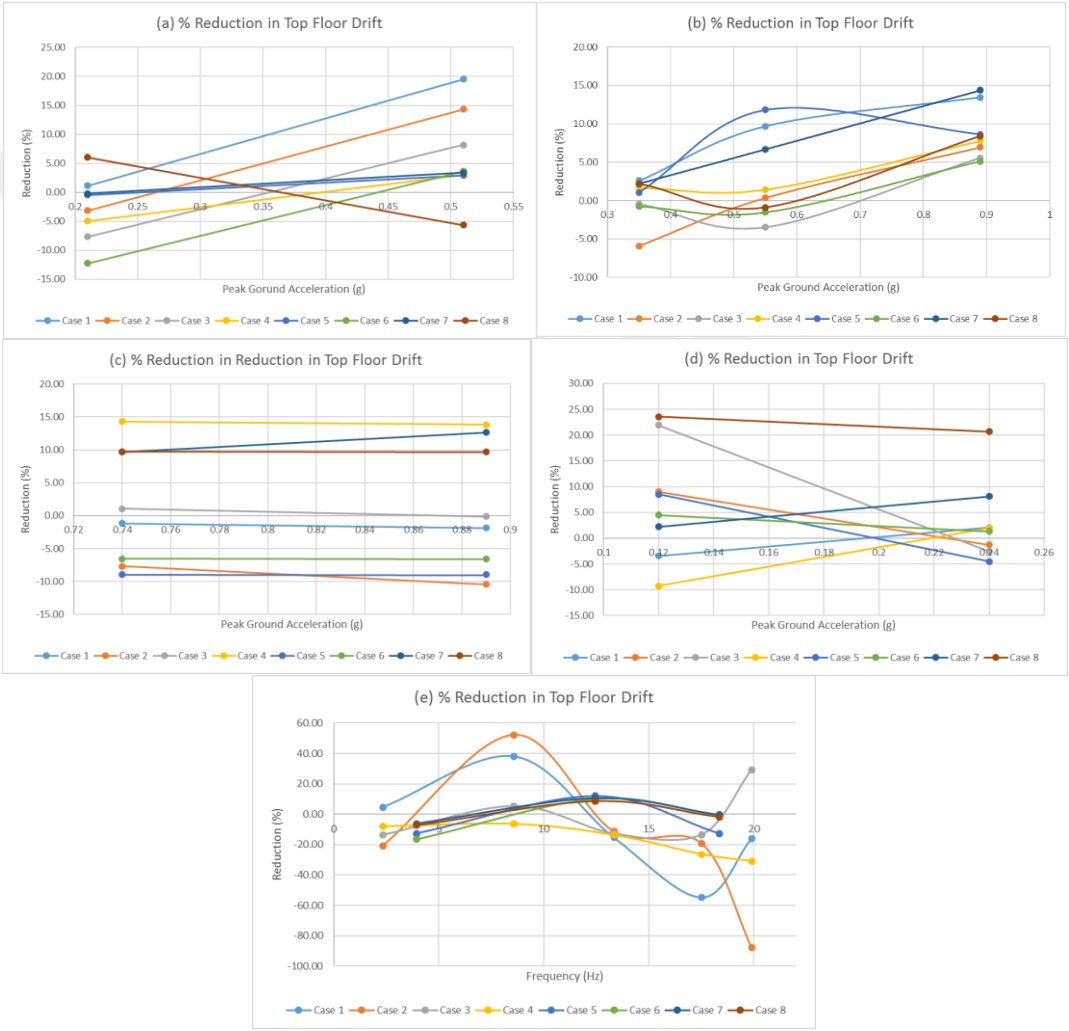

Figure 5.3. Reduction distributions of top floor drift for Kocaeli earthquake (a), El Centro earthquake (b), Kobe earthquake (c), Kocaeli Iznik record motion (d) and Cyclic sinusoidal motion (e) for all cases.

5.2.4. Effects of Geogrid Reinforced Zones on First Floor Drift

Effect of geogrid reinforcement in terms of first floor drift is presented in Figure 5.4 for each motion group. For the Kocaeli earthquake motions (Figure 5.4a), most of the cases functioned properly while Case 4 display the greatest performance among other cases at 0.51g. However, the maximum reduction value was below 12% for all cases. In terms of El Centro motions (Figure 5.4b), all cases except Case 7 functioned properly for 0.35g. Case 4 displayed the greatest reduction for 0.35g, while Case 1 provided better reduction at 0.55g and Case 5 displayed better performance at 0.89g. Reduction rates of Kobe motion (Figure 5.4c) showed that all cases except the Case 5 at 0.89g exhibited a reduction performance in various ranges, while the Case 1, Case 2, Case 3 and Case 4 displayed the greatest reduction in both PGA values. Thus, in terms of first floor drift, geogrid configurations were more efficient in 5-story building models. Iznik station record reduction values are (Figure 5.4d) highlighted that the most reduction occurred in Case 3, at 0.12g by a value of 32%. For the higher PGA of the same motion, Case 8 was more efficient. Case 1, Case 4 and Case 6 test setups produced low values of reduction for various PGA ranges. Under the effect of cyclic sinusoidal motions (Figure 5.4e) the most reduction was occurred for the Case 2 at 8.85 Hz, which contains 2 layers of geogrids and 5-story model structure. The greatest reduction was noted on the first floor drift values is assigned to Case 4, under the Kobe earthquake with 0.89g.

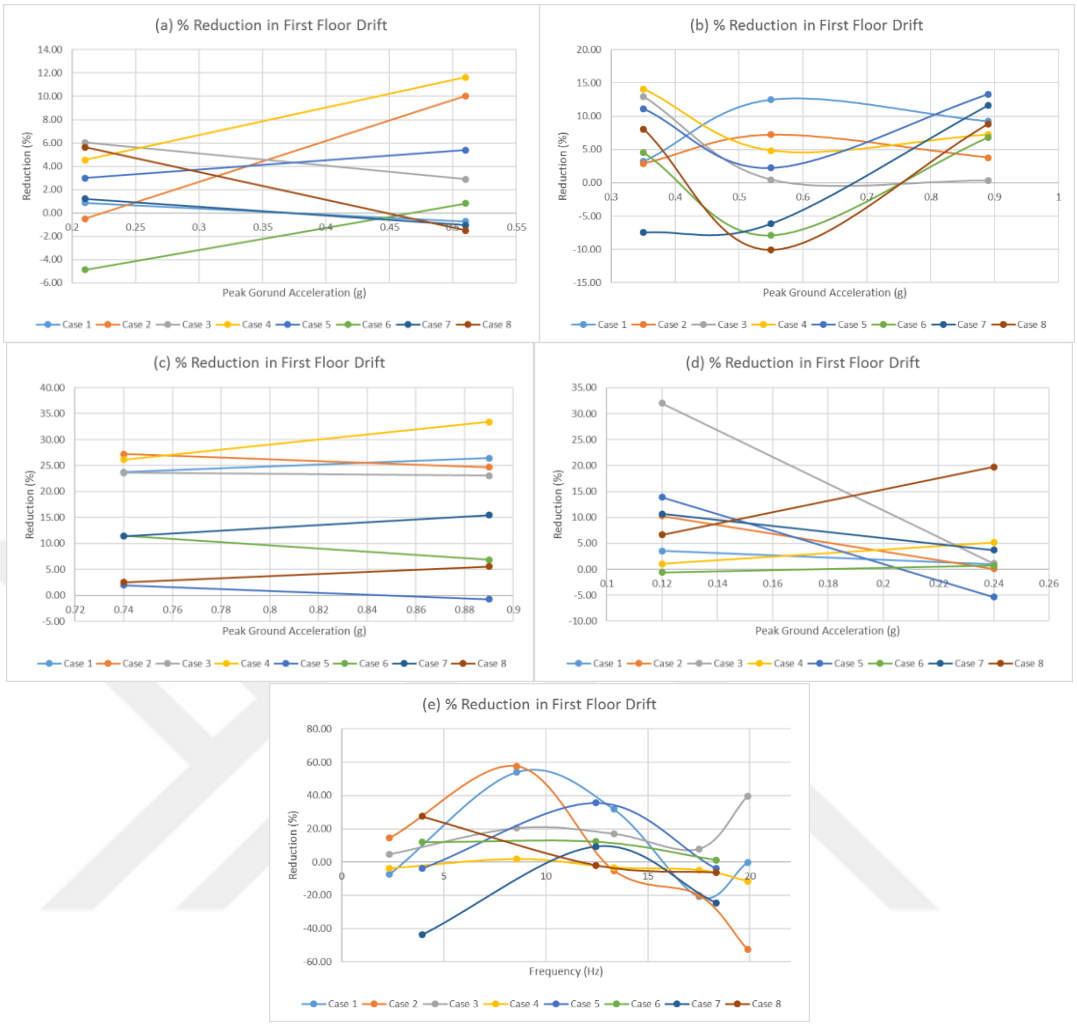

Figure 5.4. Reduction distributions of first floor drift for Kocaeli earthquake (a), El Centro earthquake (b), Kobe earthquake (c), Kocaeli Iznik record motion (d) and Cyclic sinusoidal motion (e) for all cases.

5.2.5. Effect of Geogrid Reinforced Zones on Top Floor Arias Intensity

As demonstrated in Figure 5.5; top floor arias intensity reduction parameters are presented for each motion individually. For the Kocaeli earthquake (Figure 5.5a), Case 8, Case 7 and Case 6 displayed better reduction performance near the 0.21g, respectively. The rest of the cases displayed no significant reduction; thus, top floor arias intensity was functionally reduced for 5-story setups for lower PGAs. In terms of El Centro earthquake (Figure 5.5b), Case 1 and Case 7 represented higher reduction values for the motion. Case 7, which consisted of 3 layers of geogrid reinforcement with a 3-story building model, reduced the top floor arias intensity up to 56% for 0.35g. Reduction rates of Kobe motion

(Figure 5.5c) represented that Case 1, Case 2, Case 3, Case 4 and Case 8 displayed a useful reduction ratio above 10% for all variations of PGA. The maximum reduction was exhibited by Case 1 and Case 2, which contain 5-story structure model and 1-2 geogrid reinforcement layers respectively. The reduction was above 50% for both cases at 0.74g and for Case 2 only at 0.89g. In the Iznik station record of Kocaeli motion (Figure 5.5d), Case 8 presented significant reduction values when compared with other cases, for both lower and higher PGA ranges. The reduction value is near 30% for 0.12g and 0.24g values. Case 1, Case 3, Case 4, Case 6 and Case 7 also reduced the top floor arias intensity effect in all PGA ranges. In terms of cyclic sinusoidal motions of various frequencies (Figure 5.5e), Case 2 exhibited the most reduction factor by around an 80% for 8.58 Hz, followed by Case 1. For the higher frequency values, Case 2 functioned stable. The maximum reduction on top floor arias intensity was noted for Case 7, under El Centro earthquake with the PGA of 0.35g.

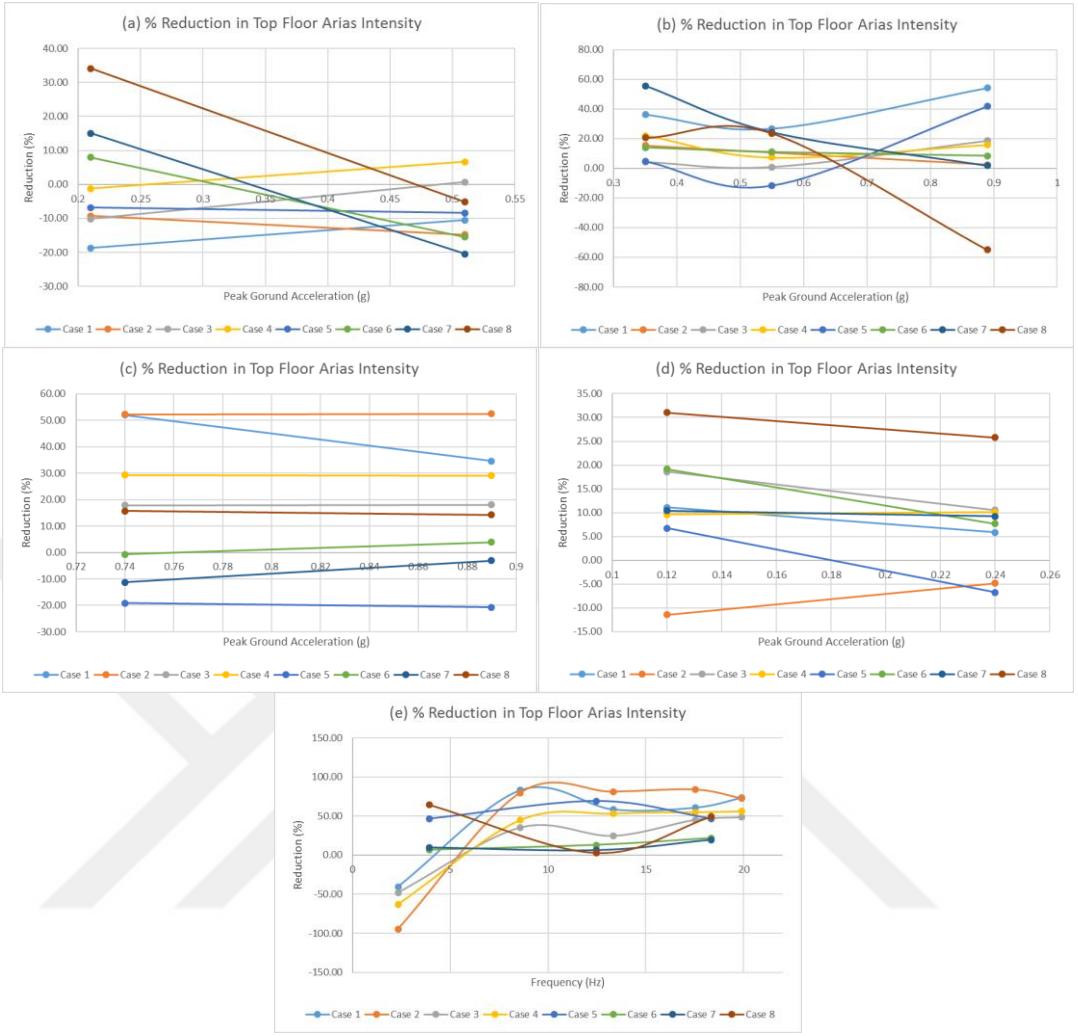

Figure 5.5. Reduction distributions of top floor arias intensity for Kocaeli earthquake (a), El Centro earthquake (b), Kobe earthquake (c), Kocaeli Iznik record motion (d) and Cyclic sinusoidal motion (e) for all cases.

5.2.6. Effect of Geogrid Reinforced Zones on Foundation Arias Intensity

Effect of geogrid reinforcement in terms of foundation arias intensity is presented in Figure 5.6 for various PGA ranges for each motion. For the Kocaeli earthquake response (Figure 5.6a), most of the cases functioned properly to reduce foundation arias intensity, except for the Case 7 and Case 8 for higher PGA values. The highest reduction was noted for Case 4, by around 27% at the 0.21g. On behalf of El Centro motion (Figure 5.6b), all cases except Case 6 and Case 7 were contributing the reduction of foundation arias intensity. Case 1, Case 4 and Case 5 are the cases with the most reduction values and maximum reduction of the mentioned parameter is measured as 30% by Case 5 in 0.89g.

Distribution chart of Kobe earthquake (Figure 5.6c) displays that all cases were able to produce a reduction value in various levels even the maximum reduction rate is below 12%. Maximum decrease ratio is generated by Case 1 at all displayed PGA values of the motion. Iznik station record reduction values are (Figure 5.6d) presented that the most reduction occurred in Case 8, at 0.24g by a value of 18%. For the lower PGA of the same motion, Case 3 was more efficient by a reduction value of 16%. Case 1, Case 5, Case 6 and Case 7 test setups produced low values of reduction, below 10%, for various PGA ranges. Under the effect of cyclic sinusoidal motions (Figure 5.6e) the most reduction was occurred by a large amount of 63% for the Case 2 and Case 4 at 17.52 Hz, which contains 5-story model structure for both cases. The greatest reduction among the earthquake motions was noted on the foundation arias intensity is generated by Case 5, under the Kobe earthquake with 0.89g by 29%.

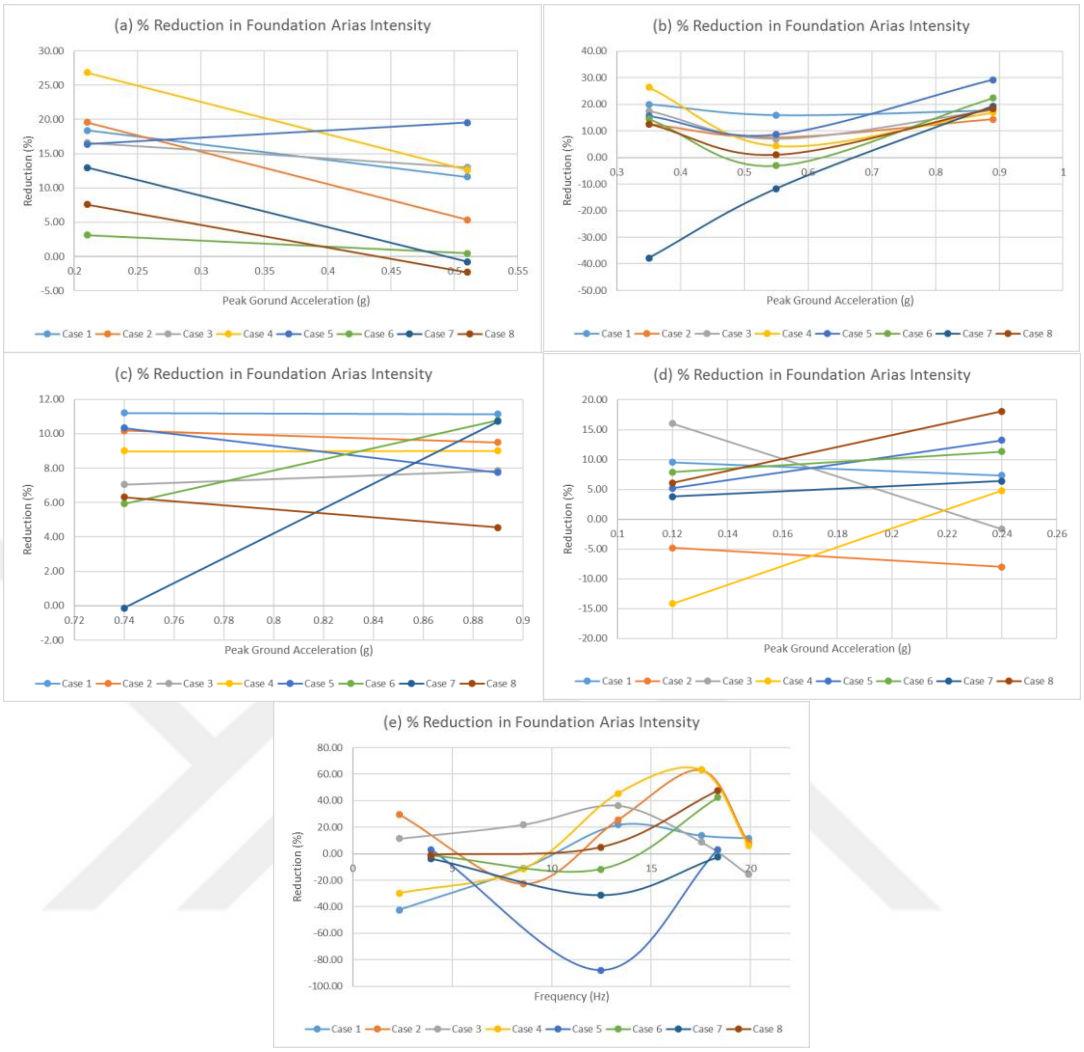

Figure 5.6. Reduction distributions of foundation arias intensity for Kocaeli earthquake (a), El Centro earthquake (b), Kobe earthquake (c), Kocaeli Iznik record motion (d) and Cyclic sinusoidal motion (e) for all cases.

5.2.7. Effect of Geogrid Reinforced Zones on Base Shear

Base shear reduction values for each motion group are presented in Figure 5.7 and reduction parameters are displayed for various PGA and frequency ranges. For the Kocaeli earthquake motions (Figure 5.7a), Case 1 and Case 2 were able to generate reduction for the higher PGA values of the motion. The reduction value of both Case 1 and Case 2 was around 15-16% for 0.51g, which were the highest reduction value. Case 8 was in a decreasing trend while the PGA was increasing. Among the El Centro motions (Figure 5.7b), Case 1, Case 4, Case 5, Case 7 and Case 8 displayed efficient reduction values for all PGA ranges and Case 7 displayed the maximum reduction under the 0.89 PGA by 13%,

which is followed by Case 1 by a 13% for the same PGA value. For the Kobe motion (Figure 5.7c), all cases displayed similar reduction values of their own for the increasing PGAs and results are generally in a steady horizontal line appearance. The highest reduction was generated by Case 4, which contains 4 layers of geogrids and 5-story model structure. For the Iznik station record (Figure 5.7d), Case 8 provided better performance by displaying positive reduction values for both lower and higher PGA values of the motion, by around a 20% for both PGA ranges. Cyclic sinusoidal motion behavior (Figure 5.7e), varied in a large reduction range and greatest reduction was generated by Case 3, for 19.90 Hz, by a reduction value of 11%, which is followed by Case 1, Case 2 and Case 5 test setups.

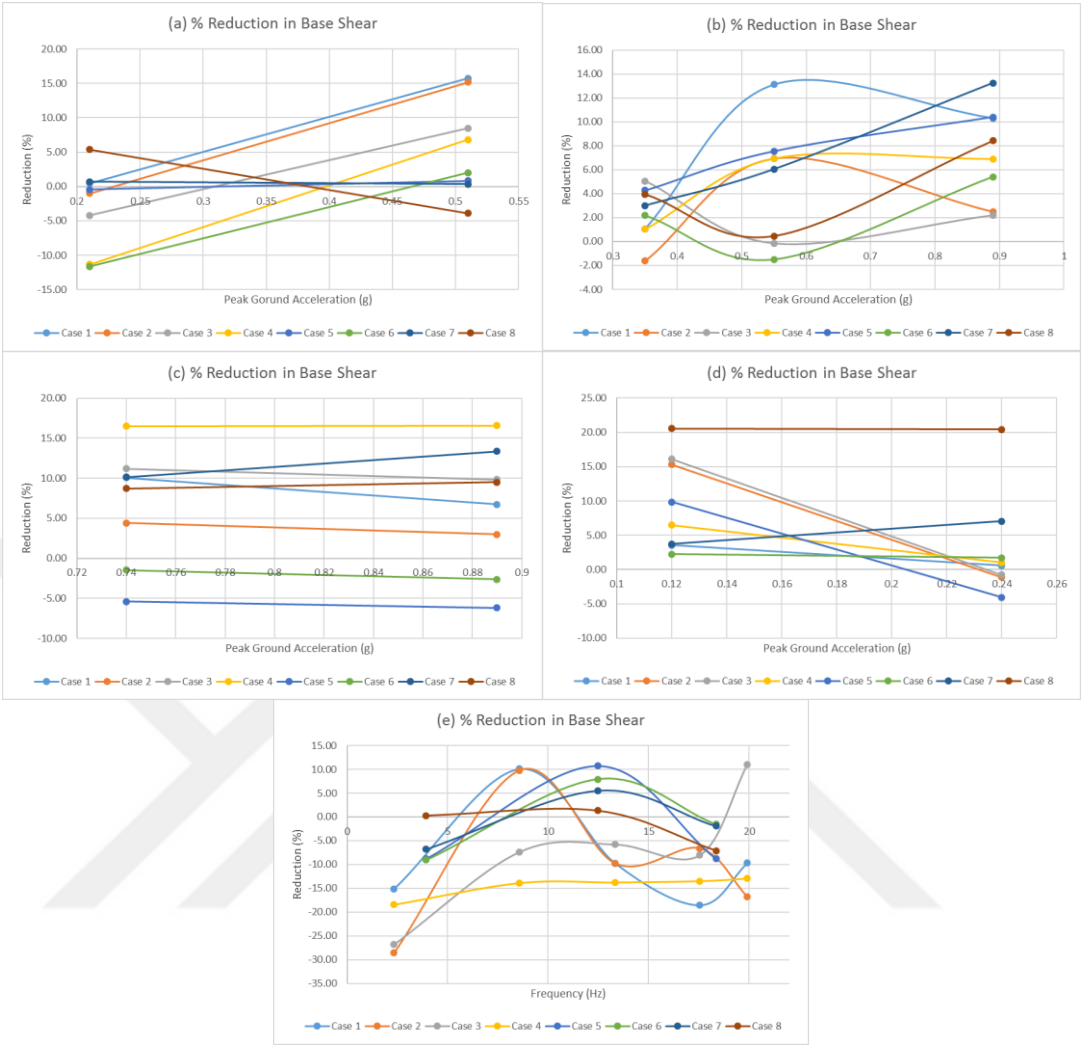

Figure 5.7. Reduction distributions of base shear for Kocaeli earthquake (a), El Centro earthquake (b), Kobe earthquake (c), Kocaeli Iznik record motion (d) and Cyclic sinusoidal motion (e) for all cases.

5.2.8. Effect of Geogrid Reinforced Zones on Base Moment

As demonstrated in Figure 5.8; base moment reduction parameters are presented for each motion individually. For the Kocaeli earthquake (Figure 5.8a), Case 1, Case 2 and Case 3 displayed better reduction performance near the 0.51g, respectively. The rest of the cases displayed no significant reduction; thereby, base moment was functionally reduced for 5-story setups for higher PGAs. In terms of El Centro earthquake (Figure 5.8b), Case 1 and Case 7 represented higher reduction values for the motion. Case 7, which consisted of 3 layers of geogrid reinforcement with a 3-story building model, reduced the base moment proportionally up to 17% for 0.89g. Reduction rates of Kobe motion (Figure 5.8c)

represented that Case 1, Case 3, Case 4, Case 7 and Case 8 presented a reduction ratio by various percentages for all PGA ranges. The maximum reduction was exhibited by Case 4, which contain 5-story structure model and 4 layers of geogrid reinforcement. The reduction is near 15% for the case at both 0.74g and 0.89g. In the Iznik station record of Kocaeli motion (Figure 5.8d), Case 8 presented significant reduction values when compared with other cases, for both lower and higher PGA ranges. The reduction value is near 23% for 0.12g and 0.24g values. Rest of the case configurations also reduced the base moment effect in lower PGA ranges. In terms of cyclic sinusoidal motions of various frequencies (Figure 5.8e), Case 2 exhibited the most reduction factor by around an 9% for 8.58 Hz, which is followed by Case 5 by a reduction factor of 9% for 12.46 Hz. The maximum reduction on base moment was detected for Case 8, under Iznik station record of the Kocaeli earthquake with the PGA of 0.12g.

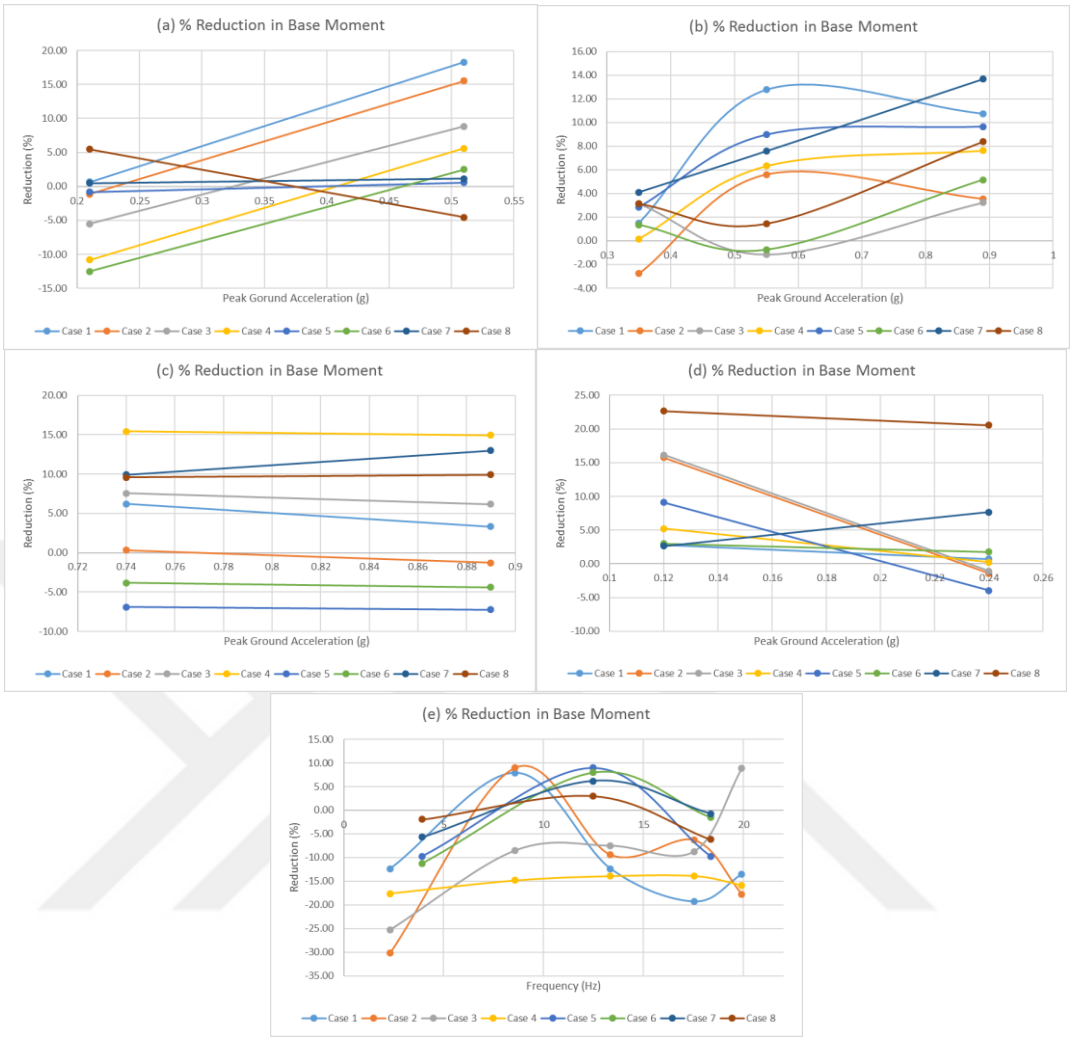

Figure 5.8 Reduction distributions of base moment for Kocaeli earthquake (a), El Centro earthquake (b), Kobe earthquake (c), Kocaeli Iznik record motion (d) and Cyclic sinusoidal motion (e) for all cases.

5.3. Effect of Geogrid Reinforced Zones on Spectral Ratios

Spectral ratios of the acceleration time response histories of the model setups were calculated by a ratio of Fourier Amplitude Spectrums of a soil-site (test setup) record to a reference site record (Safak, 2001; Calikoglu, 2017).

In the scope of this study, the effect of proposed geogrid reinforcement is investigated through the spectral ratios of A18 (top floor accelerometer for 5-story structure model) and A16 (top floor accelerometer for 3-story structure model) accelerometer data to A5 accelerometer data for the unreinforced and reinforced cases

under the same earthquake motions. Spectral ratios of the Fourier transforms were generated under the Kocaeli (0.21g), El Centro (0.35g) and Kobe earthquake (0.89g) motions. Note that from the Section 4.1, there was an increase in the acceleration within the soil deposit in the direction of the surface.

In the following parts, spectral ratios of Fourier Amplitude Spectrums of the responses under Kocaeli, Kobe and El Centro earthquakes for all cases were evaluated.

5.3.1. Spectral Ratio Comparisons of Case 1

As displayed in Figure 5.9, spectral amplitude ratios of unreinforced and reinforced cases are compared. Spectral ratio plots are generated through the Fourier amplitudes of A18/A5 accelerometers for reinforced and unreinforced cases. Since the Case 1 is N=1 for 5-story model setup, it is seen that one layer of geogrid displayed amplitude reductions as represented in the ratio amplitudes of comparison plots.

The most amplitude reduction is displayed for the Kobe earthquake motion, where the peak amplitude value is reduced around 65%, in favor of the geogrid reinforced case, on the governing mode of the structure. The reduction under the Kobe earthquake is followed by the Kocaeli earthquake motion by a reduction in amplitude by 32%. There is also a slight reduction in Fourier amplitude under the El Centro motion for the governing mode of the structure, by nearly 4%. Generally, there are slight frequency shifts, however the amplitude ratios are clearly decreased for the top floor, as an indicator parameter.

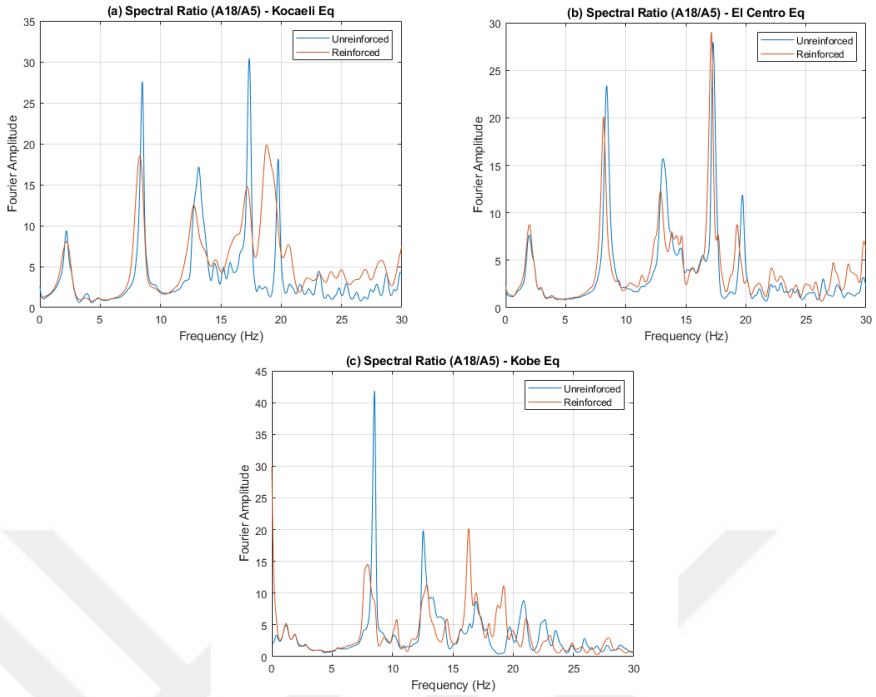

Figure 5.9. Spectral Ratio Comparisons for Case 1 – Kocaeli Earthquake (a), El Centro Earthquake (b), Kobe Earthquake (c).

5.3.2. Spectral Ratio Comparisons of Case 2

In Figure 5.10, spectral amplitude ratios for both unreinforced and reinforced cases are analyzed. As a side note, the Case 2 is N=2 for 5-story model setup and it is displayed that two layers of geogrid reinforcement affected top floor response spectrum.

Maximum difference in spectral ratio is displayed for the Kobe earthquake as similar to Case 1. As the governing mode of the structure is in the same frequency range, nearly a 65% reduction in the Fourier amplitude is observed for the mentioned mode. However, reductions were not clearly observed for both El Centro and Kocaeli earthquake motions. In Case 2, a slight frequency shift is possible to monitor for most of earthquake scenarios.

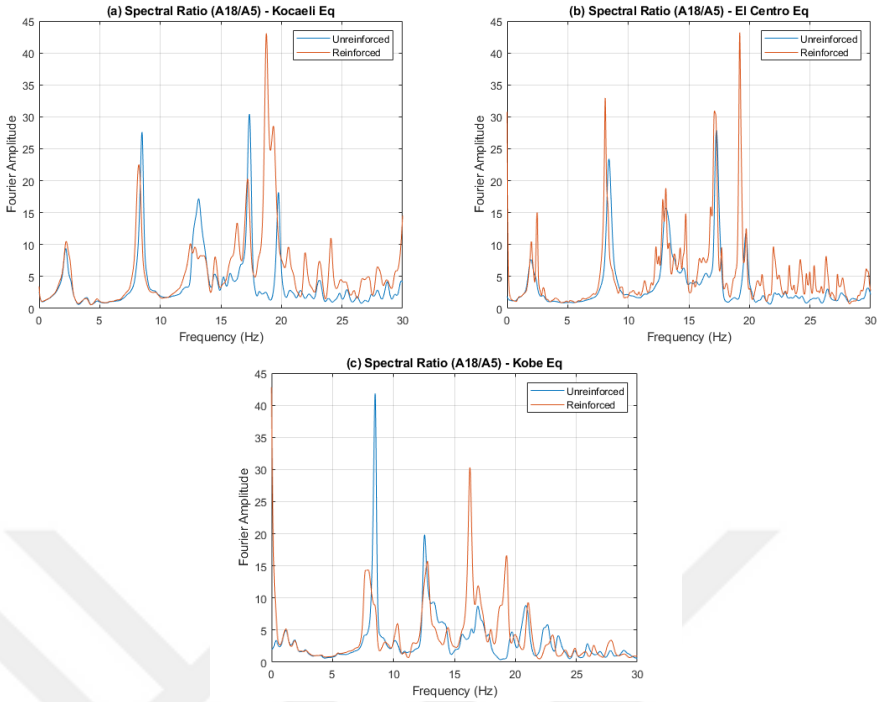

Figure 5.10. Spectral Ratio Comparisons for Case 2 – Kocaeli Earthquake (a), El Centro Earthquake (b), Kobe Earthquake (c).

5.3.3. Spectral Ratio Comparisons of Case 3

As exhibited in Figure 5.11, spectral ratio values of unreinforced and reinforced cases are compared. Since the Case 3 is N=3 for 5-story model setup, it is represented that three layers of geogrid reinforcement moderated spectral ratio values of the A18 (top floor) according to A5 accelerometer.

Governing mode amplitude of Kobe earthquake was relatively the most reduced condition and the ratio value of the governing mode is changed around 42%. Under other earthquake motions, generally an increasing trend was observed for the Case 3. Mainly, there were no significant frequency shifts and amplitude reductions for this case.

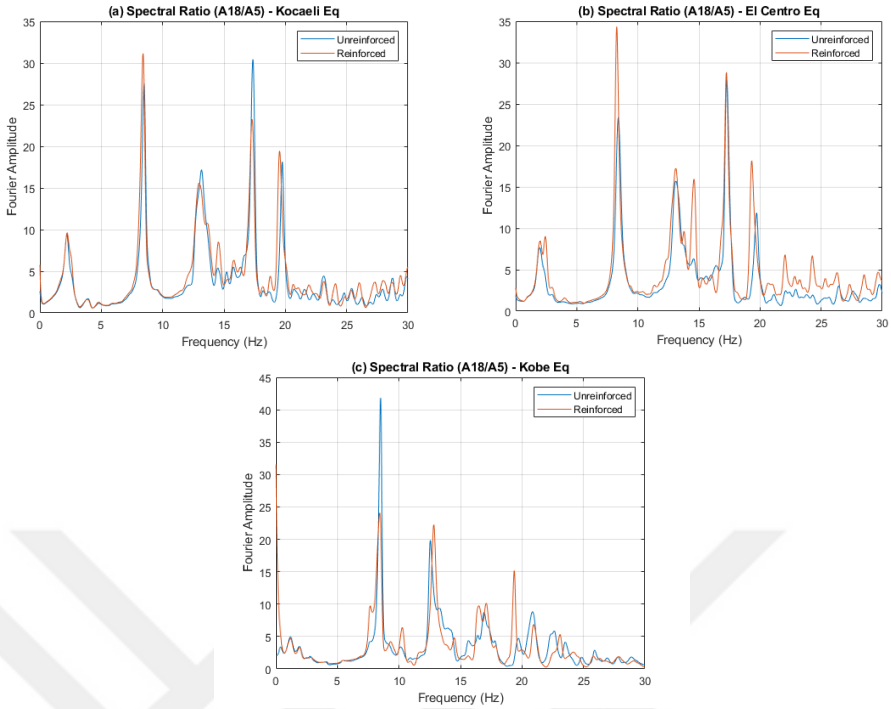

Figure 5.11. Spectral Ratio Comparisons for Case 3 – Kocaeli Earthquake (a), El Centro Earthquake (b), Kobe Earthquake (c).

5.3.4. Spectral Ratio Comparisons of Case 4

Spectral ratios in frequency domain of unreinforced and reinforced cases are examined for Kocaeli, El Centro and Kobe earthquake motions in Figure 5.12. Spectral ratio plots are generated from the spectral amplitudes of A18 (top floor) and A5 accelerometers. Case 4 is N=4 for 5-story model setup and it is presented in the figure that the configuration reduces spectral ratios under Kobe earthquake motion, while there was an increase in the amplitude value of the El Centro motion. There was around 44% reduction for the Kobe earthquake motion. There were nearly no frequency shifts were noted for the Case 4.

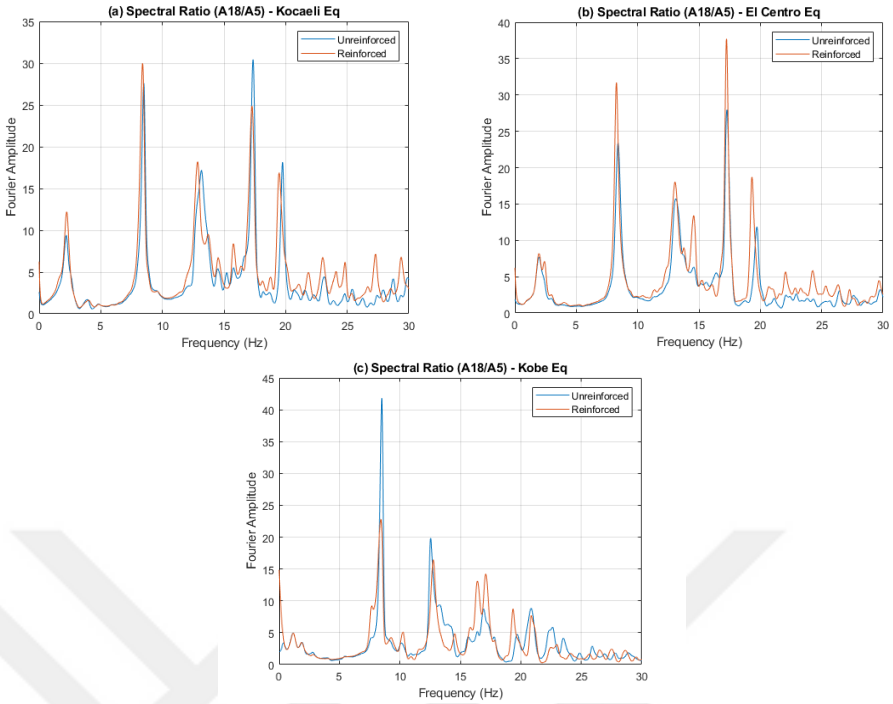

Figure 5.12. Spectral Ratio Comparisons for Case 4 – Kocaeli Earthquake (a), El Centro Earthquake (b), Kobe Earthquake (c).

5.3.5. Spectral Ratio Comparisons of Case 5

As displayed in Figure 5.13, spectral amplitudes of unreinforced and reinforced case are compared. Plots are generated from the spectral amplitudes through of A16 (top floor) and A5 accelerometers for the 3-story cases. Case 5 represents the N=1 for 3-story model setup and it only exhibits reduction for one mode under the El Centro motion.

For the governing mode of the structure, spectral ratio under the El Centro earthquake motion was decreased by the effect of reinforced zone as well as the frequency shift for the same mode. There was around 34% difference noted for the El Centro motion in comparison of spectral ratio values for the mentioned governing mode. In terms of other strong ground motions, a significant reduction is not clearly noted.

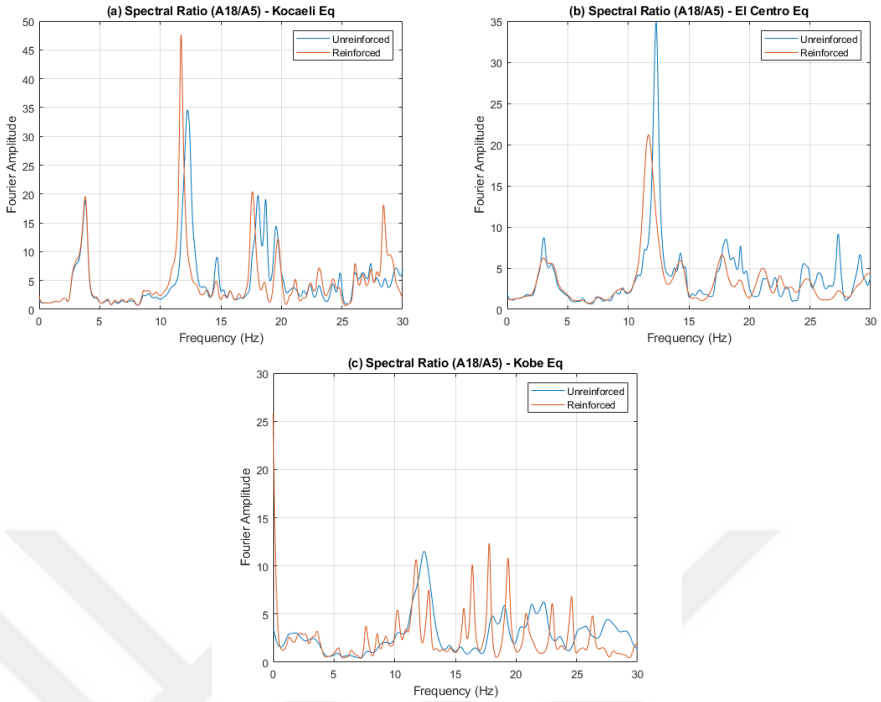

Figure 5.13. Spectral Ratio Comparisons for Case 5 – Kocaeli Earthquake (a), El Centro Earthquake (b), Kobe Earthquake (c).

5.3.6. Spectral Ratio Comparisons of Case 6

Spectral ratio plots of unreinforced and reinforced cases are analyzed in Figure 5.14. Since the Case 6 is N=2 for 3-story model setup, it can be seen that two layers of geogrid reinforcement affected top floor spectral amplitudes.

The most amplitude reduction was displayed under the Kobe earthquake motion and there were small reductions in spectral ratios under the Kocaeli earthquake motion. Governing mode of the structure displayed a reduction in spectral ratio by near 10%. For the Kocaeli earthquake motion, around 3% reduction is noted for the spectral ratios of unreinforced and reinforced cases. The amplitudes under the El Centro earthquake motion were increased for the governing modes. In general, there were no frequency shifts noted for the Case 6.

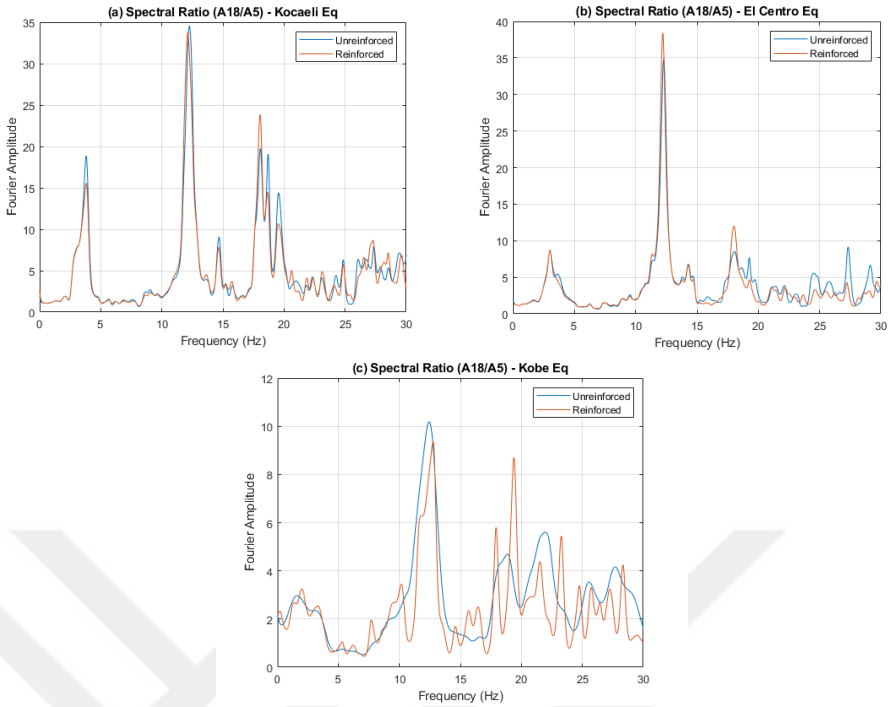

Figure 5.14. Spectral Ratio Comparisons for Case 6 – Kocaeli Earthquake (a), El Centro Earthquake (b), Kobe Earthquake (c).

5.3.7. Spectral Ratio Comparisons of Case 7

As displayed in Figure 5.15, spectral ratios of unreinforced and reinforced case are examined. Since the Case 7 is N=3 for 3-story model setup, it is presented that three layers of geogrid displayed various behavioral aspects under different earthquake motions for Case 7.

The most and only reductions were exhibited under the Kocaeli earthquake motion and there were no frequency shifts noted for the motion. Peak spectral ratio was reduced for the governing mode was around 29% for the Kocaeli earthquake. On behalf of El Centro and Kobe earthquake motions, there were no reductions noted and spectral ratios were increased for the reinforced case. Also, there were no frequency shifts noted for both El Centro and Kobe earthquakes.

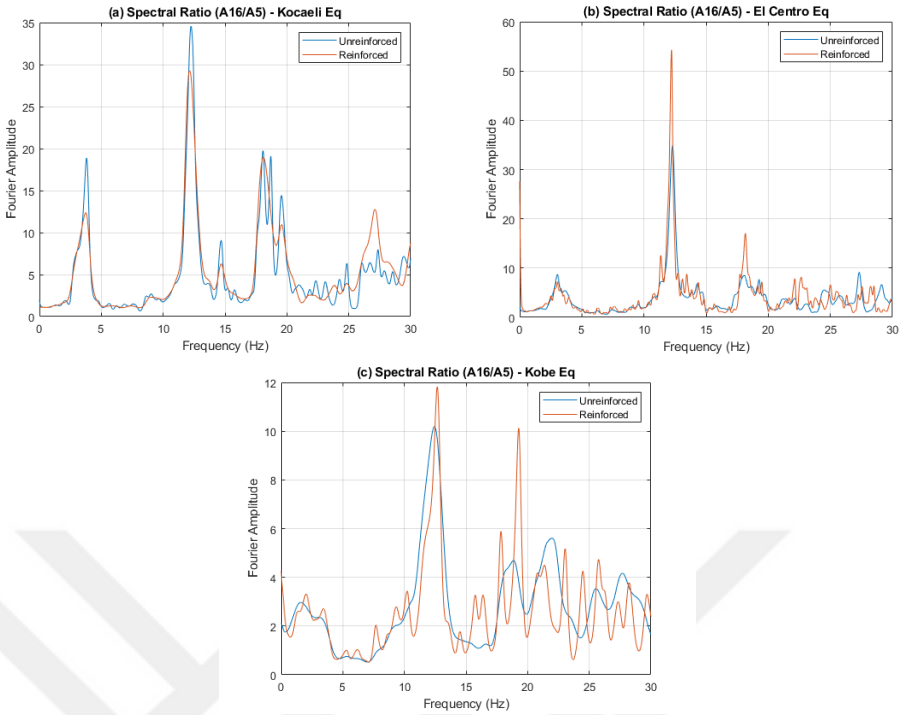

Figure 5.15. Spectral Ratio Comparisons for Case 7 – Kocaeli Earthquake (a), El Centro Earthquake (b), Kobe Earthquake (c).

5.3.8. Spectral Ratio Comparisons of Case 8

As generated in Figure 5.16, spectral ratios of top floor for unreinforced and reinforced case are examined. As a reminder, Case 8 is N=4 for 3-story model setup and the effects of four layers of geogrid on the spectral ratios are presented.

Mainly, there are reductions in terms of governing modes of the structure for all motions specifically. The most amplitude reduction of the case was displayed under the Kocaeli earthquake and followed by El Centro earthquake, by around 35% and 28% respectively. For the Kobe earthquake, a slight ratio reduction was noted by 14% for the governing mode of the structure. In general aspect, there were no significant frequency shifts produced under different motions.

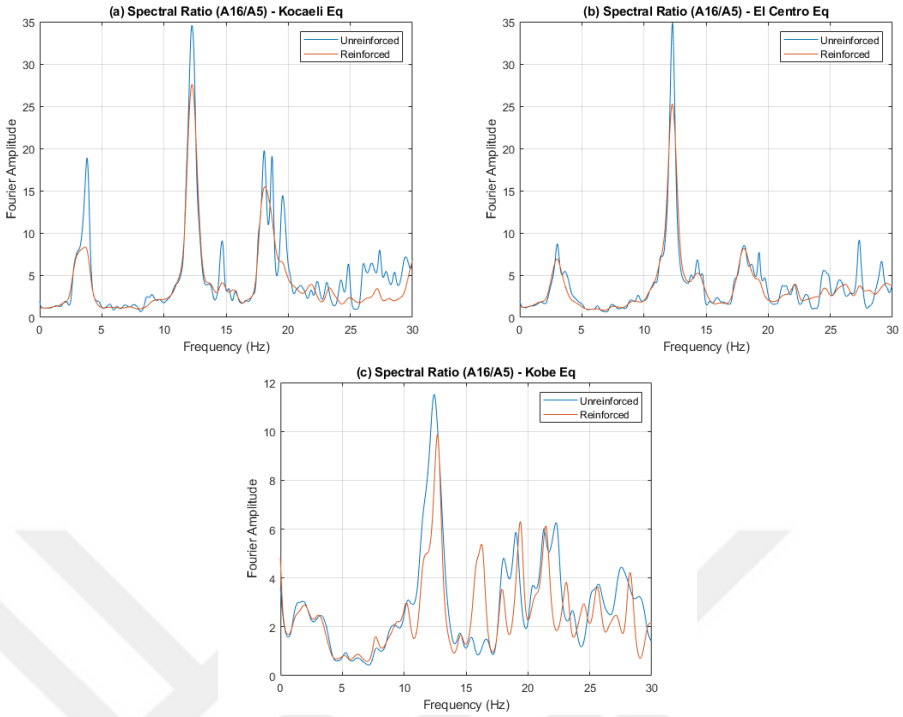

Figure 5.16. Spectral Ratio Comparisons for Case 8 – Kocaeli Earthquake (a), El Centro Earthquake (b), Kobe Earthquake (c).

6. SUMMARY AND CONCLUSION

6.1. Summary

The main objective of this thesis study is to research the effectiveness of the geogrid reinforced zones on the seismic performance of low to medium rise buildings. The experiments were performed for unreinforced and geogrid reinforced foundations. The cause of the experimental study is to observe the behavioral aspects of the test setups, search and evaluate economical and practical solutions to provide a better seismic performance for the structures. Thus, for the developing countries where other earthquake solutions are not applicable or where the workforce is rather cheap, the effects of reinforcement mechanism should be investigated.

This study is composed of six chapters and in every chapter, a different specification of the study is expressed. First chapter contains information about the introduction of the thesis, where the main objective is expressed. Second chapter extents information about literature reviews and previous studies within this concept. Characteristics and literature review of the geogrid materials, geogrid reinforcement and previous numerical and experimental studies, laminar box containers are indicated, along with the experimental techniques of the shaking table tests. Chapter three involves in the characterization and definitions of the materials and test methods of the study. The shaking table specifications, the instruments used in the measurement of the test setup responses, sand material characteristics, input ground motions and applied ground motion definitions, preparation and instrumentation of the test setups, the scaled building model characteristics and the methods used in shaking table experiments are expressed. In chapter four, the experimental outcomes of the study are displayed for every case on behalf of Kocaeli, El Centro and Kobe earthquake motions. The same considerations were also displayed for both 3-story and 5-story structures. The measured findings are visualized by figures and tables to demonstrate the effects of different configurations of the geogrid reinforcement. In the scope of section five, a parametric study is conducted to determine the behavioral aspects of the geogrid reinforced zones via various PGA values of the different earthquakes, cyclic sinusoidal motions and Kocaeli Iznik station record. Effect of geogrid reinforced zone is

expressed through all conducted experimental results and comparative figures are generated to visualize the geogrid effect. The comparisons were made through the eight performance parameter indicators and each of the evaluated individually. Spectral ratio differences of reinforced and unreinforced cases were compared also in this chapter. Inferences and comments of the experimental tests were represented in the chapter six, lastly.

Essentially, the idea of the geogrid reinforcement comes from the concept of interlocking mechanism of the soil through the apertures of the geogrids and thereby, creating and anchoring effect. This behavioral qualification of the geogrid material turned it into a reinforcement element and many studies are conducted about the phenomenon. There are many static experimental tests on the topics of the geogrid reinforcement arrangements and on the bearing capacity of the geogrid reinforced soil. However, this study alternatively aims to conduct and compare the dynamic aspects and qualifications of geogrid material and configuration variations in a dynamic test setup, in terms of a soil reinforcement material. Thus, the seismic performance of the geogrid reinforcement is researched through unreinforced and reinforced tests for different cases which are approximately around 300 tests.

Multiple layers of polypropylene (PP) geogrid materials were used to simulate geogrid reinforcement of the soil and effects of the reinforcement on soil-structure interaction as well as structural responses. Four different configurations for number of geogrid layers and two different type of test models, varying in number of stories, were adopted. For each geogrid arrangement, the effects of geogrid reinforced zones were evaluated as a soil reinforcement material through the reductions or increases in the eight performance parameters; which are top floor acceleration, foundation acceleration, top floor drift, first floor drift, top floor arias intensity, foundation arias intensity, base shear and base moment.

Eventually, as a result of the both experimental tests and parametric studies of the chapter four and five, the effects of the number of the story, number of geogrid reinforcement layers and ground motion specifications are assessed and seismic

performance, as well as the advantages and disadvantages of the geogrid reinforcement for the whole combination of cases were expressed.

6.2. Conclusions

Taking the consequences of the measurements into account, it is possible to confirm the positive effects of the geogrid reinforced zones in terms of seismic performances of the test setups. Various configurations of N parameter shifted the behavioral aspects of the experimental setup in terms of different parameters. Thereby, performance of the geogrid reinforcement layers depends on configurations and number of stories.

For the 5-story building models, all layer numbers of geogrid configuration displayed efficient reductions in the responses, however, precise and consistent results were typically displayed in N=2 and N=3 cases. For the Kocaeli earthquake which has a lower PGA value among others, two layers of geogrids were sufficient to reduce foundation acceleration, top floor acceleration and first floor drift responses of the setup, both in for RMS and peak values. As similar to that, the root mean square of the time histories of the same responses were also lessened, meaning in continuously variation of among the time history was also reduced. In addition, these reduction ratios of the mentioned parameters were more precise in terms of scalar quantities and supported by other performance parameters. As the PGA value increased for N=2, reduction factors were generally in an increasing trend, thus, displaying a direct proportion for many parameters. Under the El Centro and Kobe earthquakes, acceleration reductions were increased along with the arias intensity and base shear/base moment reduction values, gradually. For that matters, two layers of geogrid reinforcement (N=2) is a preferable solution to improve seismic performance of the building models.

As similar to N=2 case, three layers of geogrid (N=3) configurations also provides a consistent reduction in the 5-story cases. Under the Kocaeli earthquake, three reinforcement layers created consistent results but less reductions and also small amplifications in base shear and base moments when compared with two layers of geogrid reinforcements. However, under progressively increasing PGA values, three layers of geogrids displayed better reductions in peak values, however, it was still behind the arias

intensity reduction values when examined in contrast to N=2 arrangement. In three layers of geogrid reinforcement system, base shear and base moment reductions were comparatively higher than in the case with two layers of geogrids. As a complementary to N=2 setup, arias intensity reductions gradually become more stable under increasing PGA value. Thus, for mid-rise structures, three layer of geogrid reinforcement can be considered as an option.

Furthermore, N=4 setup of the geogrid reinforcement provides a great amount of peak reduction in terms of acceleration time histories and drift time histories of medium rise models, which is 5-story in this concept. However, it requires the deeper soil deposit to place a fourth layer of geogrid, thus, having a practical disadvantage while in the application phase of the reinforcement. Four layers of geogrid also moderates and lowers the peak ratios of the acceleration and drift time histories for higher PGA values, as well as the arias intensity. In addition, these performance improvements are relatively higher or close to N=3 and N=2 configurations, however, it is not able to provide same reductions on behalf of RMS calculations. Thus, four layers of geogrid reinforcement can be a case specific solution where the peak value reduction is the desired condition in the seismic performance of the structure.

Reinforced soil with one layer of geogrid (N=1) provides relatively lower performance on dissipating the seismic effects. On the other hand, for the earthquakes with higher PGA values as El Centro and Kobe earthquakes, it is a preferable solution and it requires the lowest reinforcement depth to applicate the configuration among other multi layered cases. Conversely, as a disadvantage, the generated reduction outcomes under the N=1 parameter does not always display inter compatibility with other performance criteria for the lower PGA values. Even so, it may be the most economical option for higher PGA values to provide base shear and base moment reduction, as well as providing lower foundation arias intensity.

For the 3-story building models, all geogrid configurations displayed reduction in varying ranges. Even so the reductions in the performance indicator parameters are not clear as in the 5-story building cases, precise and stable results were typically displayed in N=3 case, in accordance with mid-rise building model. As under the Kocaeli earthquake

which has a lower PGA value, three layers of geogrids were not functionally efficient in terms of every performance indicators. But, under the El Centro and Kobe earthquake motions, the reductions values are supported by more performance parameters. Three layers of geogrid reinforcement were sufficient enough to reduce the seismic responses of acceleration-time and displacement-time histories of the building model. N=3 case fundamentally represented more reductions under the lower PGA values of Kocaeli earthquake and higher PGA values of El Centro and Kobe earthquakes.

Among N=2 and N=4 configurations, the four layers of geogrid reinforcement is representing more effective performance improvement for the 3-story building model. Especially in lower PGA values of Kocaeli, El Centro and Kobe earthquakes, four layers of geogrid presented more efficient reduction ratios. Basically, peak values of the performance indicators parameters are showing a greater declining trend under the effect of four layers of geogrid. However, as mentioned in 5-story cases, it requires more effort to place four layers of geogrid into the soil deposit, thereby, making it practically uneconomical. More dissipation of seismic energy is observed in the reinforced case of four layers compared to two layers. It has been determined as common behavior at low and high PGA values of El Centro and Kobe earthquakes and only lower PGA values of Kocaeli earthquake.

One layer of geogrid (N=1) configuration under the 3-story models generated dissipation of seismic energy, however, reduction factors for different earthquakes and various PGA values are competent for every case. Thus, an economical but situation specific solution is generated by one layer of geogrid for the low rise structures. Generally, minimum PGA values of Kocaeli and Kobe earthquake motions performed better with the one layer of geogrid reinforcement. Additionally, reductions are also noted for performance parameter under the larger PGA values of El Centro earthquake. Thus, on behalf of soil reinforcement, one layer of geogrid reinforcement was not functionally efficient for all cases.

Eventually, the use of geogrid reinforcement is case specific. For the cases considered in this thesis, three layers (N=3) of geogrid reinforcement displayed better reduction values among the other reinforced zones created by same reinforcement

materials. As the number of story increases, the number of geogrid reinforcements may decrease. The two layers of geogrid also worked optimally for many performance parameters and affected the behavior of the mid-height building model.

The results of this first experimental study showed that the geogrid reinforced zone can significantly affect the seismic performance of buildings. Most importantly, it may be possible to determine the most economical and effective number of geogrid reinforcement layers that will increase the seismic performance of the structure with such modeling studies.

In summary, the seismic performance of buildings may be dependent on the geogrid reinforced zone, number of stories, properties of soil and geogrid, and ground motion characteristics such as amplitude, frequency, and time.

Briefly, the results of the evaluated parameters showed that it can be possible to mitigate the earthquake damage of the low-to-mid rise buildings by constructing the buildings on the geogrid reinforced zone. Therefore, the proposed soil reinforcement method may be beneficial for developing countries.

REFERENCES

1. Alamshahi, S. and Hataf, N., "Bearing capacity of strip footings on sand slopes reinforced with geogrid and grid-anchor, *Geotextiles and Geomembranes.* Vol. 27, pp. 217-226, 2009.

2. Alawaji, H.A., "Settlement and Bearing Capacity of Geogrid-Reinforced Sand over Collapsible Soil", *Geotextiles and Geomembranes*. Vol. 19, pp. 75-88, 2001.

3. Bhattacharya, S., D. Lombardi, L. Dihoru, M.S. Dietz, A.J. Crewe, & C.A. Taylor, "Model Container Design for Soil-Structure Interaction Studies", *Role of Seismic Testing Facilities in Performance- Based Earthquake Engineering*. Vol 5, pp. 135-158, 2012.

4. Calikoglu, M. *Experimental Study on Foundation Isolation Using Geosynthetics*, MSc. Thesis, Bogazici University, 2017.

5. Chang, K.C., Y. B. Yang & J.D. Yau, "Base Isolation", *In Earthquake Engineering Handbook*. CRC Press, 2002.

6. Cheung, W. M., X. Qin, N. Chouw, T. Larkin, and R. Orense, "Experimental and Numerical Study of Soil Response in a Laminar Box", *NZSEE Conference*. 2013.

7. Chunxia, H., Z. Hongru, C. Gouxing, and S. Zhilong, "Design and Performance of a Large-Scale Soil Laminar Shear Box in Shaking Table Test". 2008.

8. Edincliler, A., Y. S. Toksoy and O. Yildiz, "Parametric Study on Seismic Performance of Low and Mid-Rise Buildings on Geogrid Reinforced Sand". *GeoAfrica 2017 Conference.* Marrakech, Morocco, 2017.

9. Edincliler, A. and Y. S. Toksoy, "Effects of Geogrid Reinforcement to Mitigate Earthquake Hazards of Medium-Rise Buildings Under Different Earthquake Motions". *Eurasian Journal of Civil Engineering and Architecture.* Vol. 3, pp. 9-22, 2019.

10. Ecemis, N., and I. Kahraman, "Design of Laminar Shear Box for One Dimensional Shaking Table Tests", Tenth International Congress on Advances in Civil Engineering. Ankara, Turkey, 2012.

11. El-Emam, M. M., and R. J. Bathurst, "Experimental Design, Instrumentation and Interpretation of Reinforced Soil Wall Response Using a Shaking Table", International Journal of Physical Modelling in Geotechnics. Vol. 4, pp. 13-32, 2004.

12. Goztepe, B. *Experimental Study on Mitigation of Earthquake Hazards Using Rubber-Soil Mixtures,* MSc. Thesis, Bogazici University, 2016.

13. Guido, V. A., D. K. Chang and M.A. Sweeney, "Comparison of geogrid and geotextile reinforced earth slabs", *Canadian Geotechnical Journal.* Vol. 23, No.4, pp. 435-440, 1986.

14. Harris, H. G., and G. M. Sabnis, *Structural Modeling and Experimental Techniques*. CRC Press. 1999.

15. Hushmand, B., R. F. Scott, and C. B. Crouse, "Centrifuge Liquefaction Tests in a Laminar Box", *Geotechnique*. Vol. 38, No.2, pp. 253-262, 1988.

16. Iai, S., "Similitude for Shaking Table Tests on Soil-Structure-Fluid Model in 1g Gravitational Field," *Soils and Foundations*, Vol. 29, pp105-118, 1989.

17. Jafarzadeh, F., "Design and Evaluation Concepts of Laminar Shear Box for 1g Shaking Table Tests", *Thirteenth World Conference on Earthquake Engineering.* No.1391, Canada, 2004.

18. Koerner, R. M., "Designing with Geosynthetics", Pearson Education Press, Chapter 3. 2005.

19. Lombardi, D., and S. Bhattacharya, "Shaking Table Tests on Rigid Soil Container with Absorbing Boundaries", *15 WCEE*. Lisboa, 2012.

20. Omar, M. T., B. M. Das, V.K. Puri, S.C. Yen, "Ultimate bearing capacity of shallow foundations on sand with geogrid reinforcement", *Canadian Geotechnical Journal.* Vol. 30, No.3, pp. 545-549, 1993.

21. Patra, C. R., B. M. Das, C. Atalar, "Bearing capacity of embedded strip foundation on geogrid-reinforced sand", *Geotextiles and Geomembranes*. Vol. 23, pp. 454-462, 2005.

22. Prasad, S. K., I. Towhata, G. P. Chandradhara, and P. Nanjundaswamy, “Shaking Table Tests in Earthquake Geotechnical Engineering”, *Current Science.* Vol. 87, No. 10, 2004.

23. Safak, E., “Local Site Effects and Dynamic Soil Behavior", *Soil Dynamics and Earthquake Engineering,* Vol. 21, pp. 453-458, 2001.

24. Schofield, A. N., “Dynamic and Earthquake Geotechnical Centrifuge Modelling”, *First International Conference on Recent Advances in Geotechnical Earthquake Engineering and Soil Dynamics.* No.2, 1981.

25. Sekman, M. *Experimental Study on Mitigation of Earthquake Hazards Using Geosynthetics,* MSc. Thesis, Bogazici University, 2016.

26. Thevanayagam, S., and N. Ecemis, “Geotechnical Laminar Box Shaking Facility”, UB Users Workshop, University of Buffalo, 2006.

27. Turan, A., S. D. Hinchberger, and H. E. Naggar, “Design and Commissioning of a Laminar Soil Container for Use on Small Shaking Tables”, *Soil Dynamics and Earthquake Engineering.* Vol. 29, pp. 404-414, 2009.

28. Yetimoglu, T., J. T. H. Wu and A. Saglamer, “Bearing Capacity of Rectangular Footings on Geogrid-Reinforced Sand”, *Journal of Geotechnical Engineering.* Vol. 120, pp. 2083-2099, 1994.

29. Yildiz, A.A., M. Laman, M. Ornek, and A. Demir, "Numerical Analysis of Circular Foundations Supported by Sand Reinforced with Geogrid", *Second National Conference on Geosynthetics*, University of Bogazici, Istanbul, pp. 75-84, 2006 (in Turkish).

30. Wang, L., G. Chen and S. Chen, "Experimental study on seismic response of geogrid reinforced rigid retaining walls with saturated backfill sand", *Geotextiles and Geomembranes.* Vol. 43, pp. 35-45, 2015.

31. Zeng, X. & Schofield, A. N., "Design and performance of an equivalent-shear-beam container for earthquake centrifuge modelling", *Géotechnique.* Vol. 46, pp. 83-102, 1996.